



## AVERTISSEMENT

Ce document est le fruit d'un long travail approuvé par le jury de soutenance et mis à disposition de l'ensemble de la communauté universitaire élargie.

Il est soumis à la propriété intellectuelle de l'auteur. Ceci implique une obligation de citation et de référencement lors de l'utilisation de ce document.

D'autre part, toute contrefaçon, plagiat, reproduction illicite encourt une poursuite pénale.

Contact : [ddoc-theses-contact@univ-lorraine.fr](mailto:ddoc-theses-contact@univ-lorraine.fr)

## LIENS

Code de la Propriété Intellectuelle. articles L 122. 4

Code de la Propriété Intellectuelle. articles L 335.2- L 335.10

[http://www.cfcopies.com/V2/leg/leg\\_droi.php](http://www.cfcopies.com/V2/leg/leg_droi.php)

<http://www.culture.gouv.fr/culture/infos-pratiques/droits/protection.htm>

# Université de Lorraine

## Laboratoire d'Ingénierie des Biomolécules

### École Doctorale Sciences et Ingénierie des Ressources Naturelles

## THÈSE

Présentée et soutenue publiquement pour l'obtention du titre de

## DOCTEUR DE L'UNIVERSITÉ DE LORRAINE

Mention : « **Génie Biotechnologique et Alimentaire** »

Par

**Kamil ELKHOURY**

---

## Nanofunctionalization and biofabrication of natural hydrogels for tissue engineering applications

---

**Le 19 Février 2021**

Devant le jury d'examen composé de :

<b>Aldo Boccaccini</b>	Professor, University of Erlangen-Nuremberg, Germany	Rapporteur
<b>Eliana Souto</b>	Professor, University of Coimbra, Portugal	Rapporteuse
<b>Wojciech Swieszkowski</b>	Professor, Warsaw University of Technology, Poland	Examinateur
<b>Ali Tamayol</b>	Associate Professor, University of Connecticut, USA	Examinateur
<b>Frances Yen Potin</b>	Directrice de recherche, Université de Lorraine, France	Examinatrice
<b>Elmira Arab-Tehrany</b>	Professor, Université de Lorraine, France	Directrice
<b>Laura Sanchez-Gonzalez</b>	MCF, Université de Lorraine, France	Co-directrice



# Acknowledgments

This thesis was carried out at the LIBio lab (ENSAIA, Nancy, France), during which two international research mobilities were conducted at Shin lab (Harvard Medical School, Brigham and Women's Hospital, Cambridge, MA, USA) and at COMPASS lab (Aveiro Institute of Materials, Aveiro, Portugal).

First of all, I would like to thank **Elmira** very much for giving me this amazing opportunity! Thank you for supporting and guiding me all along, for never failing to motivate me with every single meeting we had, for trusting me with big decisions, and for providing me with the best opportunities that improved me immensely not only as a researcher but also as a person.

Je tiens également à remercier vivement **Laura**, merci d'avoir accepté de codiriger cette thèse et de trouver des solutions chaque fois que je suis venu te voir avec des problèmes.

I would like to thank Prof. **Aldo Boccaccini** and Prof. **Eliana Souto** for accepting the invitation to judge this work as rapporteurs. I would also like to thank Prof. **Wojciech Swieszkowski**, Dr. **Ali Tamayol**, and Dr. **Frances Yen Potin** for agreeing to take part in this jury as examiners.

Je tiens à remercier le ministère de l'Enseignement Supérieur, de la Recherche et de l'Innovation (MESRI) pour le financement de cette thèse et l'initiative de la Lorraine University of Excellence (LUE) pour le financement de ma mobilité vers les États-Unis dans le cadre du programme de mobilité internationale DrEAM.

Je remercie tous les personnels du LIBio avec qui j'ai partagé ces années de thèse, spécialement mes collègues/amis de bureau : **Auréli**e, **Aldjia**, **Sarah** et **Mahmoud**. Un grand merci à **Cyril** pour ses nombreux conseils et ses encouragements tout au long de ce projet. Je tiens à remercier aussi tous mes stagiaires : **Yasmina**, **Maria**, **Lynda**, **Auréli**e et **Alicia** pour leur contribution à l'avancement de ce projet.

I would like to thank Dr. **Su Ryon Shin** for welcoming me to her lab at Harvard University. I would also like to thank my dear friends that I met during this mobility, especially **Maggie**, **Polen**, **Mo**, and my **Mexican Familia**.

I would like to thank Prof. **João Mano** for welcoming me to his lab at the University of Aveiro. I would also like to thank my dear friends that I met during this mobility, especially **Pedro**, **Paulo**, and **Luis**.

I would like to also thank all my friends in Lebanon and the ones I met in France for the greatest moments we spent together, especially **Julie**, **Pia**, **Mariam**, **Ziad**, **Hamzeh**, **Amal**, **Elio**, **Christelle**, **Rami**, **Dalal**, **Sarah**, **Moussa**, **Narimane**, **Mayssa**, **Gracia**, **Jona**, **Elie**, and **Nicolas**.

Un très grand merci à mes meilleures amies **Nancy** et **Sarah** pour tous les moments de pur bonheur et pour leur support dans les moments difficiles.

A very big thank you to my best friends **Fawze** and **Firas** who despite the distance did not miss any opportunity to support and encourage me.

I would like to thank my family in Lebanon and all around the world, especially my uncle **Mahdi** for his big support and encouragement throughout my studies.

Finally, I want to thank very warmly my dear parents, **Khalil** and **Mahdia**, who have always been my source of motivation, support, and encouragement. Thank you for your love and for always being there for me. It is to you that I dedicate this thesis, hoping that you will always be proud of me.

# **Table of Contents**

<b>Acknowledgments .....</b>	<b>2</b>
<b>List of Publications and Communications .....</b>	<b>4</b>
<b>List of Abbreviations .....</b>	<b>6</b>
<b>Introduction &amp; Objectives .....</b>	<b>7</b>
<b>Chapter I: Literature Review .....</b>	<b>19</b>
Soft-Nanoparticle functionalization of Natural Hydrogels for Tissue Engineering Applications.....	23
Engineering Smart Targeting Nanovesicles and their Combination with Hydrogels for Controlled Drug Delivery .....	44
Biofabrication of Natural Hydrogels for Cardiac, Neural, and Bone Tissue Engineering Applications .....	69
<b>Chapter II: Evaluating Sources of GelMA Hydrogels .....</b>	<b>97</b>
Synthesis and characterization of C2C12-laden gelatin methacryloyl (GelMA) from marine and mammalian sources .....	101
<b>Chapter III: Nanofunctionalized GelMA Hydrogels .....</b>	<b>117</b>
Gelatin methacryloyl (GelMA) Nanocomposite Hydrogels embedding Bioactive Naringin Liposomes .....	121
<b>Chapter IV: Biofabricated GelMA Hydrogels .....</b>	<b>139</b>
Reprogramming exosome-liposome hybrid bioink.....	143
<b>Conclusion &amp; Perspectives.....</b>	<b>161</b>
<b>References.....</b>	<b>171</b>
<b>Abstract.....</b>	<b>212</b>
<b>Résumé.....</b>	<b>212</b>

# List of Publications and Communications

## Publications

1. **K. Elkhoury**, L. Sanchez-Gonzalez, P. Lavrador, R. Almeida, V. Gaspar, C. Kahn, F. Cleymand, E. Arab-Tehrany, J. F. Mano, Gelatin Methacrylate (GelMA) Nanocomposite Hydrogels embedding Bioactive Naringin Liposomes. *Polymers*. 12, 2944 (2020).
2. **K. Elkhoury**, P. Koçak, A. Kang, E. Arab-Tehrany, J. Ellis Ward, S. R. Shin, Engineering Smart Targeting Nanovesicles and Their Combination with Hydrogels for Controlled Drug Delivery. *Pharmaceutics*. 12, 849 (2020). **Highlighted on the Journal's Cover.**
3. E. Arab-Tehrany\*, **K. Elkhoury\***, G. Francius, L. Jierry, J. F. Mano, C. Kahn, M. Linder, Curcumin Loaded Nanoliposomes Localization by Nanoscale Characterization. *IJMS*. 21, 7276 (2020). **\*Co-first authors.**
4. M. Hasan, **K. Elkhoury**, N. Belhaj, C. Kahn, A. Tamayol, M. Barberi-Heyob, E. Arab-Tehrany, M. Linder, Growth-Inhibitory Effect of Chitosan-Coated Liposomes Encapsulating Curcumin on MCF-7 Breast Cancer Cells. *Mar. Drugs*. 18, 217 (2020).
5. J. Li, **K. Elkhoury**, C. Barbieux, M. Linder, S. Grandemange, A. Tamayol, G. Francius, E. Arab-Tehrany, Effects of Bioactive Marine-Derived Liposomes on Two Human Breast Cancer Cell Lines. *Mar. Drugs*. 18, 211 (2020).
6. R. Kadri, J. Bacharouch, **K. Elkhoury**, G. Ben Messaoud, C. Kahn, S. Desobry, M. Linder, A. Tamayol, G. Francius, J. F. Mano, L. Sánchez-González, E. Arab-Tehrany, Role of active nanoliposomes in the surface and bulk mechanical properties of hybrid hydrogels. *Mater. Today Bio*. 6, 100046 (2020).
7. A. Bianchi, É. Velot, H. Kempf, **K. Elkhoury**, L. Sanchez-Gonzalez, M. Linder, C. Kahn, E. Arab-Tehrany, Nanoliposomes from Agro-Resources as Promising Delivery Systems for Chondrocytes. *IJMS*. 21, 3436 (2020).
8. F. Cleymand, A. Poerio, A. Mamanov, **K. Elkhoury**, L. Ikhelf, J.P. Jehl, C. Kahn, M. Ponçot, E. Arab-Tehrany, J. F. Mano, Development of novel Chitosan / Guar Gum inks for extrusion-based 3D Bioprinting: Process, Printability and Properties. *Bioprinting*. 21, e00122 (2020).
9. **K. Elkhoury**, C. S. Russell, L. Sanchez-Gonzalez, A. Mostafavi, T. J. Williams, C. Kahn, N. A. Peppas, E. Arab-Tehrany, A. Tamayol, Soft-Nanoparticle Functionalization of Natural Hydrogels for Tissue Engineering Applications. *Adv. Healthcare Mater*. 8, 1900506 (2019).
10. M. Hasan, **K. Elkhoury**, C. J. F. Kahn, E. Arab-Tehrany, M. Linder, Preparation, Characterization, and Release Kinetics of Chitosan-Coated Nanoliposomes Encapsulating Curcumin in Simulated Environments. *Molecules*. 24, 2023 (2019).

## Submitted Manuscripts

11. **K. Elkhoury**, M. Morsink, L. Sanchez-Gonzalez, A. Tamayol, E. Arab-Tehrany, Biofabrication of Natural Hydrogels for Cardiac, Neural, and Bone Tissue Engineering Applications. *Bioactive Materials*.
12. **K. Elkhoury**, M. Morsink, Y. Tahri, C. Kahn, F. Cleymand, S. R. Shin, E. Arab-Tehrany, L. Sanchez-Gonzalez, Synthesis and characterization of C2C12-laden gelatin methacryloyl (GelMA) from marine and mammalian sources. *Int. J. Biol. Macromol*.
13. R. Kadri, **K. Elkhoury**, G. B. Messaoud, C. Kahn, A. Tamayol, J. F. Mano, L. Sanchez-Gonzalez, E. Arab-Tehrany, Physicochemical interactions in nanofunctionalized alginate /GelMA IPN hydrogels. *Molecules*.
14. M. Hasan, **K. Elkhoury**, N. Belhaj, S. Latifi, C. Kahn, M. Linder, E. Arab-Tehrany, Enhancing the anti-cancer activity of curcumin on MCF-7 cells through O/W nanoemulsions based on marine and plant lipids. *IJMS*.

## Manuscripts in preparation

15. **K. Elkhoury**, M. Chen, P. Koçak, E. Martinez, M. Urbina, L. Sanchez-Gonzalez, E. Arab-Tehrany, S. R. Shin, Reprogramming Exosome-liposome hybrid bioink.
16. E. Passeri\*, **K. Elkhoury\***, M. Morsink, K. Broersen, F. Yen Potin, E. Arab-Tehrany, Alzheimer's Disease treatment limitations and novel prevention strategies. \***Co-first authors**.

## Book chapters

1. **K. Elkhoury**, C. Kahn, L. Sanchez-Gonzalez, E. Arab-Tehrany, Soft Nanobiomaterials (Nanoliposomes) for Biomedical Applications. In *Soft Matter for Biomedical Applications*; H. Azevedo, Ed.; Royal Society of Chemistry: Cambridge.
2. L. Sanchez-Gonzalez, **K. Elkhoury**, C. Kahn, E. Arab-Tehrany, Composite Hydrogels of Pectin and Alginate. In *Plant and Algal Hydrogels for Drug Delivery and Regenerative Medicine*; Elsevier.
3. S. Hasan\*, **K. Elkhoury\***, A. Fattahi, S. R. Shin, Fabrication of Bioinspired and Biomimetic Devices. In *bioengineering technologies*; Springer US: New York, NY. \***Co-first authors**.

## Written Communications

- **K. Elkhoury**, L. Sanchez-Gonzalez, C. Kahn, E. Arab-Tehrany, Nanomechanical and Biological Properties of Nanofunctionalized Hybrid Hydrogels, *Nano Today*, 2019, Lisbon, Portugal.
- **K. Elkhoury**, L. Sanchez-Gonzalez, C. Kahn, E. Arab-Tehrany, J. F. Mano, Nanofunctionalized Natural Bioink for Bone Tissue Engineering, *Nano Today*, 2019, Lisbon, Portugal.

## Seminars

- **K. Elkhoury**, L. Sanchez-Gonzalez, E. Arab-Tehrany, The Nanofunctionalization of Natural Hydrogels for Tissue Engineering, *SIReNa annual seminar*, 2020, Nancy, France.
- **K. Elkhoury**, L. Sanchez-Gonzalez, E. Arab-Tehrany, Hydrogels for Tissue Engineering, *ENSAIA international seminar*, 2019, Nancy, France.
- **K. Elkhoury**, L. Sanchez-Gonzalez, E. Arab-Tehrany, Hydrogels for Biomedical Applications, *ENSAIA international seminar*, 2018, Nancy, France.

## Awards

- DrEAM International Mobility Grant, *Lorraine University of Excellence*, 2019.
- Student Travel Award, *Nano Today Conference*, Lisbon, Portugal, 2019.
- Best Poster Award, *Doctoriales de Lorraine*, Nancy, France, 2019.

# List of Abbreviations

<sup>1</sup> H NMR	Proton Nuclear Magnetic Resonance
2D	Two-dimensional
3D	Three-dimensional
ALP	Alkaline phosphatase activity
ANOVA	Analysis of Variance
AuNPs	Gold nanoparticles
BM	Basal culture medium
BMP	Bone morphogenetic protein
CAD	Computer-aided design
CFs	Cardiac fibroblasts
CNTs	Carbon nanotubes
CMs	Cardiomyocytes
Dex	Dexamethasone
DiO	3,3'-Diocadecyloxacarbocyanine perchlorate
DMEM	Dulbecco's Minimum Eagle Media
DPBS	Dulbecco's Phosphate Buffered Saline
DS	Degree of Substitution
DSC	Differential Scanning Calorimetry
DVS	Dynamic vapor sorption
ECM	Extracellular Matrix
EE	Encapsulation efficiency
ESCRT	Endosomal sorting complex required for transport
EPR	Enhanced permeability and retention
F1	Fish skin gelatin with addition of 1.25% methacrylic anhydride
F20	Fish skin gelatin with addition of 20% methacrylic anhydride
FBS	Fetal Bovine Serum
FDA	Food and Drug Administration
FRESH	Freeform reversible embedding of suspended hydrogels
FRET	Fluorescence resonance energy transfer
FTIR	Fourier Transform infrared spectroscopy
GAM	Gene-activated matrix
GelMA	Gelatin Methacryloyl
GO	Graphene oxide
HBSS	Hank's balanced salt solution
hASCs	Human adipose-derived mesenchymal/stromal stem cells
HUVEC	Human umbilical vein endothelial cells
MA	Methacrylic Anhydride
MMP	Matrix Metalloproteinase
P1	Porcine skin gelatin with addition of 1.25% methacrylic anhydride
P20	Porcine skin gelatin with addition of 20% methacrylic anhydride
PDI	Polydispersity index
PI	Photoinitiator (2-hydroxy-4'-(2-hydroxyethoxy)-2-methylpropiophenone)
RGD	Arginine-glycine-aspartic acid
rGO	reduced GO
RH	Relative humidity
RT-PCR	Reverse Transcriptase Polymerase Chain Reaction
SEM	Scanning electron microscopy
TEM	Transmission electron microscopy
Td	Degradation Temperature
Tg	Transition Temperature
TGA	Thermal Gravimetric Analysis
Tm	Melting Temperature
TNBS	2,4,6-trinitrobenzene-sulfonic acid

# **Introduction & Objectives**



Tissue engineering is an interdisciplinary field that applies both the principles of life sciences and engineering to develop biological substitutes or whole organs [1]. Beyond this initial goal, tissue engineered constructs have found new applications, such as research tools, that could improve our understanding and testing of disease. Hydrogels are materials with a high water content and one of the few biomaterials that can be used to make scaffolds mimicking the extracellular matrix (ECM). In addition to being highly biocompatible, hydrogels possess advantageous physical and biological tunability and desirable robustness in biofabrication. To avoid the potential risk of inflammatory and immunological responses from synthetic polymeric materials, naturally occurring crosslinked polymer networks are the preferred choice for the fabrication of ECM mimetic scaffolds [2].

Gelatin is one of the most popular biopolymers produced by partial hydrolysis of native collagen, which is a fibrous protein and the main constituent of the skin, bones, and connective tissue of animals. Due to its unique functional and technological properties, gelatin has been widely used for tissue engineering [3]. Gelatin contains abundant arginine-glycine-aspartic acid sequences which enhance cell attachment and contains matrix metalloproteinase target sequences which promote cell remodeling. Derived from denatured collagen, gelatin has excellent solubility, biodegradability, biocompatibility, low antigenicity, and a low gel point. However, certain limitations, such as its low mechanical modulus and rapid degradation, limit its use in biomedical applications. To overcome these drawbacks, gelatin methacryloyl (GelMA) is created by the chemical modification of gelatin, when methacrylate groups are added to side groups containing amines. This methacrylation reaction allows, in the presence of a photoinitiator, the UV light activated polymerization of the gelatin to a hydrogel stable at 37 °C [4].

The physicochemical properties of biomaterials and their biological activity affect the response of incorporated cells or tissues. The physical properties of natural hydrogels, including their mechanical and electrical properties, may differ from those observed in native tissues. In addition, the presence of various biological factors and proteins play a key role in the growth and maturation of modified tissue-like constructs. There are various ways of modulating the physical and biological properties of the environment of natural hydrogels; this includes the creation of fibers and composite constructions, the formation of double or multiple interpenetrating polymer networks, and the incorporation of nano / micro-features. These strategies have been used for the modulation of mechanical and electrical properties at the cellular or tissue level, providing topography to guide cell morphology and growth, as well as the slow release of various growth factors [3].

Among the various strategies, the incorporation of nanoparticles has attracted attention due to their high surface-to-volume ratio, ease of administration, and ability to target cellular

components rather than an entire cell or tissue [5]. Additionally, the use of nanoscale particles enables a bottom-up approach to engineering the hydrogel niche. Nanoparticles can generally be classified as hard and soft nanoparticles. Hard nanoparticles are generally referred to as those whose compression modulus is significantly different from the value of natural hydrogels. Hard nanoparticles can be made from materials such as silica and gold, quantum dots, carbon nanotubes, graphene sheets, and polymer nanoparticles. While soft nanoparticles with mechanical properties comparable to hydrogels include liposomes, exosomes, dendrimers, polymeric micelles and nanogels.

Hard nanoparticles have various intrinsic functionalities, very ordered structures, and are generally stable during circulation and storage. On the contrary, they can cause an undesirable inflammatory disease and can induce toxicity when accumulated in different tissues. Another major concern associated with the use of inorganic hard nanoparticles is their carcinogenicity. On the other hand, the soft nanoparticles exhibit properties of non-conductive insulating type associated with covalent, flexible, and organic-type structures and assemblies. In addition, these nanoparticles are generally biodegradable and are considered to be more biocompatible compared to their hard inorganic counterparts. Thus, in biomedical applications, in particular in tissue engineering, the use of soft organic nanoparticles must be prioritized.

Furthermore, one of the main challenges in bioengineering and nanomedicine is how to formulate biomaterials and nanoparticles that selectively deliver encapsulated therapeutic agents to specific cells or tissues, when the enhanced permeability and retention (EPR) effect is ineffective [6]. Liposomes have been studied for more than five decades and have become a well-established drug delivery vesicle, which has resulted in the marketing authorization of many liposome products clinically approved to treat different diseases [7]. The resemblance of liposomes to biomembranes allows for superior biocompatibility and safety over other polymeric and metal-based nanoparticles. However, liposomes require surface modification with ligands to acquire smart targeting abilities. On the other hand, some natural nanovesicles, such as exosomes, already have these targeting capabilities [8]. In addition, exosomes are produced by cells, which means they possess an even higher level of biocompatibility and lower immunogenicity than liposomes. However, exosomes have limitations in terms of efficient and reproducible loading with drugs or bioactive agents. To solve this problem, while equipping liposomes with intelligent tissue and cell targeting behavior, hybrid delivery systems of fused liposomes and exosomes have been created [9–12]. The combination of these two types of nanovesicles into a single hybrid nanovesicle will preserve the beneficial characteristics of these two complementary systems and allow the engineering of an improved drug delivery targeting system.

However, even with all these advancements and although new types of tissues and organoids are being developed and manufactured, there are still many challenges to overcome before fully functional tissues can be created [13]. One of the main challenges is to create load-bearing structures capable of mimicking the complex architecture and physical properties of native ECM. These types of structures cannot be manufactured only using conventional techniques, such as solvent casting / particle leaching, freeze drying and gas foaming, but require advanced biofabrication techniques, such as bioprinting and textile based techniques. Biofabricated textiles can form more solid support structures, while bioprinted constructions have more complex and controlled architectures [14]. These advances in biofabrication techniques have led to various novel applications in tissue engineering, from creating electroactive scaffolds, that modulate cell proliferation and differentiation, to smart scaffolds, that sustain the dynamic nature of the tissue's microenvironment, which have opened doors to immense developments in cardiac, neural, and bone tissue engineering [15–17].

Even though the field of bioprinting is still in its infancy, it has been successfully used to create functional living three-dimensional (3D) human constructs with mechanical and biological properties suitable for transplantation. Bioprinting technology can be used to 3D print almost all types of biomaterials into scaffolds and patient-specific tissues with tailored morphological, physical, and biological properties. Despite the wide range of advantages bioprinting present there still exists the inherent need for vast improvements and advancements in bioprinter technologies and processes.

Currently, most of the available hydrogel-based bioink materials lack the native characteristics present in native tissues and organs that exhibit a heterocellular architecture. A high concentration of hydrogels used in bioinks will result in high viscosity, this favors mechanical and structural integrity and allows for the bioprinting of complex shapes. However, at the same time, these bioinks will not support cell viability and proliferation. The solution here can be the use of small concentrations of nanofunctionalized hydrogels possessing improved mechanical properties in a bioink formulation.

This thesis therefore aims to formulate a soft-nanofunctionalized GelMA bioink that can be used to bioprint functional 3D scaffolds for various applications in tissue engineering. The manuscript is organized as follows:

In the first chapter, the effect of nanofunctionalization with soft nanoparticles on the physicochemical and biological properties of natural hydrogels is presented. Next, the formation of smart targeting soft nanoparticles that can be incorporated into natural hydrogels to create sustained and controlled drug delivery systems is discussed. Finally, the novel biofabrication methods used to create complex 3D structures using natural hydrogels for applications in cardiac, neural and bone tissue engineering are highlighted.

In the second chapter, the physicochemical (structural, thermal, water uptake, swelling, rheological, and mechanical) and biological (cell viability, proliferation, and spreading) properties of porcine and fish GelMA are compared. C2C12 mouse myoblasts were encapsulated in low and high methacrylation porcine GelMA hydrogels and, for the first time, in low and high methacrylation fish GelMA hydrogels, to determine their biocompatibility, as well as their potential use as skeletal muscle tissue engineering scaffolds in future studies.

In the third chapter, the formulation of an all-natural bioactive nanocomposite hydrogel comprising building blocks of salmon-derived nanoliposomes loaded with naringin and incorporated into the GelMA hydrogel network is presented. First, the optimization of the manufacturing parameters and the physicochemical characterization of blank and naringin-loaded liposomes were carried out. Subsequently, the encapsulation efficiency, *in vitro* release, and biocompatibility of the encapsulated naringin were evaluated. In addition to the loaded-liposomes' dispersion in the GelMA matrix, their effect on the swelling behavior and the surface, rheological, mechanical properties of the GelMA matrix was investigated.

In the fourth chapter, the physicochemical and biological characterization of a nanofunctionalized GelMA bioink with hybrid exosome-liposome nanoparticles was presented. This developed hybrid bioink has been used to successfully bioprint 3D cardiac patches and to directly reprogram cardiac fibroblasts into cardiomyocytes.

Finally, a general conclusion of the acquired knowledge and carried out experiments during this thesis, as well as the future perspectives concerning this work and the potential translation of the invented nanofunctionalized and biofabricated GelMA platform are discussed.

L'ingénierie tissulaire est un domaine interdisciplinaire appliquant les principes de la biologie et de l'ingénierie pour développer des substituts biologiques ou des organes entiers [1]. Au-delà de cet objectif initial, les constructions issues de l'ingénierie tissulaire ont trouvé de nouvelles applications, telles que le développement d'outils de recherche, qui pourraient améliorer notre compréhension des maladies. Les hydrogels sont des matériaux à forte teneur en eau et constituent l'un des rares biomatériaux pouvant être utilisés pour fabriquer des échafaudages imitant la matrice extracellulaire (MEC). En plus d'être hautement biocompatibles, les hydrogels possèdent des propriétés physique et biologique ajustables et une résistance recherchée pour des applications en biofabrication. Pour éviter le risque potentiel de réactions inflammatoires et immunologiques des matériaux polymères synthétiques, les réseaux de polymères réticulés naturels sont le choix préféré pour la fabrication d'échafaudages mimétiques de MEC [2].

La gélatine est l'un des biopolymères les plus utilisés, ce composé est obtenu par hydrolyse partielle du collagène natif, qui est une protéine fibreuse et le principal constituant de la peau, des os et du tissu conjonctif des animaux. En raison de ses propriétés fonctionnelles et technologiques uniques, la gélatine a été largement utilisée pour des applications en ingénierie tissulaire [3]. La gélatine contient de nombreuses séquences de type arginine-glycine-acide aspartique qui améliorent la fixation des cellules ainsi que des séquences cible d'une métalloprotéinase matricielle qui favorisent le remodelage des cellules. Dérivée du collagène dénaturé, la gélatine présente une excellente solubilité, biodégradabilité, biocompatibilité, une faible antigénicité et un point de gélification bas. Cependant, certaines limitations, telles que son faible module mécanique et sa dégradation rapide, limitent son utilisation dans les applications biomédicales. Pour pallier ces inconvénients, la gélatine méthacrylate (GelMA) est produite par modification chimique de la gélatine, lorsque des groupements méthacrylate sont fixés sur des groupes latéraux contenant des fonctions amine. Cette réaction de méthacrylation permet, en présence d'un photoinitiateur, la polymérisation de la gélatine sous rayonnement UV. L'hydrogel de GelMA ainsi obtenu est stable à 37°C [4].

Les propriétés physicochimiques des biomatériaux et leur activité biologique modifient la réponse des cellules ou des tissus incorporés dans la matrice biocompatible. Les propriétés physiques des hydrogels naturels, y compris leurs propriétés mécaniques et électriques, peuvent différer de celles observées dans les tissus natifs. En outre, la présence de divers facteurs biologiques et protéines joue un rôle clé dans la croissance et la maturation des constructions tissulaires modifiées. Il existe différentes façons de moduler les propriétés physiques et biologiques de l'environnement des hydrogels naturels ; cela inclut la création de fibres et de constructions composites, la formation de réseaux de polymères à double ou multiple interpénétration et l'incorporation de nano-/micro-caractéristiques. Ces stratégies ont été

utilisées pour l'ajustement des propriétés mécaniques et électriques au niveau cellulaire ou tissulaire, fournissant une topographie pour guider la morphologie et la croissance des cellules, ainsi que la libération lente de divers facteurs de croissance [3].

Parmi les différentes stratégies, l'incorporation de nanoparticules attire l'attention en raison des caractéristiques de ces particules (rapport surface-volume élevé, facilité d'administration et capacité à cibler des composants cellulaires plutôt qu'une cellule ou un tissu entier) [5]. De plus, l'utilisation de nanoparticules permet une approche ascendante pour concevoir les hydrogels. Les nanoparticules peuvent être classées en deux catégories, les nanoparticules dures et molles. En général, les nanoparticules dures correspondent à celles dont le module de compression est significativement différent de celui des hydrogels naturels. Les nanoparticules dures peuvent être fabriquées à partir de matériaux tels que la silice et l'or, les points quantiques, les nanotubes de carbone, les feuilles de graphène et les nanoparticules à base de polymères. Alors que les nanoparticules molles ayant des propriétés mécaniques comparables à celles des hydrogels regroupent notamment les liposomes, les exosomes, les dendrimères, les micelles polymères et les nanogels.

Les nanoparticules dures présentent diverses fonctions intrinsèques, il s'agit de structures très ordonnées, et sont généralement stables pendant la circulation et le stockage. Elles peuvent cependant provoquer une réaction inflammatoire indésirable et induire une toxicité lorsqu'elles sont accumulées dans différents tissus. Une autre préoccupation majeure associée à l'utilisation de nanoparticules dures inorganiques est leur cancérogénicité. Les nanoparticules molles présentent quant à elles des propriétés de type isolant non conducteur, associées à des structures et des assemblages de type covalent, flexible et organique. En outre, ces nanoparticules sont généralement biodégradables et sont considérées comme plus biocompatibles que leurs homologues inorganiques durs. Ainsi, dans les applications biomédicales, en particulier en ingénierie tissulaire, l'utilisation de nanoparticules organiques douces doit être privilégiée.

De plus, un des principaux défis de la bioingénierie et de la nanomédecine est de savoir comment formuler des biomatériaux et des nanoparticules qui délivrent sélectivement des agents thérapeutiques encapsulés à des cellules ou des tissus spécifiques, lorsque la perméabilité accrue et la rétention effet (RPE) est inefficace [6]. Les liposomes ont été étudiés pendant plus de cinq décennies et sont devenus une vésicule d'administration de médicaments bien établie, ce qui a permis d'obtenir l'autorisation de mise sur le marché de nombreux produits à base de liposomes cliniquement approuvés pour traiter différentes maladies [7]. La ressemblance des liposomes avec les biomembranes permet une biocompatibilité et une sécurité supérieures à celles d'autres nanoparticules de type polymériques et métalliques. Cependant, les liposomes nécessitent une modification de surface avec des ligands pour acquérir des capacités de ciblage intelligent. En parallèle, certaines nanovésicules naturelles, telles que les exosomes, possèdent

déjà ces capacités de ciblage [8]. En outre, les exosomes sont produits par des cellules, ce qui signifie qu'ils possèdent un niveau de biocompatibilité encore plus élevé et une immunogénicité plus faible que les liposomes. Cependant, les exosomes présentent des limites en termes de chargement efficace et reproductible de médicaments ou d'agents bioactifs. Pour résoudre ce problème, tout en dotant les liposomes d'un comportement intelligent de ciblage des tissus et des cellules, des systèmes de livraison hybrides de type liposome-exosome fusionnés ont été créés [9–12]. La combinaison de ces deux types de nanovésicules en une seule nanovésicule hybride permettra de préserver les caractéristiques bénéfiques de ces deux systèmes complémentaires et de mettre au point un système amélioré de ciblage de l'administration des médicaments.

Cependant, malgré tous ces progrès et bien que de nouveaux types de tissus et d'organoïdes soient développés et fabriqués, il reste de nombreux défis à relever avant de pouvoir créer des tissus pleinement fonctionnels [13]. L'un des principaux défis consiste à créer des supports capables d'imiter l'architecture complexe et les propriétés physiques des MEC natives. Ce type de structures ne peut pas être fabriqué uniquement à l'aide de techniques conventionnelles, telles que le coulage avec solvant / la lixiviation particulière, la lyophilisation et le moussage, mais nécessite des techniques de biofabrication avancées, telles que la bioimpression et les techniques à base de textile. Les textiles biofabriqués peuvent former des matrices de support plus solides, tandis que les constructions bioimprimées présentent des architectures plus complexes et contrôlées [14]. Les progrès dans les techniques de biofabrication ont conduit à diverses nouvelles applications en ingénierie tissulaire, allant de la création d'échafaudages électroactifs qui modulent la prolifération et la différenciation des cellules, aux échafaudages intelligents qui soutiennent la nature dynamique du microenvironnement du tissu et qui ont ouvert la voie à d'immenses avancées en ingénierie des tissus cardiaques, neuronaux et osseux [15–17].

Même si le domaine de la bioimpression n'en est qu'à ses débuts, cette technique a été utilisée avec succès pour créer des constructions humaines fonctionnelles en trois dimensions (3D) avec des propriétés mécaniques et biologiques adaptées à la transplantation. La technologie de la bioimpression peut être utilisée pour imprimer en 3D presque tous les types de biomatériaux en échafaudages et en tissus spécifiques au patient avec des propriétés morphologiques, physiques et biologiques adaptées. Malgré le large éventail d'avantages que présente la bioimpression, il existe toujours un besoin inhérent d'améliorations et de progrès considérables dans les technologies et les processus de bioimpression.

Actuellement, la plupart des matériaux de bioencres à base d'hydrogel disponibles n'ont pas les caractéristiques natives des tissus et des organes présentant une architecture hétérocellulaire. Une concentration élevée en hydrogel utilisée dans les bioencres se traduit par

une viscosité élevée, ce qui favorise l'intégrité mécanique et structurelle et permet la bioimpression de formes complexes. Cependant, en même temps, ces bioencres ne favoriseront pas la viabilité et la prolifération des cellules. La solution ici peut être la formulation de bioencre à partir de faibles concentrations en hydrogels nanofonctionnalisés possédant des propriétés mécaniques améliorées.

L'objectif principal de cette thèse est donc de formuler une bioencre à base de GelMA nanofonctionnalisée à l'aide de particules molles pour des applications en ingénierie tissulaire et notamment adaptée pour une technologie de type bioimpression d'échafaudages 3D fonctionnels. Le manuscrit est organisé comme suit :

Dans le premier chapitre, l'effet de la nanofonctionnalisation avec des nanoparticules molles sur les propriétés physicochimiques et biologiques des hydrogels naturels est présentée. L'élaboration de nanoparticules molles conçues pour permettre un ciblage et un relargage contrôlé dans les hydrogels naturels utilisés en tant que systèmes d'administration de médicaments d'intérêt est ensuite abordée. Enfin, les nouvelles méthodes de biofabrication utilisées pour créer des structures 3D complexes à l'aide d'hydrogels naturels pour des applications en ingénierie des tissus cardiaques, neuraux et osseux sont détaillées.

Dans le deuxième chapitre, les propriétés physicochimiques (structurelles, thermiques, d'absorption d'eau, de gonflement, rhéologiques et mécaniques) et biologiques (viabilité cellulaire, prolifération et propagation) d'hydrogels à base de GelMA non fonctionnalisés sont étudiées. L'influence de la source de gélatine utilisée et du degré de méthacrylation sur les propriétés physicochimiques et biologiques des hydrogels est déterminée. Concernant les propriétés biologiques, des myoblastes de souris C2C12 ont été encapsulés dans les hydrogels afin de déterminer leur biocompatibilité, et d'analyser leur potentiel en ingénierie tissulaire pour des applications en tant qu'échafaudage pour l'ingénierie des tissus musculaires squelettiques.

Le troisième chapitre présente la formulation d'un hydrogel entièrement naturel à base de GelMA fonctionnalisé par des nanoparticules molles de type nanoliposomes de source marine (saumon) chargés de naringine. Dans un premier temps, l'optimisation des paramètres de fabrication et la caractérisation physico-chimique des liposomes vides et chargés de naringine ont été réalisées. Ensuite, l'efficacité de l'encapsulation, la libération *in vitro* et la biocompatibilité de la naringine encapsulée ont été évaluées. De plus, la répartition des liposomes chargés dans la matrice de type GelMA a été étudiée ainsi que l'effet de l'incorporation de ces particules sur les propriétés de gonflement, de surface, rhéologiques et mécaniques de la matrice polymérique.

Dans le quatrième chapitre, la caractérisation physicochimique et biologique d'une bioencre formulée à partir de GelMA nanofonctionnalisée avec des nanoparticules molles hybrides de type exosome-liposome a été présentée. Cette bioencre hybride développée a été

utilisée avec succès pour bioimprimer des patchs cardiaques 3D et pour reprogrammer directement les fibroblastes cardiaques dans les cardiomyocytes.

Enfin, une conclusion générale aborde les expériences menées au cours de cette thèse, les connaissances acquises, ainsi que les perspectives futures concernant ce travail et le potentiel de ce support à base de GelMA nanofonctionnalisée et biofabriquée est discuté.



# **Chapter I:**

## **Literature Review**

**K. Elkhoury**, C. S. Russell, L. Sanchez-Gonzalez, A. Mostafavi, T. J. Williams, C. Kahn, N. A. Peppas, E. Arab-Tehrany, A. Tamayol, Soft-Nanoparticle Functionalization of Natural Hydrogels for Tissue Engineering Applications. *Adv. Healthcare Mater.* 8, 1900506 (2019).

**K. Elkhoury**, P. Koçak, A. Kang, E. Arab-Tehrany, J. Ellis Ward, S. R. Shin, Engineering Smart Targeting Nanovesicles and Their Combination with Hydrogels for Controlled Drug Delivery. *Pharmaceutics.* 12, 849 (2020). **Highlighted on the Journal's Cover.**

**K. Elkhoury**, M. Morsink, L. Sanchez-Gonzalez, A. Tamayol, E. Arab-Tehrany, Biofabrication of Natural Hydrogels for Cardiac, Neural, and Bone Tissue Engineering Applications. *Submitted to Bioactive Materials.*



In the first chapter of this thesis, an up to date overview of current research on the nanofunctionalization and biofabrication of natural hydrogels is presented. In a first review published in *Advanced Healthcare Materials* the nanofunctionalization of natural hydrogels with soft nanoparticles are highlighted. In addition, the impact of the incorporation of soft nanoparticles in the hydrogel's matrix is discussed. In a second review published in *Pharmaceutics* and highlighted on its cover, the generation of smart targeting hybrid nanovesicles by the membrane fusion between exosomes and liposomes is overviewed. Moreover, the nanofunctionalization of natural hydrogels using these nanovesicles and their impact on their release behavior and administration routes are discussed. In a third review submitted to *Bioactive Materials*, the various biofabrication techniques, such as 3D bioprinting and textile techniques, that can be used to create organized and robust tissue constructs from naturally-derived hydrogels are reviewed. The progress, advantages, and shortcomings of the emerging biofabrication techniques are also highlighted, along with the novel applications of biofabricated natural hydrogels in cardiac, neural, and bone tissue engineering.

Dans le premier chapitre de cette thèse, un aperçu des recherches actuelles sur la nanofonctionnalisation et la biofabrication d'hydrogels naturels est présenté. Dans une première revue publiée dans le journal *Advanced Healthcare Materials*, la nanofonctionnalisation des hydrogels naturels avec des nanoparticules molles est détaillée. De plus, l'influence de l'incorporation de nanoparticules molles dans la matrice de type hydrogel sur ses propriétés est discutée. Dans une deuxième revue publiée dans le journal *Pharmaceutics* et mise en évidence sur la page de couverture, la génération de nanovésicules hybrides intelligentes obtenues par la fusion de membranes entre les exosomes et les liposomes est présentée. En outre, la nanofonctionnalisation des hydrogels naturels utilisant ces nanovésicules et leur impact sur leur comportement de libération et leurs voies d'administration sont discutés. Dans une troisième et dernière revue soumise pour publication dans le journal *Bioactive Materials*, les différentes techniques de biofabrication, telles que la bioimpression 3D et les techniques textiles, qui peuvent être utilisées pour créer des constructions tissulaires organisées et robustes à partir d'hydrogels d'origine naturelle sont passées en revue. Les progrès, les avantages et les inconvénients des nouvelles techniques de biofabrication sont discutés, ainsi que les nouvelles applications des hydrogels naturels biofabriqués en ingénierie des tissus cardiaques, neuronaux et osseux.



**ADVANCED HEALTHCARE MATERIALS***Review***Soft-Nanoparticle functionalization of Natural Hydrogels for Tissue Engineering Applications**

Kamil Elkhoury<sup>1</sup>, Carina Russell<sup>2</sup>, Laura Sanchez-Gonzalez<sup>1</sup>, Azadeh Mostafavi<sup>2</sup>, Tyrell Williams<sup>2</sup>, Cyril Kahn<sup>1</sup>, Nicholas A. Peppas<sup>3</sup>, Elmira Arab-Tehrany<sup>1</sup>, Ali Tamayol<sup>2</sup>

<sup>1</sup> LIBio, University of Lorraine, F-54000 Nancy, France.

<sup>2</sup> Department of Mechanical and Materials Engineering, University of Nebraska, Lincoln, NE, 68508, USA.

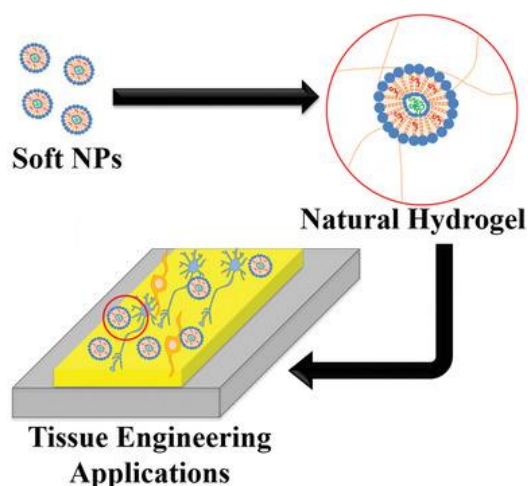
<sup>3</sup> Mary and Dick Holland Regenerative Medicine Program, University of Nebraska-Medical Center, Omaha, NE, 68198.

<sup>4</sup> Departments of Biomedical and Chemical Engineering, Departments of Pediatrics and Surgery, Dell Medical School, University of Texas at Austin, Austin, TX, 78712, USA.

Received: 18 April 2019; Accepted: 6 June 2019; Published: 12 August 2019

**Abstract**

Tissue engineering has emerged as an important research area that provides numerous research tools for the fabrication of biologically functional constructs that can be used in drug discovery, disease modeling, and the treatment of diseased or injured organs. From a materials point of view, scaffolds have become an important part of tissue engineering activities and are usually used to form an environment supporting cellular growth, differentiation, and maturation. Among various materials used as scaffolds, hydrogels based on natural polymers are considered one of the most suitable groups of materials for creating tissue engineering scaffolds. Natural hydrogels, however, do not always provide the physicochemical and biological characteristics and properties required for optimal cell growth. In this review, we discuss the structure and properties of widely used natural hydrogels. In addition, we present methods of modulation of their physicochemical and biological properties using soft nanoparticles as fillers or reinforcing agents.



**Keywords:** Nanofunctionalization; Natural Hydrogels; Soft nanoparticles; Tissue engineering.

## 1. Introduction

Tissue engineered constructs have now found various new applications, which are beyond the initial goal of their use for replacing damaged or diseased tissues. Tissue engineered constructs are emerging as research tools that could improve our understanding of biological processes [18–20] and pathophysiology of diseases [21,22]. In addition, the use of patient-specific cells and biological factors is expected to facilitate the development of personalized therapies [23–25].

More complex, yet functional tissues or organoids can be fabricated by combining the advances in biology, on-chip technologies, biomanufacturing, biomaterials, and drug delivery [26–32]. Despite recent progress, there are still many challenges that remain to be addressed [33–37]. For example, the formation of a niche that supports cellular growth, differentiation, and function is still the subject of many research studies. The natural extracellular environment is comprised of a highly defined microarchitecture formed from various proteins, polysaccharides, and glycosaminoglycans; resulting in modulation of cell-level and tissue-level physical and chemical properties [38–40].

The presence of a cocktail of factors affecting biological processes at different stages of tissue development and maturation combined with proper oxygenation, as well as nutrient transport result in the development and function of different tissues and organs in the human body.[41,42] As discussed extensively by Clegg *et al.* mimicking these properties in engineered tissue constructs, although desirable, is not trivial.[43]

To facilitate the formation of functional tissues, advanced biomaterials with controlled physical, chemical, biological, and electrical properties should be designed.[19,44–47] Hydrogels are one of the few biomaterials that possess properties required for tissue engineering applications [42,48]. Hydrogels are crosslinked three-dimensional (3D) hydrophilic polymer networks, which form matrices with a high water content of up to a thousand times their dry weight [49]. They possess tunable physical and biological properties, native extracellular matrix (ECM) similarity, high biocompatibility, and robustness in biofabrication [31,50,51]. With these combined characteristics, hydrogels are excellent candidates for biomedical applications [52–54], drug delivery [55–58], as well as tissue engineering and regenerative medicine [50,59–61].

Nonetheless, the majority of existing hydrogels cannot properly mimic all the physical, chemical, and biological properties of native ECM at the same time. Thus, the idea of developing hybrid and composite systems in which nano/micro-features are incorporated to modulate some of these properties have drawn noticeable attention [19]. Soft and hard nanoparticles can be incorporated as fillers in the hydrogel matrix, to yield nanofunctionalized hydrogels with tailored properties [62,63]. Here, we review hybrid and composite hydrogel

systems produced from natural polymers that are functionalized with soft nanoparticles. We initially discuss the properties of different types of natural hydrogels. The effects of soft nanoparticles on the physical and biological properties of natural hydrogels will also be highlighted. The challenges and potential opportunities in the field are also outlined.

## 2. Hydrogels from Natural Polymers

Hydrogels are formed from natural or synthetic polymers or their mixtures. Each of the two classes offers a set of advantages and disadvantages, listed in **Table 1**. In this section, we briefly introduce some of the natural hydrogels frequently used in tissue engineering. The readers are referred to several reviews for a more comprehensive overview of natural hydrogels [64–69,3].

**Table 1.** Advantages and disadvantages of using natural or synthetic polymers for the preparation of hydrogels [70,71].

	Natural Hydrogels	Synthetic Hydrogels
<b>Advantages</b>	<ul style="list-style-type: none"> <li>• Non-toxic</li> <li>• Biocompatible</li> <li>• Biodegradable</li> <li>• Promote cells adhesion</li> <li>• Promote cells growth</li> <li>• Promote cells proliferation</li> <li>• Promote cells differentiation</li> <li>• Promote cells ECM secretion</li> </ul>	<ul style="list-style-type: none"> <li>• Controllable microstructure</li> <li>• Controllable degradation</li> <li>• Long shelf life</li> <li>• Tailored functionality</li> <li>• Strong mechanical properties</li> <li>• Wide varieties of raw chemical resources</li> </ul>
<b>Disadvantages</b>	<ul style="list-style-type: none"> <li>• Low mechanical strength</li> <li>• Batch variation</li> <li>• Risk of disease transmission (ECM-based hydrogel)</li> </ul>	<ul style="list-style-type: none"> <li>• Low biocompatibility</li> <li>• Risk of inflammatory response</li> <li>• Risk of immunological response</li> </ul>

### 2.1 Polysaccharide-based hydrogels

Polysaccharides are carbohydrate polymers which can break into physiological breakdown upon degradation. Polysaccharides are biocompatible, usually degradable, and possess tunable mechanical properties. In addition, polysaccharides are a major constituent of native ECM. Thus, hydrogels formed from different polysaccharides have been widely used in tissue engineering, regenerative medicine, and drug delivery. The most common polysaccharide-based hydrogels that have been utilized for tissue engineering scaffolds are alginate [72], chitosan [73], hyaluronic acid [74], and cellulose [75]. Although, hydrogels formed from other polysaccharides such as chitin, gellan gum, etc. have also been utilized for tissue engineering applications [76,77].

In a recent study, alginate was used to carry platelet-rich plasma (PRP) that can release a cocktail of biological factors essential for tissue healing and growth (**Figure 1d, e**). The utilized

hydrogels could facilitate vascularization and stem cell migration. In addition, the fabrication of an interpenetrating network of polymers from alginate and a protein-based hydrogel with cell binding sequences has also been shown to significantly improve the biological activity of the hydrogels (**Figure 1a-c**). Key reasons for the popularity of alginate-based hydrogels in tissue engineering applications are its stability, ease-of-handle, and fast crosslinking process.

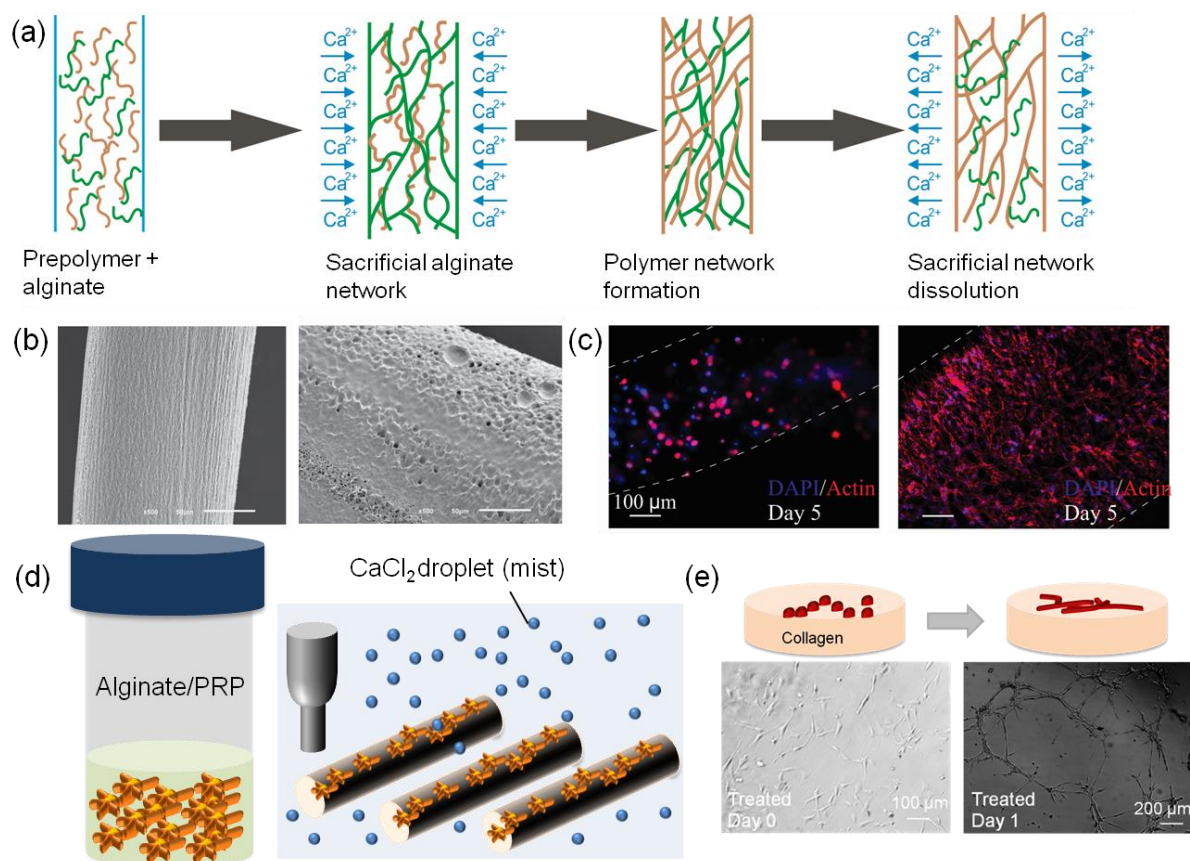


**Figure 1.** Alginate-based hydrogels in tissue engineering applications. (a) The use of alginate for engineering IPN hydrogels with various materials or its use as a sacrificial network for creating fibers from polymers and protein-based hydrogels. (b) SEM image of IPN fibers of GelMA and alginate (left) and the removal of alginate from the construct to fabricate pure GelMA fibers (right). (c) Cellular morphology shown by F-actin staining in IPN fibers of GelMA and alginate (left) and GelMA fibers after the removal alginate from the network (right). Reproduced with permission [78]. Copyright 2015, John Wiley and Sons. (d) The use of alginate for carrying PRP as a source of biological factors in tissue engineering. The hydrogel fibers could be printed in the presence of  $\text{CaCl}_2$  mist on dry substrates. (e) The effect of PRP encapsulated in alginate in releasing angiogenic factors facilitating vascularization. Reproduced with permission [23]. Copyright 2018, John Wiley and Sons.

## 2.2 Protein-based hydrogels

Proteins are a major constituent of ECM and they are responsible for the biological and mechanical characteristics of native tissues. Collagen by far is the most abundant protein in the human body. However, other proteins such as fibronectin, elastin, and laminin are also found in noticeable quantities in specific tissues. It is now widely accepted that the composition and physical properties of the environment significantly affect cellular fate and function. Thus, to mimic the native ECM, many research studies have focused on engineering scaffolds from

various proteins or a combination of them in ECM. In comparison to different natural protein-based hydrogels, those that are formed from collagen or its denatured form (gelatin) have been extremely popular in tissue engineering [3,79]. Fibronectin-, elastin-, laminin-based hydrogels have also been utilized in tissue engineering. Each of these hydrogels offers unique and interesting properties, which make them suitable for engineering specific tissues.

In one study, the effect of hydrogel composition on the growth pattern of endothelial cells was studied (**Figure 2a-d**) [80]. In this study, fractal-like dense cultures of endothelial cells with different dimensions were generated and covered by a layer of hydrogel. The results showed a distinct growth and migration pattern within the fabricated protein-based hydrogels. In that study, only hydrogels formed from Type I collagen could support the formation of vessel-like structures. Fibronectin-based gels have also shown superior support in the growth of endothelial cells and are being utilized for engineering constructs which require rapid vascularization [81]. In another noticeable example, an elastin-based hydrogel was extremely resilient against mechanical stretch and torsion (**Figure 2e,f**) [82]. As the presence of each protein is expected to affect the function of cells, efforts have been made to utilize the whole ECM to form hydrogels.

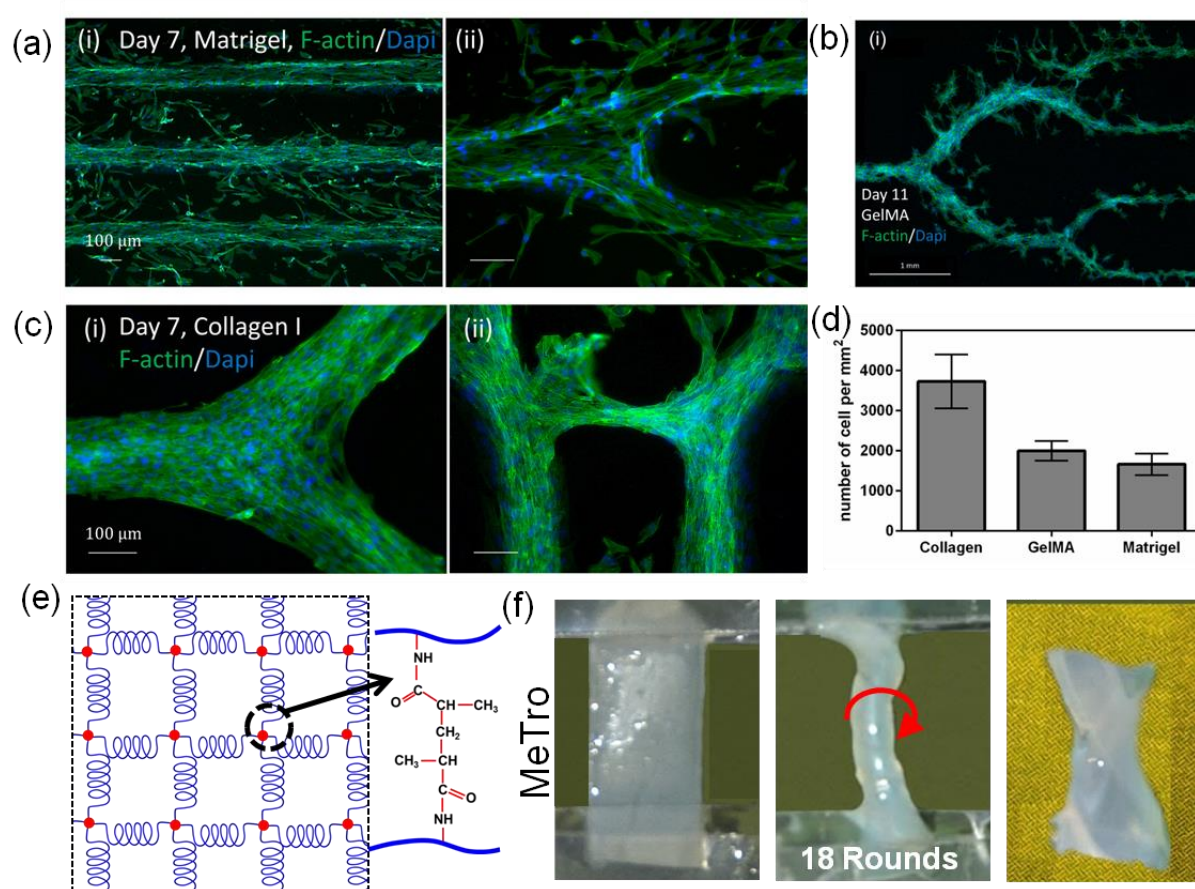


**Figure 2.** Protein-based hydrogels as scaffolding materials for tissue engineering. (a-c) The growth of endothelial cells cultured in vascular-like organizations in different protein-based hydrogels including Matrigel (a), GelMA (b), Collagen (c). The patterns of cellular migration into the hydrogel constructs were fundamentally different. Among them, only collagen supported the formation of tubular sprouts.

Reproduced with permission [80]. Copyright 2016, John Wiley and Sons. (d) The density of cells within the original patterns was also dependent on the material. (e,f) The fabrication of highly elastic hydrogel networks from photocrosslinkable methacrylated tropoelastin (MeTro). The fabricated hydrogel showed excellent torsional resilience. Reproduced with permission [82]. Copyright 2015, John Wiley and Sons.

While hydrogels offer high porosity, favorable transport properties, and tunable mechanical properties, they do have various limitations affecting the possibility of creating a tissue biomimetic environment. For example, hydrogel systems lack factors that can initiate or facilitate physiological and biological processes crucial for tissue formation and maturation. Thus, modulating their properties to become more biomimetic has been the subject of numerous research. Engineering nanocomposite hydrogels with the use of suitable nanomaterials have shown to be effective in addressing these challenges and will be discussed in the following sections.

### 3. Nanofunctionalized Hydrogels

The physicochemical properties of biomaterials and their biological activity affect the response of cells or tissues embedded within or interfaced with them. The physical properties of natural hydrogels including their mechanical and electrical properties can deviate from those observed in native tissues. In addition, the presence of various biological factors and proteins play a key role in the growth and maturation of the engineered tissue-like constructs. There have been various ways for modulating the physical and biological properties of the environment of natural hydrogels; this includes creating composite fibers and constructs, forming double or multiple interpenetrating polymer networks [83], and incorporation of nano/micro-features. These strategies have been used for modulation of the mechanical and electrical properties at the cellular or tissue level providing topography for guiding cellular morphology and growth, as well as the slow release of various growth factors [3].

Among different strategies, the incorporation of nanoparticles has drawn conspicuous attention due to their high surface-area-to-volume ratio, ease-of-delivery, and the ability to target cellular components rather than an entire cell or tissue [5]. Additionally, the use of nanoscale particles enables a bottom-up approach for engineering the hydrogel niche. For example, similar to the formation of reinforced bricks from mud and straw, nanoparticle incorporation in the hydrogel matrix will strengthen and reinforce the hydrogel structure, while adding new functionalities.

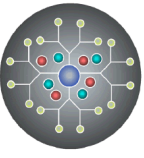
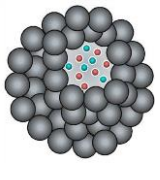
These properties have led to the widespread use of nanoparticles of various biomaterials in biomedical applications, such as controlled drug and gene delivery [84], tissue engineering and regenerative medicine [85], biosensors [86,87], bioimaging [88], and bioseparation [89].

Nanoparticles can be generally classified as hard and soft nanoparticles [90]. Hard nanoparticles typically are referred to those with a compressive modulus that is significantly

different from the value for natural hydrogels. Hard nanoparticles can be fabricated from materials such as silica and gold, quantum dots, carbon nanotubes, graphene sheets, and polymeric nanoparticles. Whereas soft nanoparticles with mechanical properties comparable to hydrogels include liposomes, dendrimers, polymeric micelles, and nanogels [91–93].

Hard nanoparticles possess various intrinsic functionalities, highly ordered structures, and are usually stable during their circulation and storage. On the contrary, they can cause an adverse inflammatory response and can induce toxicity upon their accumulation in different tissues [94,95]. Another major concern associated with the use of inorganic hard nanoparticles has been their carcinogenicity. On the other hand, soft nanoparticles (**Table 2**) manifest non-conducting, insulator-type properties associated with covalent, flexible, organic-like structures and assemblies [90]. Moreover, these nanoparticles are typically biodegradable and are considered more biocompatible in comparison to their hard inorganic counterparts. Thus, in biomedical applications especially in tissue engineering, the use of soft organic nanoparticles should be prioritized. In this review, we mainly focus on soft nanoparticles and how they can modulate various properties of natural hydrogels. A number of reviews on the use of hard nanoparticles in tissue engineering and drug delivery have recently been published [19,96].

**Table 2.** Comparing the characteristics of four soft nanoparticles: nanoliposomes, dendrimers, polymeric micelles, and nanogels. Images reproduced with permission [97,98].

Type	Nanoliposomes	Dendrimers	Polymeric Micelles	Nanogels
				
Nature	Natural	Synthetic	Synthetic	Natural Synthetic
Size	~50 nm	2-15 nm	10-100 nm	<100 nm
Preparation methods	Microfluidization Extrusion Sonication	Convergent Divergent	Direct dissolution Film casting Dialysis Oil in water emulsion	Physical self-assembly of interactive polymers Chemical synthesis in colloidal environments Chemical crosslinking of preformed polymers Template-assisted nanofabrication
Adv.	Biocompatible Biodegradable Non-toxic Non-immunogenic Controlled and targeted drug delivery Sustained release Increase drug efficacy and stability Many administration routes	Biodegradable Very small size Well-defined and flexible structure Precise controllability High deformability Stimuli-responsiveness Surface functionality	Small size Narrow distribution Easy sterilization High structural stability Low toxicity Excellent blood stability High water solubility Controlled release functions	Biocompatible Large surface area Stimuli sensitivity High water content/swellability and hydrophilicity Tunable nanoparticle size Site targeting Controllable release Increased drug stability

<b>Disadv.</b>	Low solubility Short half-life High production cost Difficult sterilization Lysosomal degradation Low efficacy active targeting	Low biocompatibility Significant liver accumulation Material's homogeneity deterioration Great batch-to-batch variability	Low biocompatibility Difficult synthesis Difficult to scale-up Limited choice of monomers Concerns over nanotoxicity and storage stability	Challenging optimization of degradation mechanism, biodistribution, and component toxicity Drug instability and rapid degradation in the bloodstream
<b>REF.</b>	[99–101]	[102,103]	[99,104–106]	[98,107,108]

### 3.1 Nanoliposomes

Liposomes are continuous, closed, and round-shaped vesicles formed from one or several phospholipid bilayers dispersed in an aqueous medium [109]. Phospholipids are amphiphilic molecules, composed of a hydrophobic lipid soluble tail segment and a hydrophilic water-soluble head segment. Liposomes have been widely used in drug and gene delivery [110–113], and in tissue engineering [114,115]. Liposomes with submicron sizes are called nanoliposomes. They are around 50-200 nm in size and are extensively used for the encapsulation and controlled release systems of bioactive agents in the food, cosmetic, and pharmaceutical industries [116–118,101]. Nanoliposomes are natural soft nanoparticles, biocompatible, biodegradable, easy-to-fabricate, easy-to-decorate, and possess low toxicity [119–121]. Nanoliposomes can be prepared by sonication, extrusion, or microfluidization method [100,101,122]. Nanoliposomes provide more surface area than liposomes and have the potential to significantly improve the controlled release, enhanced bioavailability, increased solubility, and enabled precision targeting of the encapsulated material [101]. Being amphiphilic, nanoliposomes are able to increase the in vivo and in vitro stability of hydrophobic drugs or molecules by embedding them in the lipid bilayer or encapsulating them in the central aqueous cavity [120,123].

### 3.2 Dendrimers

Medical and pharmaceutical properties of the various star and star-shaped polymers have attracted considerable attention by researchers interested in the development of various polymeric systems with architectures other than linear systems. Polymeric systems with such architectures include ladder, star, and comb polymers, which have some degree of a three-dimensional character. Star and star-shaped polymers are molecules of hyperbranched structures that emanate from a central core and consist of a large number of terminal groups with a definite geometrical growth.

Dendrimers are highly branched and symmetrical polymeric molecules composed of numerous perfectly branched monomers that originate from a central core [124]. A dendrimer molecule is composed of an interior core, several layers composed of repeating units called dendrons, and multiple active terminal groups [125]. Dendrimers are generally synthesized by the divergent and convergent methods (**Figure 4a, b**). In the first approach, synthesis is initiated

at the center of the star polymer, whereas in the second approach, synthesis starts in the outside of the dendrimer.

Dendrimers are widely used in the biomedical field, especially in nanomedicine because it is possible to control their molecular weight and chemical composition [102,124]. Thereby, it is possible to control their polyvalency properties, biocompatibility, bioactivity, and pharmacokinetics. Dendrimers provide the ability to develop drug-loaded biomaterials by simple functionalization of their external groups, and increase the efficiency of drug loading or increase electrostatic interaction with the anionic bioactive agent [126]. Moreover, they provide sustained drug release, and the ability to enhance the solubility of hydrophobic drugs. Polyamidoamine (PAMAM) dendrimers, the most common class of dendrimers, were used for bioimaging [127], as drugs [128], drug carriers [129], and gene carriers [130]. Polypeptide and polyester dendrimers were used as scaffolds for tissue repair [131,132], as well as drug carriers [133,134].

### 3.3 Polymeric micelles

Polymeric micelles are self-assemblies (10-200 nm in diameter) of amphiphilic polymers (hydrophobic core and hydrophilic shell) in an aqueous environment with remarkable therapeutic potential. They are formed through self-assembly into a core-shell micellar structure (hydrophilic shell and hydrophobic core) of block copolymers comprising two or more polymeric chains with different hydrophobicity [135]. These polymers are chemically different and covalently attached to each other. Since one of the polymers is hydrophobic and the other is hydrophilic, when they are present in an aqueous solution, many unfavorable interactions between the hydrophobic polymer and water molecules will occur. Thus, at a specific and narrow concentration range of amphiphilic polymers in aqueous solution, called the critical micelle concentration, the amphiphilic block copolymers will self-assemble into colloidal-sized particles or micelles. Resulting in the removal of the hydrophobic polymer from solution.

Preparation methods for drug-loaded polymeric micelles are dependent on the solubility of the copolymer being used. Direct dissolution or film casting methods may be employed if the copolymer is relatively water soluble, whereas dialysis method or oil in water emulsion procedure may be employed if the copolymer is not readily soluble in water [136]. On account of their small size, controlled release of drugs, aqueous solubility enhancement of carried drugs, and simple sterilization; polymeric micelles are an ideal carrier for hydrophobic drugs [137].

### 3.4 Nanogels

Nanogels are nanometer-sized (<100 nm) crosslinked colloidal particles that may also respond to environmental changes (pH, temperature, ionic strength, presence of molecules or ions, light) and to external fields (magnetic and electric) by changing their volume significantly

[107]. Nanogels can be chemically crosslinked using covalent bonds or physically crosslinked using non-covalent bonds [138–140]. This response can be used to control the release of encapsulated bioactive compounds such as drugs, proteins, DNA, and RNA [138]. Nanogel preparation methods can be divided into four categories: template-assisted nanofabrication of nanogel particles, polymerization of monomers in homogeneous or heterogeneous environments, physical self-assembly of interactive polymers, and chemical crosslinking of preformed polymers [141]. Due to their encapsulation stability, biocompatibility, water solubility, control of drug release rate, and reduction of toxicity; nanogels have been used in drug delivery as drug delivery vehicles [142] and in tissue engineering as scaffolds [143–145].

In general, among all soft nanoparticles, nanoliposomes offer superior biocompatibility, ease of surface modification, favorable pharmacokinetic profile, and long circulation time [146]. However, liposomes suffer from the disadvantages of fast elimination from the blood and the capture by the cells of the reticuloendothelial system [147]. On the other hand, polymeric nanoparticles (dendrimers, micelles, and nanogels) are superior in terms of controlled release capability, versatile drug loading, improved stability in biological fluids, desired pharmacokinetics, and high cellular internalization efficiency [148].

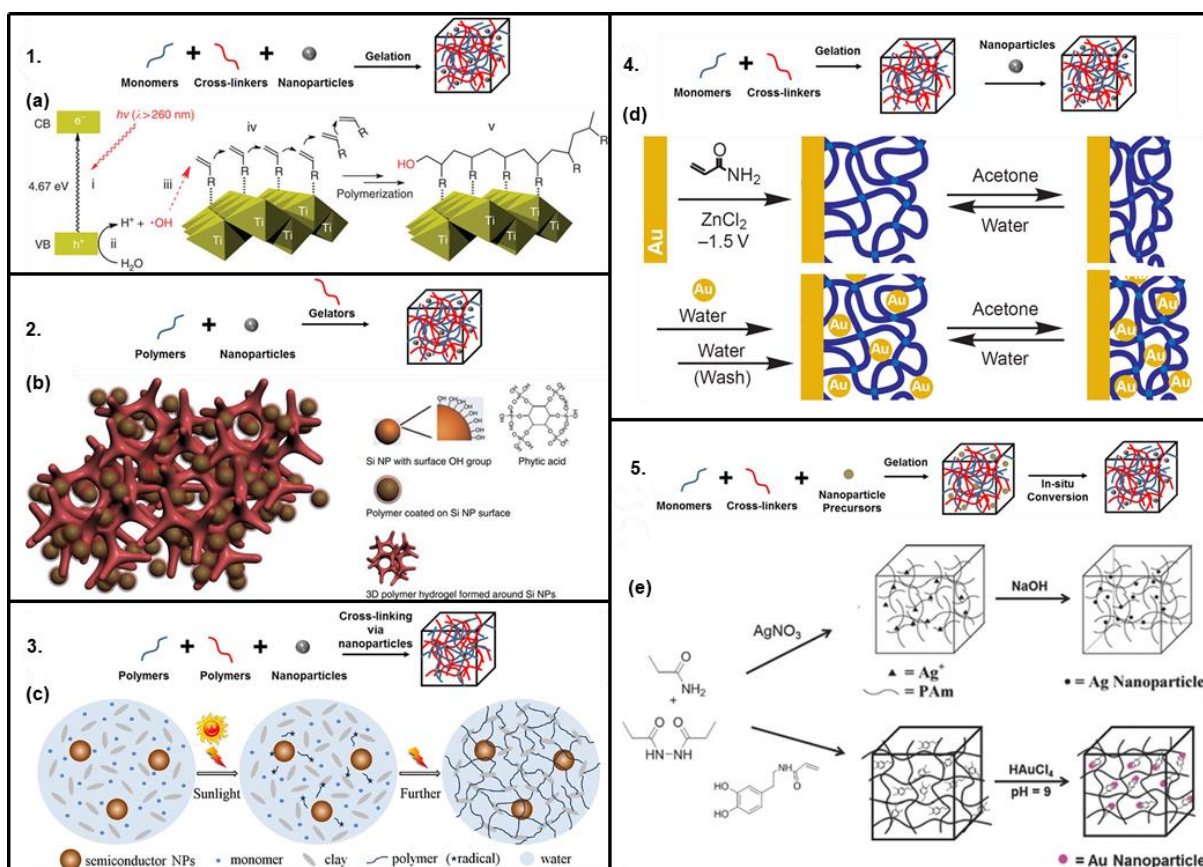


**Figure 3.** Five main nanofunctionalization techniques with their relative examples. Adapted with permission [63]. Copyright 2015, Wiley-VCH): 1. hydrogel formation in a nanoparticle suspension, 2. gel formation using nanoparticles, polymers, and distinct gelator molecules, 3. cross-linking using nanoparticles to form hydrogels, 4. physical incorporation after gelation of nanoparticles into the hydrogel matrix, and 5. formation of reactive nanoparticle within a preformed gel. (a) Schematic of the

usage of the photo catalyst, titania nano sheets, for gelation. Reproduced with permission [149]. (b) Schematic illustration of 3D porous silicon-nanoparticles/conductive polymer hydrogel. Reproduced with permission [150]. (c) Cross-linking using semiconductor nanoparticles, monomer, and clay nanostructure to form nanoparticle-hydrogel composites with enhanced mechanical properties. Reproduced with permission [151]. (d) The switch between its swollen and shrunken states resulting in the construction of a gold-nanoparticle/hydrogel composite. Reproduced with permission [152]. (e) Preparation of Ag/PAAm hydrogel composite without using thiols. Reproduced with permission [153]. Hydrogel nanofunctionalization with gold nanoparticles resulting in catalytic hydrogels. Reproduced with permission [154]. Copyright 2014, American Chemical Society.

Overall, different techniques, presented in **Figure 3**, can be used to incorporate nanoparticles into the hydrogel matrix and they can be divided into 5 groups [63]. Even though the examples presented are for hard nanoparticles, the same techniques can be used to incorporate soft nanoparticles.

- 1) The gelation of a hydrogel-forming monomer solution, in which pre-formed nanoparticles are suspended, is the easiest method. However, if the crosslink density is low, the risk of the leaching nanoparticles out of the hydrogel matrix may exist [155,156]. Liu *et al.* synthesized photo-modulable thermo-responsive hydrogels using unilamellar titania nanosheets as photocatalytic crosslinkers (**Figure 3a**) [149].
- 2) Distinct gelator molecules can be used to crosslink polymers incorporating nanoparticles into a hydrogel matrix. This method has been used to create 3D porous silicon nanoparticles/conductive polymer hydrogel composite electrodes by encapsulating the silicon nanoparticles within a conductive polymer surface coating and connecting them to a highly porous hydrogel framework (**Figure 3b**) [150].
- 3) Crosslinking groups present on the nanoparticle surface can be used to form a hydrogel matrix [157]. One recent example of this approach is the synthesis, by Zhang *et al.*, of semiconductor nanoparticle-based hydrogels by self-initiated polymerization using light irradiation (**Figure 3c**) [151]. Semiconductor nanoparticles were used here to initiate monomer polymerization under sunlight and to crosslink it to form nanocomposite hydrogels with the help of clay nanosheets.
- 4) Physical incorporation of nanoparticles can occur after the polymerization formation of the hydrogel. The physical incorporation can be achieved by either the “breathing” method or by centrifugation/thermal annealing method. The “breathing” consists of placing the swollen hydrogel into a solvent which causes it to get rid of entrapped water and shrink, then in an aqueous solution containing nanoparticles where it causes the hydrogel to swell and “breath in” the nanoparticles. Even with extra “breathing out” cycles the nanoparticles concentration in the hydrogel remains intact due to physical entanglement and to hydrogen bond interactions. This method was used to construct a gold-nanoparticle/hydrogel composite at the electrode interface (**Figure 3d**) [152]. The other approach consists on incorporating the

nanoparticles into the hydrogel matrix by repeated heating, centrifugation and re-dispersion followed by annealing. This was used by Jones and Lyon to co-assemble poly-*N*-isopropylacrylamide hydrogel particles and nanosized colloidal Au into colloidal crystals [158].

- 5) In-situ formation of nanoparticles, in which nanoparticle precursors can be loaded into the matrix before gelation, followed by nanoparticles formation supported by the hydrogel network, was developed by Langer's group [159]. This method produces mechanically strong composite hydrogels without an external reducing agent. Saravanan *et al.* used this method to synthesize silver nanoparticles containing polyacrylamide hydrogel composites by free-radical cross-linking polymerization of acrylamide monomer in an aqueous medium containing Ag<sup>+</sup> ions (**Figure 3e**) [153]. In a more recent example, Marcelo *et al.* used redox active catechol side chain in acrylamide-NIPAAm hydrogels to produce gold nanoparticles from precursors already incorporated and in the absence of any external reducing agent (**Figure 3e**) [154].

#### 4. Properties of Soft Nanoparticle-Functionalized Hydrogels

The effectiveness of the scaffolds in tissue engineering applications depends on how closely they can mimic native tissues. It has been shown that physical properties (mechanical and electrical), chemical composition, pore size distribution, and biological activity affect cellular growth, alignment, differentiation, and function. On the contrary, some natural hydrogels resembling the structure and in some cases the composition of native ECM fail to offer suitable mechanical and electrical properties, both at cellular and tissue levels. In addition, biological factors essential for cellular functions including phenotyping, differentiation, and maturation are typically not available in natural hydrogels. The incorporation of soft nanoparticles is a promising method for modulating the properties of scaffolds made of natural hydrogels, inherently affecting the response of incorporated cells. As the evaluation of biomaterial biocompatibility/biological response continues to be a challenge [160], the use of biocompatible soft nanoparticles is favored in comparison to their hard counterparts. In this section, we highlight how the incorporation of soft nanoparticles within natural hydrogels can improve the physical and biological outcome for various tissue engineering applications.

##### 4.1 Hydrogels with modulated physical properties

Physical specifications of hydrogel constructs, such as mechanical properties and electric conductivity, play a vital role in maintaining their 3D architecture, in mechanical interaction with cells, and in inducing cell-to-cell signaling [14]. Providing high tensile strength to the fragile hydrogels while mimicking the electrical stimulations that occur naturally in the body, is extremely important when engineering load-bearing or electrophysiologically active tissues

[161]. While imitating the electrical conductivity in tissues remains work in progress, functionalizing hydrogels to reinforce their soft structures to mimic the elastic moduli of native tissues is essential. The elastic modulus of bone has been found to be directly correlated to specimen size, however, it has been previously reported that trabecular and cortical bone have an averaged modulus around 4.59 and 5.44 GPa, respectively [162]. In comparison, muscle and connective tissue can range on average from 12 – 134 kPa [163]. Myocardial tissue also has a wide range of elastic modulus, which is dependent on the beginning and end of diastole; ranging from tens of kPa to several hundred [164]. More recently, dynamic loading was used to determine the shear and bulk modulus of soft tissues: liver (37 – 340 kPa, 0.28 GPa), heart (60 – 148 kPa, 0.49 GPa), stomach (8 – 45 kPa, 0.48 GPa), and lung (10 – 54 kPa, 0.15 GPa) [165]. Physical properties can be improved with the incorporation of predominantly hard nanoparticles within the hydrogel network [166], however, there are a few examples that have demonstrated changes in mechanical properties of hydrogel constructs with the incorporation of soft nanoparticles.

For example, Xiao *et al.* created an amphiphilic block copolymer that self-assembled into micelles of 21 nm diameter and incorporated them in poly(acrylamide) hydrogels [167]. By varying the block copolymer micelle concentration, the mechanical properties of these highly elastomeric block copolymer micelle crosslinked hydrogels were able to be controlled. The increase in micelle concentration from 7.5 to 15 mg.mL<sup>-1</sup> achieved a 4-fold increase in Young's modulus and a 2-fold increase in tensile stress.

Soft nanoparticles can interact with the polymer chains or can help with the further crosslinking of the hydrogel network to improve its mechanical properties. In one study, Duan and Sheardown used polypropyleneimine octaamine dendrimers to crosslink a highly concentrated collagen solution (2–4%) using the water-soluble carbodiimide EDC [168]. When compared with the natural human cornea, as well as EDC and glutaraldehyde cross-linked collagen, the dendrimer crosslinked collagen showed better optical transparency, mechanical properties, adhesion ability, and glucose permeability. This was due to an increase in free amine groups that react with activated carboxylic acid groups to crosslink the collagen hydrogel. The presence of dendrimers did not adversely affect the biocompatibility of the gels, which was confirmed by the *in vitro* culture of human corneal epithelial cells on dendrimer cross-linked collagen gels. Human corneal epithelial cell growth and adhesion were supported in these dendrimer crosslinked collagen gels with no cell toxicity; implying that they might be suitable scaffolds for corneal tissue engineering.

Rahali *et al.* functionalized GelMA hydrogels with naturally derived nanoliposomes and reported that the incorporation of nanoliposomes enhanced the mechanical stability of the functionalized GelMA hydrogels; proven by their higher resistance to twist and shear [169].

Similarly, it was also demonstrated that the incorporation of nanoliposomes within alginate/GelMA hydrogels affected the rheological properties of the formed hydrogels, as well as their mechanical properties [170]. This observation was related to the ability of the alginate-gelatin mixture to tune the mechanical properties of refined architectures.

Overall, modulating the physical properties of hydrogels is important in optimizing the cellular response. The incorporation of soft nanoparticles can moderately modulate the local and global mechanical properties; however, they are generally electrically non-conductive and cannot positively affect global conductivity. Despite their moderate effects in comparison to hard inorganic particles; soft nanoparticles offer better biocompatibility, along with superior drug transportation abilities, and factors further assisting the modulation of the cellular environment.

#### *4.2 Hydrogels with enhanced availability of biological factors and drugs*

It is very important for tissue engineering scaffolds to possess strong mechanical properties similar to native tissues, a well-defined 3D microstructure with interconnected pores, and a suitable biodegradability rate. Another key factor is the presence of biological factors within the scaffolds to facilitate tissue regeneration and growth [171]. Be that as it may, usually natural hydrogels lack sufficient growth factors essential for cellular functions. To address this challenge, the field of drug delivery goes hand-in-hand with tissue engineering to design an ideal scaffold. Scaffolds have evolved from releasing single molecules within simple hydrogel systems to releasing multiple molecules in a sequential manner from advanced systems [172–176]. Many drug delivery and tissue engineering applications, summarized in **Table 3**, are based on soft nanoparticles. These nanoparticles have also been incorporated within hydrogels as carriers for controlled or on-demand release of necessary drugs and growth factors. As a result, scaffolds produced from hydrogels formed from natural polymers functionalized with natural soft nanoparticles are highly desirable.

The addition of bioactive molecules to biomaterial scaffolds, such as growth factors, can significantly enhance regenerative scaffolds [177]. However, larger pore sizes of natural hydrogels in comparison to the size of active compounds reduce their residence time within the hydrogel limiting their effectiveness. Thus, nanoparticles that can prolong the release time of active compounds could potentially overcome this challenge. Liposomes could be used as carriers for delivery systems by covalent conjugation of carboxyl groups of HA to amine groups of liposomes. This has the potential to increase the circulation time in the body and accumulation of encapsulated drugs in the intended site. Taetz *et al.* used conjugated liposome as a siRNA carrier to lung cancer cells [178]. Furthermore, one example of this involves a minimally invasive bone reconstruction system was created by Pederson *et al.*, which consisted

of a combination of calcium and phosphate-loaded liposomes with an acid-soluble collagen solution [179]. This liposome/collagen precursor fluid forms a mineralized collagen gel when heated from room temperature to body temperature (37 °C). Self-assembling collagen contained within a liposome-encompassing suspension was then shown to be integrated into an injectable mineral/collagen biomaterial. In another instance, Samadikuchaksaraei *et al.* employed nanoliposomes as the nucleation site for the synthesis of nano-hydroxyapatite particles under hydrothermal conditions [180]. A nano-hydroxyapatite/gelatin nanocomposite scaffold was conditioned with osteoblasts and showed an increase in biocompatibility, biodegradation, and osteoinduction. These findings suggest that this method can be used to develop a variety of bone tissue engineering scaffolds.

Ochi *et al.* introduced a new technique for tissue-engineered cartilage transplantation, illustrated in **Figure 4c**, with a minimally invasive procedure [181]. The novel scaffold was composed of a collagen hydrogel (Atelocollagen) embedded with human chondrocytes. The group also suggested that integrating magnetic liposomes for controlled release of cytokines or growth factors (FGF or TGF- $\alpha$ ) can ameliorate cell proliferation and ECM synthesis during cultivation. In this study, magnetic liposomes were successfully concentrated and maintained within the defect area to further improve the bioavailability of the incorporated factors.

Stem cells are able to generate mature cells of a particular tissue upon proper differentiation [182]. Transforming growth factor-beta 1, TGF- $\beta$ 1, is a mammalian protein that plays a role in stem cells differentiation [183], proliferation [184], and metabolic activities [185]. In one study, Dostert *et al.* tested the effect of TGF- $\beta$ 1 encapsulated in salmon-derived nanoliposomes on human mesenchymal stem cells (hMSCs) [186]. The group reported that TGF- $\beta$ 1 encapsulated in nanoliposomes had a higher impact on cellular proliferation in comparison to free TGF-  $\beta$ 1. In addition, the studied concentrations of nanoliposomes, free TGF- $\beta$ 1, and TGF- $\beta$ 1 encapsulated in nanoliposomes did not induce any inhibitory effects.

Nanogels-functionalized hydrogels have also been utilized as drug carriers. Cholesterol-bearing pullulan nanogel-crosslinking hydrogel (CHPA/hydrogel), prepared by Michael addition, were used as a scaffold to deliver low amounts of bone morphogenetic proteins (BMP), which stimulated osteoblasts and induced bone formation [172]. Fujioka-Kobayashi *et al.* used cholesteryl and acryloyl group-bearing pullulan (CHPOA) nanogels to prepare fast-degradable hydrogels (CHPOA/hydrogels) for the controlled delivery of two growth factors: recombinant human bone morphogenetic protein 2 (BMP2) and recombinant human fibroblast growth factor 18 (FGF18), as seen in **Figure 4d, e** [187]. This study concluded that the CHPOA/hydrogel system was able to efficiently deliver BMP2 and FGF18 to a bone defect site and induce effective bone repair, which suggests that this system can be successfully used for bone tissue engineering. Joo *et al.* created a novel formulation of a hybrid liposome-based hyaluronic acid-

chitosan nanogel using a self-assembly process [188]. This hydrogel was successfully used to encapsulate and release recombinant human bone morphogenetic protein 7 (BMP7), also known as osteogenic protein-1.

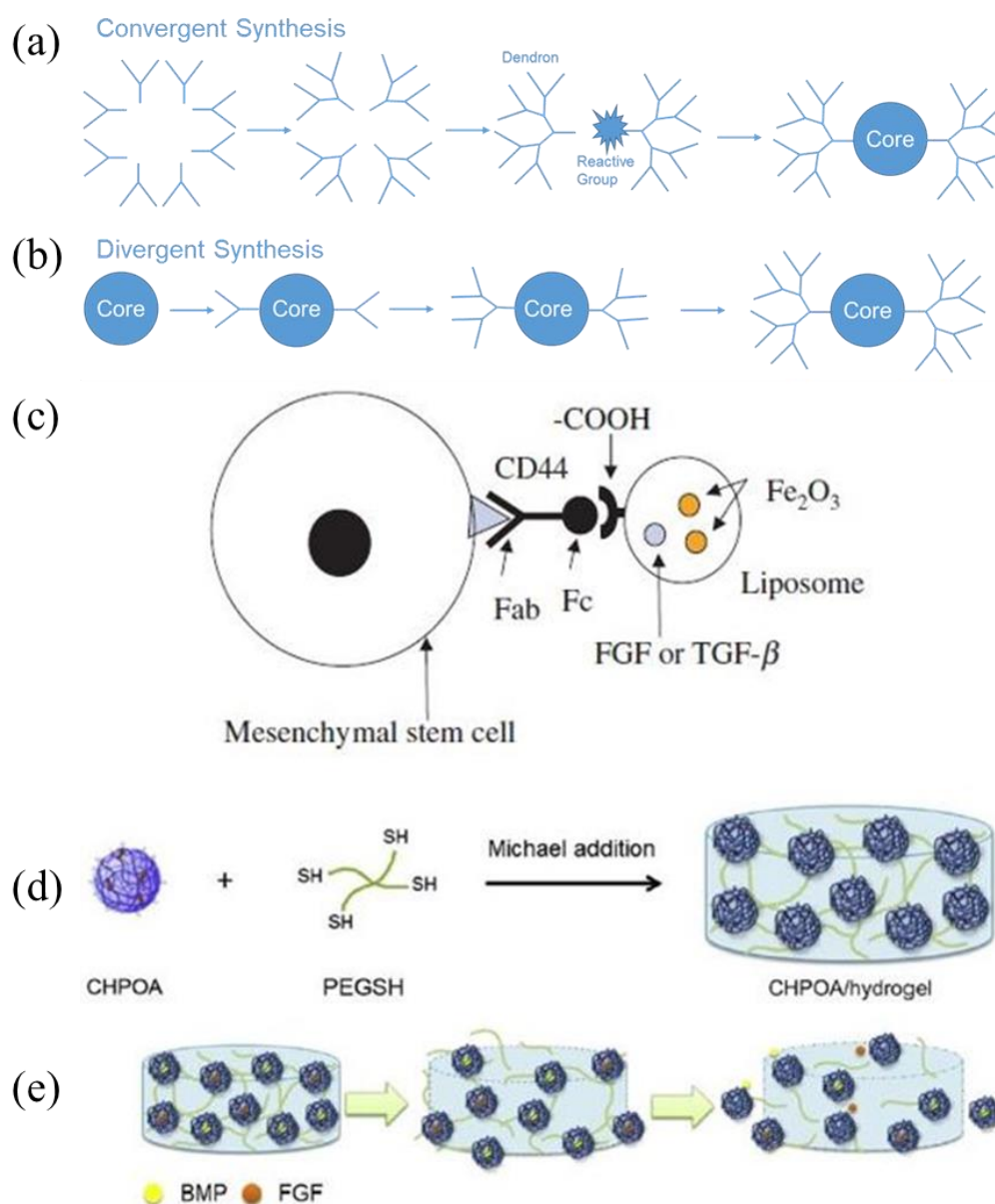


**Figure 4.** Scheme for (a) convergent and (b) divergent synthesis of dendrimers. (c) Schematic of autologous bone marrow mesenchymal stem cell–liposome complex. Reproduced with permission [181]. (d) Synthesis of the CHPOA/hydrogel block by Michael addition. (e) Schematic representation of nanogels releasing FGF18 and BMP2 after disintegration. Reproduced with permission [187]. Copyright 2009, American Chemical Society.

The addition of soft nanoparticles to natural hydrogels addresses the need for growth factors that natural hydrogels alone cannot provide. Tissue regeneration and growth are key concerns for current and future development of bioengineered scaffolds in bone, cartilage, and muscle tissues. Considering that it is essential for tissue-engineered scaffolds to mimic native tissues, the ability to have controlled the release of growth factors and drugs encapsulated in soft nanoparticles is pertinent.

### 4.3 Hydrogels with enhanced cell-cell signaling

Intercellular communication can occur via extracellular vesicles known as exosomes. They behave as a vectorized signaling method that originates within a donor cell and is received at the periphery, cytosol, or nucleus of a target cell [189]. Exosomes derived from stem cells provide an alternative approach to culturing cells *in vitro*. Scaffolds employing exosomes have the advantage of providing the extracellular signaling needed without the difficulty of retaining the multipotent properties of mesenchymal stem cell [190,191]. In one experiment, led by Liu *et al.*, exosomes were isolated from stem cells and integrated into a photoinduced imine crosslinking hydrogel glue [190]. The result was an acellular tissue patch used to regenerate articular cartilage. In another experiment, conducted by Shi *et al.*, exosomes were isolated from GMSCs and combined with a chitosan/silk hydrogel, for the treatment of diabetic ulcers in rat models [192]. Nonetheless, further research is still required on how these mechanisms work [193].

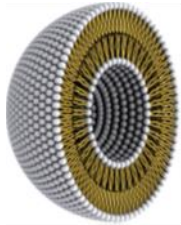
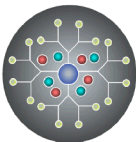
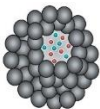
### 4.4 Scaffolds capable of gene and plasmid delivery

Biological factors can direct cellular growth, differentiation, and maturation. However, biological factors typically possess low half-lives and can get deactivated, both in the presence of other chemokines or cytokines. Nevertheless, recent advancements in biology have enabled cellular reprogramming through the use of plasmids and gene editing tools. Moreover, adverse side effects caused by the burst release of supraphysiological quantities of recombinant proteins can be prevented by the delivery of genes-encoding growth factors, rather than the protein itself. As soft nanoparticles possess excellent cell affinity and can be internalized once interfaced with cells, they have emerged as attractive tools for plasmid delivery and cell transfection.

Gene-activated matrix (GAM) is a gene transfer technology that also provides a structural template for cell proliferation and ECM synthesis. Peng *et al.* coupled this technology with soft nanoparticles to create a porous scaffold for periodontal tissue regeneration [194]. The GAM was composed of chitosan/plasmid DNA nanoparticles, encoding platelet-derived growth factors, embedded in a porous chitosan/collagen composite scaffold. This GAM was used to culture periodontal ligament cells, which achieved high proliferation, formed a periodontal connective tissue-like structure after 2 weeks, and maintained a fibroblast figure. In another study, Raftery *et al.* developed and optimized chitosan-pDNA nanoparticles that facilitated MSC transfection *via* incorporation into collagen-based scaffolds [195].

The incorporation of soft nanoparticles in many studies has shown that functionalized natural hydrogels offer the necessary biodegradability, biocompatibility and support native tissue proliferation. Consequently, soft nanofunctionalized hydrogels are the preferred choice for biomaterial scaffolds, that can perform enhanced functions of native ECM.

**Table 3.** Biomedical applications of functionalized natural hydrogels by soft nanoparticles. Images reproduced with permission [97,98].

Nanoparticle	Natural Hydrogel	Application	Properties	REF.
	Alginate	Bone tissue engineering siRNA delivery Protein delivery system	Physical Biological Biological	[196] [197] [198]
	Collagen	Cartilage tissue engineering Bone tissue engineering Wound healing	Biological Biological Biological	[181] [179] [199]
	Chitosan	Cancer	Biological	[200]
	Hyaluronic acid	Bone tissue engineering Ocular pathologies	Physical Physical	[180] [201]
	Collagen	Corneal tissue engineering Gene delivery system	Physical Biological	[168] [202]
	Hyaluronic acid	Cartilage tissue engineering	Physical	[203]
	Cholesterol-bearing pullulan	Bone tissue engineering	Biological	[187]
	Chitosan	Bone tissue engineering	Biological	[188]

## 5. Conclusions and Future Directions

Conventional and novel applications of tissue engineering require the design of scaffolds that are biocompatible and biodegradable, facilitate cellular growth and nutrient transport, and mimic the architecture and physical properties of native tissues [64]. The utilized biomaterial in the fabrication of scaffolds plays a key role in achieving this goal. Natural hydrogels have been widely used as scaffolds for tissue engineering due to their excellent biocompatibility, tunable biodegradability, and low cytotoxicity.

To improve their biological activity, these hydrogels can be functionalized by soft nanoparticles. Although soft nanoparticles are highly biocompatible and do not negatively impact cellular functions, they cannot significantly modulate the physical properties of the functionalized scaffolds. Thus, the development of soft nanoparticles that can improve the

electrical and ionic conductivity of the hydrogels would be an important step towards engineering scaffolds for the culture of neural, muscular, and cardiac tissues.

An emerging area in the field of drug delivery is the development of smart systems for on-demand administration of active compounds [204]. This concept is also important in tissue engineering applications where different spatial and temporal concentrations of biological factors are needed at different stages of tissue formation. Towards this end, engineering soft nanoparticles that can respond to external and internal stimuli would be a major step forward. The use of bioresorbable electronics for forming electrically enabled scaffolds in which the drug delivery can be triggered using embedded electronics is another possibility.

One of the areas that are expected to achieve significant attention is the development of scaffolds that can direct cellular fate during tissue growth. Soft nanoparticles are excellent choices for delivering plasmids or factors into cells and thus can be used for engineering such biologically active scaffolds. The biofabrication of hydrogels functionalized with different soft nanoparticles and controlling their spatial distribution could potentially enable directing the spatial organization of cells during tissue maturation.

It has become evident that hydrogels for wound care applications and drug delivery systems have substantial potential to be utilized in pharmaceutical applications. In recent years, a number of materials attributed to hydrogels have been approved by the Food and Drug Administration (FDA) [205]. Hydrogels can be considered a Class I, II, or III medical devices dependent upon added biologics and drugs [206]. Their approval process, therefore, begins with a 501(k) premarket notification. Commercialization of hydrogel products has a bright future, the demand for patient-specific treatments and healing processes continues to grow.





*pharmaceutics*

IMPACT  
FACTOR  
4.421



# Engineering Smart Targeting Nanovesicles and Their Combination with Hydrogels for Controlled Drug Delivery

Volume 12 · Issue 9 | September 2020



[mdpi.com/journal/pharmaceutics](https://mdpi.com/journal/pharmaceutics)  
ISSN 1999-4923



Review

## **Engineering Smart Targeting Nanovesicles and their Combination with Hydrogels for Controlled Drug Delivery**

Kamil Elkhoury<sup>1,2</sup>, Polen Koçak<sup>1,3</sup>, Alex Kang<sup>1</sup>, Elmira Arab-Tehrany<sup>2</sup>, Jennifer Ellis Ward<sup>4</sup>, Su Ryon Shin<sup>1</sup>

<sup>1</sup> Division of Engineering in Medicine, Department of Medicine, Brigham and Women's Hospital, Harvard Medical School, Cambridge, MA 02139, USA.

<sup>2</sup> LIBio, University of Lorraine, F-54000 Nancy, France.

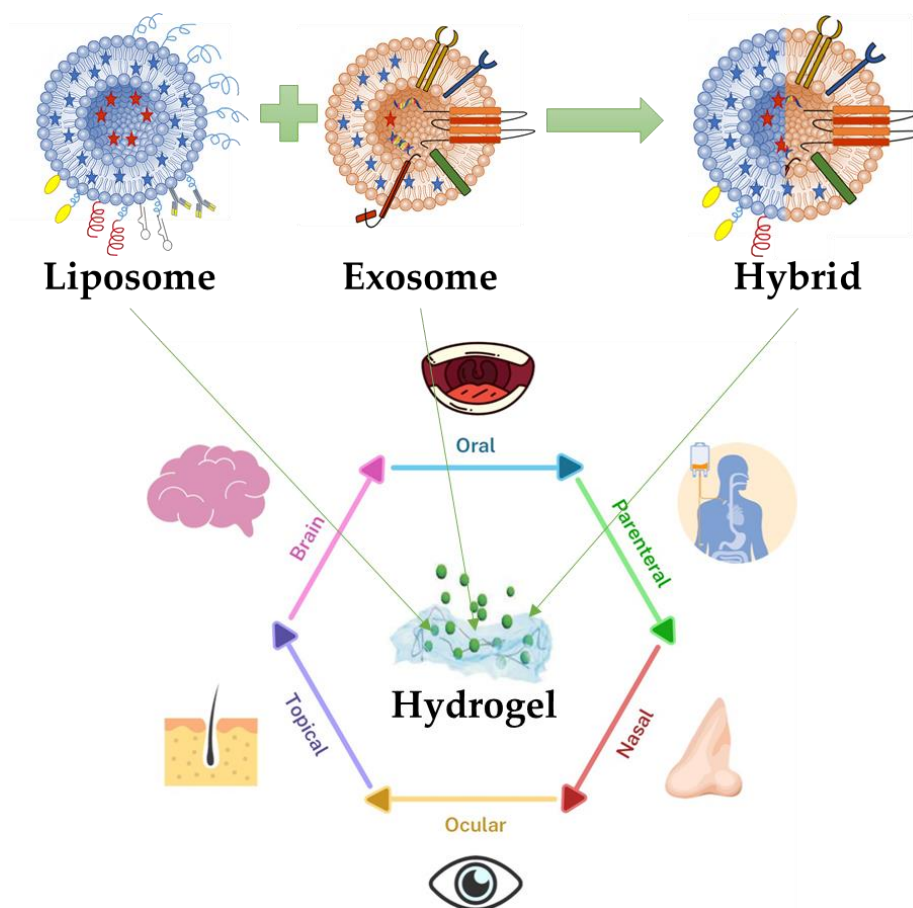
<sup>3</sup> Department of Genetics and Bioengineering, Faculty of Engineering and Architecture, Yeditepe University, TR-34755 Istanbul, Turkey.

<sup>4</sup> Division of Genetics, Department of Medicine, Brigham and Women's Hospital, Harvard Medical School, Boston, MA 02115, USA.

Received: 8 August 2020; Accepted: 2 September 2020; Published: 7 September 2020

### **Abstract**

Smart engineered and naturally derived nanovesicles, capable of targeting specific tissues and cells and delivering bioactive molecules and drugs into them, are becoming important drug delivery systems. Liposomes stand out among different types of self-assembled nanovesicles, because of their amphiphilicity and non-toxic nature. By modifying their surfaces, liposomes can become stimulus-responsive, releasing their cargo on demand. Recently, the recognized role of exosomes in cell-cell communication and their ability to diffuse through tissues to find target cells have led to an increase in their usage as smart delivery systems. Moreover, engineering “smarter” delivery systems can be done by creating hybrid exosome-liposome nanocarriers via membrane fusion. These systems can be loaded in naturally derived hydrogels to achieve sustained and controlled drug delivery. Here, the focus is on evaluating the smart behavior of liposomes and exosomes, the fabrication of hybrid exosome-liposome nanovesicles, and the controlled delivery and routes of administration of a hydrogel matrix for drug delivery systems.



**Keywords:** Liposomes; Exosomes; Targeting Nanovesicles; Hydrogel; Controlled Drug Delivery.

## 1. Introduction

Today, one of the key challenges in bioengineering and nanomedicine is how to formulate biomaterials and nanoparticles that selectively deliver encapsulated therapeutics to specific cells or tissues, when the enhanced permeability and retention (EPR) effect is inefficient. Liposomes have been studied and investigated for more than five decades and have become a well-established drug delivery vesicle, resulting in the marketing authorization of many clinically approved liposome-based products to treat different diseases [7]. Liposomes' resemblance to biomembranes enables superior biocompatibility and safety over other polymeric and metal based nanoparticles, as well as the ability to deliver lipid-soluble and water-soluble molecules at the same time [207,208]. However, liposomes require surface modification with ligands to acquire smart targeting capabilities. On the other hand, some natural nanovesicles, such as exosomes, already possess these targeting capabilities. The smart behavior is granted to exosomes by the donor cells in the form of cellular and lipid adhesion molecules expressed on their surfaces that allow them to target specific types of receptor cells [8]. Furthermore, since exosomes are produced by the cells, they offer an even higher level of biocompatibility and a lower immunogenicity than liposomes, which increases their stability in systemic circulation and enhances their uptake profile and therapeutic efficacy *in vitro* and *in vivo* [209,210].

However, exosomes have limitations in terms of efficient and reproducible loading with drugs or bioactive agents. To address this issue, while equipping liposomes with smart tissue and cell targeting behavior, many research groups have created hybrid liposome-exosome delivery systems [9–12].

In fact, exosomes and liposomes have many similarities (**Figure 1**), as both of them are nanovesicles composed of one lipid bilayer, ranging in size from 40 nm to 120 nm. Due to these similarities, artificial or synthetic exosome-mimetic nanovesicles are normally derived from liposomes [209]. However, liposomal and exosomal nanovesicles have major differences as well, with the main one being the complex surface composition of exosomes. The lipid composition and membrane proteins of exosomes differentiate them from other nanovesicles. Their unique lipid composition dictates their *in vivo* fate as they play an important role in specific interactions with serum proteins. Their membrane proteins (i.e. tetraspanins) facilitate their cellular uptake and increase the efficiency of their targeting ability. Compared to synthetic nanovesicles (micelles, liposomes and polymeric nanoparticles), exosomes are less cytotoxic, more biocompatible, can evade phagocytosis, and have an extended blood half-life [211–213]. Recently, head-to-head comparisons between liposomes and exosomes have been questioned because of the poor selection of controls [214]. However, all these comparisons have shown that the advantages of exosomes are the disadvantages of liposomes and vice-versa. Therefore, as mentioned before, combining these two nanovesicle types into one hybrid nanovesicle will preserve the beneficial features of both of these complimentary systems and allow for the engineering of an enhanced drug delivery targeting system.

The most common way of administering drug-loaded liposomes and exosomes is *via* injection. However, it is not a very effective method because it is difficult for the nanovesicles to be retained at the targeted site, and thus rapid clearance is the only inevitable outcome. One possible solution to avoid multiple injections and to release the drug over a long period of time is to embed nanovesicles in a hydrogel system. Hydrogels have been commonly used as drug delivery matrices, as, in addition to the protection they provide to the encapsulated drugs or nanovesicles, they are able to form a drug depot following their administration at the targeted defected site and control the release rate of both nanovesicles and drugs in a time dependent manner [215–220]. Both natural and synthetic biodegradable hydrogel systems have been used for the development of these depot-forming controlled release systems. However, the main advantages of naturally derived hydrogels used as extracellular matrices (ECMs) mimicking systems are their biocompatibility, their biodegradability, and promotion of cell adhesion, growth, proliferation, differentiation, and natural ECM secretion [2]. As a result, natural hydrogels are usually the preferred choice when choosing a drug delivery system. Many of the hydrogel limitations, such as low tunability and low mechanical properties, could be overcome

*via* the synergistic effect of the incorporated nanovesicles [2,19,221]. Furthermore, the ability of drugs and nanovesicles of different sizes to be loaded and released from hydrogel systems allows for delivery *via* administration routes other than injection or oral. This will allow broader biomedical usages for the embedded nanovesicles, such as wound healing, bone and spinal cord regeneration, and direct cell reprogramming.

Here, we provide a comprehensive insight for liposomes, exosomes, and their hybrid nanovesicles with recent improvements in their formulation as drug delivery nanovesicles. The fabrication of hybrid nanovesicles from membrane fusion will also be highlighted. In addition, natural hydrogels used as controlled delivery systems and their usual routes of administration will be outlined.

## 2. Liposomes as Drug Delivery Vesicles

Liposomes were first discovered in the 1960s when the British Dr. Bangham noticed that phospholipids formed a closed bilayer upon contact with water [109,222]. Phospholipids are amphiphilic molecules, which, when surrounded in an aqueous medium, the hydrophobic acyl chains drive the thermodynamically favorable formation of a lipid sphere [223,224]. This formation is enhanced by electrostatic interactions, such as van der Waals forces and hydrogen bonding [225,226]. The liposomal vesicle is made up of an aqueous core encircled by a lipid bilayer and is able to encapsulate both hydrophobic and hydrophilic bioactive molecules [116,227]. Hydrophobic molecules are entrapped in the lipid bilayer with a higher efficiency than the entrapment of hydrophilic molecules in the aqueous core, due to the lower volume of hydration in the liposome core [223]. Based on their surface characteristics, liposomes can be categorized as conventional PEGylated/stealth liposomes, or ligand-targeted (**Figure 1**). Clinically approved liposome-based products cover 6 main therapeutic areas [7]:

- Cancer therapy: DaunoXome® (non-PEGylated), Depocyt® (non-PEGylated), Doxil® (PEGylated), Marqibo® (non-PEGylated), Mepact® (non-PEGylated), Myocet® (non-PEGylated), Onivyde™ (PEGylated).
- Fungal diseases: Abelcet® (non-PEGylated), Ambisome® (non-PEGylated), Amphotec® (non-PEGylated).
- Analgesics: DepoDur™ (non-PEGylated), Exparel® (non-PEGylated).
- Photodynamic therapy: Visudyne® (non-PEGylated).
- Viral vaccines: Epaxal® (non-PEGylated), Inflexal® V (non-PEGylated).
- Rare genetic disease treatment: ONPATTRO®/Patisiran (non-PEGylated).

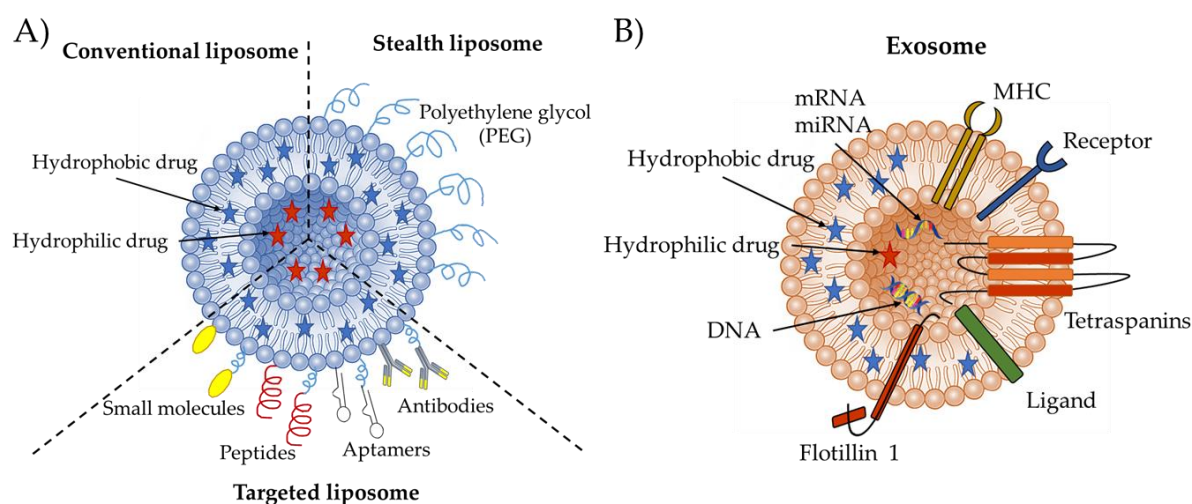


**Figure 1.** Schematic illustration of A) conventional, PEGylated/stealth, and ligand-targeted liposome, and of (B) exosome structures.

### 2.1. Conventional Liposomes

Liposomes can be formed from naturally occurring lipids that are extracted and purified, or from commercially available synthetic lipids. Conventional liposomes can be classified according to their size and lamellarity. They can be small (~100 nm) or large (~1,000 nm) vesicles and can be composed of a single (unilamellar) bilayer or multiple (multilamellar) bilayers. The number of bilayers and the size of liposomes affect their encapsulation efficiency, drug release profile, physical stability upon storage, and cell internalization [228,229]. The size of liposomes and the number of bilayers are controlled *via* the chosen method of preparation. Multilamellar vesicles can be formed by the thin-film hydration method, large unilamellar vesicles can be produced by the freeze-thaw method, and small unilamellar vesicles can be generated with sonication or multiple extrusions through a polycarbonate membrane. Liposomes are widely used as drug delivery vesicles mainly because they are biocompatible and can increase the bioavailability while reducing the toxicity of encapsulated drugs, but also because their surface properties, charge, and size can be simply engineered to deliver their cargo into cells *via* adsorption onto the cell membrane, fusion with the cell membrane, micropinocytosis, or endocytosis [230].

However, the surface of the conventional liposome is usually impaired through opsonization by physical interactions with specific circulating proteins in blood. The opsonizing proteins include fibronectin, laminin, type I collagen, C-reactive protein, immunoglobulins, and complementary proteins. Though opsonization is an important natural process and is crucial for the immune response to clear dangerous pathogens, it hinders the ability of liposomes to circulate in the blood pool for a prolonged period [231]. Opsonized liposomes are recognized and cleared by the mononuclear phagocytic system (MPS) or reticuloendothelial system (RES), which are located in the liver and spleen. Another limitation of conventional liposomes is their

tendency to release their cargo during circulation. To avoid this problem and to increase the circulation time of a liposomes, a hydrophilic polymer called polyethylene glycol (PEG) can be added to their surface, to create what is known as PEGylated or stealth liposomes [232,233].

### 2.2. *Stealth Liposomes*

The term “stealth” used in biomedical research is derived from the “low observable technology” applied to military tactics, which mainly refers to invisible nanovesicles that can avoid clearance from the bloodstream [234]. The development of long-circulating liposomes is crucial to avoid clearance by the organs of the MPS and to achieve prolonged persistence and targeted delivery of drugs. This invisibility can be achieved by decorating the outer liposome surface with stealth polymeric substances, such as PEG [235,236].

Polymeric materials, whether natural or synthetic, should be biocompatible to reduce the amount of interaction between the liposome surface and the opsonizing proteins to circumvent an immune response. PEGylated liposomes are heavier than conventional liposomes and are thus eliminated from the body by a different mechanism. This increased weight helps them to avoid enzymatic degradation and clearance *via* glomerular filtration [237–239]. The weight of PEGylated liposomes governs their clearance fate, as the heavy ones with weights above 20 kDa are primarily eradicated by the liver, whereas the lighter ones are eliminated through renal filtration [239]. PEGylated liposomes alter the pharmacokinetic profile of encapsulated drugs and thus decrease their toxicity and increase their therapeutic index. Doxil®, a typical PEGylated liposome encapsulating the chemotherapy drug doxorubicin, was the first nanodrug approved by the Food and Drug Administration (FDA) in 1995 [240]. Encapsulated doxorubicin in PEGylated liposomes maintained a presence in human circulation for more than 350 hours and achieved a human circulation half-life time of around 90 hours [241,242].

When they accumulate in the body, PEGylated liposomes mainly accumulate in tumor tissues rather than in normal tissues, thus creating a local drug depot in their accumulation area. This depot increases the drug tissue concentration and promotes a higher therapeutic effect. However, due to the EPR effect, a concentration of PEGylated liposomes in a targeted area is possible, but the efficient release of drugs is not guaranteed, even after endocytosis by the cells, as the PEG coating can sometimes constrain the drugs’ endosomal escape [243]. Moreover, a homogeneous distribution of liposomes in the targeted area is hard to achieve, especially in complex microenvironments, which can hinder sufficient treatment. Thus, active targeting drug delivery with improved strategies are required to promote efficient treatment.

### 2.3. *Targeted Liposomes*

Through membrane fusion or endocytosis, liposomes can deliver drugs inside the cell membrane, as both membranes are composed of phospholipids. Therefore, active targeting

liposomes that enter targeted cells *via* receptor-mediated endocytosis should be engineered to achieve an efficient cell-specific uptake. Conjugating the appropriate targeting ligands, such as small molecules, aptamers, monoclonal antibodies, and peptides, on the surface of liposomes can modulate the cell-type-specific uptake and tissue distribution of PEGylated liposomes. The overexpression levels of the corresponding receptors or proteins on the cell surface, which these targeting ligands are bound to, influence the cellular uptake efficiency [244].

To improve cell targeting specificity, the liposomal surface can be functionalized with small molecules which possess a high binding affinity to receptors present on the cell surface. Many cancer cells overexpress folate receptors, which makes the small molecule folate a great candidate to direct the delivery of liposomes containing cancer therapeutics towards cancer cells [245–247]. The overexpression of sigma receptors in many cancer cell lines has paved the way for another small molecule ligand possessing a high binding affinity to these receptors: anisamide [248–250]. Banerjee *et al.* attached the anisamide moiety to liposomes and included a PEG spacer between them to improve the ligand targetability and stability, and to increase the circulation half-life [251]. This was the first study to use anisamide to target and deliver doxorubicin encapsulated in liposomes to prostate cancer cells overexpressing sigma receptors.

Aptamers are RNA or DNA sequences which exhibit high affinities and specificities towards specific cells and tissues [252]. Aptamers' target specificities are adopted thanks to their unique three-dimensional structures. Baek *et al.* inserted RNA aptamer-conjugated micelles into liposomes loaded with doxorubicin to target LNCaP prostate epithelial cells expressing the prostate specific membrane antigen (PSMA), thus minimizing the systemic toxicity and side effects of the anticancer drug [253].

Receptor-specific cell-targeting and nonspecific cell-penetrating peptides are the two peptide categories used for liposome surface functionalization [254]. When compared to nontargeted liposomes, peptide-targeted liposomes showed superior therapeutic efficacy, which was caused by the enhanced cellular uptake in target cells [255,256]. The conjugation of peptides to liposomes can be achieved through thioester linkages, sulfanyl bonds, disulfide bonds, peptide bonds, and maleimide linkages [232,257]. Ding *et al.* constructed cell-penetrating peptides-modified, pH-sensitive PEGylated liposomes that displayed improved targeting and cellular internalization efficiencies on MCF-7 cancer cells [258].

The surface functionalization of liposomes *via* covalent coupling to the modified PEG termini distal with monoclonal antibodies (mAbs) or their fragments, such as fragment antigen-binding and single-chain variable fragment, can generate immunoliposomes with reduced side effects and the ability to target cells which overexpress the antigens to these antibodies [259]. Immunoliposomes have been extensively studied for cancer therapy, however, they can also be used to treat many other diseases, such as autoimmune and degenerative diseases, inflammatory

and cardiovascular diseases, and infectious pathologies. Various methods have been reported for coupling antibodies to the PEGylated liposome surface, with the most common ones involving the conjugation between the PEG chains' distal ends and the antibodies [260]. The chronic neurodegenerative disease, Alzheimer's disease, is caused by the accumulation of neurofibrillary tangles and amyloid plaques (A $\beta$ ), two core pathological hallmarks, in the brain. Ordóñez-Gutiérrez *et al.* functionalized the surface of PEGylated liposomes by using a monoclonal anti-A $\beta$  antibody to capture A $\beta$  in the periphery and showed that these immunoliposomes had a higher therapeutic efficacy than the free monoclonal antibody [261].

### 3. Exosomes as Drug Delivery Vesicles

Cell to cell communication is important for the integrity of organisms and for maintaining tissue homeostasis. In fact, these cell communication mechanisms mostly require the coordination of signaling molecules and receptors [262]. Recently, cell to cell communication mediated *via* nanovesicles, mostly exosomes, has become popular due to the ability to shuttle various bioactive molecules between producing and target cells [2]. The first term of 'exosome' was described 50 years ago as cellular garbage released *via* shedding of the plasma membrane [263]. According to the literature, exosomes can be released from almost every cell type, including lymphocytes, mesenchymal stem cells (MSC), cancer cells, epithelial and endothelial cells and dendritic cells [264–269]. Studies indicate that extracellular vesicles contain receptors involved in antigen presentation, including class I and II MHC molecules, co-stimulatory molecules such as CD83 and CD40, exosomes derived from B and T cells, and mast production [270].

Depending on the originating cell or organism, the exosome's contents may vary, but generally all exosomes encompass nucleic acid molecules (mRNAs, functional microRNAs, and non-coding RNAs), proteins, small molecule metabolites and lipids [271]. Additionally, the exosome's surface contains receptors (HSP70), which are valuable for transporting materials to recipient cells and for identifying exosomes [272]. There are numerous methods to isolate exosomes, such as ultracentrifugation, differential centrifugation, chromatography, two phase aqueous systems named as polymer-based precipitation, filtration, and immunological separation. The development of a gold standard universal method that is efficient, with a high yield, but without compromising biologic function, is an active research goal [273].

Besides their ability to communicate between cells due to their small nano-metric size ( $\sim$ 30–150 nm [274]), exosomes are found in both the nucleus and in the cytoplasm and are also involved in the RNA processing of cells [275]. Exosomes differ from other extracellular vesicles with their unique biogenesis pathways, lipid compositions, and cargo that they can carry [272]. These vesicles, which can be obtained from all bodily fluids, have been demonstrated to have

an important role in many biological functions such as intercellular communication, signal transmission, genetic material transfers and regulation of the immune response.

### *3.1. Biogenesis of Exosomes*

The secretion of exosomes is mediated by multivesicular bodies (MVBs). The formation of exosomes *via* the MVBs pathway is eventuated by the endosomal membrane's inward budding into the endosomal lumen. Later, the MVBs deliver their endosomal cargo to the lysosomes for degradation. Other than delivering cargo to lysosomes, these vesicles play a role in molecule secretion *via* plasma membrane fusion [276]. After the membrane fusion, exosomes that are found in the MVBs are dispatched into the extracellular space and then are received by a recipient cell either by plasma membrane fusion, receptor ligand binding, or endocytosis [277].

Intraluminal vesicle formation necessitates the endosomal sorting complex, which is needed for the transport (ESCRT) functions [278]. These mechanisms are composed of four different ESCRT proteins (0 to III), which cooperate to aid MVB formation, the budding of the vesicles, and protein cargo classification and sorting [279,280]. ESCRT dependent exosome biogenesis is initiated by the identification and sequestration of ubiquitinated proteins into the endosomal membranes' particular units *via* ESCRT-0 binding subunits. Afterwards, the exosome will cooperate with ESCRT I-II, and will be combined with ESCRT-III, which plays a role in supporting the total complex of the budding process. Finally, after separating the buds and forming ILVs, the MVB membrane and the ESCRT-III complex will also be separated with the separation protein Vps4s' energy [278]. Studies have mentioned that exosome biogenesis is related to an ESCRT regulation mechanism, and different ESCRT compartments and ubiquitin proteins have already been investigated in exosomes obtained from different types of cells. In addition, it has been reported that the exosomal protein Alix, associated with several ESCRT mechanism proteins such as TSG101 and CHMP4, participates in sorting exosome cargo and membrane budding through syndecan interactions [281]. These studies have led to a hypothesis that implies ESCRT mechanisms play a large role in exosome biogenesis.

### *3.2. Molecular Composition of Exosomes*

Exosome composition may vary from cell to cell, an indication that the contents of an exosome are not only a mirror of the donor cell, but also a reflection of the sorting process [282]. Exosome cargo is comprised of various proteins, nucleic acids such as DNA, mRNA, miRNA, small molecules and lipids, which are found both inside and on the surfaces of exosomes [283,284]. A proteomic analysis of exosomes has demonstrated that some proteins originate from the cell or tissue of origin, and some proteins are common among all exosomes [281]. Typically, exosomes contain proteins with different functions, for example: tetraspanins (CD9

CD81, CD63 and CD82) involved in cell penetration, invasion, and fusion; heat shock proteins such as HSP70 and HSP90, which are involved in the stress response, which is also related to antigen binding and delivery; MVB formation proteins (Alix, TSG101) found in exosome secretion; and proteins responsible for membrane translocation and fusion (Annexin and Rab) [285]. Among these proteins, some of which participate in exosome biogenesis like Alix, flotillin, and TSG101, are secreted upon plasma membrane spillage, while others are specifically found in exosomes and can be used as an exosome marker proteins, such as HSP70, TSG101, CD63 and CD81 [285].

### 3.3. Exosomes and Signaling

Previously, exosomes were believed to be cellular garbage with mediocre lysosomal degradation capacity. However, studies showed that exosomes were involved in various physiological processes, their functions *in vivo* continued to be explained, and now they are recognized as very significant for cell-to-cell communication and cellular signaling.

It is known that there are several different exosome based mechanisms in cell-cell communication. The first is that the proteins in the exosome membrane activate intracellular signaling by interacting with receptors on target or receptor cells. Another mechanism is that the membrane proteins of exosomes can be cut by soluble fragments and proteases and can thus act as soluble ligands that bind to the receptors of the cell surface. Finally, exosomes can be engulfed by target cells and can release their cargo molecules to trigger downstream events in the recipient cells [286].

The secretion of exosomes by many different cells such as epithelial cells, stem cells, hematopoietic cells, cancer cells, and neural cells has shown that these nanovesicles can be effective in cellular physiology and pathology. Exosomes play a role in maintaining normal homeostasis, and may exert both a protective or detrimental role in human pathologies, such as cardiovascular diseases [287]. MicroRNAs are short non-coding RNAs which regulate gene expression and are enriched in exosomes, and alterations in their levels are associated with cardiovascular diseases. The cells of the heart, such as cardiomyocytes, fibroblasts and endothelial cells, secrete exosomes in response to injuries, and mediate paracrine crosstalk through microRNA levels between cardiac cell types in conditions such as cardiomyocyte hypertrophy [288,289]. In the immune system, exosomes are known to play a significant role in regulating signals by intervening innate and adaptive immune responses. Notably, there is some evidence that exosomes play a role in the spread of antigens or MHC-peptide complexes.

In addition, according to proteomic studies, exosomes have been shown to contain proteins located in cellular signaling pathways. The effects of these proteins on targeting and cellular signaling have not yet been fully disclosed, but sheds light on new studies. In particular

studies, the Wnt signaling pathway, which is also known as the signal transduction pathway and plays important roles in embryo development, tissue regeneration, and cancer metastasis, has attracted attention. However, the mechanisms by which Wnt proteins can target cells are mostly unknown. Indeed, membrane bound palmitoylated Wnt proteins are not likely to be released into the extracellular space as soluble proteins. All in all, recent studies suggest that the packaging of exosomes and the release of their cargo may be promising for the downregulation of cellular signaling pathway activity [290–292]. Exosomes have potential as both a therapeutic target and may serve as biomarkers of disease.

#### 4. Engineering Hybrid Exosome-Liposome Systems

Recent studies have revived the usage of exosomes for targeted drug delivery, with surface modifications or by producing hybrid synthetic nanovesicles. Exosomes are nanosized particles that have great potential to increase anticancer responses and targeted drug delivery. Exosomes modified by genetic or non-genetic methods can increase the cytotoxicity and targeting ability of therapeutic agents, thereby improving their effectiveness for the drug delivery [209].

As mentioned briefly above, exosomes can transmit signal molecules such as miRNA, mRNA, proteins and lipids [265]. Due to their small sizes, they have the ability to escape phagocytosis and can carry and deliver the cargo in circulation. Exosomes can also pass through the blood brain barrier and placental barrier [267]. Because of their high drug delivery potential, studies have focused on the engineering of exosomes using both surface modification and hybridization with synthetic nanocarriers, such as liposomes (**Figure 2**) [11].

Therefore, to increase the delivery efficiency of exosomes, Sato *et al.* tried to form an exosome-liposome hybrid fusion using the freeze-thaw method. The aim of this study was to modify the exosome surface to reduce the immunogenicity of the exosome and also increase the colloidal stability. The result of the study demonstrated a new way to hybridize exosomes into a biological nanocarrier, which could be used to transport exogenous hydrophobic lipids, as well as hydrophilic cargos to recipient cells via membrane fusion method [9].

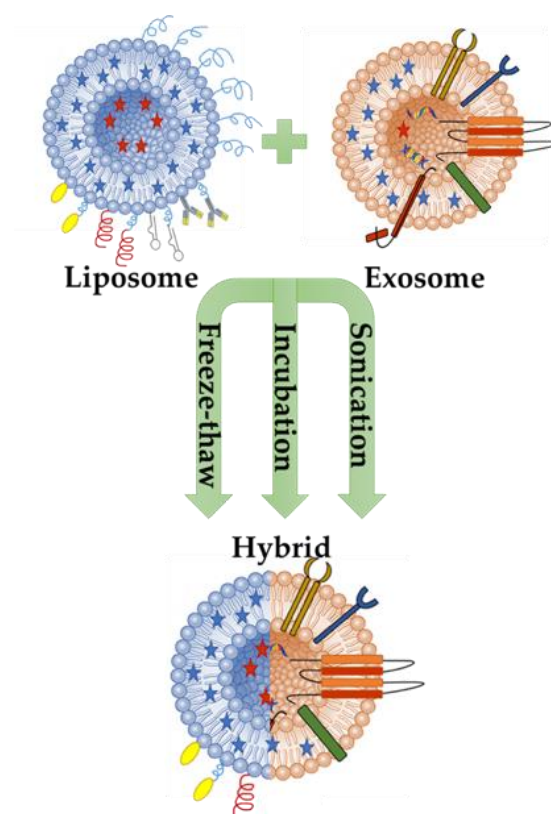


**Figure 2.** Schematic illustration of hybrid exosome-liposome nanovesicles formed by three main methods: Sonication, Incubation, and Freeze-thaw cycles.

According to the literature, the exosome's lack of size tunability could be disadvantageous for the encapsulation of bioactive molecules with various sizes. Current evidence for drug delivery is mostly related to micro RNAs and siRNAs, or particles with a smaller size than cas9 expressing plasmids. Therefore, new strategies should be developed for increasing the efficacy of both encapsulation and targeting for drug delivery. In one study, the successful delivery of the CRISPR-Cas9 system in MSCs was achieved *via* hybrid exosomes produced through simple incubation with liposomes [11].

Exosomal membrane engineering, in other words, modifying exosomes through membrane fusion with synthetic liposomes, aims to make exosome liposome hybrids to increase the half-life of exosomes in blood. In addition, due to the hydrophobic properties of lipid molecules, lipids have been shown to prevent the direct loading of exosomes. It is not easy to make genetic changes in the exosome lipid membrane because there is more than one protein in the lipid biosynthesis process, and the process of separating the lipid from the parent cell to exosome has not been clearly demonstrated.

Therefore, in recent studies, new strategies have been proposed for the preparation of hybrid particles designed by the fusion of the exosomal and liposomal membranes *via* freeze-thaw cycles [293]. The fabrication of these hybrid particles is one of the strategies used to abstain possible safety problems associated with the usage of allogenic nanovesicles, and to avoid the inefficient isolation yield or the long time required to produce and isolate exosomes.

In addition, studies have focused on the development of optimized microfluidic based approaches, and ready-to-use GMP compatible equipment is available to expand production.

Although current studies have shown that it is possible to determine the exosomal lipidic and protein content using lipidomic and proteomics tools, the issue of whether these methods will lead to the production of efficient targeting liposomes *in vivo* is still being explored. Indeed, extracellular vesicles have been known to have targeting potential for some types of cells over the past 5 years, but in most cases, they have failed to show the expected therapeutic results following systemic administration. Subsequent unsuccessful trials have revealed some shortcomings in the methods utilizing exosomes as targeted drug delivery nanovesicles. Now, the main prerequisites for using nanovesicles to deliver and target specific drugs are: (i) efficient loading with a drug/molecule to elicit a therapeutic effect; (ii) good stability during circulation in the bloodstream before achieving therapeutic goals (preservation of size, structure and drug load); (iii) the ability to block the uptake of macrophages and the capability of traveling for a long time to reach their cellular targets and cargos; and (iv) being nontoxic, nonimmunogenic, and biocompatible. Because of the many similarities between liposomes and exosomes (as noted in section 2 above), both nanovesicles have been used as hybrid molecules to improve targeted drug delivery.

All in all, studies on exosomes, nano-sized vesicles encapsulating proteins, and nucleic acids have grown in number over the past years due to their important roles in cell-cell communication. While the composition and biogenesis of mammalian-derived exosomes have been the focus of several studies, others have demonstrated the usage of these vesicles both as diagnostic and therapeutic tools for the drug delivery. In addition, the biocompatible properties of exosomes and liposomes with appropriate modifications can increase the cellular targeting efficiency as a drug delivery system. One of the main focuses of this review is to summarize examples of exosome and liposome modifications, and the delivery of therapeutic molecules, as well as passive and active loading approaches.

### **5. Nanovesicles-Hydrogels Interactions**

Hydrogels are mainly noted for their composition and ability to maintain a stable structure. As a result of these desired properties, hydrogels have been extensively studied as engineerable ECM mimics for tissue engineering and drug delivery applications [50]. Natural proteins or polysaccharides, such as collagen, alginate, chitosan, gelatin, or hyaluronic acid (HA), can be used to form hydrogels [294]. Natural hydrogels are better suited for drug delivery applications compared to nanovesicles, mainly because of their formulation stabilities and drug administration routes. For example, liposome-based technology presents several shortcomings such as instability, rapid clearance from blood circulation, capture by the reticuloendothelial

system, and rapid degradation [295]. To combat this, encapsulating nanovesicles in hydrogels can protect them from rapid clearance and can enhance their membrane integrity and mechanical stability. Additionally, hydrogels' physical, mechanical, and biological properties can be improved and tuned by the incorporated nanovesicles [2]. Other properties such as charge, pore size, hydrophobicity, and hydrophilicity can be also be tuned by nanofunctionalization with nanovesicles to form controlled release composite hydrogel delivery systems that have been used for many biomedical applications (**Table 1**).

**Table 1.** Comparison of liposomes, exosomes, and hybrid particles embedded in natural hydrogel delivery systems and their applications.

Hydrogel	Loaded molecule	Release duration	Cell type	Application	Ref.
Liposomes					
Gelatin methacryloyl (GelMA)	Deferoxamine, bovine serum albumin, and paclitaxel	5, 11 and 35 days	MC3T3-E1 and HUVECs	Bone regeneration	[215]
GelMA	Gemcitabine	4 days	MG63 cells	Osteosarcoma treatment	[296]
GelMA	Melatonin	25 days	MC3T3-E1 cells	Osteoporosis treatment	[297]
GelMA	SDF-1 $\alpha$	7 days	MSCs	Wound healing	[298]
GelMA and alginate	-	-	Keratinocytes	Wound healing	[299]
Collagen, gelatin, and alginate	Moxifloxacin and dexamethasone	1 day	Ocular epithelial cells	Corneal wound healing	[300]
Chitosan and alginate	mRNA	14 days	Fibroblasts and dendritic cells	Vaccine delivery	[301]
Chitosan	Carboxyfluorescein, rifampicin, and lidocaine	5.5 h	-	Wound dressings	[295]
Chitosan	-	-	HaCaT and hASCs	Tissue engineering scaffolds	[302]
Chitosan	$\alpha$ -tocopherol	6 days	L929 cells and cardiomyocytes	Cardiac tissue engineering	[303]
Exosomes					
Hyaluronic acid and Gelatin	-	-	hBMSCs	Cartilage regeneration	[190]
Hyaluronic acid and alginate	-	14 days	MC3T3-E1	Bone regeneration	[304]
Oxidative hyaluronic acid and Poly- $\epsilon$ -L-lysine	-	21 days	HUVECs	Skin regeneration	[216]
Modified hyaluronic acid	-	21 days	EPCs	Myocardial preservation	[305]
Silk fibroin	miR-675	36 days	H9C2 cells	Vascular dysfunction treatment	[306]
Chitosan	-	1 day	HUVECs	Hindlimb ischemia treatment	[218]
Alginate	-	10 days	HUVECs	Myocardial infarction treatment	[307]
Alginate	-	7 days	HeLa cells	Wound healing	[219]
Chitosan	miR-126-3p	6 days	HMEC-1 and fibroblasts	Wound healing	[308]
Chitosan and silk	-	-	GMSCs	Wound healing	[309]
Hybrid					
-	-	-	HeLa cells	Drug delivery	[9]

-	GFP mRNA	-	HUVECs, MSCs, and MDCK cells	Drug delivery	[10]
-	CRISPR/ Cas9	-	MSCs and HEK293FT cells	Gene editing	[11]
-	doxorubicin	2 days	4T1, K7M2, and NIH/3T3 cells	Tumor targeted drug delivery	[12]

### 5.1. Liposome-Loaded Hydrogels

Gelatin is a natural protein that is produced by denaturing collagen. Due to its favorable biodegradability, biocompatibility, and low antigenicity, gelatin is mostly used in biomedical and pharmaceutical applications. However, rapid degradation and a low mechanical modulus are two main limitations for using unmodified gelatin in biomedical applications. To surpass these limitations, gelatin is usually chemically modified into gelatin methacryloyl (GelMA) by the addition of methacrylate groups to the amine-containing side groups [310]. In the presence of a photoinitiator, this methacrylation reaction allows for the light polymerization of gelatin into a hydrogel. Undamaged cell adhesive arginine-glycine-aspartic acid (RGD) motifs and matrix metalloproteinase degradable amino acid sequences help in retaining the excellent biocompatibility and bioactivity of gelatin by the fabricated GelMA hydrogels.

Although GelMA is biocompatible and can be used for depot drug delivery, its big pores cannot control the release of drugs and often leads to a burst release. To solve this issue, many groups have embedded liposomes loaded with bioactive molecules in the GelMA matrix. In addition to offering a controlled release, the liposome integration improves the GelMA's mechanical properties due to the hydrogen bonding that forms between the GelMA polymer chains and the phospholipid bilayers. Cheng *et al.* reported that such a mechanically enhanced liposome-GelMA hydrogel can sustain stretching, torsion, and compression, and studied the controlled release of deferoxamine, a hydrophilic drug, from this composite hydrogel (**Figure 3 A**) [215]. 80% of deferoxamine was released from the GelMA hydrogel in the first 4 hours compared to about 25% released from the liposome-GelMA hydrogel. The controlled release of the composite hydrogel led to a significant promotion of angiogenesis and osteogenic differentiation *in vitro* and *in vivo*, influencing the adhesion or proliferation of MC<sub>3</sub>T<sub>3</sub>-E<sub>1</sub> and HUVECs cells.

In a more recent study, Xiao *et al.* generated a sustained Melatonin (MT) release system composed of MT liposomes embedded in a GelMA-Dopamine (DOPA) hydrogel, and studied its release behavior and ability to induce implant osseointegration in an osteoporotic state (**Figure 3 B**) [297]. As for the release behavior, the samples exhibited various release characteristics depending on the density of the hydrogel network, with 5% GelMA constructs having only 5 days of sustained release and 20% GelMA constructs exhibiting up to 25 days of sustained release. The developed system could be used for the treatment of implant loosening

in patients with osteoporosis, as it was shown to be able to suppress osteoblast apoptosis, promote osteogenic differentiation and improve bone quality around the prosthesis.

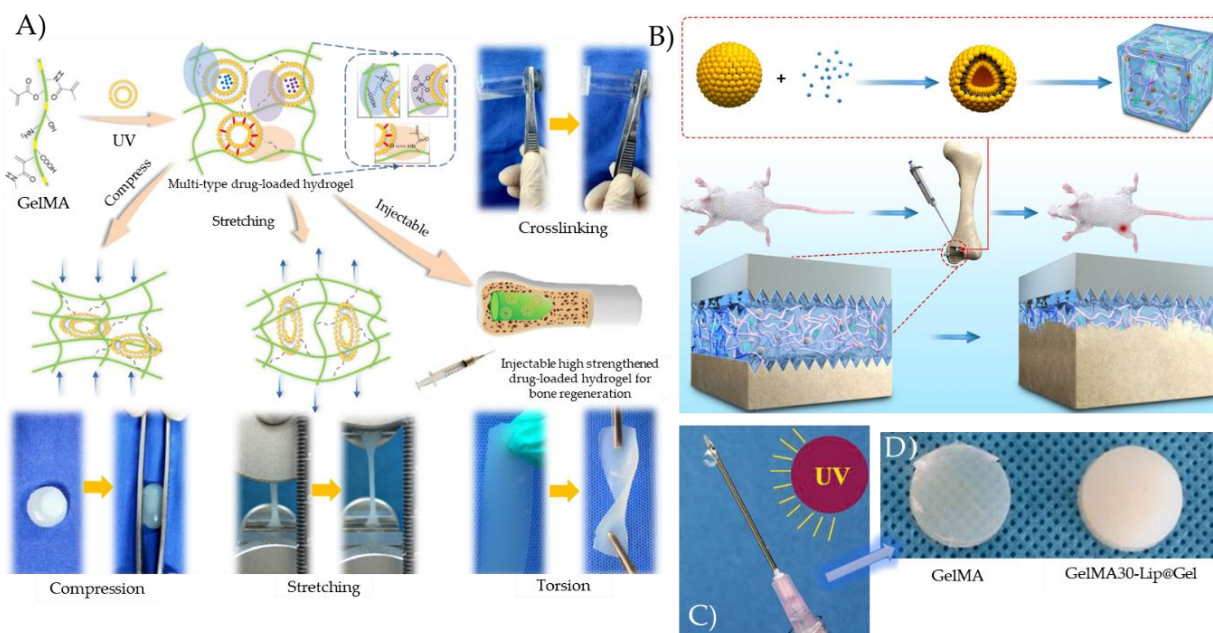


**Figure 3.** A) liposome-GelMA hydrogel with controlled release of bone regeneration drugs and enhanced mechanical properties. Reproduced/Adapted with permission from [215], Elsevier, 2018. B) The bone regeneration mechanism promoted by Melatonin-loaded liposomes embedded in a GelMA-Dopamine hydrogel. Adapted from [297], Hindawi, 2020. C) The mechanism of UV induced crosslinking and D) the appearance of UV crosslinked GelMA and Gemcitabine-loaded liposomes embedded in GelMA (GEM30-Lip@Gel). Adapted from [296], Taylor & Francis, 2018.

Wu *et al.* reported that the double-network crosslinked structures that formed between GelMA and liposomes significantly improved the hydrogel's mechanical properties (**Figure 3 C,D**) [296]. The inclusion of liposomes in the GelMA matrix in their study presented a sustained controlled release of the anticancer drug Gemcitabine for 4 days, whereas the free drug was released from a pure GelMA hydrogel in only 6 hours. The loaded liposome-GelMA hydrogel killed MG63 cells *in vitro* and inhibited osteosarcoma *in vivo*, presenting itself as a promising implant for the treatment of osteosarcoma. In the field of wound healing, Kadri *et al.* reported that the nanofunctionalization of IPN GelMA-alginate hydrogels with rapeseed-derived liposomes significantly improved their mechanical properties and induced keratinocyte growth [299]. In another study, Yu *et al.* developed a liposome-GelMA hydrogel delivery system that controlled the release of the pro-healing chemokine stromal cell derived factor-1 $\alpha$ , which might be used for clinical wound healing applications [298].

Chitosan is mainly composed of deacetylated ( $\beta$ -1,4-linked glucosamine) and acetylated (N-acetyl-D-glucosamine) units with different degrees of deacetylation (70-95%) and molecular weights (10-1,000 kDa) [41]. Chitosan's low toxicity, biocompatibility, and biodegradability has led to its widespread use in hydrogels for tissue engineering and drug delivery applications [311]. Chitosan is also positively charged, which gives it antibacterial properties. Chitosan-

based formulations exhibit good mucoadhesive characteristics and are capable of achieving a prolonged presence in the intestines and improving drug bioavailability in the GI tract. Although chitosan can be a very promising hydrogel for drug delivery applications, it has a limited capacity for controlling drug release. To overcome this disadvantage, liposomes and other nanovesicles can be embedded in the chitosan matrix to deliver drugs at a controlled rate.

Peers *et al.* studied the release of a model water-soluble dye (carboxyfluorescein), an antibiotic (rifampicin), and an anesthetic (lidocaine) from liposome-chitosan hydrogels [295]. The water-soluble molecules were first encapsulated in Dipalmitoylphosphatidylcholine (DPPC) liposomes, then embedded into chitosan physical hydrogels. This incorporation did not modify the hydrogel's rheological properties. The release was sustained for longer periods in small unilamellar vesicles embedded in a chitosan hydrogel, compared to multilamellar vesicles embedded in a chitosan hydrogel and chitosan hydrogels without liposomes. Indeed, the liposome-chitosan hydrogel proved to be a promising candidate for the depot drug delivery of water-soluble antibiotics and anesthetics, which might have biomedical applications such as wound dressings.

Li *et al.* encapsulated curcumin inside liposomes and coated them with thiolated chitosan to form injectable and *in situ*-formable liposomal hydrogels [312]. The thermosensitive liposome-chitosan hydrogels could quickly transform from a fluidic state at room temperature to a gelled state at 37 °C. The release of curcumin was effectively delayed by the liposomal hydrogel encapsulation, which could improve the hydrogel's water solubility and bioavailability *in vivo*. The cytocompatible liposome-chitosan hydrogels were able to suppress and kill MCF-7 breast cancer cells when loaded with curcumin. In summary, the injectable, *in situ*-formable, and thermosensitive liposome-chitosan hydrogels show great promise as scaffolds for the controlled drug delivery of curcumin or other anticancer drugs for breast cancer treatment or after tumor resection.

Fibrin is a blood coagulation product *in vivo* in the presence of thrombin enzymes, which catalyze the cleavage of fibrinogen to fibrin [313]. Fibrin is especially effective due to its unique properties, such as biodegradability and nontoxicity. In addition, fibrin's components can be easily modified, such as the gel's structure, mechanical properties, and degradation [314]. Wang *et al.* found that fibrin could be combined with liposomes and chitosan hydrogels to carry hydrophilic drugs with low-molecular weights [313]. This is especially important because fibrin, in addition to liposomes, can allow for a depot delivery system that controls the release of biologically active peptides or hydrophilic drugs. The gradual release of bioactive components can be achieved when using fibrin and liposome technology [315]. As for liposome-based hydrogels using alginate, they have been used for slow drug release as well as

highly increased efficacy when compared to polymeric-based systems or liposome-based systems only [316,317].

### 5.2. Exosome-Loaded Hydrogels

Unlike liposomes, exosomes embedded in hydrogels are mostly used as bioactive molecules rather than as nanovesicles for the controlled delivery of drugs and molecules. The controlled release of exosomes from hydrogel systems increases their therapeutic efficiency by creating a depot of exosomes in the injury area, thus reducing the speed of their clearance from the body. Exosomes embedded in HA, gelatin, chitosan, and polypeptide-based hydrogels have been used for cartilage and bone defect repair, wound healing, and ischemia treatment, to name a few [216,218,190,304].

Liu *et al.* embedded stem cell-derived exosomes in a photoinduced imine crosslinked hydrogel formed from the reaction of aldehyde groups generated under light irradiation of o-nitrobenzyl alcohol moieties modified HA and amino groups distributed on gelatin (**Figure 4A**) [190]. The exosome-hydrogel patch showed retained exosomes at defect sites and successfully integrated with native cartilage. It showed also good biocompatibility and remarkable operability, which suggests that it can be used as a scaffold for cartilage defect repair. In another study, to maintain stable exosomes at the deficient area and to repair bone degeneration in rats *in vivo*, Yang *et al.* successfully embedded stem cell derived exosomes in an injectable, hydroxyapatite-embedded, *in situ* crosslinked HA-alginate composite hydrogel system (**Figure 4C**) [304]. Their exosome-hydrogel system could significantly enhance bone regeneration.

Other than repairing cartilage, exosome-hydrogel systems can be used to repair chronic wounds. Wang *et al.* demonstrated this by producing a multifunctional, self-healing, injectable, and antibacterial polypeptide-based hydrogel that can control the release of embedded exosomes to treat chronic wounds [216]. This exosome-hydrogel system significantly increased the cellular proliferation, migration, and vascularization *in vitro* and significantly improved the wound healing of diabetic full-thickness cutaneous wounds *in vivo*. The exosome-hydrogel system also decreased the scar tissue area while inducing the appearance of abundant skin appendages which accelerated the diabetic wound healing process. This suggests that the controlled release of exosomes from the hydrogel had a synergistic wound healing ability.

Hindlimb ischemia treatment is another area in which exosome-hydrogel systems can be applied. Zhang *et al.* incorporated MSC-derived exosomes in a chitosan hydrogel matrix, which was injectable and could retain exosomes at the injury sites (**Figure 4D**) [218]. One of the main findings of their study was that the exosome-chitosan hydrogel promoted the therapeutic effects of exosomes, which led to an improvement in endothelial cells' survival and angiogenesis, and an accelerated ischemic hindlimbs recovery. This exosome-chitosan system may be considered

as a potential cell-free ischemia therapy. Han *et al.* demonstrated that miR-675, which is an aging process modulator, can be loaded in exosomes, that, in turn, can be embedded in a silk fibroin hydrogel to provide a sustained *in vitro* release and treat aging-induced vascular dysfunction (**Figure 4B**) [306].

Lv *et al.* revealed that exosomes incorporated in an alginate hydrogel were more efficient at stimulating angiogenesis, inhibiting cardiac apoptosis and fibrosis, while improving scar thickness and cardiac function when compared to only MSC-derived exosomes [307]. Shafei *et al.* loaded adipose-derived stem cell exosomes in an alginate-based hydrogel and concluded that this bioactive scaffold wound dressing technique induced collagen synthesis, wound closure, and tube formation in the wounded tissue [219].

A controlled-release of exosomes from synovium MSC was combined with chitosan and was observed by Tao *et al.* to stimulate human dermal fibroblast viability and proliferation. Furthermore, in a diabetic rat model, they found that this system improved the re-epithelialization stage of wound healing, activated vessel formation, and improved the collagen production *in vivo* [308]. In addition, Shi *et al.* studied exosomes from gingival MSC combined with a chitosan/silk hydrogel and their effects on a diabetic rat skin defect model, and found that this hydrogel could increase the wound healing of diabetic skin defects [309].

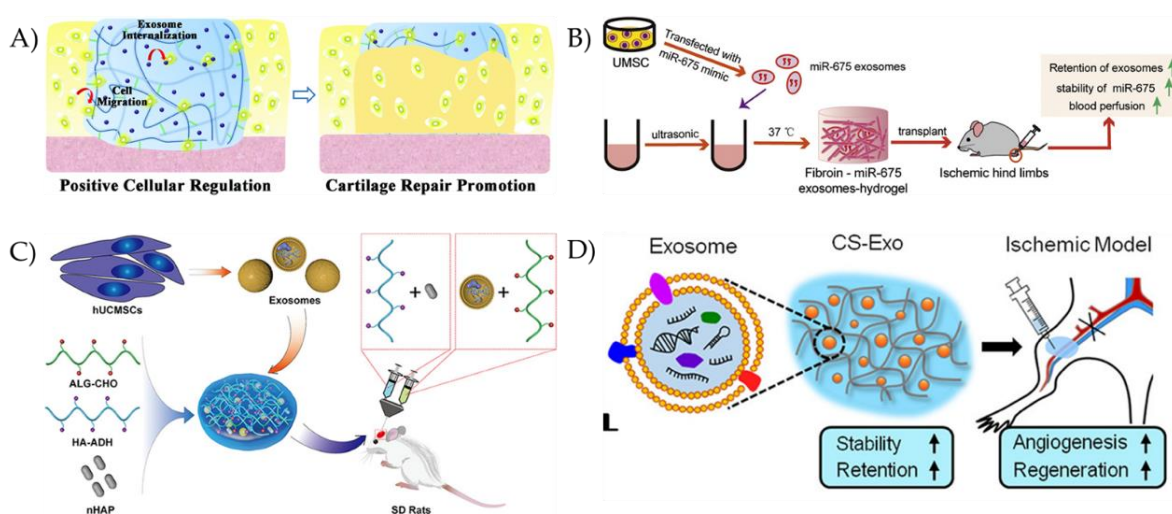


**Figure 4.** A) Schematic illustration of the exosome-hydrogel scaffold for cartilage regeneration. Reproduced/Adapted with permission from [190], Royal Society of Chemistry, 2017. B) Schematic illustration of the miR-675-loaded exosome-silk fibroin hydrogel system for age-induced vascular dysfunction treatment. Adapted from [306], Elsevier, 2019. C) Schematic illustration of the exosome-hyaluronic acid-alginate hydrogel system for bone regeneration. Reproduced/Adapted with permission from [304], American Chemical Society, 2020. D) Schematic illustration of the exosome-chitosan hydrogel system for muscle regeneration. Reproduced/Adapted with permission from [218], American Chemical Society, 2018.

### 5.3. Hybrid Nanovesicle Releasing Hydrogels

To the best of our knowledge, no groups have examined the applications of hybrid exosome-liposome particles embedded in natural or synthetic hydrogels *in vitro* or *in vivo* yet.

The only studies that have been done up until now using these hybrid particles, were only using free-standing nanovesicles [9–12]. Embedding these hybrid particles in hydrogels is a very pertinent topic to investigate, since, as mentioned before, it can maximize the advantages of the targeting ability of exosomes and the versatility of liposomes while increasing the presence of these smart particles at the desired site, thus increasing their efficiency and the controlled release of bioactive compounds. Furthermore, building programmable release platforms is achievable using responsive hydrogels that can be chemically-, biologically-, electrically-, photo-, thermo-, or pH-responsive [318,319]. Coupling smart nanovesicles (hybrid exosome-liposome particles) with smart hydrogel systems (stimuli-responsive hydrogels) can create “smarter” delivery systems that can have big impact on drug and gene delivery, tissue engineering, and regenerative medicine fields.

### 6. Advantages of Hydrogel Systems for Efficient Drug Delivery

Despite all their advantages, such as targeting ability, controlled release of bioactive molecules and drugs, and biocompatibility, liposomes, exosomes, and hybrid particles are limited in their administration route, since they can only be administered *via* injection. Moreover, when they are injected in the body, these nanovesicles are quickly cleared from blood circulation and accumulate rapidly in the liver, spleen, lungs, and gastrointestinal tract. These challenges and limitations led to a shift from encapsulating and delivering drugs in nanovesicles only to embedding these loaded delivery nanosystems in hydrogels. When suspended in the hydrogel matrix, the controlled release period is extended from hours to days and even weeks, and the drug or nanovesicle delivery can be achieved *via* several administration routes and not only *via* injection, such as oral, nasal, parenteral, ocular, topical, and brain delivery (**Figure 5**).

Oral drug delivery is among the most common forms of drug delivery due to its ease and positive patient compliance. Gastroretentive drug dosage forms are favorable in order to prolong the gastric residence time so that bioavailability and therapeutic effects are improved. Oral routes are also favored due to the ability to protect the drug from enzymatic degradation [320]. Gutowska *et al.* focused on a new hydrogel delivery method that can exhibit delayed, zero-order, or on-off release profiles. The controlled delivery of the drug can assist with problems such as drugs decomposing too quickly in the stomach, or irritated stomach leading to adverse effects in the upper GI tract [321,322].

The parenteral route seems to be the favored route of administration for many drugs such as peptides and proteins. Hydrogels can be created to prolong drug release and gradually release the bioactive components to the patient. In addition, hydrogels can also increase drug half-life, increase bioavailability, protect drugs from enzymatic degradation, and decrease the frequency of drug administration, which could then lead to increased patient compliance [323]. Another

positive component for some injectable hydrogels, such as chitosan, is that they are usually fluid at room temperature and viscous at body temperature. This gelation allows for sustained drug release and improved bioavailability.

The nasal route of delivery is typically used to treat certain ailments such as nasal allergies, congestion, and infections. However, recently, this route has been used for the delivery of small molecular weight polar drugs, proteins and peptides, in order to provide rapid uptake of the drug, something other routes fail to achieve [324]. Illum *et al.* reported in her paper that the most important limiting factor in the nasal route of drug delivery is the low membrane permeability. Another barrier that exists is the short nasal residence due to the mucosal turnover. Additionally, chitosan hydrogels have been known to be effective for nasal delivery due to their mucoadhesive, viscoelastic, and biocompatible properties. In turn, chitosan hydrogels can increase nasal residence time. Developments in the delivery route from nose to brain, and in maximizing rapid and highly concentrated drugs in the brain to elicit an efficient therapeutic response, are promising. Wu *et al.* studied a thermosensitive hydrogel and its prospective use for nasal drug delivery. The solution, when applied to the nasal cavity, turned into a viscous hydrogel at body temperature, reducing the rate of nasal mucociliary clearance and causing the drug to slowly release. Furthermore, Wu *et al.* explored quaternized chitosan as an absorption enhancer, leading to the capacity to open tight junctions between epithelial cells. They found that the hydrogel decreased the concentration of blood glucose (40-50% of the initial concentration) for 4-5 hours post-administration, with no signs of cellular toxicity after application [325].

The ocular route has been met with some resistance in the field of drug delivery due to anatomical and physiological barriers that protect the eye from toxicants, though there are multiple ways to deliver drugs *via* the ocular route. These include topical, intravitreal, intracameral, and subtenon, among others. The benefits that follow include patient compliance, direct delivery to vitreous and retina, sustaining drug levels, and ease of administration. Some challenges that exist include higher tear dilution and turnover rate, toxicity due to high dosage, and cataracts, among others [326]. Gulsen *et al.* suggests that the mainstream route of eye-drops is ineffective, as 95% of the drug contained in the drops is lost due to tear drainage or absorption by the conjunctiva. Gulsen and coworkers proposed to encapsulate the drug in nanoparticles and to place them on the lens material. These contact lenses would ultimately release and deliver drugs over a long period of time [327]. Especially in treating ocular diseases and issues, a non-invasive delivery method, a maintained drug release, safety, and a high efficiency of drug encapsulation are desired. Thus, Kang Derwent and Mieler designed a sustained-release localized drug delivery system that was able to control the release of anti-VEGF agents to combat ocular vascular disease [328]. The developed hydrogel had thermoresponsive

characteristics, so once the liquid was injected to the juxtasclear region *via* a small-gauge needle, the solution became a solid gel that released the encapsulated protein or anti-VEGF agent. Kang Derwent and Mieler argued that this system optimized the antiangiogenic effects and minimized the potential ectopic effects of a large bolus delivery. They concluded that thermosensitized hydrogels had the ability to deliver drugs to the posterior segment of the eye in a steady, controlled fashion [328]. In Liu *et al.*, they came up with an alginate hydrogel that supported human corneal epithelial cell growth using BSA as a drug model. Studies have shown that a composite hydrogel has the mechanical strength and optical clarity for use as a therapeutic lens and/or a corneal substitute for transplantation in corneal damage or diseases [329].

Topical, or transdermal drug delivery has been one of the more favored routes of drug delivery in recent years. There are three types of transdermal delivery systems: first-generation, second-generation, and third-generation. The first generation delivery systems provide the delivery of lipophilic, small sized and low-dose drugs, while the second generation delivery systems use chemical boosters, ultrasound and iontophoresis that do not depend on cavitation. Finally, third-generation delivery systems use microneedles, thermal ablation, microdermabrasion, electroporation, and cavitation ultrasound to target the stratum corneum [330]. Overall, the topical route allows scientists to address the issue of low bioavailability and difficulties that arise from other routes of delivery. Targeting the stratum corneum while specifically protecting deeper tissues is a milestone that makes the topical route poised to make a widespread impact. In Calixto *et al.*, they studied the effects of polyacrylic polymer hydrogels for topical use. They found that the polymer concentration raised the elastic, mechanical and bioadhesive characteristics of the hydrogel. Additionally, in an *in vitro* drug release test, they found that hydrogels controlled the release of the drug, improving the therapy outcome. They concluded that the polymeric hydrogels were promising platforms for bioadhesive topical drug delivery systems for the treatment of skin diseases [331]. In Reimer *et al.*, they created a povidone-iodine (PVP-I) liposome hydrogel that allowed for both moist and antiseptic treatment, and studied its effects [332]. In addition to the antimicrobial properties of PVP-I, it has been concluded that liposomes provided specificity to the target area, the ability to retain moisture, drug retardation, and prevented infections while activating the wound healing process.

Drug delivery *via* the brain is a difficult route due to the blood-brain barrier and the challenges it presents. Drugs, antibiotics, and neuropeptides all cannot overcome the barrier. However, nanoparticles seem to have the possibility to achieve desired therapeutic effects [333]. Nanoparticles have the potential to treat very aggressive brain tumors, among other things. The most likely mechanism would be through endocytosis by entering the endothelial cells of the brain blood capillaries [333]. Wang and co-workers also noted that the use of a hydrogel released in the subventricular zone to stimulate repair after a stroke decreased the stroke cavity

size, increased neurons in the peri-infarct region and migratory neuroblasts, and decreased apoptosis [334].

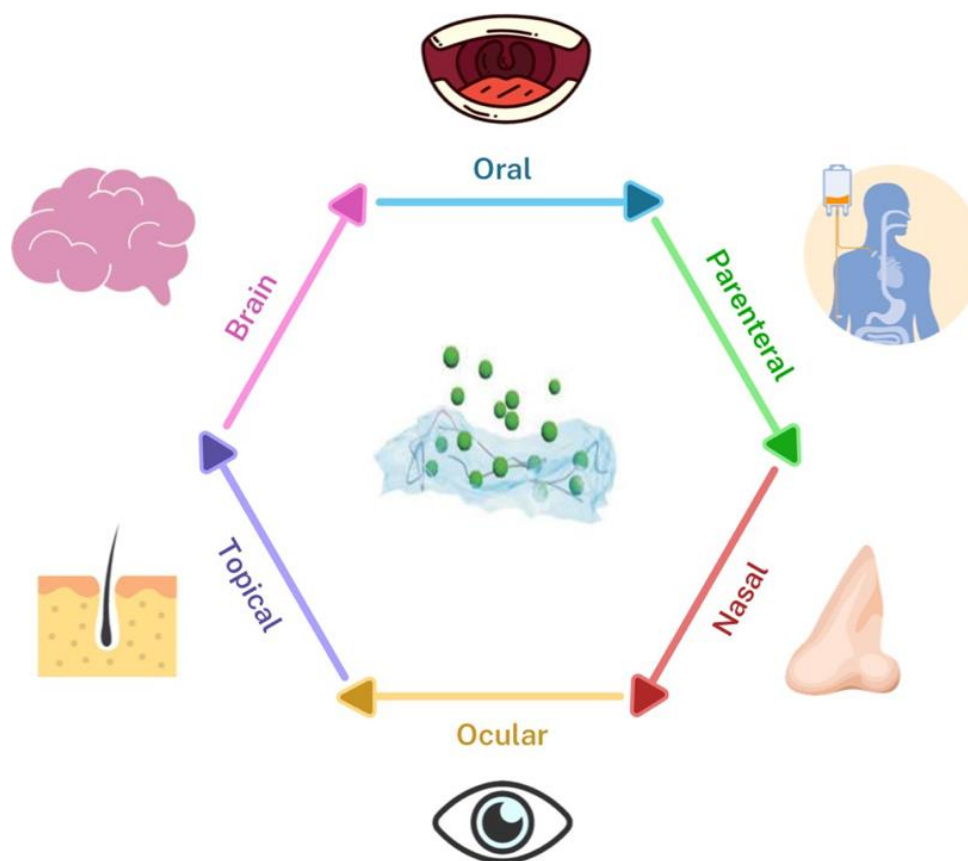


**Figure 5.** Schematic representation of the routes of administration of nanovesicle embedded hydrogel-based delivery platforms.

## 7. Conclusion and Future Perspective

Since its discovery in 1965, liposome technology has massively advanced in terms of versatility. Liposomes have been extensively studied as drug delivery nanovesicles due to their ability to deliver bioactive molecules of different sizes and to target specific cells/tissues through the chemical modifications of their surfaces. On the other hand, surface chemical modifications are not required to create targeting exosomes, as they naturally possess this ability due to cellular and lipid adhesion molecules expressed on their surface. However, challenges in loading large bioactive molecules efficiently in exosomes have called for the development of a novel hybrid system based on the membrane fusion between liposomes and exosomes. This novel system has so far seen applications in cancer and gene editing and possesses great potential to be applied for many targeted drug delivery applications.

Many challenges related to liposomes and exosomes still persist. Without any doubt liposomes are considered the most successful family within the field of nanomedicine. However, after 60 years of research, the full potential of the liposomes has yet to be fulfilled, as only a handful of liposomal drug formulations have reached the market. The main causes behind the low transition rate of liposomes from bench to bedside are their potential cytotoxic

effects, leakage, stability problems, batch to batch reproducibility, effective sterilization methods, and scale-up problems. For exosomes, the field is still in its infancy, as clinical trials have just begun, and many challenges still need to be answered, such as inefficient drug loading, variable compositions and complex structures, possible safety issues, and the lack of optimized purification methods needed for large-scale production. A more comprehensive review about the challenges that the clinical translation of nanoparticles faces was written and recently updated by Anselmo and Mitragotri [335,336].

It has become evident that hydrogels have substantial potential to be used for pharmaceutical applications. There exist many challenges and hurdles that need to be surpassed before clinically approving a hydrogel product. These challenges were recently discussed in detail in a comprehensive review by Mandal *et al.* [337]. Nevertheless, in recent years, the FDA has approved a number of marketed hydrogel-based products such as Belotero balance®, Revanesse® Versa™, SpaceOAR®, Teosyal® RHA, Radiesse®, and TraceIT® [205,337]. Depending on the added drugs and bioactive compounds, hydrogels can be classified Class I, II, or III medical devices by the FDA [206]. A bright future stands ahead for commercialized hydrogel products, as the demand for patient-specific healing processes and treatments continues to grow by the day. Whether natural or synthetic, diffusion controlled or stimuli-responsive, a number of hydrogels have been developed for controlled drug delivery, each presenting a set of advantages and limitations. One approach used to limit the disadvantages of preferred natural hydrogels is nanofunctionalization with soft and hard nanoparticles. Nanofunctionalization with targeting nanovesicles can, in addition to ameliorating the mechanical properties of polymers, deliver drugs to one cell type in a certain tissue, which can be useful in reprogramming and transdifferentiation applications.

Going forward, engineering effective targeted controlled drug delivery systems is of major importance and can achieve a huge breakthrough in treating many diseases, especially for cancer. These systems can form a depot around the tumor area, releasing smart nanovesicles encapsulating anticancer drugs in a controlled manner. This will lead to an increase in drug concentration in the tumor environment and to the targeting of cancer cells, while preserving healthy cells. In this review, we showed that hybrid exosome-liposome nanovesicles are great candidates for targeted drug delivery. However, because only a couple of groups have investigated such systems, more time is needed before we can fully judge the ability of this hybrid system. No research has been done yet on coupling this hybrid system with natural, synthetic, or stimuli-responsive hydrogels. Although, previous investigations of exosomes or liposomes embedded in hydrogels are promising.



Review

## **Biofabrication of Natural Hydrogels for Cardiac, Neural, and Bone Tissue Engineering Applications**

Kamil Elkhoury<sup>1</sup>, Margaretha Morsink<sup>2</sup>, Laura Sanchez-Gonzalez<sup>1</sup>, Ali Tamayol<sup>3</sup>, Elmira Arab-Tehrany<sup>1</sup>

<sup>1</sup> LIBio, Université de Lorraine, Nancy, F-54000 France.

<sup>2</sup> Department of Applied Stem Cell Technologies, University of Twente, Enschede, 7500AE The Netherlands.

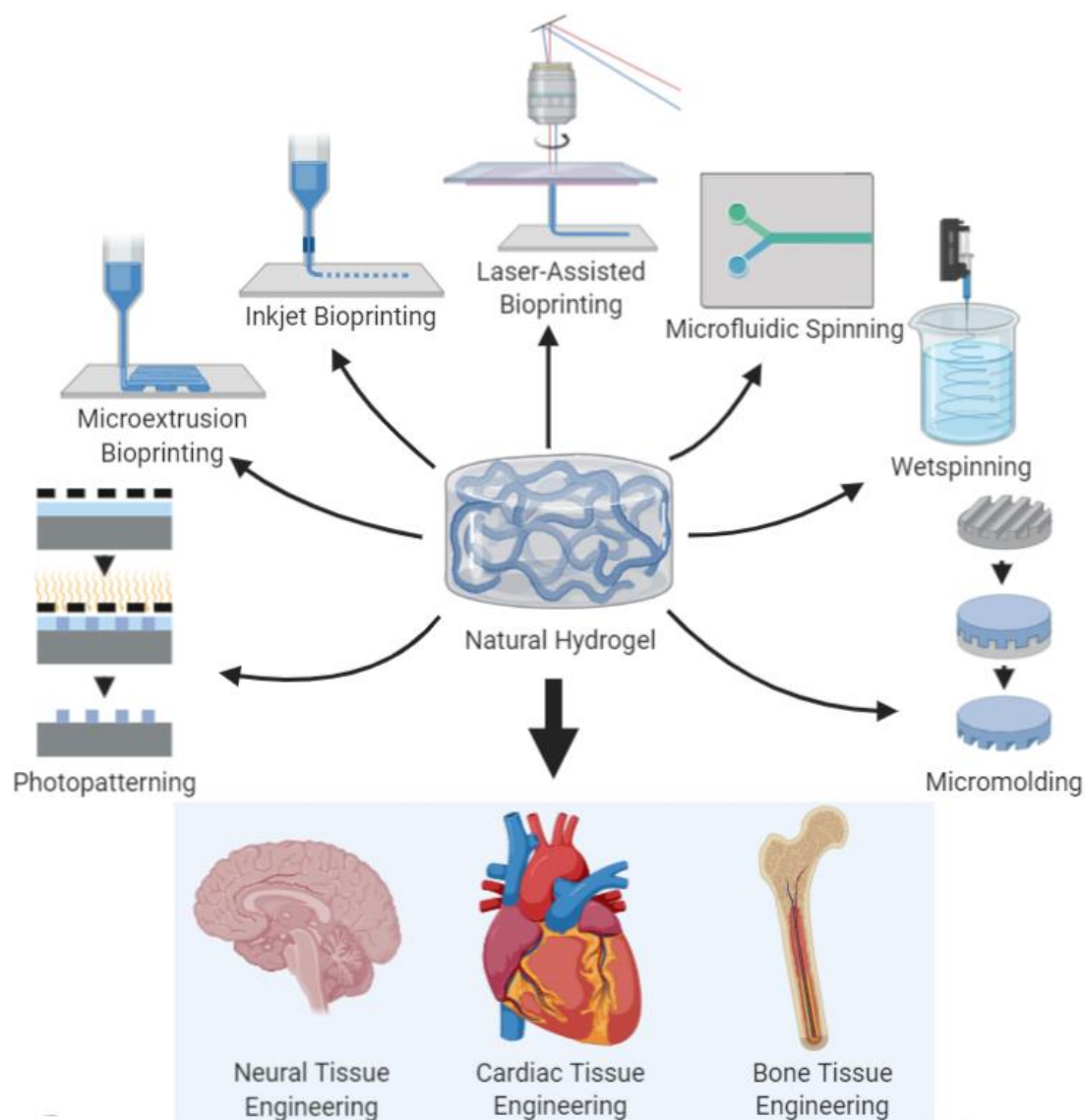
<sup>3</sup> Department of Biomedical Engineering, University of Connecticut, Farmington, CT, 06030 USA.

### **Highlights**

- Different biofabrication techniques of natural hydrogels were overviewed.
- The progress, advantages, and disadvantages of the novel biofabrication strategies were discussed.
- Novel applications of biofabricated natural hydrogels in cardiac, neural, and bone tissue engineering were presented.
- Overlooked challenges facing the translation of biofabricated scaffolds and their potential solutions were highlighted.

### **Abstract**

Natural hydrogels are one of the most promising biomaterials for tissue engineering applications, due to their biocompatibility, biodegradability, and extracellular matrix mimicking ability. To surpass the limitations of conventional fabrication techniques and to recapitulate the complex architecture of native tissue structure, natural hydrogels are being constructed using novel biofabrication strategies, such as textile techniques and three-dimensional bioprinting. These innovative techniques play an enormous role in the development of advanced scaffolds for various tissue engineering applications. The progress, advantages, and shortcomings of the emerging biofabrication techniques are highlighted in this review. Additionally, the novel applications of biofabricated natural hydrogels in cardiac, neural, and bone tissue engineering are discussed as well.



**Keywords:** Hydrogel; Microfabrication; Bioprinting; Textiles; Tissue engineering; Regenerative medicine.

## 1. Introduction

Tissue engineering, as defined by Langer and Vacanti in 1993, is an interdisciplinary field that applies both the principles of life sciences and engineering to develop biological substitutes or entire organs [1]. Beyond that initial goal, tissue-engineered constructs have found a variety of new applications, such as being research tools that could improve our understanding and testing of diseases [338–342]. Furthermore, the development of personalized therapies is expected to be further facilitated by utilizing patient-specific cells and biological factors [343,344,23,345]. Recently, tissue engineered constructs have even explored as tools for food production.

Hydrogels are high water content materials and one of the few biomaterials that can be used to fabricate extracellular matrix (ECM) mimicking scaffolds [299,346]. Moreover, in addition to being highly biocompatible, hydrogels possess an advantageous physical and

biological tunability, and desirable robustness in biofabrication [347–349]. To avoid the potential risk of inflammatory and immunological responses of synthetic polymeric materials, the naturally-derived crosslinked polymeric networks are the preferred choice for fabricating ECM mimetic scaffolds [2,6,65,3].

Even though new types of tissues and organoids are being developed and fabricated, many challenges remain to be addressed before being able to create fully-functional tissues [13]. One of the main challenges is to create load-bearing structures that can replicate the complex architecture and physical properties of the native ECM. These type of structures cannot be fabricated using conventional techniques only, such as solvent casting/particulate leaching, freeze-drying, and gas foaming, but requires advanced biofabrication techniques, such as bioprinting and textile-based techniques [350,351]. Biofabricated textiles can form stronger supporting structures, whereas bioprinted constructs have more complex and controlled architectures [14].

These advances in biofabrication techniques have led to various novel applications in tissue engineering, from creating electroactive scaffolds, that modulate cell proliferation and differentiation, to smart scaffolds, that sustain the dynamic nature of the tissue's microenvironment, which have opened doors to immense developments in cardiac, neural, and bone tissue engineering [15–17].

Here, we review the various biofabrication processes that can create organized and robust tissue constructs from naturally-derived hydrogels. Their main advantages and disadvantages, as well as their recent progress and recent cardiac, neural, and bone tissue engineering applications are discussed. The challenges and potential opportunities in the field of biofabricated natural hydrogels are also outlined.

### **2. Biofabrication of natural hydrogel-based scaffolds**

Mimicking the architectural features of native tissues is important in recapitulating their function with engineered tissue constructs [352]. The important aspect of controlling scaffold porosity and microarchitecture is directing tissue formation and function [353]. Scaffold porosity and pore interconnectivity affect its stiffness [354], ECM secretion [355], as well as cell survival, proliferation, and migration [356]. Original scaffold manufacturing approaches, such as solvent casting/particulate leaching, freeze-drying, and gas foaming present the ability to produce and control the size and porosity of interconnected porous structures. Yet, they do not allow the fabrication of complex geometries or controlled cellular distribution within the scaffold for developing functional and biomimetic tissues [14].

Advanced manufacturing techniques, such as microfabrication tools, fiber-based technologies, and three-dimensional (3D) bioprinting have been developed, emerging as strong

tools in tissue engineering. These technologies provide a way to overcome the limitations of conventional techniques, along with allowing the precise control over mechanical properties, structural properties, microarchitecture, pore size, pore geometry, pore interconnectivity, and cellular distribution of complex engineered cell-laden scaffolds [357]. Fiber-based technologies and 3D bioprinting have been applied to a multitude of tissue engineering applications because of their robustness in creating structures with biomimetic architectures and properties enhanced by microfabrication tools [358–360]. In this section, we will discuss various biofabrication technologies that can be used for engineering structured constructs and scaffolds from natural hydrogels.

### 2.1 Microfabrication techniques

Numerous modern microfabrication techniques have been explored to control the microstructure of natural hydrogels to tune the cell-material interactions and cell behaviors. Photopatterning and micromolding are two of the most widely used, cutting-edge microfabrication techniques that generate 3D cell-laden hydrogel microstructures with controlled morphological, structural, and physical properties [161].

**Photopatterning**, also known as photolithography, is a technique consisting of using light to imprint patterns into materials [161]. First, a mask is created, containing the pattern to be implemented; it possesses transparent areas to pass the light and other opaque areas to block the light. Microengineered hydrogels are created via light irradiation forming the micropatterns. Areas under the transparent region of the mask are crosslinked and under the opaque parts it remains uncrosslinked; that of which are washed out afterward. Since light is used to crosslink these hydrogels, they should be photocrosslinkable. For this purpose, hydrogels can be made photocrosslinkable by conjugating acrylamide- or acrylate-based groups to the prepolymer backbone, such as in the case of gelatin methacryloyl (GelMA) [3] and methacrylate hyaluronic acid (HA) [361]. A photoinitiator is added to commence the polymerization reaction by forming radicals upon light irradiation.

Photopatterning is a flexible easy-to-use technique and allows precise spatial control over the cellular microenvironment without the need for sophisticated equipment. Furthermore, it allows the fabrication of 3D cell-laden hydrogel constructs containing various cell types by patterning different cells through sequential photopatterning. Determining the suitable ultraviolet exposure time, the fabrication of only planar constructs, and the use of multiple photomasks to control cell distribution are the main challenges faced by the photopatterning technique [50].

GelMA hydrogels were photopatterned through UV crosslinking by Nichol *et al.* and loaded with human umbilical vein endothelial cells (HUVECs) [4]. The results showed high

cell viability after the biofabrication process and the hydrogel's mechanical properties were found to be directly affected by the UV exposure time and methacrylation degree. In a follow-up study, Aubin *et al.* photopatterned cell-laden GelMA hydrogel encapsulating fibroblasts, myoblasts, ECs, and cardiac stem cells with different widths to control the alignment and elongation [362]. The study proved that the widths of the photopatterned rectangular microconstructs had a significant impact on the morphology and self-organization of cells. Although UV is the most common light source for photocrosslinking of hydrogels, researchers have tried to use light sources with higher wavelengths to reduce the risk of DNA damage [363,364]. However, it should be noted that the use of higher wavelength light sources might reduce the achievable resolution.

**Micromolding** consists of employing molds fabricated from plastics, polymers, and metals to microfabricate both physically and chemically crosslinked hydrogel constructs [50]. Micromolding is a rapid, robust, biocompatible, cost-effective, easy-to-use, and scalable technique. Most popular molds used today are fabricated from polymers such as poly(methyl methacrylate) (PMMA) and elastomers such as polydimethylsiloxane (PDMS) [365].

This technique can be used to create complex structures with high resolution via layer-by-layer fabrication and an assembly step. Layers of cationic, neutral, and anionic polymers are usually deposited onto a solid substrate, such as silica particles or sugar beads. This is well-known as the layer-by-layer technique and synonymously as electrostatic self-assembly. The multilayers are stabilized by the electrostatic forces. One or more drugs could be incorporated into the layers. Meanwhile, the layer-by-layer method has been extended to other materials such as proteins and colloids. Moreover, hollow nano and microspheres are obtained through layer-by-layer adsorption of oppositely charged polyelectrolytes on template nano- and microparticles.

In one study, a liver-like structure containing perfusable channels was created by He *et al.* from HepG2 cells encapsulated within micromolded agarose hydrogel; a natural hydrogel with good biocompatibility and mechanical properties [366]. Negative PDMS molds, injected with a collagen solution containing HUVECs, were used to fabricate this liver construct that had high cellular viability over 3 days of culture *in vitro*. Despite the many advantages, the fabrication of 3D vascularized geometries is not possible without the combination of other fabrication techniques, such as rapid prototyping strategies. Besides, the restriction to planar structures and the reduction in feature quality at high height to width ratios are two other major drawbacks of the micromolding technique.

Generally, micromolding is remarkably flexible and arguably the simplest microfabrication technique for hydrogels. On the other hand, photopatterning has rapidly evolved into a very powerful and flexible tool with many reported variations. There is still a

need to incorporate and control the release of growth factors within hydrogels at predefined patterns; to stimulate cellular growth, proliferation, healing, and cellular differentiation of embedded cells. This is a problem that could be solved by microfabricating cell-laden hydrogels that are nanofunctionalized, preferably with soft nanoparticles [2].

### 2.2 Fiber-based technologies

Fibrous scaffolds offer anisotropic mechanical and architectural properties, which mimics those observed in some native tissues such as tendons, ligaments, and muscles [367,368]. These scaffolds can be fabricated using several different techniques such as random, organized stacking of fibers, or assembly using textile processes. Regardless of the assembly process, fibers are the essential component of such scaffolds. There exist only a few fabrication technologies that allow the engineering of continuous fibers from hydrogels including interfacial complexation, wet spinning, and microfluidic spinning.

**Interfacial complexation** consists of fabricating fibers at the interface of two oppositely charged polyelectrolyte solutions through polyion complex (PIC) formation [369,370]. Forceps or a bent needle were used to fabricate fibers, of 10-20  $\mu\text{m}$  diameters with a range of tensile strength of 20-200 MPa, by drawing upwards the contact interface of two oppositely charged polyelectrolyte droplets placed in close proximity [371]. The main advantage of this technique is that it produces fibers at room temperature under aqueous conditions, which allows the encapsulation of biologics; such as cells, proteins, and the fabrication of cell-laden hydrogel fibers [371,372]. The simplicity of this technique does not make large scale production easy to achieve. In addition, the limited type of materials that can be used and the small range of the fabricated fiber diameters, similar to the diameter of a cell, are two other major drawbacks of this technique. Natural polymers, mainly cellulose, chitosan, and alginate, were used previously to create cell-laden hydrogel fibers by interfacial complexation [371,372]. In one study, Leong *et al.* fabricated cell-laden alginate-chitosan hydrogel fibers using interfacial polyelectrolyte complexation to create aligned and spatially defined prevascularized tissue constructs with endothelial vessels [373]. Other previous studies have shown that vascular integration of the used tissue construct with the host is successfully promoted by the creation of a preformed microvascular network within the construct [374–376]. However, since this method is limited in the number of materials and fibers size range, the industrial-scale production of cell-laden structures is challenging [358].

**Wet spinning** consists of continuous extrusion of a prepolymer from a spinneret orifice into a bath containing crosslinking reagents [369,377]. Wet spinning enables the fabrication of cell-laden hydrogels with a diameter in the range of 100  $\mu\text{m}$  to several millimeters. The fabricated fibers with larger diameters carry the risk for the occurrence of weak points due to

improper network crosslinking in regions far from the fiber surface. The large diameter of the fibers can also limit oxygen and nutrient diffusion, negatively impacting the survival of encapsulated cells [14]. In recent work, Mirani *et al.* 3D printed a grooved positive mold that was used in a casting process to fabricate grooved extruders that in turn were used in a developed wet spinning device (**Fig. 1 A**) [378]. Sodium alginate solution was continuously extruded into a calcium chloride bath by the fabricated grooved extruders to produce grooved solid and hollow hydrogel fibers with controlled porosity, surface morphology, and cross-sectional shape. In addition to fabricating complex 3D structures using these fibers *via* textile technologies (weaving, braiding, and embroidering), the grooved fibers were able to induce alignment along the grooves of myoblasts, cardiac fibroblasts, cardiomyocytes, and glioma cells, as opposed to their random alignment on unpatterned fibers.

Yang *et al.* produced shear-patterned natural alginate hydrogel microfibers with aligned submicron topography [379]. Submicron topography alignment of the wet spun hydrogel microfibers was controlled by varying the rotary rate of the receiving pool and perfusion rate of the prepolymer. Rat neuron-like PC12 cells and human osteosarcoma MG63 cells were successfully cultured in the wet spun biocompatible hydrogel microfibers. The study investigated the effect of different rotation rates of the receiving pool, different perfusion rates of alginate on the fiber topography, and the effect of this topography on the cell orientation along with the fiber axis. The results showed that the bigger the rotation rate and the smaller the perfusion rate the higher the submicron topography alignment was and that the cells cultured on shear-patterned fiber (SP fiber) showed oriented distribution, unlike the random distribution of cells cultured on a petri dish (**Fig. 1 B-E**).

**Microfluidic spinning** consists of creating biofibers in a microchannel by co-flowing a prepolymer and a crosslinker in a coaxial fashion [357,380]. Fibers with a variety of structures can be produced by microfluidic spinning; this includes flat fibers, spiral curls, solid cylinders, Janus structures, hollow tubes, and bamboo-like architectures using coaxial laminar flows [381]. Microfluidic spinning enables the fabrication of cell-laden hydrogels and of microfibers in a mild environment in which most natural polymers can be spun into hydrogel-based microfibers without the use of additives [382]. Multi-compartment fiber production that mimics the native tissue's heterogeneous 3D structures, usually consisting of various types of cells, is possible when using programmable microvalves. Nonetheless, this technique is relatively slow. Other limitations include the risk of nozzle clogging during production and the need for fast solidification of fiber materials [14]. The lack of suitable materials that satisfy microfluidic fabrication is another shortcoming that was targeted by Zuo *et al.*, who developed a combination of alginate-GelMA composite hydrogel with capillary-based microfluidic technology [383]. The microfluidic-based on composite microfibers showed improved mechanical properties

compared to the one based on pure alginate. It successfully mimicked blood vessel-like microtubes by encapsulating HUVECs in the middle layer and mimicked bone ECM by encapsulating human osteoblast-like cells (MG63) in the outer layer (**Fig. 1 F-I**). Generally, microfluidic spinning is the most suitable spinning technique for creating cell-laden hydrogels; as it offers superior control over the fiber size, shape, and overall biochemical composition [14,357,384].

After cell-laden fibers are fabricated, textile technologies such as weaving, knitting, and braiding, can be used to fabricate tissue engineering scaffolds with tailored microarchitecture to optimize different properties and cellular behavior [78,350].

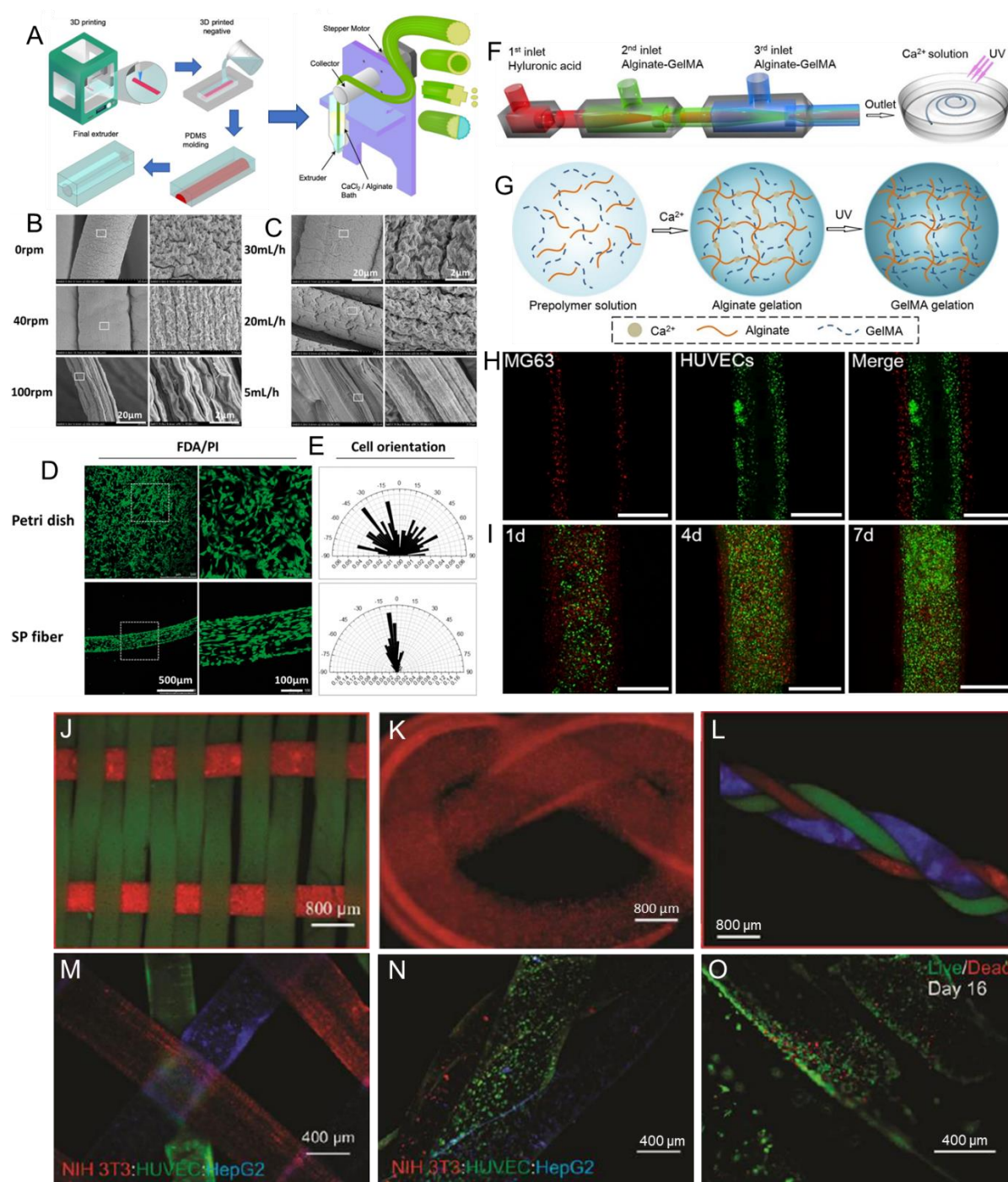


**Fig. 1.** A) Schematic illustration of the fabrication process of the grooved extruders, the wet spinning device, and the hydrogel solid and hollow grooved fibers. Reproduced with permission [378]. Copyright 2020, American Chemical Society. Wetspun shear-patterned alginate hydrogel microfibers: SEM Images of the orientation trend of submicron topography on hydrogel microfibers fabricated with (B) different rotation rate  $\omega$  (rpm) of receiving pool and (C) different perfusion rate  $Q$  (ml/h) of alginate, and (D) the spreading and (E) orientation of PC12 cells that were cultured on a petri dish and a shear-patterned fiber (SP fiber) after 3 days. Reproduced with permission [379]. Copyright 2017, Oxford University Press. Microfluidic fabrication of a GelMA-alginate composite natural hydrogel: (F) Ca-alginate reaction and UV exposure resulting in the formation of microfibers, (G) Schematic illustration of network formation of the composite natural hydrogel, (H) fluorescent image of cell distributions in the microfibers (HUVECs stained with CM-FDA (green) encapsulating in middle layer and MG63 stained with CM-DIL (red) encapsulating in outer layer) and (I) Confocal images of cell-laden alginate-GelMA composite hydrogel microfibers after incubation for 1, 4, and 7 days. Reproduced with permission [383]. Copyright 2016, Elsevier. Micrographs showing: (J) woven alginate:GelMA fibers, (K) knitted alginate:gelatin fibers, and (L) braided alginate:GelMA fibers. Micrographs showing: (M) a multilayer construct form from different stained cell types (NIH-3T3-red; HUVEC-green; HepG2-blue), (N) three different cell-laden alginate:GelMA fibers forming a braided cell-laden structure, and (O) high cellular viability after 16 days of culture in the braided fibers. Reproduced with permission [78]. Copyright 2015, Wiley-VCH GmbH.

**Weaving** consists of creating fabrics and 3D constructs by interlacing two different sets of warps at right angles [369]. Weaving can create lightweight, flexible, and strong structures with controlled geometry, porosity, morphology, and strength; achievable in a less mechanically harsh process, but possess a low porosity with small pores [357,369]. Woven natural hydrogel fibers have been used to control the cellular distribution within a construct. For example, Onoe *et al.* assembled cell-laden hydrogel fibers to create complex constructs with a controlled cellular pattern [385]. The microfibers had a core-shell structure, where the core was composed of gelated ECM proteins encapsulating differentiated cells or somatic stem cells, while the shell was composed of Ca-alginate hydrogel. In another study, Tamayol *et al.* created woven constructs (**Fig. 1 J**) from wetspun cell/bead-laden alginate/GelMA hydrogel fibers [78]. The pure natural hydrogel fibers were able to endure the weaving fabrication process and generated a woven construct that could be handled manually. The alginate/GelMA fibers successfully encapsulated NIH-3T3 fibroblasts for 5 days.

**Knitting** consists of forming symmetric loops and complex patterns by intertwining threads or yarns in the form of stitches [369,384]. The knitting process is highly flexible and can create complex structures having the ability to stretch using computer-aided design (CAD) systems. On the other hand, it is a complex technique, and adjusting the knitted construct properties in different directions is challenging [14,357]. Pure natural hydrogel fibers were used by Tamayol *et al.* to create a gelatin knot (**Fig. 1 K**) [78]. A fiber of alginate/gelatin was initially used to form the knot and was then treated with an EDTA solution to remove alginate from the construct.

**Braiding** consists of forming complex structures or patterns in a cylinder or rod shape by intertwining three or more fiber strands [357,369]. Braiding offers many advantages; such as

high structural integrity, high flexibility, plus high axial, in-plane, and through-plane mechanical properties [14]. As with the other techniques, there are some disadvantages as well; geometrical limitations, inherently limiting its application and creating less porous structures [14]. Akbari *et al.* braided three different composite fibers that were comprised of a load-bearing core fiber, a sheath of cell-laden natural alginate, and GelMA hydrogels; containing NIH 3T3 cells, HepG2 cells, and HUVECs, respectively, as a model for the liver [384]. However, the only pure natural hydrogel fibers that were used to produce braided constructs, were fabricated by Tamayol *et al.* from microbead-laden alginate/GelMA hydrogel fibers (**Fig. 1 L**) [78]. In the same study, 3D constructs formed from separate HUVEC-, HepG2-, and NIH-3T3-laden alginate/GelMA hydrogel fibers were stacked, braided, and assessed as a model of liver tissue (**Fig. 1 M-O**).

Textile techniques provide the ability to engineer tissue-like structures and scaffolds with controlled microarchitecture and cellular distribution by knitting, weaving, or braiding cell-laden fibers spun from biocompatible natural hydrogels. Additionally, these biotextiles are highly porous; in turn making them permeable to growth factors, nutrients, and oxygen. Cell-laden fiber assembly is a promising technique for building complex organs by protecting cells from the immune system during their growth, proliferation, and ECM secretion. The main challenges for the use of biotextiles for tissue engineering are the automation of the process combining textile machinery and biomaterials used to create tissues and organs. The low mechanical strength of cell-laden fibers makes their processing with the harsh textile techniques difficult, as the final structure will be too fragile to be used. The latter problem can be addressed by either coating a mechanically strong core material with a cell-laden natural hydrogel layer to create cell-laden fibers, or by creating cell-laden fibers from nanofunctionalized cell-laden natural hydrogels with nanoparticles that reinforce their structure [2,386].

Therefore, forming stronger fibers in an automated large-scale process is a necessity if tissue engineering scaffolds will be produced using fiber-based techniques. For this, new textile machines providing control over humidity, oxygen, CO<sub>2</sub> levels, environment sterility, and nutrient access to cells encapsulated in the fibers of the generated textiles are required.

### 2.3 Bioprinting

3D printing or additive manufacturing (AM) consists of producing a three-dimensional object of almost any shape or geometry by forming successive layers of material under computer control using digital model data [23,387,388]. 3D bioprinting is the utilization of 3D printing technology and bioinks (bioprintable materials) to fabricate complex 3D functional living tissues by combining living cells, biomaterials, and biochemicals, using several different methods with different characteristics summarized in **Table 1** [389–393]. Bioprinted scaffolds

can be fabricated using several different methods, each of which possesses its own advantages, disadvantages, and material demands. In general, a typical process for bioprinting 3D tissues encompasses 6 steps and in each step, a choice should be made based on the final application and the desired properties: Imaging (X-ray, computed tomography CT, magnetic resonance imaging MRI), design approach (biomimicry, self-assembly, mini-tissues), material selection (natural polymers, synthetic polymers, ECM), cell selection (differentiated cells, pluripotent stem cells, multipotent stem cells), bioprinting technique (inkjet, microextrusion, laser-assisted), and finally the application (maturation, implantation, *in vitro* testing).

**Table 1.** Comparison of inkjet, laser-assisted, and microextrusion bioprinting techniques [389–393].

	<b>Inkjet</b>	<b>Laser-assisted</b>	<b>Microextrusion</b>
<b>Natural bioink</b>	Alginate, agarose, cellulose, collagen, fibrin, gelatin, silk fibroin	Alginate, collagen	Alginate, agarose, cellulose, chitin, chitosan, collagen, fibrin, gelatin, hyaluronic acid, silk fibroin
<b>Material viscosity</b>	Low ( $<12$ mPa/s)	Low ( $<300$ mPa/s)	High ( $>6 \times 10^7$ mPa/s)
<b>Preparation time</b>	Short	Medium to long	Short to medium
<b>Resolution</b>	High ( $10$ - $50$ $\mu\text{m}$ )	High ( $10$ - $100$ $\mu\text{m}$ )	Medium ( $20$ - $200$ $\mu\text{m}$ )
<b>Print speed</b>	Fast ( $1$ - $10000$ droplets/s)	Medium ( $200$ - $1600$ mm/s)	Slow ( $10$ - $50$ $\mu\text{m/s}$ )
<b>Printer cost</b>	Low	High	Medium
<b>Cell viability</b>	High ( $>90$ %)	High ( $>90$ %)	Low ( $75$ - $90$ %)
<b>Cell densities</b>	Medium ( $10^6$ - $10^7$ cells/mL)	High ( $>10^8$ cells/mL)	High ( $10^8$ - $10^9$ cells/mL)

*Inkjet printers* are the most widely used printers for 2D and 3D printing; they consist of delivering controlled liquid volumes to locations that have already been defined. Inkjet bioprinters are low-cost printers with high printing speeds and can enable several polymerization mechanisms. Disadvantages of inkjet bioprinting include: their limited ability to handle liquids with limiting ranges of viscosity, restriction to thin structures, applied mechanical and thermal stresses (which reduces cell viability), and they produce solutions with low cell density [14]. Inkjet printing technology has been used for several tissue engineering applications, such as bone [394,395], cartilage [396], neural [397], cardiac [398], and skin [399]. For example, Gao *et al.* successfully 3D inkjet bioprinted, human stem cells, and PEG-GelMA

hybrid scaffold for bone and cartilage tissue engineering; which showed improved mechanical properties and precise deposition of cells [400].

Recently, Teo *et al.* have created fine 3D microstructured alginate hydrogels in a single step using a micro-reactive inkjet printing technique (**Fig. 2 C**), based on the in-air collision of the precursor and cross-linker microdroplets [401]. This novel technique surpasses the limitations of conventional single- and full-reactive inkjet printing techniques (**Fig. 2 A,B**), mainly the time-consuming gel substrate preparation and the complicated cross-linker bath optimization, which opens new paths for tissue engineering by 3D bioprinting microarchitectures analogous to human tissues.

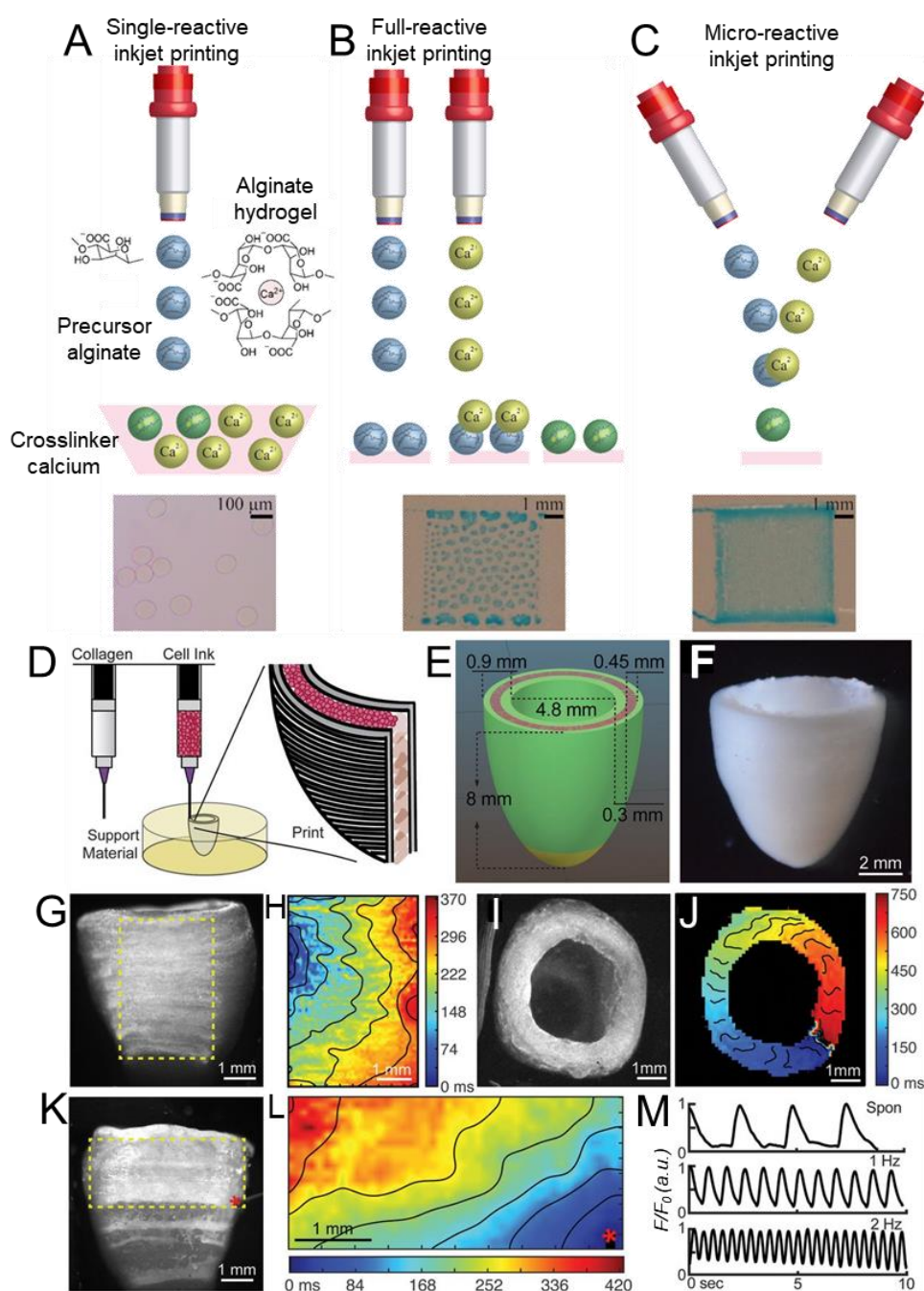


**Fig. 2.** Illustration of (A) single-, (B) full-, and (C) micro-reactive inkjet printing approaches to fabricate alginate hydrogel. Reproduced with permission [401]. Copyright 2019, American Chemical Society. D)

Schematic representation of the dual-material FRESH printing process and (E) the construct dimensions. F) Micrograph of the final printed model. G,I) Side and top view of the calcium imaging of the printed structure and H,J) their respective spontaneous and directional propagation calcium wave that indicates the transmission of the action potential across embedded cardiomyocytes. K,L) Calcium signal propagation observed after point stimulation. M) Transient calcium waves measured during spontaneous and induced (1-2 Hz) contractions. Reproduced with permission [402]. Copyright 2019, AAAS.

**Laser-assisted bioprinting** is based on laser-induced forward transfer; a method that was developed for the purpose of patterning and transferring metals, of which has then been successfully applied to DNA [403], peptides [404], cells [405], and other biological materials [406]. Laser-assisted bioprinting is ideal for low viscosity materials; it facilitates high cell density and achieves a microscale resolution and high cell viability [14]. There are some disadvantages to laser-assisted bioprinting; such as high cost, complexity, limited polymerization mechanisms, narrow viscosity range, and it is restricted to thin structures [14]. Laser-assisted printing technology has been used for many tissue engineering applications, such as bone [407], cardiac [402], and skin [408–410]. Gruene *et al.* bioprinted a natural hydrogel, composed of alginate and ethylenediaminetetraacetic acid blood plasma, using laser-assisted bioprinting to study the effects of different processing parameters [411]. In another study, Koch *et al.* demonstrated the 3D arrangement of vital cells using laser-assisted bioprinting as multicellular grafts similar to native skin model by successfully bioprinting fibroblasts and keratinocytes embedded in collagen [409].

**Microextrusion bioprinting** consists of continuously dispensing biological materials and biomaterials through nozzles connected to bioink cartridges and is composed of a temperature-controlled dispensing system, a fiber-optic light source, a video camera, and a piezoelectric humidifier. Microextrusion technology has been used for several tissue engineering applications, such as bone [412,413], cartilage [414,415], neural [416,417], cardiac [418,419], skin [420,421], liver [422,423], and skeletal muscle [414,424]. Microextrusion bioprinting can create thick vertical structures, facilitate high viscosity and high cell density solutions, and enable several polymerization mechanisms; however, it possesses a tendency of nozzle clogging, achieving interlayer bonding is challenging, and in high-resolution structures, the nozzle shear can reduce cell viability [14]. Using this bioprinting technique, Billiet *et al.* biofabricated 3D printed macroporous cell-laden GelMA constructs for a tissue engineering application and succeeded in maintaining high cell viability (>97%) [425]. Nanocellulose–alginate bioink was successfully utilized by microextrusion bioprinters to fabricate human chondrocyte-laden natural hydrogels that maintained high cell viability and proliferation during *in vitro* culture [426,427]. This shows that the nanocellulose–alginate bioink has the potential of being used for articular cartilage tissue engineering.

Recently, microextrusion bioprinting in a support bath has been used by Lee *et al.* to enable the biofabrication of collagen, the primary component of the extracellular matrix in the human body, in a novel method called FRESH (freeform reversible embedding of suspended hydrogels) [402]. FRESH is based on the extrusion of bioinks within a gelatin-based thermoreversible support bath that be flushed away at 37°C. A human cardiac left ventricle, presenting contractile functions and synchronous electroconductivity, could be bioprinted (**Fig. 2 D-M**) using FRESH from a cardiomyocytes-laden fibrinogen bioink confined in a collagen ink. Lee *et al.* successfully bioprinted five components of the human heart spanning capillary to a full-organ scale using the FRESH method [402].

Lately, “time” is added as a fourth dimension to further develop the bioprinting technology from 3D bioprinting to 4D bioprinting [428,429]. The instances where external stimuli, such as cell fusion or self-assembly are present, cause objects to change their shape. 4D bioprinting promotes dynamic, structural, and cellular changes of tissue over time [430]. This will help overcome the static nature of 3D bioprinting and create tissue-like models that resemble the ones found in nature.

Generally, there is still not a clear classification or definition of 4D bioprinting, but two main approaches can be considered. The first approach is based on the deformation of bioprinted materials. These materials are responsive biocompatible materials, comparatively like natural hydrogels, that are able to change their shape or function according to external stimuli (i.e. water absorption, thermal stimulation, pH value, light, surface tension, and cell traction) [431]. Kirillova *et al.* fabricated hollow self-folding tubes by bioprinting shape-morphing cell-laden hydrogels composed of two natural biopolymers; alginate, and hyaluronic acid [432]. In this case, 4D bioprinting provided a unique control over the diameters and architectures of these self-folding tubes. The average internal tube diameter was as low as 20 µm, comparable to the diameters of the smallest blood vessels. These tubes maintained high viability of the printed marrow stromal cells for 7 days.

The second 4D bioprinting approach is based on the maturation of engineered tissue constructs that can be achieved by cell coating, cell self-organization, and matrix deposition. For example, vascular graft maturation can be promoted by coating an endothelial cell layer in the lumen of bioprinted engineered vascular grafts to prevent thrombosis [433,434]. Similarly, a connective tubular graft was formed from the cell self-organization of printed cellular toroids that contained human ovarian granulosa cells [435]. Likewise, matrix deposition from hMSCs seeded onto bioprinted tissue constructs prolonged its degradation time from 2 days to more than 2 weeks in media [436].

In general, 4D bioprinting presents the advantages of creating 3D complex tissue constructs based on responsive biomaterials and generating tissue constructs with

functionalities similar to those of native tissues [428,431]. Unfortunately, the presence of a stimulus can be a possible limitation of 4D bioprinting because it may damage or kill living cells [430]. Thus, the stimulus must be regulated or refined to prevent this problem from occurring to a significant degree.

Even though the bioprinting field is still in its early stages, it has successfully created several 3D functional living human constructs with mechanical and biological properties suitable for transplantation. Bioprinting technology can be used to print almost all types of biomaterials into scaffolds with tailored morphological, physical, and biological properties. These tailored properties can mimic native tissue properties and provide the required microenvironment for cells to grow, proliferate, and differentiate. Furthermore, patient-specific tissues can be bioprinted thanks to advancements in computer-aided manufacturing (CAM), medical imaging, and computer-aided design (CAD). Despite the wide range of advantages bioprinting present there still exists the inherent need for vast improvements and advancements in bioprinter technologies and processes.

Bioprinting still operates at a relatively low process speed; it takes hours to fabricate one construct because bioprinters use a relatively low resolution to cover a large area. Biomaterials used in bioprinting processes are in gel or sol-gel form and not in solid form; such as in the case of 3D printers, bioprinters still lack full automation [437]. Currently, most of the available hydrogel-based bioink materials lack the native characteristics present in native tissues and organs that exhibit a heterocellular architecture. A high concentration of hydrogels used in bioinks will result in high viscosity, this favors mechanical and structural integrity and allows for the bioprinting of complex shapes. However, at the same time, these bioinks will not support cell viability and proliferation. The solution here can be the use of small concentrations of nanofunctionalized hydrogels possessing improved mechanical properties in a bioink formulation. In terms of bioprinters commercially available on the market today, they have a high cost and limited variety.

Overall, there is vast room for improvements to be made in regard to bioprinters and bioinks; the range of compatible bioinks must be extended by using nanofunctionalized hydrogel-based bioinks, the methods of bioinks and cells deposition printed with increased precision and specificity must be developed and automated, the speed and resolution of fabrication must be increased, and finally, the high cost and size of bioprinters must be decreased.

### **3. Tissue engineering applications**

Using hydrogel scaffolds for tissue engineering applications is highly advantageous, as they offer attractive characteristics for multiple applications. For example, hydrogels offer a

range of mechanical properties, including desired stiffness and porosity, and allow for the incorporation of cells and bioactive molecules. Especially natural hydrogels appeal to tissue engineering applications, as they allow for improved cell adhesion, degradation of the material *in vivo* due to proteolytic activity, and exhibit inherent biocompatibility and lack cytotoxicity. Biocompatibility and biodegradability are of high importance, as adverse reactions to cells and tissue could lead to severe complications upon clinical use [438]. Moreover, the degradation rate of the scaffold should match the regeneration rate of the tissue, as this would allow for the most beneficial healing [439]. The hydrogel scaffold acts as the ECM and can integrate various growth factor hubs, specific to the tissue application, to allow for the most effective regeneration, and mimics the tissues' natural environment. It is therefore important that the mechanical properties of the scaffold match those of the inherent tissue [438,440]. Moreover, by using natural polymers, its natural structure and molecules, including RGD sequences and bioactive peptides, remain intact, which improves cell functionality, proliferation, differentiation, angiogenesis, amongst other beneficial effects [441]. In addition, biofabrication techniques using these natural hydrogels could allow for beneficial structures by mimicking the organization of the tissue, as well as improved incorporation of cells into the scaffold [442]. Moreover, the incorporation of various (nano)materials to tune the suitability and functionalize the scaffold to specific applications has been extensively examined [2]. The versatile properties of various biopolymers, including cellulose, gelatin, alginate, hyaluronic acid, and collagen, have been exploited by many researchers [443–445]. This chapter reviews the most recent advances in tissue engineering application using biofabricated natural hydrogels for the heart, nerves, and bone.

### 3.1 Cardiac Tissue Engineering

Cardiovascular diseases, including acute myocardial infarcts, are the leading cause of death worldwide. Interruption of the blood flow in the heart leads to ischemia, which causes severe damage to the heart tissue, including loss of cardiomyocytes (CMs). Moreover, infarcts initiate the wound healing response, which induces several morphological and functional changes to the heart tissue, including excessive matrix deposition, rendering the tissue non-functional (**Fig. 3 A**). The infarcted region in the heart can lead to severe complications and reduced quality of life. As of yet, there is no cure for repairing the damaged cardiac tissue other than organ transplantation. However, engineering cardiac tissues for tissue regeneration is an emerging therapeutic strategy. Especially using natural hydrogels, cardiomyocytes or stem cells can be grown on a cardiac patch, which can be implanted onto the infarcted site of the heart, which could possibly lead to amelioration of the disease [446,447].

There are several factors that should be considered when engineering cardiac patches or cardiac tissue. In addition to being biocompatible and biodegradable, the scaffolds for cardiac tissue engineering should be able to mimic and transduce the heartbeat. This encompasses a contractible and conducive biomaterial, with according mechanical and electrophysiological properties [448]. As the heart has a low inherent regenerative capacity, it is of high importance to allow for maturation and differentiation of implanted cells into conductive and contractile CMs [449]. Therefore, the most recent advances in cardiac tissue engineering have employed nanofunctionalization of natural hydrogels, using carbon nanotubes (CNTs), gold nanoparticles (AuNPs), or graphene and its derivatives [15].

Lee and coworkers have employed GelMA hydrogel with the incorporation of CNTs, graphene oxide (GO), and reduced GO (rGO) for cardiac tissue engineering and characterized the effects of the nanofunctionalization on cardiac functionality [450]. They postulate the importance of guiding the tissue regeneration using mechanical and electrophysiological cues derived from the carbon derivatives. All scaffolds exhibited electrophysiological properties and were conductive and posed the proper mechanical stiffness for the heart. Moreover, they found that the different types of functionalization allowed for different types of maturation of the tissue. CNTs led to a ventricular-like tissue, whereas GOs guided to atrial-like tissue, and rGO-GelMA resulted in a mixed phenotype of the CMs. This is likely a result of the integrin-mediated differentiation of the CMs, which was stimulated differently by using different carbon nanoparticles. Moreover, the engineered cardiac tissue showed similar gene expression of specific cardiac genes, such as Troponin I and Connexin-43 (Cx-43) to native cardiac tissue, as well as a similar alignment of fibers (**Fig. 3 B**). The use of carbon nanoparticles is highly advantageous in cardiac applications, due to its electroconductive behavior, in addition to low density, high aspect ratio, large surface area, and strong mechanical resistance. However, carbon nanoparticles pose debatable cytotoxicity [451]. For all tissue engineering applications, it is of the utmost importance to perform proper testing of toxicity and safety, and therefore cytotoxicity should be evaluated carefully [452].

Other researchers have employed the beneficial effects of GelMA as well for their cardiac constructs. Koti *et al.* created 3D bioprinted cardiac constructs using GelMA and optimized extruder pressure as well as UV exposure, which is necessary to crosslink GelMA into a functional hydrogel [453]. In addition, they incorporated fibronectin, a naturally occurring ECM molecule, which showed enhanced CM survival and spreading. However, there are no mentions of electrical conductivity, which could pose a serious limitation. Moreover, Zhu *et al.* have incorporated gold nanorods (GNRs) and created a biocompatible 3D bioprinted construct, which exhibited proper spreading and organization of CMs, as well as provided an electrically active microenvironment [437]. The GNRs improved the cell-cell interactions, by traversing the

pores within the hydrogel, in addition to advancing the synchronized beating of the CMs. Last, Li *et al.* used gold nanowires in GelMA, resulting in synchronized contractile behavior, as well as ideal electrophysiological properties [454]. This allowed for enhanced maturation and differentiation of CMs, creating a promising hydrogel for cardiac constructs.

AuNPs are highly attractive nanomaterials to incorporate within natural hydrogels for cardiac tissue engineering, as they are biocompatible and induce proper electrophysiological behavior to CMs [455]. Other than its use in GelMA, AuNPs have been incorporated into chitosan [456,457] and collagen [458,459] as well. The chitosan scaffold by Saravanan *et al.* not only incorporated AuNPs but also used GO to functionalize the hydrogel [457]. The scaffold exhibited desirable degradation properties, support of cell attachment and maturation, no cytotoxicity, and showed an increase in electrical conductivity and signal propagation. In addition, Cx-43 levels increased upon the addition of the conductive nanomaterials. *In vivo*, the scaffold showed improved heartbeat, contractility, and conductivity, creating a clinically attractive strategy. The AuNP nanofunctionalized collagen hydrogel was developed by Hosoyama *et al.* and showed that by using spherical AuNPs the Cx-43 expression was increased, compared to pristine collagen and incorporation of silver nanoparticles (AgNPs) (**Fig. 3 C**) [459]. In addition, recovery of infarcted myocardium in neonatal mice was observed upon the use of AuNP functionalized collagen. The AuNP collagen cardiac patch showed reduced scar size *in vivo*, no sign of arrhythmias, nor displacement of the spherical AuNPs, and therefore poses a promising novel therapeutic strategy for myocardial infarction.

Other researchers have employed collagen for the creation of cardiac constructs as well. Yu *et al.* incorporated different amounts of CNTs in a collagen hydrogel and evaluated the cardiac function of encapsulated CMs. They found that the CNT-collagen hydrogel was able to support cardiac function, as there were an improved rhythmic contraction and desirable mechanical stiffness with respect to the pristine collagen hydrogel [460].

Alginate hydrogel lends itself well for cardiac tissue engineering applications, because of its biocompatibility and ECM resemblance [461]. Researchers have been employing alginate formulations to help cardiac regeneration, and it is one of the first biomaterials tested in clinical trials [462]. A recent prospective on clinical trials using injectable alginate for patients with heart failure showed promising results for cardiovascular health, compared to the control group, indicating its high clinical potential [463]. However, there are still limitations to the use of alginate for cardiac applications, including the difficulty of recellularization due to low cell attachment [462]. Recently, Hayoun-Neeman and coworkers have employed peptides to improve cell attachment to overcome this limitation of alginate [464]. They have incorporated the arginine-glycine-aspartate (RGD) peptide, as well as heparin-binding peptide (HBP) into the alginate hydrogel and seeded stem cell-derived CMs. They monitored the cell function for

35 days, which showed increased expression of Cx-43 and alignment (**Fig. 3 D**), and similar results were found for the expression of Troponin I, T, and C, indicating a matured cardiac construct.

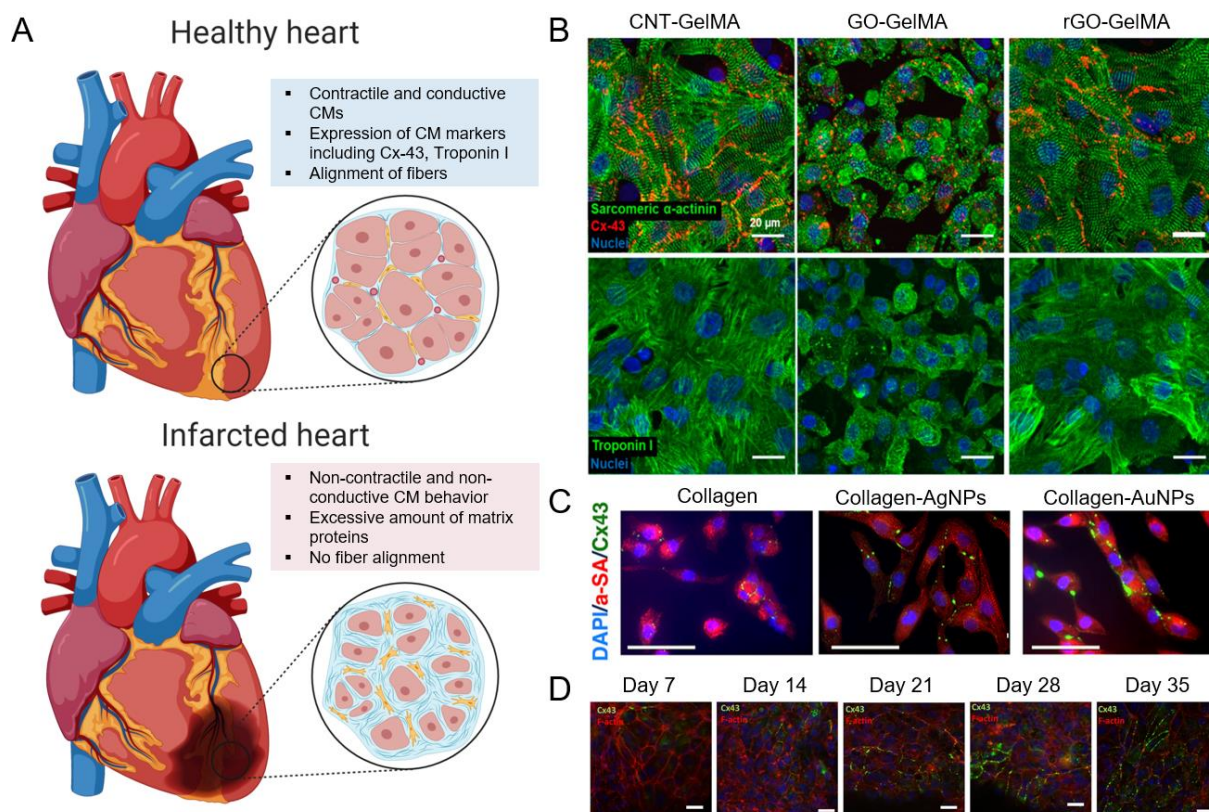


**Fig. 3.** Applications of natural hydrogels in cardiac tissue engineering. A) Schematic representation of healthy cardiac tissue vs. infarcted cardiac tissue. It can be seen the infarcted region does not exhibit contractile nor conductive behavior, as a result of an excessive amount of matrix. Created with BioRender.com B) Carbon functionalized GelMA constructs, exhibiting increased Cx-43 and Troponin I expression, as well as improved cellular alignment. Reproduced with permission [450]. Copyright 2019, American Chemical Society. C) Collagen hydrogels functionalized with AuNPs shows the best expression of cardiac maturation marker Cx-43 and improved cellular alignment. Reproduced with permission [459]. Copyright 2018, American Chemical Society. D) Alginate hydrogel functionalized with RGD and HBP peptides shows increasing Cx-43 presence over the course of 35 days. Reproduced with permission [464]. Copyright 2019, Wiley-VCH GmbH.

In conclusion, biofabricated and nanofunctionalized natural hydrogels, using either conductive nanomaterials or cell adhesive peptides, pose a great potential for cardiac regeneration. However, the questionable cytotoxicity of the electro-active components could pose problems upon clinical translation. Therefore, research should focus on the optimization of biocompatibility of carbon nanotubes, for example by using coatings. This will eventually allow for the clinical application of electro-active scaffolds for cardiac tissue engineering.

### 3.2 Neural Tissue Engineering

Neural tissue engineering is the repair and regeneration of the central nervous system (CNS) and the peripheral nervous system (PNS) [465]. The inherent regeneration capacity of neural tissue is very low, resulting in the requirement for external scaffolds and guidance to

allow for regeneration [466]. Impairment of the neural tissue can be a result of trauma, as well as various neurodegenerative diseases including Alzheimer's Disease, Parkinson's Disease, and amyotrophic lateral sclerosis. Moreover, stroke is a large cause of brain impairment as well. These neural impairments largely decrease the quality of life of the patients and they occur frequently worldwide, resulting in great demand for the regeneration of the tissue [467]. Current strategies involve the use of (natural) hydrogels as a scaffold for neural cultures, however, biofabrication techniques are increasingly used to desirable structures to enhance neural regeneration (**Fig. 4 A**). Hydrogels allow transducing of mechanical cues to the neural cells, thereby mimicking the native ECM [468]. Moreover, the inclusion of magnetic particles to create a magnetic field or the addition of growth factors or conductive materials prove to be useful to enhance the functionality of the scaffold [469]. Similarly to cardiac tissue, neural tissue inherently requires electrical conductance to allow for cell-cell signaling and therefore conductive hydrogels have positive effects on the cell proliferation, differentiation, and paracrine activity, and thereby regeneration of the tissue [470]. The next paragraph discusses the most recent advances in neural tissue engineering using natural hydrogels.

Collagen is a highly used natural hydrogel for the repairment of the brain and neural regeneration, as a result of its biocompatible, biodegradable, and versatile nature. Collagen can be used as an injectable scaffold, allowing to locally deliver neuroprotective soluble factors, as well as delivery of encapsulated stem cells with regenerative capacity, or to provide structural support for the axons to grow and adhere [471]. Moreover, collagen hydrogels are one of the first hydrogels in clinical trials for peripheral nerve damage, such as CelGro (ACTRN12616001157460), Neuromaix [472], and NeuraGen [473]. O'Rourke *et al.* have successfully used collagen tubes combined with a neural stem cell line to regenerate a murine sciatic nerve injury model [474]. They showed the engineered tissue performed well in the regeneration of axon, the formation of neurites, and exhibited functional electrical behavior, in addition to angiogenesis. Additionally, this network outperformed autografts, which is the current golden standard treatment of neural injuries, thereby proving the functional use of stem cell lines. Schuh *et al.* have combined collagen with fibrin to create a functional nerve conduit [475]. *In vivo* transplantation of the scaffold into a sciatic rat model showed enhanced axonal count compared to the collagen control in the middle and distal region of the nerve.

Others have used fibrin hydrogels as well for neural tissue engineering applications, due to its excellent biocompatibility, plasticity, flexibility, ability to incorporate cells and growth factors, and because it is a component of the native ECM [476]. Hasanzadeh *et al.* have incorporated multiwalled-CNTs (MWCNTs) as well as polyurethane (PU) into the fibrin gel scaffold to increase its conductivity to promote neural regeneration [477]. They assessed the

functionality of human endometrial stem cells and found that cell adherence, viability, and proliferation were optimal in the fibrin/PU/MWCNT hydrogel compared to the fibrin control.

Gelatin, as mentioned before, is a denatured form of collagen, which can be produced at low cost, provides high biocompatibility, and has improved cellular attachment sites, allowing for improved cellular adhesion and proliferation. In neural applications, gelatin is often electrospun, sometimes in combination with other polymers, which allows for the manipulation of functional properties. Especially the orientation of the nanofibers is easily controlled using electrospinning, ideal for neural engineering [478,479]. Electrospinning of gelatin fibers resulted in Schwann cell alignment, as well as optimal axon behavior and organization, allowing for the formation of artificial nerves [480]. Additionally, electrospinning of gelatin in combination with decellularized ECM proved high effectiveness in cellular function and proliferation [481]. However, gelatin can also be used without electrospinning. Researchers have tried to enhance the electrical properties of these gelatin scaffolds in various ways. For example, Gunasekaran *et al.* have created gelatin hydrogels and functionalized them with carbon black in order to create an electrically tunable scaffold, with lower electrical impedance compared to pristine gelatin [482]. Moreover, Wang *et al.* combined a gelatin/chitosan scaffold with PEDOT (poly(3,4-ethylenedioxythiophene)) nanoparticles, which is a biocompatible, conductive polymer, allowing for increased electrical conductivity of the scaffold compared to the non-functionalized gelatin/chitosan hydrogel [483]. In addition, cell adhesion and proliferation of PC12 neuronal rat cells, as well as neurite growth, was improved upon functionalization of the scaffold with PEDOT, shown by increased expression of GAP43, a neuronal regeneration marker, and of SYP, a synapse formation marker (**Fig. 4 B**).

The modification of gelatin with Methacrylic anhydride is often used for brain and neural tissue engineering as well. Rifai *et al.* investigated PC12 neural line's proliferation, signal propagation, and cytotoxicity when cultured on GelMA substrates, showing no sign of neurotoxic effects and good signal propagation [484]. Ye *et al.* have successfully implemented a 3D printing approach to create nerve guidance conduits for peripheral nerves by using GelMA and a PC12 culture [485]. They showed proper cell proliferation and survival, and in addition, the 3D bioprinted conduits allowed for neural differentiation. This was shown by culturing neural crest stem cells on the GelMA conduits and showing the abundance of an early neuron-specific marker (Tuj1), and neuron axon specific marker (PGP9.5). Enhanced green fluorescence protein (EGFP) indicates the presence of the neurons (**Fig. 4 Ci**). Moreover, sprouting of neurons and proper cell junctions were shown as well (**Fig. 4 Cii-iii**).

Alginate's pristine use has been demonstrated by Sitoci-Ficici *et al.*, which used an alginate hydrogel system to successfully recover small spinal cord injuries, which were lesions less than 4 mm [486]. However, alginate is most often used in hybrid constructs, to improve its

inherent qualities and improve the functionality of the scaffold. For example, Golafshan *et al.* incorporated graphene and polyvinyl alcohol to increase the toughness and electrical conductivity, which is required for nervous tissue [487]. Culture with PC12 cells showed good biocompatibility, attachment, and spreading. Homaeigohar *et al.* implemented citric acid-functionalized graphite nanofilaments (CAFGNs) into alginate, rendering the hydrogel electroactive [488]. The culture of PC12 on pristine alginate versus CAFGN-alginate showed increased cell proliferation and adhesion upon the addition of CAFGN, as well as improved neurite formation. In addition, *in vivo* implantation of both hydrogels in a guinea pig model showed a decrease in inflammation over the course of 2 weeks, indicating both hydrogels have good biocompatibility. Verification of improved functionality upon CAFGN addition *in vivo* is lacking. Wang *et al.* used a combination of chitosan and alginate for neural applications, showing the proliferation of neural stem cells, as well as olfactory ensheathing cells, showing great potential for neural tissue engineering [489]. Chitosan in combination with hyaluronic acid has been tested *in vivo* in sciatic murine models [490]. They showed an increased number of myelinated nerve fibers, increased myelin sheath thickness, and no difference in scar tissue when comparing chitosan hydrogels to HA only, chitosan only, and no treatment (**Fig. 4 D**). The chitosan/HA hydrogel shows great clinical potential for neural impairment and neural tissue engineering.

Silk fibroin is also often used for neural regeneration, most frequently by electrospinning it into nanofibers. The strong mechanical properties, good biocompatibility, and minimal immunogenicity allow versatile use of silk fibroin in neural tissue regeneration [467]. Li *et al.* have coated electrospun silk fibroin using laminin, which enhanced survival and neuron differentiation [491]. Nune *et al.* have employed silk fibroin electrospun fibers as well, and incorporated melanin to improve the electrical signal propagation [492]. The use of neuroblastoma cells showed good cell adherence and viability, and improved cell differentiation was observed as a result of the melanin incorporation.

In conclusion, many advances have been made towards the clinical suitability of natural hydrogels for neural tissue engineering applications. Some successful natural hydrogels, namely collagen, are already in clinical trials, highlighting the promising nature of the biomaterial. However, similar to cardiac tissue engineering, the optimal scaffold should allow for electrical signal propagation. Therefore, researchers should apply various functionalization techniques, possibly mimicking the advances in cardiac tissue engineering, to produce a conductive scaffold. Here the biocompatibility should strongly be taken into account as well.

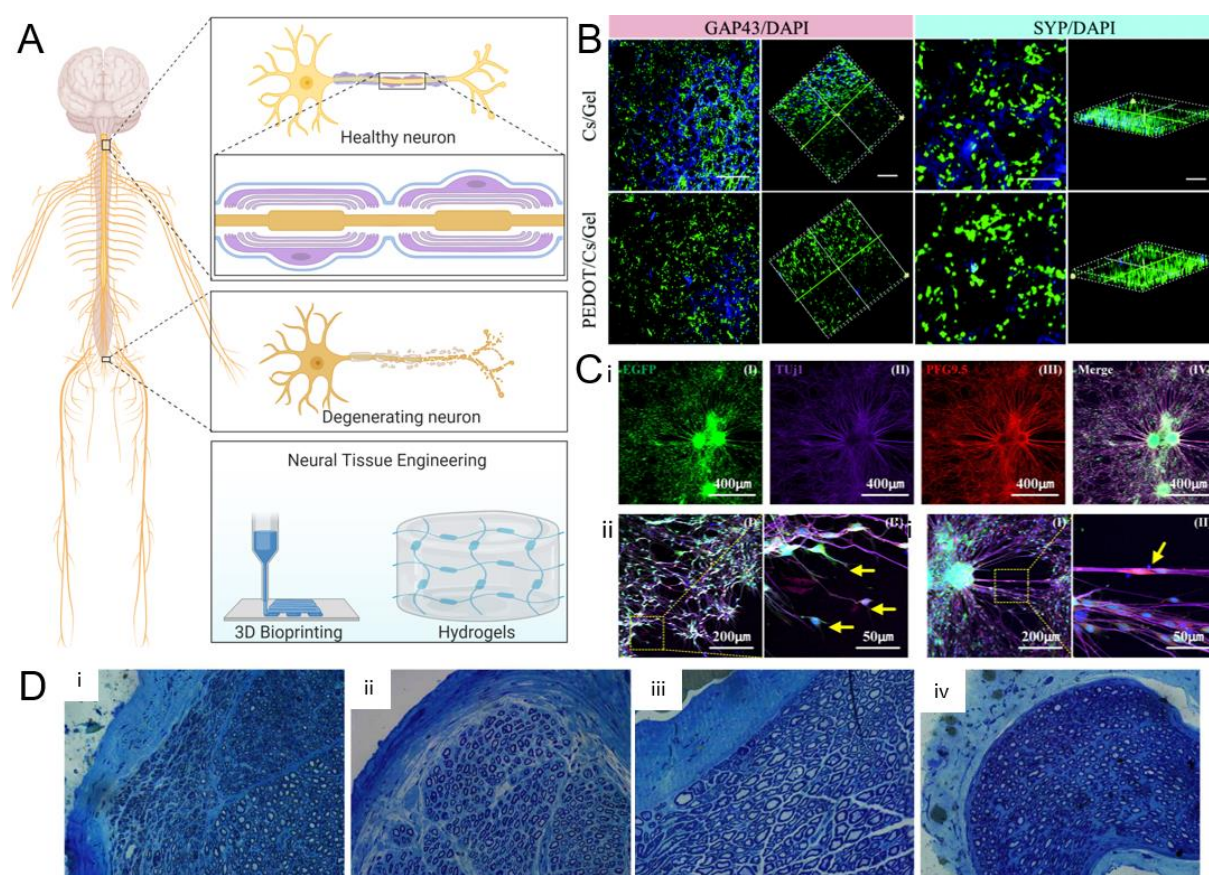


**Fig. 4.** Neural tissue engineering. A) Schematic representation of the nervous system, neural degeneration, and neural tissue engineering. Created with BioRender.com B) Use of chitosan/gelatin hydrogel functionalized with PEDOT nanoparticles, enhancing the neuronal regeneration and functionality shown by neural regeneration marker GAP43 and synaptic formation marker SYP, compared with the pristine chitosan/gelatin hydrogel. Reproduced with permission [483]. Copyright 2017, The Royal Society of Chemistry. C) 3D bioprinted GelMA neuronal conduits with NCSCs, showing i) Tuj1 and PGP9.5 positive cells, indicating early neuronal differentiation ii) sprouting of neurons, indicated by yellow arrows, and iii) differentiated neural cell junction indicated by yellow arrow. Reproduced with permission [485]. Copyright 2020, Elsevier. D) Toluidine blue staining indicating myelinated neurons 12 weeks after implantation of the scaffold, showing i) chitosan, ii) chitosan/HA, iii) no implant, iv) HA, showing the most arranged and distinct axons in the chitosan/HA group, indicating the hybrid scaffold has the most optimal functionality in neural regeneration. Reproduced with permission [490]. Copyright 2018, Spandidos.

### 3.3 Bone Tissue Engineering

Bone has a naturally high regenerative potential to recover small fractures and cracks, however larger bone defects, typically larger than 2 cm, cannot recover by themselves [493]. These larger defects can be a result of degenerative diseases, traumatic injuries, or surgical removal [494,495]. Bone grafts can be used to ameliorate and assist in the regeneration process of the defect bone tissue. There is a high clinical need and demand, making up an estimated cost of \$5 billion in the United States alone [496]. The bone grafts that are currently in clinical use mostly comprise of autologous or allogeneic transplantation, which, in general, are biocompatible, do not invoke an immune response, and manage bone function. Especially autografts which include bone formation inducing factors, such as bone morphogenetic proteins (BMPs) or other growth factors, are of great interest. However, the limitation of such autografts

is that a surgical procedure is required to harvest the tissue, and a second procedure to implant the autograft, which could all lead to very serious side effects, including defects at the donor site and other surgical risks. In addition, these procedures are highly costly [33]. Therefore, great efforts are put into research into bone tissue engineering applications of natural hydrogels, which would omit the surgical risks and donor site morbidity. It includes the creation of a biocompatible, osteogenic scaffold, which incorporates cells and in some cases growth factors to allow for optimal bone regeneration [497]. Bone tissue engineering aims to produce smart scaffolds, which sustain the dynamic nature of the microenvironment of the bone and allow for remodeling, in addition to the primary goal of bone regeneration. The scaffold replaces the bone matrix and should therefore mimic the properties of bone ECM, which include cell attachment sites, growth factor hubs, and strong mechanical properties (**Fig. 5 A**) [498]. In the next paragraph, the most promising applications of natural hydrogels and their functionalization for bone tissue engineering applications are outlined.

Collagen is one of the main protein components of the bone ECM and therefore lends itself well for bone tissue engineering applications, in addition to being biodegradable and biocompatible. Moreover, it contains many naturally occurring RGD sequences, which allow for optimal cell attachment [499]. One of the first examples of bone tissue engineering used a collagen hydrogel to regenerate nasal bone tissue [500]. Stuckensen *et al.* cryostructured collagen hydrogel precursors, resulting in a porous scaffold mimicking native bone ECM, without the use of additional growth factors [501]. hMSCs could easily enter and attach to the matrix and maintained metabolic activity. Moreover, *in vivo* implantation of the scaffold in mice showed promising results for the regeneration of the meniscus. In addition, bone tissue consists of hydroxyapatite (HA) for about 70%, the combination of collagen functionalized with HA forms a highly advantageous scaffold for bone applications [502–504]. Many researchers have exploited the hybrid collagen-HA scaffold as a scaffold to culture bone marrow cells [505], and more importantly to ameliorate bone defects [506]. Chen *et al.* produced a collagen scaffold, which contained a gradual layer of HA, fabricated using the freeze-drying process in layers (**Fig. 5 B**) [506]. This gradient mimicked the natural structure of bone tissue and showed increased cell proliferation, as well as native bone functionality, including osteogenic differentiation and alkaline phosphatase activity (ALP).

As gelatin is a processed form of collagen, it poses similar advantages for bone tissue engineering, including the cell attaching RGD sequences. However, as it is easily degradable and does not exhibit strong mechanical properties which are required for the bone, modifications are necessary [507]. Therefore Grazia Raucci *et al.* have crosslinked gelatin with carbodiimide and functionalized it with HA nanoparticles as well as BMP-2 peptide attachment [508]. They characterized the cell response to both bioactive components and found HA increases cell

proliferation and induces osteogenic differentiation of hMSCs, quantified by ALP expression. Moreover, the BMP-2 peptide addition showed even higher values of ALP, indicating both promising candidates for bone tissue regeneration. Another well-known modification of gelatin is GelMA. The use of different concentrations of GelMA for bone tissue engineering was characterized by Celikkin *et al.* [509]. They showed the cell attachment and osteogenic potential of hMSCs through DNA content, ALP activity, and calcium deposition over the course of 4 weeks and found 5% GelMA was superior to 10% GelMA, as a result of its high porosity and pore size, high mass swelling, and other mechanical characteristics. Moreover, as X-ray is a highly used tool to visualize bone tissue, X-ray attenuation can be an important design characteristic for clinical applications. Therefore, Celikkin *et al.* have functionalized GelMA with gold nanoparticles and 3D printed scaffolds which enhanced the X-ray attenuation without compromising the biological activity and osteogenic potential of the scaffold [509]. Others have synthesized a highly methacrylated GelMA, exhibiting strong mechanical properties, elastic behavior, and low degradations rates, which are used as bioinks for bone tissue engineering [510]. They showed high cell viability and function, including attachment, as well as osteogenic behavior, shown by the ALP activity, calcium deposition, and expression of osteogenic genes. Byambaa *et al.* bioprinted 5% GelMA hydrogels as well for bone applications, which contained a hollow HUVEC (human umbilical vein endothelial cells) filled vessel, allowing to perfuse the bone tissue by mimicking a blood vessel [511]. To improve their design, they conjugated silicate nanoplatelets to the GelMA to facilitate osteogenesis, and they added VEGF (Vascular Endothelial Growth Factor) in different concentrations to promote vascularization (**Fig. 5 Ci**). The alizarin red staining showed high osteogenesis of calcium deposition by hMSCs (**Fig. 5 Cii**), as well as increased expression of osteogenic marker OCN (**Fig. 5 Ciii**) and RUNX2 (**Fig. 5 Civ**). Moreover, this proves the proliferation and cell survival over 21 days *in vitro*.

Alginate poses great possibilities for bone tissue engineering as well, however, requires some modifications to improve its suitability. To start, alginate does not exhibit the RGD sequences such as gelatin and collagen, and therefore the addition of RGD peptides opts for the promotion of cell attachment, which in addition allows for various micropatterning techniques. Moreover, alginate lends itself well to the addition of bone minerals, such as calcium, ideal for bone tissue [498]. For example, Luo *et al.* incorporated RGD sequences into alginate hydrogels in addition to bone-forming peptide-1 to promote osteogenesis [512]. They encapsulated hMSCs into the hydrogel and showed good proliferation of hMSCs, as well as osteogenic differentiation, shown by expression of OCN, Col1A1, and RUNX2, compared to the alginate hydrogel without RGD sequence and bone-forming peptide-1 (**Fig. 5 D**).

Another commonly used natural hydrogel for bone tissue engineering is silk fibroin, however, it has some limitations such as difficulty controlling gelation and crosslinking, and

unsuitability for bioprinting. Therefore, researchers have made efforts in modifying silk fibroin to enhance its applicability for bone tissue engineering. Shi *et al.* developed a silk fibroin hydrogel, which can assemble under physiological conditions with the inclusion of a polysaccharide binder, which enables self-healing properties of the hydrogel [513]. Moreover, calcium phosphate is incorporated into the self-healing silk fibroin hydrogel to promote osteogenesis. This was shown by implantation *in vivo* and the formation of new bone tissue was observed after 8 weeks (**Fig. 5 E**).

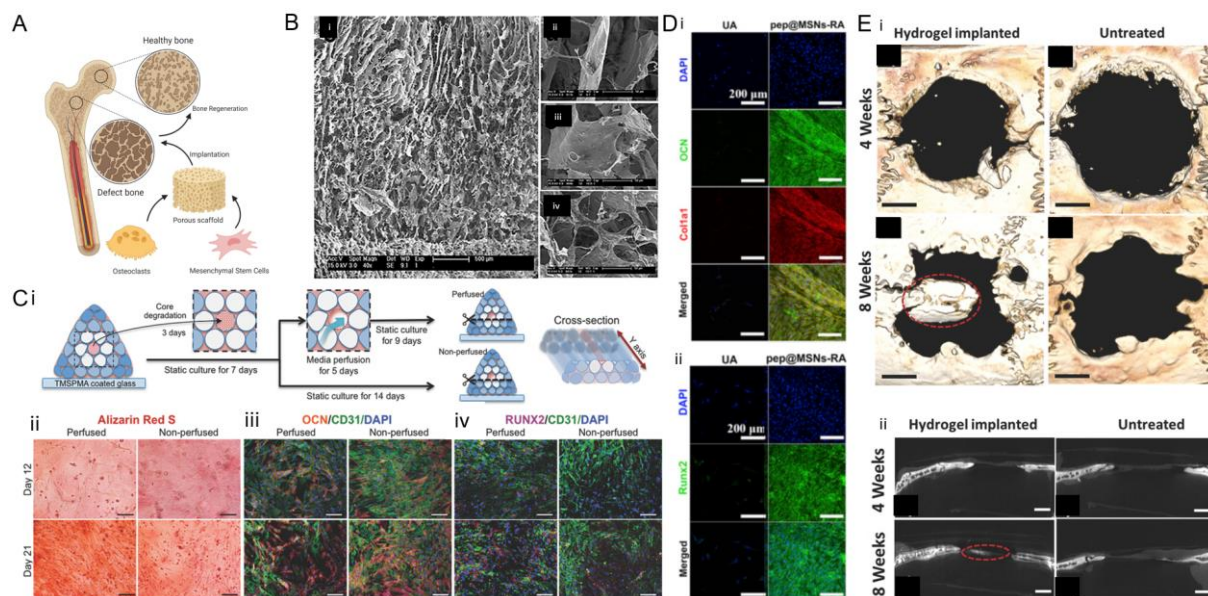


**Fig. 5.** Bone Tissue Engineering applications. A) Schematic representation of defect bone and tissue engineering approach using cells in a hydrogel scaffold. Created with BioRender.com B) SEM images of bone tissue-engineered collagen scaffold with different percentage of HA functionalization. i) Overview of a scaffold, ii) 30% HA, iii) 50% HA, and iv) 70% HA. Reproduced with permission [506]. Copyright 2017, Wiley-VCH GmbH. C) Formation of 3D bioprinted scaffold for bone tissue engineering with a degradable middle vessel to incorporate HUVECs, allowing for vessel formation and perfusion, which is schematically displayed in i). ii)-iv) show increased osteogenic function in the perfused tissue by alizarin Red, OCN, and RUNX2 visualization. Reproduced with permission [511]. Copyright 2017, Wiley-VCH GmbH. D) Osteogenesis in RGD functionalized alginate gel with bone formation peptide-1 (pep@MSNs-RA), shown by i) OCN and Col1A1 immunostaining and ii) RUNX2 immunostaining, compared to control (UA). Reproduced with permission [512]. Copyright 2018, Elsevier. E) *In vivo* implantation of self-healing silk fibroin hydrogel modified with calcium phosphate and polysaccharide crosslinking showing healing of the bone in microCT analysis in i) 3D reconstruction and ii) sagittal cross-section views. Reproduced with permission [513]. Copyright 2017, Wiley-VCH GmbH.

All in all, promising results have been obtained for bone tissue engineering using natural hydrogels. The use of bone-specific growth factors induces increased bone formation, rendering a highly successful scaffold. For example, the silk fibroin scaffold is already able to induce bone tissue regrowth after 2 months, which should be tested over a longer period of time to notice the long term effects. Additionally, clinical trials should be conducted in order to push forward to clinical translation of the proper biomaterials, as many steps have already been taken by *in vivo* implantation and characterization of the response.

#### 4. Conclusions and Outlook

Novel applications focusing on the biofabrication of cardiac, neural, or bone tissues, require the design of advanced biocompatible and biodegradable scaffolds that can mimic the complex architecture of native tissues. Here, the choice of biomaterial used in the biofabrication of such scaffolds is critical. Natural hydrogels have been widely used for tissue engineering applications due to their biocompatibility and biodegradability, but more importantly to avoid the risk of inflammatory and immunological responses that can be caused by synthetic hydrogels [2].

The advances in biofabrication techniques, specifically fiber-based techniques and bioprinting techniques, hold great promise in the fields of tissue engineering and regenerative medicine. Biofabrication techniques, of which each of them offers a set of advantages and suffers from limitations when it comes to engineering complex tissues, have been discussed in this review. Biotextiles are better suited for engineering load-bearing tissues but not for very complex architectures. Whereas 3D bioprinting offers superior control over the structure's architecture and resolution but cannot produce load-bearing structures. Interestingly, 4D bioprinting is one of the emerging biofabrication technique that is highly promising for the fabrication of tubular organs (blood vessels and glands) but still requires optimization to increase the array of bioprinted biomaterials and their printing resolution and tune the after-folding shape and its mechanical properties.

There are two important challenges, that have been overlooked in the literature, negatively impacting the translation of biofabricated scaffolds: 1) quality control measures and defects induced throughout the fabrication process; 2) the implantation of biofabricated scaffolds. Biofabrication tools are susceptible to defects and it is probable that scaffolds contain defects which deviates from the intended architecture, mechanical properties, homogeneity of composition, etc. These defects can affect the scaffolds performance and create bottlenecks in receiving regulatory approvals for their clinical use [514]. The identification of proper quality control measures is an emerging area.

Hydrogel scaffolds are not suturable and thus their implantation *in vivo* has remained a major challenge. The use of biocompatible adhesive materials in biofabrication of scaffolds can potentially address some of the challenges. In addition, recently the concept of *in vivo* printing has emerged as a promising strategy that allows direct formation of a scaffold within the host body. So far both extrusion-based [515,516] and stereolithography-based [517] approaches have been used for *in vivo* printing of scaffolds. Upon the use of proper hydrogels and their *in situ* crosslinking, the scaffolds adhere to the surrounding tissue without the need for suturing.

The emerging applications of biofabricated natural hydrogels in cardiac, neural, and bone tissue engineering have also been discussed in this review. For cardiac regeneration, engineering

electro-active scaffolds by embedding carbon nanotubes, gold nanoparticles, or graphene and its derivatives in natural hydrogels such as alginate, collagen, or gelatin can pave the way towards clinical applications. The advances in electro-active scaffolds for cardiac tissue engineering can find applications in neural regeneration since neural tissues also require scaffolds that allow electrical signal propagation. The translation of natural biocompatible hydrogels, such as collagen, is beginning to gain pace in this field. Similar to its cardiac and neural counterparts, the bone tissue engineering field has also witnessed promising results related to the use of natural hydrogels. One flagrant example is the ability of silk fibroin scaffolds to induce bone tissue regrowth in a two-month period. However, longer-term tests and clinical trials should be undertaken before a final judgment is possible.

Moving forward, to achieve a successful translation of biofabricated hydrogel products, many challenges and hurdles remain to be solved. These challenges were recently detailed and discussed by Mandal *et al.* [337]. Nonetheless, this has not stopped the FDA from approving a number of marketed hydrogel-based products that are usually classed as Class I, II, or III medical devices, depending on the encapsulated drugs or bioactive compounds [6,205,206,337]. Even though a bright future stands ahead for commercialized hydrogel products, due to the recent developments in biofabrication techniques, the big challenge of engineering large-scale functional tissues and organs, which has been rightfully labeled as the “Mars mission of bioengineering” [518], is yet to be “colonized”.

# **Chapter II:**

## Evaluating Sources of GelMA Hydrogels

**K. Elkhoury**, M. Morsink, Y. Tahri, C. Kahn, F. Cleymand, S. R. Shin, E. Arab-Tehrany, L. Sanchez-Gonzalez, Synthesis and characterization of C2C12-laden gelatin methacryloyl (GelMA) from marine and mammalian sources. *Submitted to Int. J. Biol. Macromol.*



As detailed in the first chapter, natural hydrogels are the preferred choice for tissue engineering applications, mainly to avoid the potential risk of immunological and inflammatory responses initiated by synthetic hydrogels. Gelatin is one of the most popular biopolymers that can be chemically modified to produce a photocrosslinkable, biodegradable, and biocompatible natural hydrogel named GelMA. However, mammalian source with all its clinical, religious, and economical restrictions, are still the most popular source of GelMA. In this chapter, the quest to find safer and more accepted source of GelMA is pursued. For this, the physicochemical (structural, thermal, water uptake, swelling, rheological, and mechanical) and biological (cell viability, proliferation, and spreading) properties of low and high methacrylated porcine and fish derived GelMA are characterized and compared in an article submitted to *Polymers*. Moreover, mouse C2C12 myoblasts were encapsulated in the GelMA matrices to determine their potential use as skeletal muscle tissue engineering scaffolds.

Comme expliqué dans le premier chapitre, les hydrogels naturels sont le choix préféré pour les applications en ingénierie tissulaire, principalement pour éviter le risque potentiel de réponses immunologiques et inflammatoires initiées par les hydrogels synthétiques. La gélatine est l'un des biopolymères les plus couramment utilisés qui peut être modifié chimiquement pour produire un hydrogel naturel photoréticulable, biodégradable et biocompatible appelé GelMA. Cependant, le porc avec toutes ses restrictions cliniques, religieuses et économiques, reste la source la plus courante de GelMA. Dans ce chapitre, la recherche d'une source de GelMA plus sûre et mieux acceptée est menée. Pour ce faire, les propriétés physicochimiques (structurelles, thermiques, d'absorption d'eau, de gonflement, rhéologiques et mécaniques) et biologiques (viabilité, prolifération et propagation des cellules) de la matrice hydrogel de type GelMA obtenue à partir de gélatine de poisson a été caractérisée et comparée aux propriétés de la matrice GelMA développée à partir de gélatine de porc dans un article soumis au journal *Polymers*. L'influence du degré de méthacrylation sur les propriétés de la matrice est analysée pour ces deux sources de gélatine. En outre, des myoblastes C2C12 de souris ont été encapsulés dans les matrices de GelMA afin de déterminer leur potentialité en tant qu'échafaudages d'ingénierie des tissus musculaires squelettiques.



### Article

## Synthesis and characterization of C2C12-laden gelatin methacryloyl (GelMA) from marine and mammalian sources

Kamil Elkhoury<sup>1,2</sup>, Margaretha Morsink<sup>2,3</sup>, Yasmina Tahri<sup>1</sup>, Cyril Kahn<sup>1</sup>, Franck Cleymand<sup>4</sup>, Su Ryon Shin<sup>2</sup>, Elmira Arab-Tehrany<sup>1</sup>, Laura Sanchez-Gonzalez<sup>1</sup>

1 LIBio, Université de Lorraine, F-54000 Nancy, France.

2 Division of Engineering in Medicine, Department of Medicine, Harvard Medical School, Brigham and Women's Hospital, Cambridge, MA, 02139 USA.

3 Translational Liver Research, Department of Medical Cell BioPhysics, Technical Medical Centre, Faculty of Science and Technology, University of Twente, Enschede, The Netherlands.

4 Institut Jean Lamour, CNRS—Université de Lorraine, F-54000 Nancy, France.

### Abstract

Gelatin methacryloyl (GelMA) is widely used for tissue engineering applications as an extracellular matrix (ECM) mimicking scaffold due to its cost-effectiveness, ease of synthesis, and high biocompatibility. GelMA is widely synthesized from porcine skin gelatin, which labors under clinical, religious, and economical restrictions. In order to overcome these limitations, GelMA can be produced from fish skin gelatin, which is eco-friendly as well. Here, we present a comparative study of the physicochemical (structural, thermal, water uptake, swelling, rheological, and mechanical) and biological (cell viability, proliferation, and spreading) properties of porcine and fish skin GelMA with low and high methacrylation degrees, before and after crosslinking, to check whether fish skin can replace porcine skin as the source of GelMA. Porcine and fish skin GelMA presented similar structural, thermal, and water uptake properties prior to crosslinking. However, subsequent to crosslinking, fish skin GelMA hydrogels had a higher mass swelling ratio and a lower elastic and compressive Young's moduli than porcine skin GelMA hydrogels having similar methacrylation level. Both types of GelMA hydrogels showed great biocompatibility toward encapsulated mouse myoblast cells (C2C12), however, an improved cell spreading was observed in fish skin GelMA hydrogels, and cell proliferation was only induced in low methacrylated GelMA. These results suggest that fish skin GelMA is a promising substitute for porcine skin GelMA for biomedical applications and that low methacrylated fish skin GelMA can be used as a potential scaffold for skeletal muscle tissue engineering.

**Keywords:** Fish Skin; Porcine Skin; Gelatin; Hydrogels; Skeletal Muscle Injury.

---

### 1. Introduction

Hydrogels are crosslinked networks of hydrophilic polymers that are mainly noted for their propensity for water and maintaining a stable structure. For this, hydrogels have been widely used as engineerable extracellular matrix (ECM) mimics for many different biomedical applications ranging from tissue engineering to drug and gene delivery [52,2,50,3,6]. Gelatin is

one of the most popular biopolymers produced via the partial hydrolysis of native collagen, which is a fibrous protein and the principal constituent of animal skin, bone, and connective tissue [519]. Because of its unique functional and technological properties, gelatin has been widely used for tissue engineering [3,299], drug delivery [520,521], food [522], and cosmetic applications [523]. Gelatin contains abundant arginine-glycine-aspartic acid (RGD) sequences that enhance cell attachment [524] and contains target sequences of matrix metalloproteinase (MMP) that promote cell remodeling [525]. Derived from denatured collagen, gelatin possesses excellent solubility, biodegradability, biocompatibility, low antigenicity, and a low gelling point [526]. However, some limitations, such as its low mechanical modulus and its rapid degradation, limit its use in biomedical applications.

To surpass these disadvantages, gelatin methacryloyl (GelMA) is created by the chemical modification of gelatin (**Figure 1A**), as methacrylate groups are added to the amine-containing side groups [310]. This methacrylation reaction allows, in the presence of a photoinitiator, the light polymerization of gelatin into a hydrogel that is stable at 37 °C. As it is mechanically stronger than unmodified gelatin hydrogels, GelMA hydrogels have been used to microfabricate complex structures using different micro- and biofabrication techniques, such as photopatterning [4], micromolding [527], self-assembly [528], microfluidics [529], textile techniques [530], and bioprinting techniques [531].

The physicochemical properties of GelMA depend on both the source of gelatin, mammalian or marine, and its level of methacrylation. Economical, environmental, clinical, and religious restrictions shifted preference of gelatin sources from mammalian to marine. Fish skin is a major waste byproduct of the fish-processing industry [532,533], so economically, it is an inexpensive material to acquire, and environmentally, valorizing its use will decrease pollution. Clinically, when extracting gelatin from mammalian sources, there exists a risk of zoonosis, such as Bovine Spongiform Encephalopathy [534]. The usage of gelatin derived from mammalian sources, porcine or bovine skin, is not acceptable for some major religions of the world, including Judaism, Islam, and Hinduism, constituting ~40% of the human population, whereas fish skin gelatin is acceptable [519,535]. Therefore, using fish skin GelMA scaffolds could open up tissue engineering applications, including skeletal muscle tissue engineering, for tens of millions of people in a safe and environmentally friendly manner.

Other studies have previously compared fish and porcine skin GelMA [535,536]. However, these comparisons were made using fish and porcine GelMA produced with different methacrylation levels. This study offers a more complete overview by comparing fish and porcine GelMA with similar methacrylation levels (low and high). Furthermore, previous studies did not compare the fish and porcine GelMA's structural, thermal, water sorption, and rheological properties, which are fully characterized in this report. Moreover, GelMA from

porcine origin has been extensively used for tissue engineering applications, including skeletal muscle tissue engineering. Researchers have employed the mouse myoblast cell line (C2C12) in order to assess the suitability of porcine skin GelMA for skeletal muscle tissue engineering applications, showing promising results [515,537–539]. However, none of the previous studies have assessed the suitability of fish skin GelMA for this application. To the best of our knowledge, this is the first study that investigates the use of fish skin GelMA hydrogels as C2C12 myoblasts-laden scaffolds.

In this report, we compare the physicochemical (structural, thermal, water uptake, swelling, rheological, and mechanical) and biological (cell viability, proliferation, and spreading) properties of porcine and fish skin GelMA. Mouse C2C12 myoblasts were encapsulated in low and high methacrylated porcine skin GelMA hydrogels and, for the first time, in low and high methacrylated fish skin GelMA hydrogels, to determine their biocompatibility, as well as their potential for being investigated as skeletal muscle tissue engineering scaffolds in future studies.

## 2. Materials and Methods

Gelatin from porcine skin (Type A, 300 bloom), gelatin from cold-water fish skin, methacrylic anhydride (MA), Irgacure 2959 (PI) (2-hydroxy-4'-(2-hydroxyethoxy)-2-methylpropiophenone), deuterium oxide (99.9 atom % D), 2,4,6-Trinitrobenzene-sulfonic acid solution, and Dulbecco's phosphate-buffered saline (DPBS) were all purchased from Sigma Aldrich (Saint-Quentin-Fallavier, France). Dulbecco's Minimum Eagle Media (DMEM), Fetal Bovine Serum (FBS), L-Glutamine, penicillin, streptomycin, LIVE/DEAD Viability/Cytotoxicity Kit, and PrestoBlue Kit were all purchased from Thermo Fisher Scientific (Waltham, MA, USA).

### 2.1 GelMA synthesis

GelMA was synthesized, from porcine and cold water fish skin, according to the general method first adopted by Van Den Bulcke *et al.* [310]. In brief, gelatin was mixed at 10% (w/v) into DPBS at 60 °C and stirred until fully dissolved. Then, 1.25% (v/v) and 20% (v/v) of MA was added in a dropwise manner to the gelatin solution at 50 °C, at a rate of 0.5 mL/min under stirred conditions and allowed to react for 1 h. After 1 h, the reaction was stopped following 5X dilution with additional warm (40 °C) DPBS. To remove salts and unreacted MA, the mixture was dialyzed for 5 days at 40 °C against distilled water using 12–14 kDa cutoff dialysis tubing. The solution was finally lyophilized, generating a porous white foam that was stored at -20 °C until further use.

## 2.2 Fourier-transform infrared

Fourier-transform infrared (FTIR) spectra of freeze-dried GelMA were recorded using a Tensor 27 mid-FTIR Bruker spectrometer (Bruker, Karlsruhe, Germany) equipped with a diamond ATR (Attenuated Total Reflectance) module and a DTGS (Deuterated-Triglycine Sulfate) detector between 4000 and 400  $\text{cm}^{-1}$  at 4  $\text{cm}^{-1}$  resolution. Raw absorbance spectra were smoothed using a nine-points smoothing function. After elastic baseline correction using 200 points,  $\text{H}_2\text{O}/\text{CO}_2$  correction was then applied.

## 2.3 Determination of GelMA degree of substitution

2,4,6-trinitrobenzene-sulfonic acid (TNBS) assay was performed to determine the GelMA's degree of substitution (DS) according to the method developed by Habeeb [540]. Briefly, GelMA and gelatin samples were first dissolved in 0.1 M sodium bicarbonate buffer at a concentration of 1.6 mg/mL, then mixed with an equal volume (0.5 mL) 0.01% TNBS solution and incubated for 2 h. To stop the reaction, two solutions of 0.25 mL of 1 M HCl and 0.5 mL of 10% (w/v) sodium dodecyl sulfate were added. The amino group concentration (AC) of each sample was determined from a glycine standard curve after measuring their absorbance at 335 nm. The DS was calculated according to the current formula:

$$\text{DS (\%)} = (1 - \text{AC of gelatin} / \text{AC of GelMA}) \times 100$$

To verify the DS, proton nuclear magnetic resonance ( $^1\text{H-NMR}$ ) spectra were collected at 40 °C in deuterium oxide at a frequency of 400 MHz using an AVANCE III 400 NMR spectrometer (Bruker, Karlsruhe, Germany). 50 mg of each GelMA sample was dissolved in 1 mL of deuterium oxide at 40 °C. The peak area of aromatic amino acids (7.5 – 7.3 ppm) in the GelMA samples was employed as a reference in each spectrum. Baseline correction was applied before obtaining the areas of the peaks of interest. The peak area (PA) of lysine methylene protons appearing between 3.1 – 2.9 ppm was used for calculation of the DS following the equation:

$$\text{DS (\%)} = (1 - \text{PA of GelMA} / \text{PA of gelatin}) \times 100$$

## 2.4 Thermal gravimetric analysis

The thermal resistance of GelMA samples (~ 5 mg) was examined using a Discovery thermal gravimetric analysis (TGA) 5500 (TA instruments, New Castle, DE, USA) in open pans under nitrogen atmosphere at a gas flow rate of 25 mL/min and a heating rate of 20 °C/min from 35 to 600 °C. The degradation temperature ( $T_d$ ) was determined from the onsets of percent change in derivative weight versus temperature.

### 2.5 Differential scanning calorimetry

The differential scanning calorimetry (DSC) measurement of GelMA samples (~ 5 mg) was carried out using a Discovery DSC250 (TA instruments, New Castle, DE, USA) under a dynamic inert nitrogen atmosphere, with a flow rate of 50 mL/min in a Tzero hermetic aluminum capsule. Cooling was performed to -80 °C at a rate of 20 °C/min, followed by heating to 250 °C at a rate of 10 °C/min for all samples.

### 2.6 Dynamic vapor sorption (DVS)

Water sorption isotherms were determined gravimetrically using the DVS technique (Surface Measurement Systems, SMS, London, UK). The DVS apparatus monitors the moisture sorption capacity of a sample as a function of relative humidity (RH) of the surrounding air. The changes in sample weight over time at a fixed temperature and the desired RH (between 0 and 70%) were recorded. About 55-60 mg of GelMA were placed on the quartz sample pan. The program was initially set to maintain the humidity at 0% for 6 h (drying phase). The samples were then submitted to successive steps of 10% RH increase, up to 70% RH.

### 2.7 GelMA hydrogel preparation

GelMA solution was prepared by dissolving 10% (w/v) of the freeze-dried prepolymer into a DPBS solution at 50 °C. Then, 0.5% (w/v) of PI was added and the temperature was increased to 70 °C to reach complete solubilization. GelMA solution was UV crosslinked (360-480 nm) in a specific PDMS mold for 40 s to create hydrogel discs.

### 2.8 Mass swelling ratio

The mass swelling ratio was evaluated using five cylindrical samples (2 cm diameter, 2 mm height). The samples were kept in DPBS for 24 h. The excessive water was gently removed using a paper tissue, and the swollen weight of the samples was measured using a precision balance. Later, the samples were lyophilized for 3 days and their dry weight was measured. The mass swelling ratio was given by the following formula:

$$\text{Mass swelling ratio} = \text{Swollen weight of the sample} / \text{Dry weight of the sample}$$

### 2.9 Rheological testing

Amplitude sweep tests at a frequency of 1 Hz were performed using a Kinexus pro rheometer (Malvern Instruments Ltd., Worcestershire, United Kingdom) equipped with a plane-plane geometry with a diameter of 20 mm. The hydrogel was loaded into a 1 mm gap between the plates and allowed to relax until the normal force was zero. The amplitudes of shear stress were carried out over a pressure range from 0.01 Pa to 250 Pa. The test was done with a constant frequency of 1 Hz at 37 °C and the measuring system was covered with a humid chamber to

minimize the evaporation of the water. Three different hydrogel discs are tested for each type of hydrogel with the same experimental parameters.

### *2.10 Mechanical testing*

The mechanical measurements were performed using a universal testing machine (Lloyd-LRX, Lloyd Instruments, Fareham, UK). The samples were prepared in a cylindrical shape (2 cm diameter and 2 mm height). Compression tests were performed at a crosshead speed of 1 mm/min until fracture occurred. Prior to all measurements, the zero-gap was determined. Five samples of each condition were tested. The compressive modulus was determined as the slope of the linear region corresponding to the elastic part (10–20% strain) of the stress-strain curve.

### *2.11 Cell culture*

C2C12 cells were cultured in DMEM containing 4.5 g/L of glucose, supplemented with 10% FBS, 2 mM of L-Glutamine, 100 units/mL of penicillin, and 100 µg/mL of streptomycin. Cells were maintained at 37 °C, 100% humidity, and 5% CO<sub>2</sub> and were passaged every 2 days.

### *2.12 Encapsulation of cells in GelMA*

Cells were counted and resuspended as 4x10<sup>6</sup> cells/mL. 25 µL of cell suspension (100 000 cells) were combined with 25 µL of 20% GelMA and 1% PI so that the final concentration of GelMA would be 10% and 0.5% PI. Hydrogels were crosslinked by UV light (Omnicure S2000, Excelitas Technologies, Salem, MA, USA) (800 mW) for 40 seconds on one side and directly placed in cell culture medium in a well plate. Hydrogels with encapsulated cells were maintained at 37 °C and 5% CO<sub>2</sub>.

### *2.13 Viability of cells in GelMA and proliferation assay*

The viability of the encapsulated cells was assessed using a standard Live/Dead staining kit and using the metabolic assay PrestoBlue on days 1 and 3. Calcein AM and Ethidium Homodimer-1 comprised the Live/Dead staining kit and were used according to the manufacturer's protocol with an incubation time of 30 minutes. Afterward, fluorescent images were taken using a fluorescence microscope (Axio Observer D1, Carl Zeiss, Weimar, Germany), and ImageJ (v1.52p, NIH) software was used for image analysis. PrestoBlue proliferation assay was performed according to the manufacturer's instructions with an incubation time of 2.5 hours. Cell growth was evaluated using spectrophotometry with absorption measurements at 570 nm and 600 nm.

### 3. Results and Discussion

#### 3.1 Structural properties

Spectrophotometric techniques were first used to characterize the chemical structure of the engineered prepolymers. In addition to the functional group and conformational analyses of chemical reactions, FTIR and  $^1\text{H-NMR}$  are widely used for chemical identification. FTIR was used essentially to characterize the presence of specific chemical groups in the GelMA. The results show the spectrum of porcine and fish skin GelMA (**Figure 1B**). Gelatin's characteristic peaks were clearly noticed by the presence of peptide bonds (N–H stretching), indicated by a peak at  $3200\text{ cm}^{-1}$ , and by the presence of amide I, II, and III, indicated by peaks at  $1650$ ,  $1550$ , and  $1400\text{ cm}^{-1}$  respectively [541,542]. The peaks that can be assigned to the methacrylic anhydride (MA) were indicating saturated and unsaturated C-H stretching ( $2850$ ,  $2950$ ,  $3150$ , and  $3800\text{ cm}^{-1}$ ), and H-C-H wagging ( $100\text{ cm}^{-1}$ ). The spectra broad peak at  $3300\text{ cm}^{-1}$  can be associated with the stretching of the hydrogen-bonded hydroxyl groups, derived from the modification of the gelatin with the MA [169].

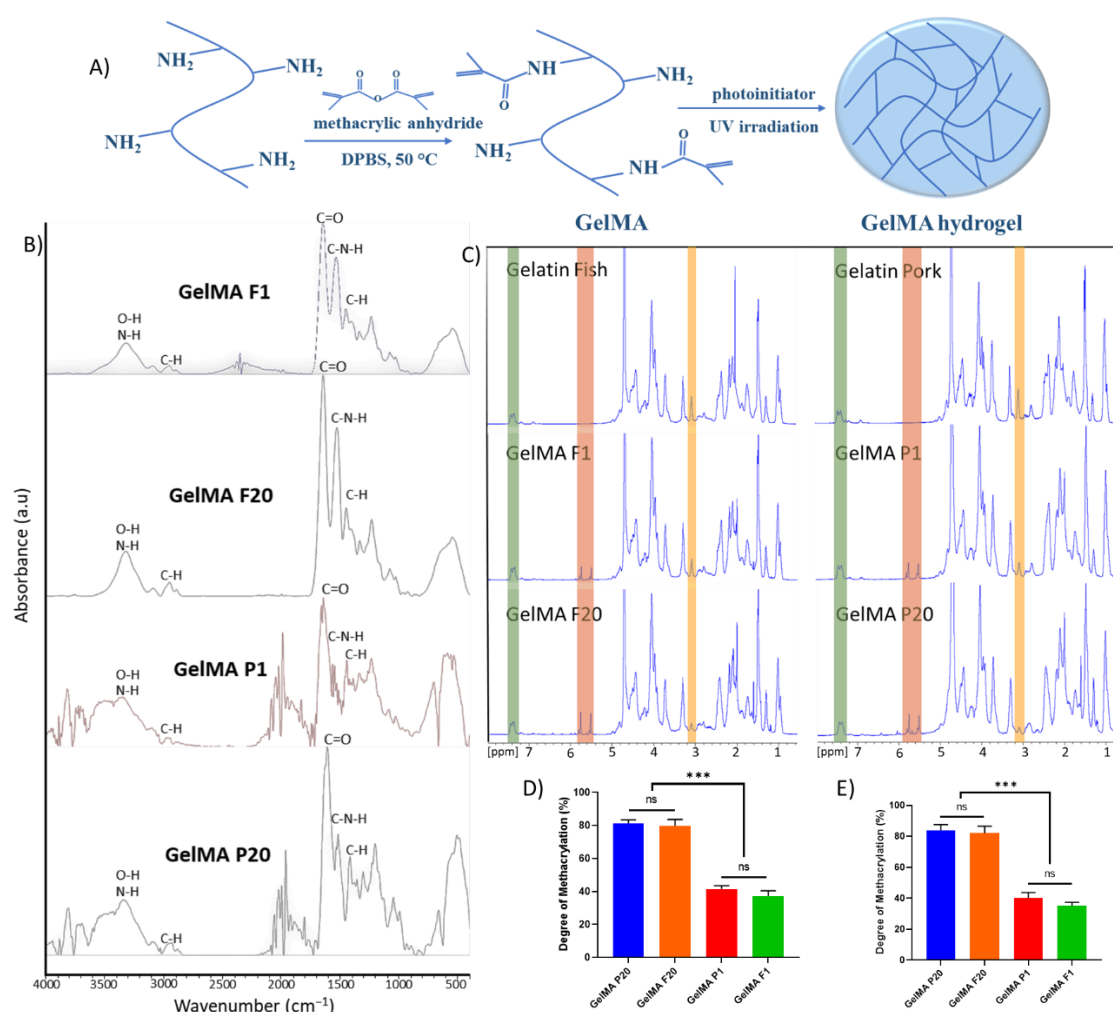


**Figure 1.** A) Schematic representation of the preparation of GelMA and its hydrogel. B) FTIR spectra of fish (F) and porcine (P) skin GelMA. C)  $^1\text{H-NMR}$  verification of F and P skin GelMA. Peaks correspond to acrylic protons (2H) of aromatic amino acids (Green), methacrylamide grafts of lysine

groups, and those of hydroxyl lysine groups (Red), methylene protons (2H) of unreacted lysine groups (Yellow). D) Degree of substitution (DS) of F and P skin GelMA as determined by  $^1\text{H-NMR}$ . E) DS of F and P skin GelMA as determined by TNBS assay. The reported data are the means of three replicates. Parametric data were analyzed using a one-way ANOVA followed by Tukey's test. Significance was indicated as \*( $p < 0.05$ ), \*\*( $p < 0.01$ ) and \*\*\*( $p < 0.001$ ).

Porcine and fish skin GelMA were synthesized using various concentrations of MA to create prepolymers with different degrees of methacrylation. Since reactive amine groups on the polypeptide backbone are the main target of MA [4],  $^1\text{H-NMR}$  analysis and TNBS assay were used to quantify the DS of GelMA. Results presented in **Figure 1C-E** confirmed the substitution of free amine groups in GelMA. These results showed that the addition of a high MA volume percentage (20%) produced a high DS for both porcine GelMA (P20) ( $81.3 \pm 2.2\%$   $^1\text{H-NMR}$ ;  $84.3 \pm 3.6\%$  TNBS) and fish skin GelMA (F20) ( $79.8 \pm 3.8\%$   $^1\text{H-NMR}$ ;  $81.7 \pm 4.6\%$  TNBS). However, the addition of a lower volume percentage of MA (1.25%) produced a low DS for porcine skin GelMA (P1) ( $41.6 \pm 1.9\%$   $^1\text{H-NMR}$ ;  $40.4 \pm 3.6\%$  TNBS) and fish skin GelMA (F1) ( $37.3 \pm 3.2\%$   $^1\text{H-NMR}$ ;  $35.2 \pm 2.4\%$  TNBS). On the one hand, the methacrylation degree was not significantly different between porcine and fish skin GelMA from the same methacrylation level, but on the other hand, it was found to be significantly different between low and high methacrylated GelMA no matter their initial source. The results presented for the DS of porcine skin and fish skin GelMA were found to be in agreement with previously published results [4,535,536].

### 3.2 Thermal properties

To explore the stability of GelMA, TGA was conducted (**Figure 2A**). About 15% (wt/wt) weight loss was observed between 30 and 250 °C, where the highest loss occurred below 110 °C. This result was attributed to the loss of moisture, whereas a weight loss of about 65% (wt/wt) was observed between 250 and 600 °C which can be associated with protein degradation [543,544]. The remaining residue was around 20% at 600 °C for all samples.

The Td is the temperature at which the maximum reduction in mass occurs and it is calculated from the first-order derivative of TGA curves [544]. Porcine skin GelMA, P20 ( $334.8 \pm 3.1$  °C) and P1 ( $336.1 \pm 2.0$  °C) had Td values close to that of fish skin GelMA, F20 ( $334.2 \pm 4.2$  °C) and F1 ( $336.6 \pm 3.2$  °C). The obtained Td values are similar to the previously reported Td value of gelatin [545], which suggests that the methacrylation of gelatin did not significantly affect its degradation temperature. The Td values of all GelMA samples were not significantly different (**Figure 2a**), which suggests that they possess similar thermal stability.

DSC thermograms of GelMA are presented in **Figure 2B**. Generally, three peaks were presented by all prepolymers that could be related to their transition due to moisture loss, transition temperature (Tg), and melting temperature (Tm) [546]. Since all samples were solid

at room temperature, it can be assumed that they are in the glassy region. One small endothermic peak in the range of 55–85 °C for fish skin GelMA and 70–100 °C for porcine skin GelMA was observed, with the corresponding maximum at  $72.7 \pm 1.7$  °C for F20,  $74.9 \pm 2.1$  °C for F1,  $86.7 \pm 1.8$  °C for P20, and  $91.2 \pm 1.8$  °C for P1. This small endothermic peak is related to water evaporation together with helix-to-coil transition [547]. Both phenomena are interconnected since water molecules stabilize the helix structure and helix-coil transition is naturally driven by the loss of water.

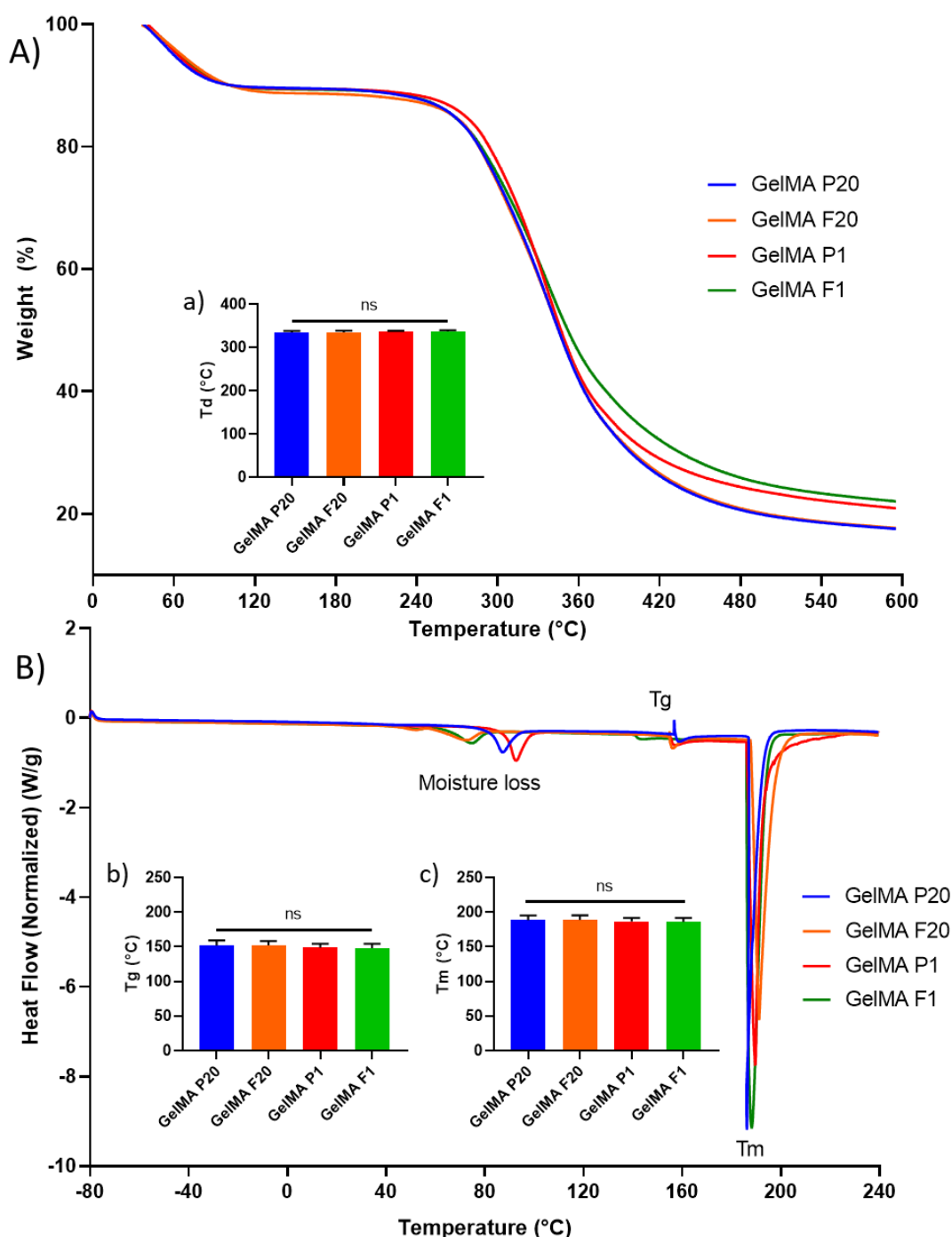


**Figure 2.** A) Thermal gravimetric analysis (TGA) curves of fish (F) and porcine (P) skin GelMA and their respective (a) degradation temperature  $T_d$  (°C) values. B) Differential scanning calorimetric (DSC)

curves showing the moisture loss, transition temperature (T<sub>g</sub>), and melting temperature (T<sub>m</sub>) peaks of F and P skin GelMA and their respective (b) T<sub>g</sub> (°C) and (c) T<sub>m</sub> (°C) values. The reported data are the means of five replicates. The reported data are the means of three replicates. Parametric data were analyzed using a one-way ANOVA followed by Tukey's test. Significance was indicated as \*(p < 0.05), \*\*(p < 0.01) and \*\*\*(p < 0.001).

By increasing the temperature, a thermodynamic change occurs above T<sub>g</sub>, due to the increased thermal motion of the sample [548]. T<sub>g</sub> values of fish skin GelMA, F1 (148.1 ± 6.3 °C) and F20 (152.3 ± 5.9 °C), were similar to that of porcine skin GelMA, P1 (148.8 ± 5.4 °C) and P20 (152.0 ± 7.1 °C) with the same methacrylation level. T<sub>g</sub> is influenced by factors such as molecular weight and crosslinking. The longer the chain length, the greater the molecular weight, resulting in increased stiffness of the polymer structure. Since the methacrylate groups have a higher molecular weight than amino groups, T<sub>g</sub> of GelMA with a high methacrylation degree is higher than that of GelMA with a low methacrylation degree. However, this increase is not significant (**Figure 2b**).

Beyond T<sub>g</sub>, the polymer chains move freely, and the material behaved like rubber until it eventually reaches its T<sub>m</sub> [548]. T<sub>m</sub> is considered a first-order transition and correlated to the melting of crystallites of partially degraded collagen helix into gelatin. Upon comparison of GelMA from the same source, it was shown that the lower DS, P1 (186.9 ± 5.0 °C) and F1 (186.1 ± 5.7 °C), had a lower T<sub>m</sub> than those with a high DS, P20 (188.6 ± 6.5 °C) and F20 (188.0 ± 5.0 °C). It can be seen that for GelMA with the same DS, T<sub>m</sub> was comparable. However, as for T<sub>g</sub> values, T<sub>m</sub> values are also not significantly different for all GelMA samples. DSC results suggest that the thermal properties of GelMA samples are analogous regardless of their source or methacrylation level.

### 3.3 Physical properties

From both scientific and commercial points of view, parameters related to the polymer water vapor sorption are crucial, as they play a big role in the modification of its properties, and thereby its range of applications [549–551]. The hydration behavior of proteins, such as collagen or gelatin, directly affects their chemical and enzymatic reactivities, as well as the formation of their secondary structure [549]. Moreover, the GelMA sorption behavior is an important parameter to study for future incorporation of nanoparticles or bioactive molecules within its matrix [549]. The influence of the methacrylation degree on the water vapor uptake of GelMA was studied at 25 °C. The linearly increasing prepolymer masses during sorption as a function of the relative humidity are presented in **Table 1** and **Figure 3A**. The water vapor uptake was higher for GelMA with low methacrylation degrees compared to high methacrylated GelMA. This can be attributed to the higher porosity of low methacrylated GelMA [4].

**Table 1.** Effect of methacrylation degree on the water vapor sorption of porcine (P) and fish (F) skin GelMA.

Target RH (%)	Change in Mass (%) - dry			
	GelMA P20	GelMA F20	GelMA P1	GelMA F1
0.0	0.00	0.00	0.00	0.00
7.8	2.80	2.26	1.85	3.27
15.6	4.43	3.74	3.61	4.96
23.3	5.92	5.15	5.25	6.51
31.1	7.29	6.53	6.77	7.91
38.9	8.73	8.06	8.30	9.37
46.7	10.25	9.61	9.96	10.90
54.4	11.90	11.28	11.84	12.50
62.2	13.68	13.05	14.07	14.41
70.0	15.97	15.06	16.64	16.54

The swelling behavior of hydrogels is an essential parameter to study after crosslinking, as it affects the hydrogel's mechanical properties and solute diffusion [4]. This behavior depends on the hydrogels' structural properties, hydrophilicity, crosslinking density, and interaction with the solvent [535,552]. To study this swelling behavior, porcine and fish skin GelMA hydrogels with different methacrylation degrees were fully swelled in DPBS at 37°C for 24 h to obtain their swollen weight and then lyophilized for three days to obtain their dry weight. Using the swollen and dry weight of GelMA, the mass swelling ratio was calculated. The low methacrylated GelMA had a higher mass swelling ratio than the high methacrylated GelMA (**Figure 3B**). Fish skin GelMA had a significantly higher mass swelling ratio than porcine skin GelMA for both methacrylation degrees. This might be due to the presence of fewer hydrophobic amino acids in fish skin than in porcine skin GelMA, which makes fish skin more hydrophilic than porcine skin GelMA [553,554]. These results are in full agreement with previously reported results [4,535,536].

Rheological measurements were carried out to assess the elastic properties of GelMA hydrogels. Results, presented in **Figure 3C**, show that the elastic modulus  $G'$ , also known as real modulus or storage modulus, of fish porcine GelMA was lower than the  $G'$  of porcine skin GelMA within the same level of methacrylation. Additionally,  $G'$  is higher for the high methacrylated GelMA of the same source. This difference in elasticity can be explained by the higher amount of proline and hydroxyproline present in porcine skin GelMA [555]. These two amino acids stabilize the ordered conformation during gel formation. On the other hand, increasing the level of methacrylation increased the elasticity of GelMA. Van Den Bulcke *et al.* suggested that high methacrylated GelMA are composed of more chemical bonds, and thus have a denser network with higher elastic modulus and network properties than low methacrylated GelMA [310].

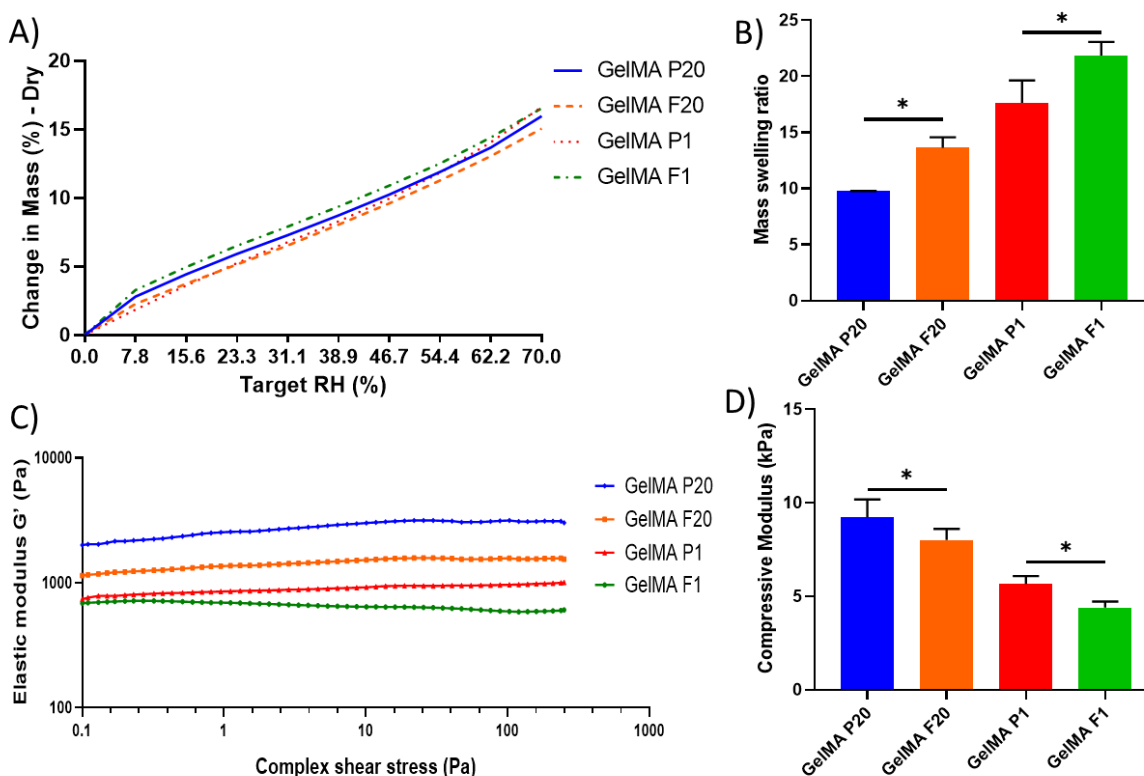


**Figure 3.** A) The isotherm curves for water sorption in fish (F) and porcine (P) skin GelMA. B) The mass swelling ratios of F and P skin GelMA hydrogels. C) Amplitude sweep data showing elastic modulus ( $G'$ ) as a function of complex shear stress of F and P skin GelMA. D) The compressive modulus of F and P skin GelMA hydrogels. The reported data are the means of five replicates. The reported data are the means of five replicates. Parametric data were analyzed using a one-way ANOVA followed by Tukey's test. Significance was indicated as \*( $p < 0.05$ ), \*\*( $p < 0.01$ ) and \*\*\*( $p < 0.001$ ).

It has been reported that cell behavior, function, proliferation, and differentiation are significantly affected by the mechanical properties of hydrogels [556–559]. Unconfined compression tests on swollen hydrogels were used to study the effect of the source and the methacrylation level of GelMA hydrogels on its mechanical properties. As shown in **Figure 3D**, the compressive Young's modulus was significantly different between porcine skin GelMA (P20 =  $9.23 \pm 0.95$  kPa and P1 =  $5.66 \pm 0.43$  kPa) and fish skin GelMA (F20 =  $8.01 \pm 0.6$  kPa and F1 =  $4.40 \pm 0.31$  kPa), and between high methacrylated and low methacrylated GelMA as well. Yoon *et al.* previously reported a significant difference between high methacrylated fish and porcine skin GelMA and between fish skin GelMA with different methacrylation degrees [535]. Wang *et al.* reported it between high methacrylated porcine skin and low methacrylated fish skin GelMA [536]. Nichol *et al.* reported this significance between low and high methacrylated porcine skin GelMA [4].

Lysine is a major methacrylation site and is present in good amounts in gelatin from both sources [533,553,560]. Since more polymeric chains are crosslinked in high methacrylated GelMA, their mechanical properties will be stronger than low methacrylated GelMA. Porcine

gelatin contains higher amounts of hydrophobic amino acids (methionine, phenylalanine, proline, isoleucine, leucine, valine, and alanine) than fish gelatin, which can form stronger hydrophobic interactions in porcine skin GelMA [536]. Moreover, fish gelatin also contains fewer amounts of imino acids (proline and hydroxyproline) than porcine gelatin, which are responsible for the higher structural stability of porcine skin GelMA [535]. Therefore, both the source of gelatin and the level of methacrylation affect the compressive Young's modulus of GelMA. However, the level of methacrylation of GelMA has a higher effect on the compressive Young's modulus of GelMA.

### 3.4 Biological properties

In order to assess the suitability of the fish and porcine skin GelMA hydrogel employment for tissue engineering applications, the cell viability of C2C12 cells was evaluated upon 3D encapsulation. Biocompatibility was assessed using live/dead staining, displayed in **Figure 4A**, and quantified in **Figure 4B**, as well as using a PrestoBlue metabolic assay, shown in **Figure 4C**. The viability of C2C12 cells was not significantly different in the porcine and fish-derived GelMA hydrogels, as they exhibited around 90% viability on day 1 and 80% viability on day 3. Similar viability results were obtained using NIH 3T3 fibroblasts in 3D porcine and fish skin GelMA [535,536] and in fish skin GelMA [561]. The cell viability in all hydrogels was high, indicating a great potential for tissue engineering applications. Viability can be improved by optimizing the UV exposure time for each cell application, as the UV dosage and the number of free radicals formed during photopolymerization affect the cell viability [562]. The non-significant difference in cell viability as a result of methacrylation degree was also found by Zhu *et al.* [563], where human hepatocellular carcinoma cells were encapsulated in porcine GelMA with different degrees of methacrylation.

Moreover, the cell morphology showed a good spreading of C2C12 cells in the fish-derived GelMA, which was previously observed for NIH 3T3 fibroblasts [535]. The spreading of C2C12 cells in porcine GelMA was observed by Costantini *et al.* [537], as there was more cell spreading for lower stiffness GelMA with an increased swelling ratio. This is likely a result of different cell signaling pathways upon mechanotransducing cues [537,562]. Zaupa *et al.* also showed an increased capacity of cell remodeling in fish skin GelMA over mammalian GelMA (bovine), despite the similar Young's moduli of the differently derived GelMA [564]. The larger swelling ratio allows for cell-cell contact, which increases proliferation and cell spreading.

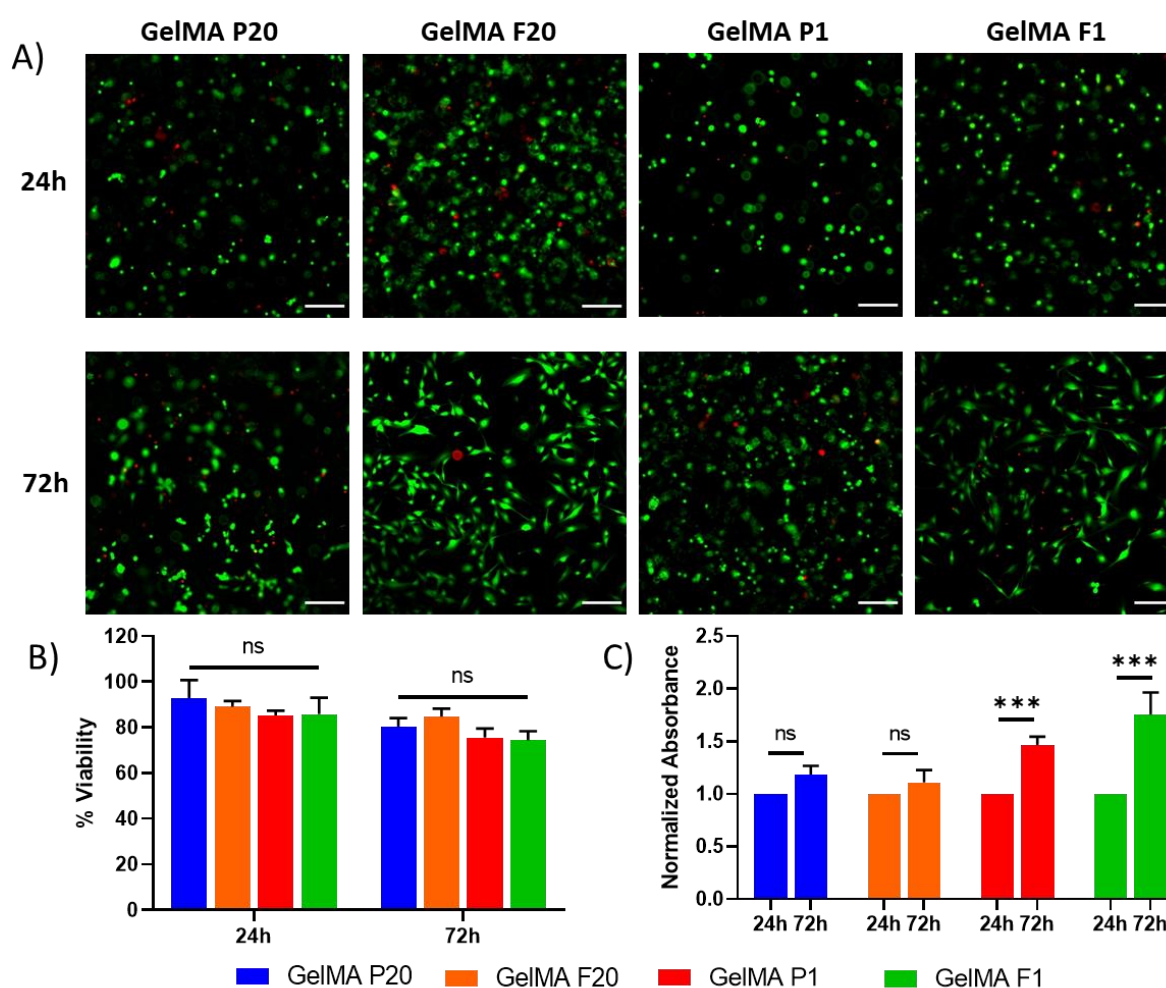


**Figure 4.** Viability of C2C12 cells in F and P skin GelMA hydrogels. A) Live/dead images of 3D cultured C2C12 cells, where green denotes live cells and red denotes dead cells. Scale bar = 200  $\mu\text{m}$ . B) Quantification of live/dead to % viability on day 1 and day 3. C) Normalized absorbance of PrestoBlue assay on day 1 and day 3 showing the proliferation of C2C12 cells. The reported data are the means of three replicates. Parametric data were analyzed using a two-way ANOVA followed by Holm-Sidak's test. Significance was indicated as \*( $p < 0.05$ ), \*\*( $p < 0.01$ ) and \*\*\*( $p < 0.001$ ).

Pepelanova *et al.* showed that the DS did not significantly impact the cell spreading of mesenchymal stem cells, however, the higher degree had less cell spreading than the lower degree, corroborating these results [562]. The influence of the level of the methacrylation does not seem to affect the cell viability and cell spreading, however, the proliferation rate is enhanced upon a lower level of methacrylation. This can be a result of the increased swelling ratio, allowing more nutrients to reach the cells as a result of the larger pore sizes [4,565]. Moreover, cell proliferation is improved as it is not hindered by the polymer network, allowing for direct cell-cell contact and signaling [562].

In conclusion, the biocompatibility of porcine GelMA is already largely established, and these results show the feasibility of using fish skin GelMA for tissue engineering applications. Further work is required to indicate how the pore size and material stiffness work together to optimize the cell microenvironment specific to an application. Additionally, as other researchers

have shown, fish skin GelMA is more easily degraded by human metalloproteinases and collagenases which could lead to better incorporation and application *in vivo* [564].

#### 4. Conclusions

Throughout this study, the potential of replacing the widely used porcine skin GelMA with fish-derived GelMA was explored. The physicochemical and biological properties of porcine and fish skin GelMA produced with low and high methacrylation degrees were studied and compared. The DS was found to be independent from the source of GelMA as it was similar between polymers with the same methacrylation degree and significantly different between low and high methacrylated GelMA. The methacrylation level and the source of GelMA did not affect the thermal and water uptake properties. However, fish skin GelMA hydrogels had a significantly higher mass swelling ratio and a lower elastic and compressive Young's moduli than porcine skin GelMA. On the other hand, with the increase in methacrylation degree, the mass swelling ratio decreased, and the elastic and compressive Young's moduli increased. Even though cell proliferation was only induced in low methacrylated GelMA and a better spreading was only observed in fish skin GelMA, all GelMA hydrogels showed great biocompatibility towards the encapsulated C2C12 myoblasts. Notably, low methacrylated fish skin GelMA showed the best proliferation and spreading of the laden C2C12 myoblasts, which encourage future investigations as a potential scaffold for skeletal muscle tissue engineering. All in all, for clinical, environmental, religious, and economical reasons, GelMA derived from marine sources might be a promising substitute to mammalian sourced GelMA for biomedical applications. Future studies will focus first on the *in vitro* differentiation of laden C2C12 myoblasts into myotubes and then on the biofabrication, using a handheld bioprinter [515], and the nanofunctionalization, with plant- and marine-derived nanoliposomes [208,224,116,227,566], of fish skin GelMA for the *in vivo* treatment of skeletal muscle injuries.



# **Chapter III:**

## **Nanofunctionalized GelMA Hydrogels**

**K. Elkhoury**, L. Sanchez-Gonzalez, P. Lavrador, R. Almeida, V. Gaspar, C. Kahn, F. Cleymand, E. Arab-Tehrany, J. F. Mano, Gelatin Methacrylate (GelMA) Nanocomposite Hydrogels embedding Bioactive Naringin Liposomes. *Polymers*. 12, 2944 (2020).



As discussed in the first chapter, the nanofunctionalization of natural hydrogels with soft nanoparticles can improve their properties and prolong the release duration of encapsulated molecules. To test this theory, in this article published in *Polymers*, Gelatin methacryloyl (GelMA) hydrogels are nanofunctionalized with salmon-derived nanoliposomes loaded with naringin and their swelling and release behavior, as well as their surface, rheological, and mechanical properties are characterized before and after nanofunctionalization. The encapsulation efficiency, release profile, and biocompatibility of naringin-loaded nanoliposomes, as well as the dispersion of liposomes in the GelMA matrix post-bioprinting are also characterized. Since naringin is a citrus flavonoid, known for its tremendous potential in inducing stem cells osteodifferentiation, and natural salmon nanoliposomes are highly enriched in omega-3 and omega-6 poly-unsaturated fatty acids, known to play an osteoprotective role, the developed nanofunctionalized GelMA hydrogel might have a potential application as a bone tissue engineering scaffold.

Comme discuté dans le premier chapitre, la nanofonctionnalisation des hydrogels naturels avec des nanoparticules molles peut améliorer leurs propriétés et prolonger la durée de libération des molécules encapsulées. Pour tester cette théorie, dans l'article publié dans le journal *Polymers* et présenté dans ce chapitre, les hydrogels à base de GelMA sont nanofonctionnalisés avec des nanoliposomes produits à partir de lécithine de saumon chargés de naringine et leur propriétés physico-chimiques (gonflement, surface, rhéologiques et mécaniques) sont caractérisées avant et après nanofonctionnalisation. La répartition des liposomes dans la matrice GelMA, l'efficacité d'encapsulation, le profil de libération de la molécule active et la biocompatibilité des nanoliposomes chargés de naringine sont également étudiés. Étant donné que la naringine est un flavonoïde d'agrume, connu pour son énorme potentiel d'induction de l'ostéodifférenciation des cellules souches, et que les nanoliposomes naturels produits à partir de lécithine de saumon sont hautement enrichis en acides gras polyinsaturés oméga-3 et oméga-6, connus pour jouer un rôle ostéoprotecteur, l'hydrogel GelMA nanofonctionnalisé développé pourrait s'avérer une voie prometteuse pour des applications en tant que matrice d'ingénierie des tissus osseux.



Article

## Gelatin methacryloyl (GelMA) Nanocomposite Hydrogels embedding Bioactive Naringin Liposomes

Kamil Elkhoury<sup>1,2</sup>, Laura Sanchez-Gonzalez<sup>1</sup>, Pedro Lavrador<sup>2</sup>, Rui Almeida<sup>2</sup>, Vítor Gaspar<sup>2</sup>, Cyril Kahn<sup>1</sup>, Corentin Peyret<sup>1</sup>, Franck Cleymand<sup>3</sup>, Elmira Arab-Tehrany<sup>1</sup>, João F. Mano<sup>2</sup>

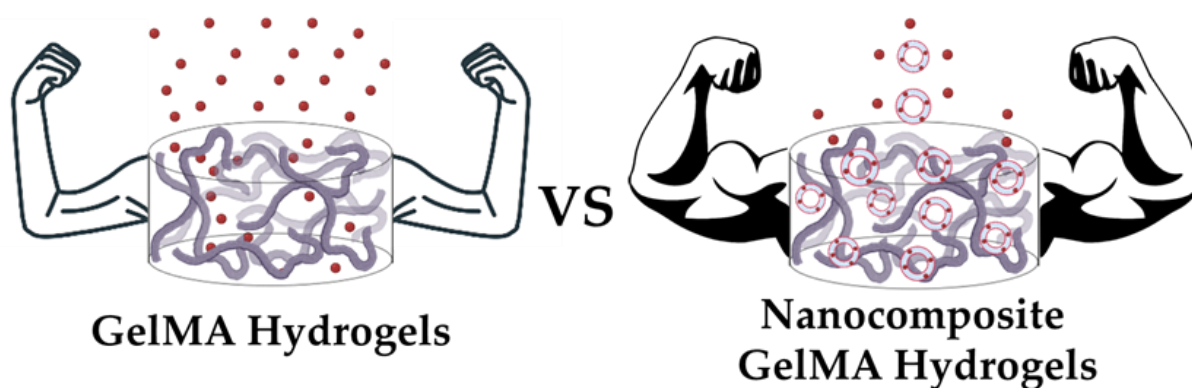
1 LIBio, Université de Lorraine, F-54000 Nancy, France.

2 Department of Chemistry, CICECO - Aveiro Institute of Materials, University of Aveiro, 3810-193 Aveiro, Portugal.

3 Institut Jean Lamour, CNRS - Université de Lorraine, F-54000 Nancy, France.

### Abstract

The development of nanocomposite hydrogels that take advantage of hierarchic building blocks is gaining increased attention due to their added functionality and numerous biomedical applications. Gathering on the unique properties of these platforms, herein we report the synthesis of bioactive nanocomposite hydrogels comprising naringin-loaded salmon-derived lecithin nanosized liposomal building blocks and gelatin methacryloyl (GelMA) macro-sized hydrogels for their embedding. This platform takes advantage of liposomes' significant drug loading capacity and their role in hydrogel network reinforcement, as well as of the injectability and light-mediated crosslinking of bioderived gelatin-based biomaterials. First, the physicochemical properties, as well as the encapsulation efficiency, release profile, and cytotoxicity of naringin-loaded nanoliposomes (LipoN) were characterized. Then, the effect of embedding LipoN in the GelMA matrix were characterized by studying the release behavior, swelling ratio, and hydrophilic character, as well as the rheological and mechanical properties of GelMA and GelMA-LipoN functionalized hydrogels. Finally, the dispersion of nanoliposomes encapsulating a model fluorescent probe in the GelMA matrix was visualized. The formulation of naringin-loaded liposomes via an optimized procedure yielded nanosized (114 nm) negatively charged particles with a high encapsulation efficiency (~99%). Naringin-loaded nanoliposomes administration to human adipose-derived stem cells confirmed their suitable cytocompatibility. Moreover, in addition to significantly extending the release of naringin from the hydrogel, the nanoliposomes inclusion in the GelMA matrix significantly increased its elastic and compressive moduli and decreased its swelling ratio, while showing an excellent dispersion in the hydrogel network. Overall, salmon-derived nanoliposomes enabled the inclusion and controlled release of pro-osteogenic bioactive molecules, as well as improved the hydrogel matrix properties, which suggests that these soft nanoparticles can play an important role in bioengineering bioactive nanocomposites for bone tissue engineering in the foreseeable future.



**Keywords:** Naringin; Liposomes; Human Mesenchymal Stem Cells; GelMA; Bone Tissue Engineering.

## 1. Introduction

The main goal of bone tissue engineering is to engineer cell-free or cell-rich biomaterial-based strategies that outperform the widely applied bone allografts and autografts [567]. In the context of cell-based therapies, human mesenchymal/stromal stem cells, either adipose (hASCs) or bone-marrow-derived, arise as particularly attractive adult stem cell sources owing to their low immunogenicity, immunosuppressive and anti-inflammatory activities, ease of isolation *via* minimally invasive techniques, and multi-lineage differentiation potential (i.e. adipose, muscle, cartilage or bone tissue precursors) [568]. Considering hASCs differentiation toward osteogenic lineages, the widely explored pro-osteogenic differentiation strategies involving Dexamethasone (Dex) or bone morphogenetic protein type 2 (BMP-2) administration are often associated with reduced effectiveness and deleterious side effects, which limits their success as stimulatory bioactive molecules for cell-based therapies.

Recently, naturally available compounds that can potentially bioinstruct the pro-osteogenic lineage differentiation process are gaining particular interest due to their cytocompatibility and potent bioactivity. One of the most promising naturally available compounds is the citrus-derived phytotherapeutic naringin. This natural flavanone glycoside cannot only enhance the proliferation and differentiation of osteoprogenitor cells into osteoblasts but simultaneously inhibits osteoclastic activity [569]. Additionally, naringin presents well-established antioxidant, anti-inflammatory, anticancer, and antimicrobial activities that are beneficial in a wide array of biomedical strategies [569,570]. This flavanone offers several advantages when compared to recombinant BMP-2 or other synthetic pro-osteogenic pharmaceuticals, such as repressing adipogenesis while solely promoting the osteogenic commitment of mesenchymal stem cells, and the ability to enhance the secretion of BMP-2 in osteoprogenitor cells while exerting a synergistic osteogenic effect with this osteoinductive protein [571–575].

Recent studies showcasing naringin's multifunctional activities and specialized pro-osteogenic toolset underline the tremendous potential for this flavonoid in inducing stem cells osteodifferentiation [569,576–579]. However, like other natural compounds, naringin presents some drawbacks that limit its clinical efficacy, such as extensive metabolism upon administration and poor *in vivo* bioavailability [580,581]. To overcome such drawbacks, self-assembled lipid nanocarriers, that can encapsulate both hydrophobic and hydrophilic bioactive compounds, may be exploited to protect and deliver naringin, while aiming to maintain its therapeutic levels over extended periods [566]. Nanoliposomes produced from natural lecithin are natural lipid nanocarriers, composed of phospholipids that permit self-sealing in aqueous media [117,123,170,582,583]. They are biocompatible and have been vastly explored for applications in different fields including food [118], cosmetics [100], drug delivery [6,116,208], and tissue engineering [122,186,299]. Furthermore, the composition of the lipids used for nanoliposome bilayers is of special interest in augmenting cells and tissue response [224,227]. In this work, natural salmon lecithin used as the nanoliposome building block is highly enriched in mono and poly-unsaturated fatty acids (PUFAs), mainly linolenic acids ( $\omega$ -3) and linoleic acids ( $\omega$ -6), which have demonstrated to play an osteoprotective role by simultaneously preventing bone resorption and increasing bone mass *in vivo* [584,585]. Collectively, naringin-loaded soft nanoliposomes with intrinsic bioactivity have not been reported to date and appear highly promising candidates for bone tissue engineering strategies either as standalone systems or included in hydrogel networks.

The successful repair of critical bone defects depends on the interaction between the implant and the injured area. Hydrogels have been recently used for various tissue engineering applications due to their high water-binding capacity, porous structure, and tunable degradation properties [3]. Moreover, hydrogels' shape can be tuned to different morphologies using different biofabrication techniques such as 3D bioprinting and fiber-based technologies [14]. From all different hydrogels previously used for bone tissue engineering applications, Gelatin methacryloyl (GelMA) hydrogel represents one of the most promising candidates for manufacturing scaffolds for bone tissue repair owing to its advantageous chemical tunability, biocompatibility, and promising *in vitro* and *in vivo* bone regeneration [586–588]. Also, in addition to gelatin being obtained from the denaturation of collagen, which is the major protein in bone tissues, recent results have shown that GelMA can significantly induce *in vitro* calcium deposition and osteogenic differentiation, as well as *in vivo* endochondral bone formation, having thus a great potential for being used in bone tissue engineering [509,589,590].

However, GelMA hydrogel networks are typically characterized by large internal pores, which allied to its hydrophilic nature, further hinders efficient loading of osteogenic hydrophobic compounds, and often leads to excessive burst release. Drugs are usually released

within hours if they were encapsulated directly in GelMA hydrogels, whereas if they were loaded in liposomes before being embedded in the GelMA matrix, their release can be prolonged to several days [296]. In this context, embedding nanoparticles within the GelMA matrix overcomes the hydrogel's poor drug loading and allows additional control over drug release kinetics, promoting a more sustained and prolonged release profile of the bioactive cargo [2]. Moreover, it has been reported that the inclusion of liposomes in the GelMA matrix enhances its strength, toughness, and flexibility, with no significant difference found between blank and loaded liposomes [215].

Gathering on this, herein we formulated an all-natural bioactive nanocomposite hydrogel comprising naringin loaded salmon-derived nanoliposome building blocks and embedded in a photocrosslinkable GelMA hydrogel network. First, the optimization of manufacturing parameters and the physicochemical characterization of blank and naringin-loaded liposomes were performed. Afterward, the encapsulation efficiency, *in vitro* release, and biocompatibility of encapsulated naringin were evaluated. In addition to the loaded-liposomes' dispersion in the GelMA matrix, their effect on the swelling behavior and the surface, rheological, mechanical properties of the GelMA matrix was investigated.

## 2. Materials and Methods

Human adipose-derived mesenchymal/stromal stem cells (hASCs , ATCC PCS- 500-011<sup>®</sup>) were purchased from LGC Standards S.L.U. (Barcelona, Spain). naringin (>95% purity) and Amicon Ultra-4 mL (100 kDa molecular weight cut-off (MWCO)) were all purchased from Laborspirit (Lisbon, Portugal). Salmon lecithin was obtained by enzymatic hydrolysis as described by Linder *et. al* [591]. A low-temperature enzymatic methodology was used to extract lipidic fractions, without requiring any organic solvents. Float-A-Lyzer G2 (3500–5000 Da MWCO) dialysis membranes were purchased from Reagente 5 (Porto, Portugal). Fetal bovine serum (FBS, E.U. approved, South American origin), minimum Essential Medium  $\alpha$ -modification ( $\alpha$ -MEM), antibiotic, and alamarBlue<sup>®</sup> were purchased from Alfacene (Lisbon, Portugal). 3,3'-Diocetadecyloxycarbocyanine perchlorate (DiO), and Dulbecco's PBS (dPBS) were purchased from Thermo Fisher Scientific (Oeiras, Portugal). Gelatin from porcine skin (Type A, 300 bloom), methacrylic anhydride (MA), Irgacure 2959 (PI) (2-hydroxy-4'-(2-hydroxyethoxy)-2-methylpropiophenone), and 2,4,6-Trinitrobenzene-sulfonic acid solution (TNBS) were all purchased from Sigma Aldrich (Saint-Quentin-Fallavier, France).

### 2.1 Preparation of blank and loaded nanoliposomes

For nanoliposomes formulation, 200 mg of salmon lecithin were dissolved in 9.8 mL of distilled water. The suspension was then mixed for 4 h under stirring in an inert atmosphere

(nitrogen) and then sonicated at 40 kHz and 40% of full power for 240 s (1 s on and 1 s off cycles) to obtain a homogeneous solution of blank nanoliposomes.

For producing drug-loaded liposomes the film hydration method was employed. In brief, 200 mg of salmon lecithin and 100 mg of naringin were dissolved in a mixture of chloroform-methanol at a ratio of 2:1 (9 mL). Afterward, the lipid-drug solution was included in a round-bottom flask and transferred to a rotary evaporator (Rotavapor<sup>®</sup> Büchi R-300, Büchi Labortechnik AG, Switzerland). After complete evaporation of organic solvents under vacuum, a thin lipid film was formed. Thin-film hydration was promoted (9.8 mL of distilled water) and the resulting suspension was stirred at 800 rpm for 4 h under a nitrogen atmosphere. The samples were then sonicated at 40 kHz and 40% of full power for 240 s (1 s on and 1 s off) to obtain a homogeneous colloidal dispersion of naringin-loaded nanoliposomes.

### 2.2 Nanoliposomes characterization

The average hydrodynamic particle diameter, polydispersity index (PDI), and  $\zeta$ -potential of the prepared blank and drug-loaded nanoliposomes were characterized by DLS with a Zetasizer Nano ZS equipment (Malvern Instruments Ltd., Malvern, UK). Prior to measuring size and  $\zeta$ -potential, the samples were diluted (1:200) with ultrapure distilled water. Measurements were performed at 25 °C with a fixed scattering angle of 173°, the refractive index at 1.471, and absorbance at 0.01. The measurements were performed in standard capillary electrophoresis cells equipped with gold electrodes (DTS 1070). At least three independent measurements were performed for each condition.

Blank and loaded nanoliposomes colloidal stability was examined by observing changes in size, PDI, and  $\zeta$ -potential upon storage. Nanoliposomes were characterized *via* DLS at different time points, namely 0, 20, and 40 days.

### 2.3 Transmission electron microscopy (TEM) analysis

Blank and naringin-loaded nanoliposomes structures were observed using transmission electron microscopy (TEM) *via* a negative staining method according to Colas *et al.* protocol [592]. Briefly, to reduce the concentration of nanoliposomes, samples were diluted with ultrapure distilled water (25-fold). To stain nanoliposomes, equal volumes of the diluted solution and an aqueous solution of ammonium molybdate (2%), used as a negative staining agent, were mixed. After the staining procedure, samples were kept at room temperature for 3 min, followed by a 5 min incubation on a copper mesh coated with carbon. Finally, samples were observed using a Philips CM20 TEM (Philips, Amsterdam, Netherlands) associated with a TEM CCD camera (Olympus, Tokyo, Japan).

### 2.4 Encapsulation efficiency

The encapsulation efficiency (EE) of naringin was obtained *via* ultraviolet-visible absorbance of its peak ( $\lambda = 282$  nm) which corresponds to the benzoyl moiety. Briefly, after naringin-loaded nanoliposomes were prepared, they were dialyzed with Float-A-Lyzer G2 dialysis devices (3.5–5 kDa MWCO) in 40 mL dPBS for 3 h and analyzed by UV–vis at  $\lambda = 282$  nm. Dialyzed blank nanoliposomes established the control for UV–vis quantification. The absorbance was measured in a quartz microplate (Hellma<sup>TM</sup> transparent 96-well quartz plate, VWR, Lisbon, Portugal) using a microplate reader equipped with a tungsten halogen lamp (Synergy HTX Biotek, Izasa Scientific, Carnaxide, Portugal). A calibration curve of naringin in dPBS was created to quantify the EE. EE was calculated using Equation (1):

$$EE (\%) = (1 - N_r/N_i) \times 100 \quad (1)$$

where EE (%) is the encapsulation efficiency,  $N_r$  the amount of naringin present in the dialysate and  $N_i$  the initial amount of naringin added.

### 2.5 *In vitro* release profile of naringin loaded in nanoliposomes

To mimic the physiological scenario, the *in vitro* release profile of naringin was examined in dPBS at pH 7.4. Briefly, 2 mL of freshly produced naringin-loaded nanoliposomes was transferred to the Float-A-Lyzer G2 dialysis device and submerged in 40 mL of dPBS. The release profile was investigated at 37 °C and stirred at 600 rpm. At specific time points (1, 2, 3, 24, 48, 72, 96, 120, 144, 168, and 192 h), 1 mL of samples was recovered from the dialysate and replaced by 1 mL of fresh dPBS. A standard naringin calibration curve in dPBS was used to quantify the cumulative release.

### 2.6 Cytotoxicity and cellular proliferation assays

Cells were maintained in a humidified 5 % CO<sub>2</sub> incubator at 37 °C and manipulated in a biosafety cabinet. hASCs were routinely cultured in basal culture medium (BM) comprised of  $\alpha$ -MEM supplemented with 1% v/v of an antibiotic mixture and 10% v/v heat-inactivated FBS. BM was exchanged every 3-4 days. Cells were subcultured before reaching confluence.

AlamarBlue ® cell viability assay was used to evaluate the cell metabolism of hASCs. Cells were seeded in a 96-well plate overnight in BM at a density of  $3.5 \times 10^3$  cells per well ( $n = 10$ ). Later, cells were incubated with BM containing naringin-loaded liposomes at concentrations of 25, 50, and 100  $\mu\text{g mL}^{-1}$  of naringin. The medium was switched to BM and alamarBlue after 24 and 96 h. The media was then transferred to a black, clear-bottom 96-well plate and resorufin fluorescence was quantified at an excitation/emission of  $\lambda_{\text{ex}} = 540$  nm/  $\lambda_{\text{em}} = 600$  nm, in a multimode microplate reader.

### 2.7 GelMA synthesis and hydrogels preparation

GelMA was synthesized, from porcine skin gelatin type A, according to the general method first adopted by Van Den Bulcke *et al.* [310]. In brief, gelatin was mixed at 10% (w/v) into dPBS at 60 °C and stirred until fully dissolved. Then, 0.6 g of MA/ 1 g of gelatin was added dropwise to the gelatin solution, at 50 °C and a rate of 0.5 mL min<sup>-1</sup> under stirring and allowed to react for 1 h. After 1 h, the reaction was stopped following 5X dilution with warm (40 °C) dPBS. To remove salts and unreacted MA, the mixture was dialyzed for 5 days at 40 °C against distilled water using 12–14 kDa cutoff dialysis tubing, in the dark. The solution was finally freeze-dried, generating a porous white foam that was stored at -20 °C until further use. The degree of substitution (D.S.) was determined by the TNBS assay [540], (D.S.: 76.4 ± 1.1%, n=3).

GelMA solution was prepared by dissolving 10% (w/v) of the freeze-dried biopolymer into a dPBS solution at 50 °C. Then, 0.5% (w/v) of PI was added and the temperature was increased to 70 °C to reach complete solubilization. GelMA solution was UV crosslinked (360–480 nm) in a specific PDMS mold for 40 s to create hydrogel discs. Nanocomposite GelMA hydrogels were prepared using the same protocol by mixing naringin-loaded liposomes at a concentration of 50 µg mL<sup>-1</sup> of naringin with the GelMA solution before UV crosslinking.

### 2.8 In vitro release profile of naringin embedded in GelMA

To study the release profile, naringin and naringin-loaded nanoliposomes were embedded in GelMA discs that were transferred to 12-14 kDa cutoff dialysis tubing containing 5 mL of dPBS and submerged in 15 mL of dPBS. The release profile was investigated at 37 °C and stirred at 600 rpm. At specific time points (1, 2, 3, 24, 48, and 72 h), 2 mL of samples was recovered from the dialysate and replaced by 2 mL of fresh dPBS. A standard naringin calibration curve in dPBS was used to quantify the cumulative release.

### 2.9 Mass swelling ratio

The mass swelling ratio was evaluated by using five cylindrical samples (2 cm diameter, 2 mm height). The samples were kept in dPBS at 37 °C for 24 h. The excessive water was gently removed using a paper tissue, and the swollen weight of the samples was measured using a precision balance. Later, the samples were freeze-dried for 3 days and their dry weight was measured. The mass swelling ratio was calculated as the ratio of the mass value after swelling to the mass value of dried samples after lyophilization.

### 2.10 Surface properties

The polar component ( $\gamma^P$ ), dispersive component ( $\gamma^D$ ), and the surface tension ( $\gamma$ ) of hydrogels were quantified according to the Owens and Wendt method [593]. This quantification

was achieved using water ( $\gamma_{\text{Liq}} = 72.8 \text{ mN m}^{-1}$ ;  $\gamma_{\text{Liq}}^{\text{D}} = 21.8 \text{ mN m}^{-1}$ ;  $\gamma_{\text{Liq}}^{\text{P}} = 51 \text{ mN m}^{-1}$ ), diiodomethane ( $\gamma_{\text{Liq}} = 50.8 \text{ mN m}^{-1}$ ;  $\gamma_{\text{Liq}}^{\text{D}} = 50.8 \text{ mN m}^{-1}$ ;  $\gamma_{\text{Liq}}^{\text{P}} = 0 \text{ mN m}^{-1}$ ), and glycerol ( $\gamma_{\text{Liq}} = 63.4 \text{ mN m}^{-1}$ ;  $\gamma_{\text{Liq}}^{\text{D}} = 37 \text{ mN m}^{-1}$ ;  $\gamma_{\text{Liq}}^{\text{P}} = 26.4 \text{ mN m}^{-1}$ ) according to the following equations:

$$\gamma = \gamma^{\text{D}} + \gamma^{\text{P}} \quad (2)$$

$$\gamma_{\text{Liq}} (1 + \cos\theta) = 2(\sqrt{\gamma^{\text{D}} \times \gamma_{\text{Liq}}^{\text{D}}} + \sqrt{\gamma^{\text{P}} \times \gamma_{\text{Liq}}^{\text{P}}}) \quad (3)$$

Where  $\theta$ ,  $\gamma$ ,  $\gamma^{\text{P}}$ ,  $\gamma^{\text{D}}$ ,  $\gamma_{\text{Liq}}$ ,  $\gamma_{\text{Liq}}^{\text{D}}$ , and  $\gamma_{\text{Liq}}^{\text{P}}$  are the contact angle, the surface tension, the dispersive and the polar components of the hydrogel's surface and the tested liquid. All the surface tension parameters are expressed in  $\text{mN m}^{-1}$  and the contact angle is expressed in degree.

The contact angle measurements were carried out using three liquids (water, diiodomethane, and glycerol), with well-known polar and dispersive components *via* the sessile drop method on a goniometer (Drop Shape Analyzer 30, KRÜSS GmbH, Hamburg, Germany). First, a  $2 \mu\text{L}$  droplet of each liquid was deposited on the hydrogel surface with a precision syringe. Then, the contact angle was measured between the tangent at the drop boundary and the baseline of the water drop. Three measurements per hydrogel were carried out.

### 2.11 Rheological testing

Amplitude sweep tests at a frequency of 1 Hz were performed using a Kinexus pro rheometer (Malvern Instruments Ltd., Worcestershire, United Kingdom) equipped with a plane-plane geometry with a diameter of 20 mm. The hydrogel was loaded into a 1 mm gap between the plates and allowed to relax until the normal force was zero. The amplitudes of shear stress were carried out over a pressure range from 0.01 Pa to 500 Pa. The test was done with a constant frequency of 1 Hz at  $37 \text{ }^\circ\text{C}$  and the measuring system was covered with a humid chamber to minimize the evaporation of the water. Three different hydrogel discs are tested for each type of hydrogel with the same experimental parameters.

### 2.12 Mechanical testing

The mechanical measurements were performed using a universal testing machine (Lloyd-LRX, Lloyd Instruments, Fareham, UK). The samples were prepared in a cylindrical shape (2 cm diameter and 2 mm height). Compression tests were performed at a crosshead speed of 1 mm/min until fracture occurred. Prior to all measurements, the zero-gap was determined. Five samples of each condition were tested. The compressive modulus was determined as the slope of the linear region corresponding to the elastic part (10–20 % strain) of the stress-strain curve.

### 2.13 3D bioprinting and confocal laser scanning microscopy analysis

GelMA embedded, DiO-loaded nanoliposomes bioink (containing Irgacure 2959 photoinitiator, 0.1 % in PBS pH=7.4) was used to 3D bioprint disc-shaped constructs using a pneumatic extrusion bioprinter INKREDIBLE+ (CELLINK, Gothenburg, Sweden) equipped with a 23G nozzle, operating at pressures ranging from 60-70 kPa. GelMA-nanoliposomes were UV crosslinked (360-480 nm) for 40 s to generate nanocomposite hydrogels (Omniscure S-2000, 0.86 W/cm<sup>2</sup>). Confocal laser scanning microscopy imaging was performed in an LSM 880 Airyscan microscope (Carl Zeiss, Oberkochen, Germany) equipped with GaAsP/PMT detectors and a 20x/NA 0.8 Plan-Apochromat objective. Acquired data was post-processed in Zeiss ZEN v2.3 blue edition software.

## 3. Results and Discussion

### 3.1 Nanoliposomes formulation and characterization

The applied sonication parameters during the naringin loading process (**Figure 1 A**) can affect the minimum size that can be achieved. The size of the naringin-loaded nanoliposomes (~114 nm) was found to be smaller than that of the blank nanoliposomes (~144 nm) (**Figure 1 B, C**), which suggests the presence of a strong interaction between naringin and salmon lecithin nanoliposomes that leads to core compaction [117,594]. The size was further confirmed with the TEM images (**Figure 1 D, E**) that also revealed liposomes spherical morphology. The formulated liposomes were relatively monodisperse, presenting a low PDI (< 0.25) associated with a narrow size distribution [595]. For nanoliposomal formulations used for drug delivery applications, a PDI value lower than 0.3 indicates a homogenous population and is considered to be acceptable [596].  $\zeta$ -potential for both blank (-45 mV) and loaded (-52 mV) nanoliposomes was negative, which is probably caused by the negatively charged phospholipids of salmon lecithin, such as phosphatidylserine, phosphatidic acid, phosphatidylglycerol, and phosphatidylinositol that can be exposed at the nanoliposomes surface [186].

Particle size, polydispersity index (PDI), and  $\zeta$ -potential of blank and naringin-loaded nanoliposomes were measured directly after preparation, as well as after 20 and 40 days to assess their colloidal stability. The results presented in **Table 1** indicate that throughout the storage period nanoparticles' size increased but stayed in the nanometric range (< 200 nm), the  $\zeta$ -potential decreased for higher negative values, and the particles maintained their relative narrow distribution with PDI values <0.3. Nanoliposomes stability was probably due to the high negative  $\zeta$ -potential value because the higher this value, the stronger the repulsion between two adjacent particles is, and thus the higher the stability of the nanoliposomal formulation will be.

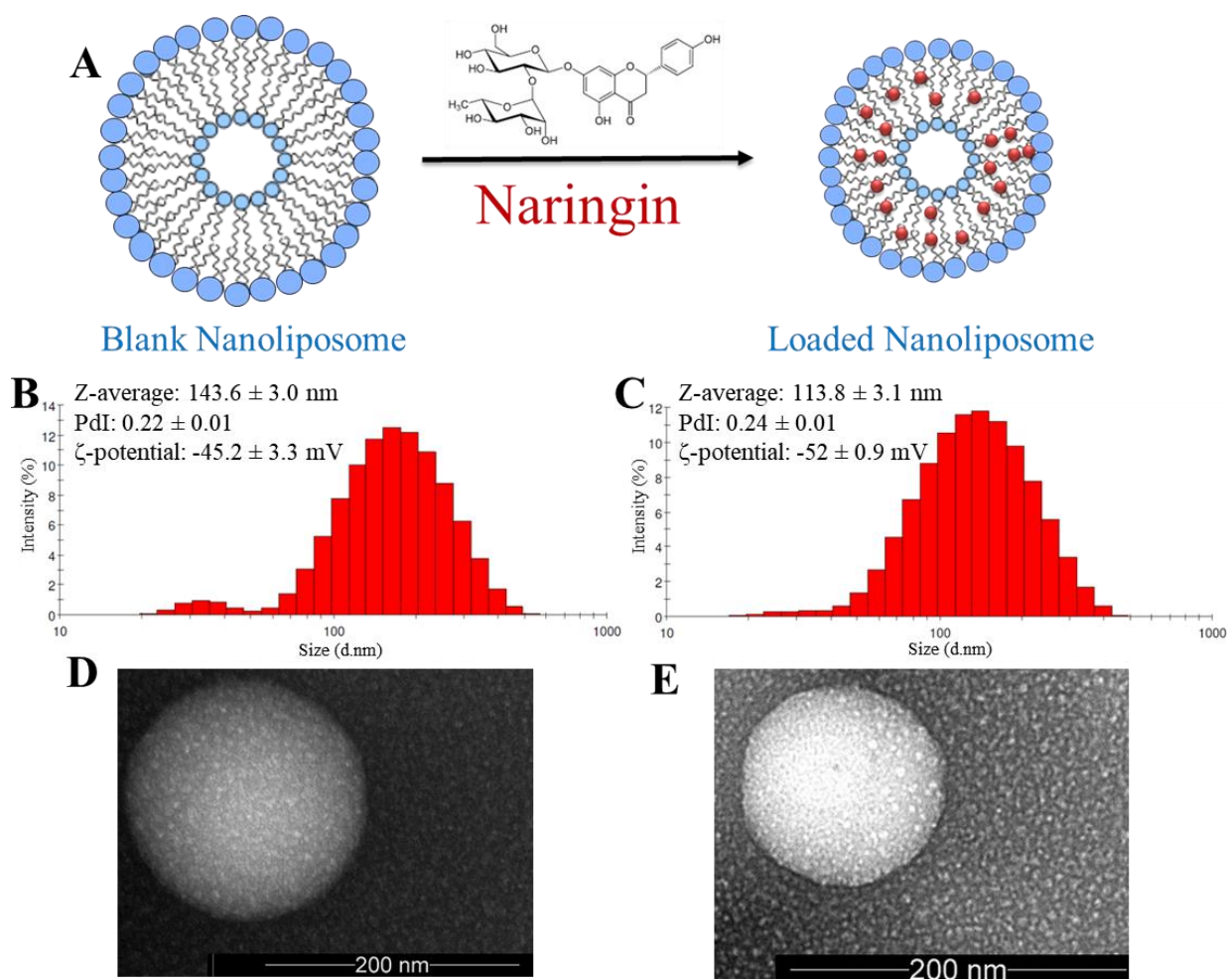


**Figure 1.** (A) Schematic representation of blank and naringin-loaded nanoliposomes. Physicochemical characterization *via* DLS of (B) blank and (C) loaded nanoliposomes. TEM images of (D) blank and (E) loaded nanoliposomes.

**Table 1.** Blank nanoliposomes (BL) and naringin-loaded nanoliposomes (LL) mean particle size, polydispersity index (PdI), and  $\zeta$ -potential at day 0, 20, and 40.

	Day	BL	LL
Size (nm)	0	143.6 ± 3.0	113.8 ± 3.1
	20	148.6 ± 5.2	131.0 ± 1.3
	40	168 ± 9.9	152.1 ± 1.6
PdI	0	0.22 ± 0.01	0.24 ± 0.01
	20	0.27 ± 0.01	0.29 ± 0.01
	40	0.28 ± 0.02	0.27 ± 0.02
$\zeta$ -potential (mV)	0	-45.2 ± 3.3	-52.0 ± 0.9
	20	-49.2 ± 0.9	-53.8 ± 0.4
	40	-56.9 ± 1.0	-54.8 ± 0.4

### 3.2 Encapsulation efficiency and release profile of naringin loaded in nanoliposomes

Nanoliposomes achieved a high EE of naringin ( $99.7 \pm 0.07\%$ ) that was quantified by UV-vis analysis and extrapolated from naringin's calibration curve. This encapsulation efficiency was consistent with other studies using liposomes to encapsulate naringin [594] and its aglycone derivative, Naringenin [597]. Nanoliposomes achieved a higher EE of naringin than that of methoxy-poly(ethylene glycol)-maleimide-thiol-poly(l-lactide) (mPEG-MS-PLA) polymeric nanomicelles which achieved an EE of  $87.2 \pm 4.6\%$  [576].

A biphasic release was observed for naringin-loaded nanoliposomes (**Figure 2 A**). The release profile showed a slow release of about 4 % only within the first three hours, followed by sustained drug release over the next 8 days. The obtained release profile is comparable to those obtained in the literature [576]. Interestingly, the salmon derived nanoliposomes exhibited only a 40 % release after 24 h, suggesting that nanoliposomes provide a more sustained release compared to previously reported polymeric nanomicelles (~65 % at 24h) [45]. This suggests that salmon-derived lipids prevent the initial burst release and provide a controlled extended release of the encapsulated flavonoid. This can improve naringin's *in vivo* bioavailability and stability, which might lead to improvements in its therapeutic effect, and prevent any unwanted interactions with other molecules [569,594].

Previously, a significant pro-osteogenic effect between free and encapsulated naringin was observed [569,576]. These findings suggest that the controlled release of this flavonoid might affect the promotion of osteodifferentiation. This osteodifferentiation can be further increased by the high percentage of  $\omega$ -3 PUFAs present in salmon nanoliposomes. Previously, these nanoparticles have been found to be composed of around 50% PUFAs, of which about 10% EPA and 24% DHA, and an  $\omega$ -3/ $\omega$ -6 ratio of 3.8 [123]. These  $\omega$ -3 PUFAs have been found to be able to stimulate the expression of Cbfa1 transcription factor involved in the initiation and modulation of osteoblast differentiation [598,599]. Moreover,  $\omega$ -3 PUFAs can regulate bone metabolism, decrease osteoclastogenesis, and modulate the number of proinflammatory cytokines which improves calcium accretion in bone [600]. The high ratio of  $\omega$ -3 to  $\omega$ -6 can protect against the bone mass loss, since it was found that  $\omega$ -6 diminishes the *opg/rankl* gene expression in osteoblasts which stimulates MSC differentiation into adipocytes, favors the osteoclastic activity, and reduces the production of osteoblasts [601]. So, these  $\omega$ -3 rich nanoliposomes can protect the bones formed by the osteodifferentiation of hASCs induced using naringin.

### 3.3 Cellular viability

Although salmon nanoliposomes have been found to be cytocompatible toward cortical neurons and Wharton's jelly human stem cells [117,186,583], investigating a possible cytotoxic response with a new cell type is an important requirement. Naringin has already been tested for its cytotoxicity toward hASCs in the range of 5–50  $\mu\text{g mL}^{-1}$  [576]. However, evaluating the cytotoxicity of naringin-loaded in nanoliposomes is important for the envisioned final application as bone regenerative nanocomposite hydrogels. For this hASCs were incubated with different concentrations of naringin-loaded nanoliposomes (LipoN 25, 50, and 100), corresponding to naringin concentrations of 25, 50, and 100  $\mu\text{g mL}^{-1}$  and nanoliposomes

concentrations of 50, 100, and 200  $\mu\text{g mL}^{-1}$ . Results show that LipoN 25 and LipoN 50, contrary to LipoN 100, showed no cytotoxicity at 24 h and 96 h (**Figure 2 B**).

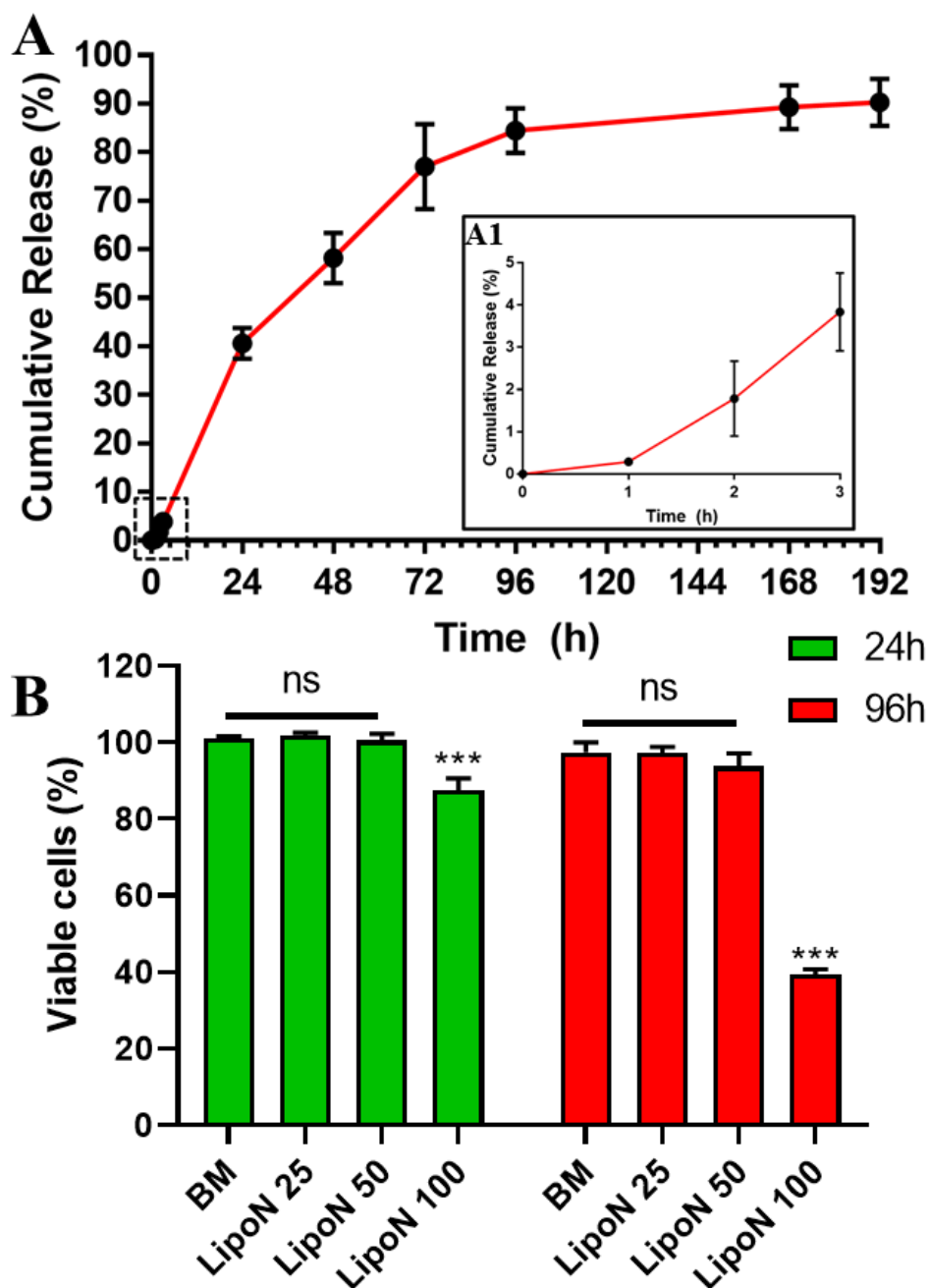


**Figure 2.** (A) Naringin-loaded nanoliposomes *in vitro* cumulative release profile in dPBS (pH = 7.4) at 37 °C. (A1) The zoomed section representing the cumulative release during the first 3 h. Data are presented as mean  $\pm$  s.d. ( $n = 3$ ). (B) hASCs cell viability at 24 and 96 h following incubation with basal culture medium (BM) and different naringin concentrations (25, 50, and 100  $\mu\text{g mL}^{-1}$ ) loaded in nanoliposomes (LipoN, 50). Data are represented as mean  $\pm$  s.d.,  $n=5$ . The reported data were analyzed using a two-way ANOVA followed by Holm-Sidak's test. Significance was indicated as \*( $p < 0.05$ ), \*\*( $p < 0.01$ ) and \*\*\*( $p < 0.001$ ).

These findings are in complete agreement with previous studies. Naringin has been found to be biocompatible and to significantly induce cell proliferation of osteoprogenitor cells [574,602,603]. Whereas, Mahmoud *et al.*, Latifi *et al.*, and Dostert *et al.* previously reported the

biocompatibility of low concentrations of salmon-derived nanoliposomes [117,186,583]. These results suggest that naringin-loaded salmon-derived nanoliposomes with a maximum naringin concentration of  $50 \mu\text{g mL}^{-1}$  (LipoN 50) present high biocompatibility toward hASCs. Having confirmed this parameter, the nanosized blocks, LipoN 50, were embedded in GelMA and subjected to UV-mediated photocrosslinking to yield naringin-loaded nanocomposite hydrogels (GelMA-LipoN).

### 3.4 *In vitro* release profile of naringin embedded in GelMA

GelMA-N (GelMA hydrogels embedding free naringin) and GelMA-LipoN presented different release behaviors and profiles (**Figure 3 A, B**), as the nanocomposite GelMA hydrogels released significantly fewer quantities of naringin than the liposome-free GelMA hydrogels. This might be due to the small size of the phytotherapeutic that can easily pass through the microsized pores of GelMA. According to the results, the amount of naringin released from GelMA-LipoN was significantly extended compared to GelMA-N. GelMA-N released 65% of naringin in the first 3 hours, compared to the ~4% released by GelMA-LipoN. At 72 hours, less than 10% of naringin remained in GelMA-N compared to more than 45% in nanocomposite hydrogels. The obtained release profiles of GelMA and nanocomposite GelMA are comparable to those obtained in the literature for naringin and other therapeutic molecules [296,604,605]. This suggests that GelMA scaffolds can be successfully loaded with LipoN and provide a controlled extended release of the encapsulated flavonoid, which might improve its *in vivo* bioavailability and hence its therapeutic effect.

### 3.5 Swelling behavior

The swelling behavior of crosslinked nanocomposite hydrogels is an essential parameter, as it affects the diffusion of solutes and the mechanical properties of these platforms along time [4]. The swelling behavior is governed by the crosslinking density, hydrophilicity, and structural properties of the hydrogel, as well as by its interactions with the solvent [535,552]. To study this behavior, GelMA and GelMA-LipoN were fully swelled in dPBS at  $37^\circ\text{C}$  for 24 h to obtain their swollen weight and then freeze-dried for three days to obtain their dry weight. Using the swollen and dry weight of GelMA, the mass swelling ratio was then calculated. GelMA had a higher mass swelling ratio than GelMA-LipoN (**Figure 3 C**). The decrease in swelling ratio of GelMA-LipoN hydrogels is considered an advantageous property since scaffolds will undergo a limited shape transformation once contacted with body fluids [296]. The low swelling ratio may also assure a higher residence time of the nanoliposomes in the nanocomposite hydrogels matrix by preventing their premature clearing.

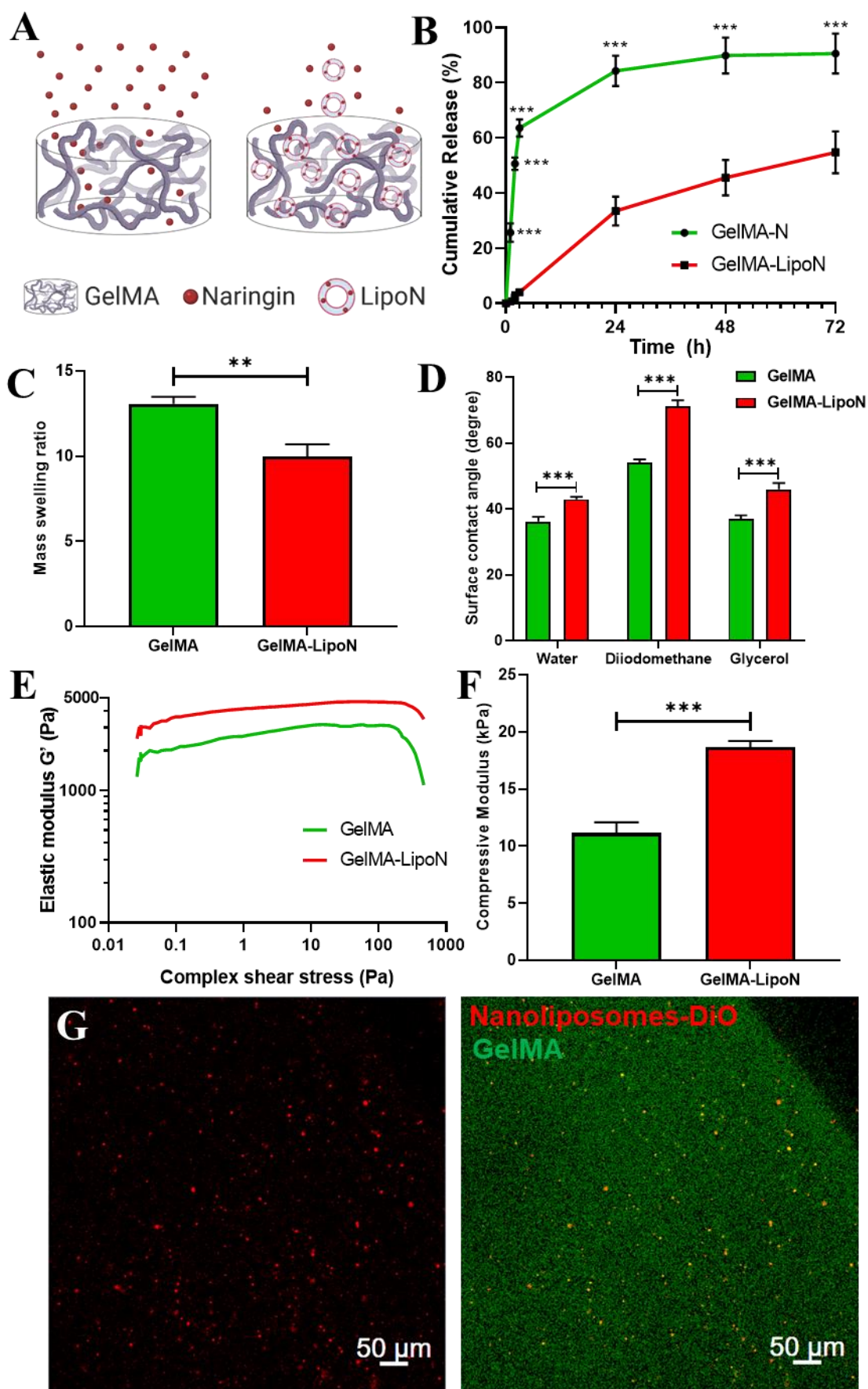


**Figure 3.** (A) Schematic representation of the different release behavior of naringin embedded directly in GelMA (GelMA-N) versus when first encapsulated in liposomes (GelMA-LipoN). Created with BioRender.com. (B) The *in vitro* cumulative release profile of GelMA-N and GelMA-LipoN in dPBS (pH = 7.4) at 37 °C. (C) The mass swelling ratios of GelMA and GelMA-LipoN hydrogels. (D) The surface contact angle of GelMA and GelMA-LipoN hydrogels measured using water, diiodomethane,

and glycerol. (E) The elastic modulus ( $G'$ ) as a function of complex shear stress and (F) the compressive modulus of GelMA and GelMA-LipoN hydrogels. (G) Confocal micrographs of DiO-loaded nanoliposomes embedded in a bioprinted 3D GelMA construct. Red channel: nanoliposomes-DiO. Green Channel: GelMA autofluorescence. Data are represented as mean  $\pm$  s.d.,  $n=3$ . The reported data of C and F were analyzed using a Student's t-test and of B and D using a two-way ANOVA followed by Holm-Sidak's test. Significance was indicated as \*( $p < 0.05$ ), \*\*( $p < 0.01$ ) and \*\*\*( $p < 0.001$ ).

A plausible explanation for this decrease in the mass swelling ratio is that the level of intermolecular crosslinking through noncovalent forces (electrostatic interactions or hydrogen bonds) have increased when nanoliposomes were embedded in GelMA. These hydrogen bonds can be created between phosphorous or other liposomal molecules and nitrogen or other elements in the GelMA network. Those newly formed bonds will increase the micro-crosslinking level of GelMA, which will thus lead to a decrease in pores' size and in the volume of retained fluid, since hydrogels with smaller pores are able to withhold a smaller volume of fluid [4,535,536].

### 3.6 Contact angle

The water contact angle on the GelMA hydrogel was significantly lower than on the GelMA-LipoN hydrogel ( $36.2^\circ \pm 1.4^\circ$  vs  $42.9^\circ \pm 0.7^\circ$ , **Figure 3 D**), revealing a much lower water affinity of the GelMA-LipoN's surface. Such behavior can be attributed to the newly formed hydrogen bonds on the GelMA surface following loaded-nanoliposomes embedding which will not only have a repulsive reaction to the droplet of water but also reduce the porosity which will lead to lower capillarity forces, and thus decrease water absorption. Indeed, the surface free energy of the GelMA was increased after the introduction of the loaded-liposomal soft nanoparticles (**Table 2**), due to a higher polar contribution. All in all, the embedment of loaded-nanoliposomes decreased the hydrophilic character of the GelMA matrix, which means that the GelMA-LipoN scaffolds offer better barrier properties.

**Table 2.** The surface tension of hydrogels ( $\gamma$ ) and its polar ( $\gamma^P$ ) and dispersive ( $\gamma^D$ ) components.

	GelMA	GelMA-LipoN
$\gamma^P$ (mN m <sup>-1</sup> )	28.8 $\pm$ 0.6	31.7 $\pm$ 1.1
$\gamma^D$ (mN m <sup>-1</sup> )	29.2 $\pm$ 0.5	21.2 $\pm$ 1.7
$\gamma$ (mN m <sup>-1</sup> )	58.0 $\pm$ 0.4	52.9 $\pm$ 2.0

### 3.7 Rheological and mechanical properties

Rheological measurements were carried out to assess the elastic properties of GelMA hydrogels. Results, presented in **Figure 3 E**, show that the elastic modulus  $G'$ , also known as real modulus or storage modulus, of GelMA hydrogels ( $\sim 2000$  Pa) was lower than  $G'$  of GelMA-LipoN hydrogels ( $\sim 3500$  Pa). Moreover, to investigate the impact of the integration of nanoliposomes in the GelMA matrix on the hydrogel's mechanical properties, a compression test was performed on hydrogel samples. **Figure 3 F** shows the compressive modulus that was

calculated from the slope of the linear region corresponding to the elastic part (10–20 % strain) of the stress-strain curve. It can be seen that the integration of nanoliposomes has led to a significant increase in the compression modulus from  $11.14 \pm 0.94$  kPa for GelMA to  $18.87 \pm 0.53$  kPa for GelMA-LipoN. The higher elastic and compression moduli of GelMA-LipoN might be caused by the newly formed hydrogen bonds that can produce a double crosslinked structure and thus can sustain higher external stress and load. Gen *et al.* previously reported a higher elastic modulus in GelMA hydrogels embedding liposomes [215]. Wu *et al.* previously reported a similar significant increase in the compressive modulus following liposomes integration in the GelMA matrix [296]. Creating composite hydrogels with improved mechanical properties is of great importance for bone tissue engineering applications since these scaffolds will provide a temporary structural and mechanical support to the laden proliferating and differentiating stem cells, leading to the synthesis of mineralized bone matrices that will replace the scaffold itself [606].

### 3.8 Nanoliposomes dispersion in nanocomposite hydrogels matrix

The confocal micrographs of the GelMA-LipoN (**Figure 3 G**) show that nanoliposomes encapsulating DiO presented a good dispersion within 3D bioprinted GelMA scaffolds without any significant aggregation being visualized. In addition to the naringin controlled release, the nanoliposomes stability upon dispersion in complex protein-based mixtures is another valuable property, that can assure the equal presence of the drug encapsulated inside the nanocomposite platforms to all encapsulated stem cells, which can maximize its effect. Similar liposomal distribution was previously observed in chitosan/gelatin hydrogels by Ciobanu *et al.* [607]. This homogeneous distribution can be very valuable for nanocomposite platforms engineering with the purpose of being applied in tissue engineering when used as implantable controlled delivery systems or as cell-laden scaffolds.

## 4. Conclusions

Throughout this study, the development and characterization of a potential bone regenerative nanocomposite hydrogel were achieved. The nanofunctionalized platform was comprised of a naturally available drug encapsulated in salmon-derived nanoliposomes and embedded in modified gelatin hydrogels. The inclusion of naringin in nanoliposomes resulted in a high encapsulation efficiency and a controlled drug release profile. The loaded nanoliposomes (LipoN 25 and LipoN 50) showed no cytotoxicity toward hASCs. Taken together with previous studies, the findings of this study provide evidence that nanoliposomes loaded with naringin are highly biocompatible and can be safely used for bone tissue engineering applications. Since nanoliposomes are derived from salmon fish, they are rich in  $\omega$ -

3 PUFAs which offers a double functionality of being bioactive on their own and being able to encapsulate bioactive molecules, increasing further their efficacy.

Moreover, the embedment of nanoliposomes in GelMA has not just improved its mechanical and rheological properties but also decreased its swelling ratio and hydrophilic character and extended the release of naringin. So, nanoliposomes have toughened the GelMA scaffold, made it more resistant to shape transformations, and improved its barrier properties and drug release behavior. To add to all these advantages, nanoliposomes did not form any aggregates and had a homogeneous distribution in the GelMA construct after the bioprinting process, which suggests that the natural nanocomposite hydrogel composed of naringin-loaded nanoliposomes embedded in GelMA may be a promising bioink candidate for the bioprinting of cell-laden bioactive pro-osteogenic constructs. Since GelMA printed structures suffer from a poor resolution [562], the developed nanocomposite hydrogel will be further evaluated and optimized as a bioink to balance between its printability and functionality. Future studies will focus also on the ability of naringin-loaded nanoliposomes to induce the osteodifferentiation of hASCs in 2D cell culture, as well as in 3D cell culture when encapsulated inside the GelMA hydrogel matrix.



# **Chapter IV:**

## Biofabricated GelMA Hydrogels

**K. Elkhoury**, M. Chen, P. Koçak, Y. Li, E. Martinez, M. Urbina, L. Sanchez-Gonzalez, E. Arab-Tehrany, S. R. Shin, Reprogramming exosome-liposome hybrid bioink. *In preparation.*



Direct cardiac reprogramming is one area that would benefit immensely from the development of a targeting system, like the one presented in the first chapter, since the delivery of reprogramming miRNAs needs to be targeted towards cardiac fibroblasts. For this, in this work, the fabrication of a soft hybrid exosome-liposome targeting nanoparticles was attempted. The physicochemical properties, miRNA encapsulation efficiency, biocompatibility, cellular uptake, and targeting ability of the produced hybrid nanoparticles were characterized. Since hydrogel environments generally produce higher reprogramming efficiencies, the smart hybrid nanoparticles were embedded in gelatin methacryloyl (GelMA) hydrogels. The hybrid GelMA's pore size, mechanical properties, biocompatibility, and efficient miRNA delivery were characterized. The reprogramming ability of the hybrid GelMA was investigated for 14 days using the cardiac marker Troponin I. Finally, the biofabrication and microfabrication versatility of the hybrid biomaterial was investigated. Since the hybrid GelMA hydrogel was successfully used to reprogram cardiac cells and to biofabricate complex architectures, it can be considered a very promising bioink for direct reprogramming applications.

La reprogrammation cardiaque directe est un domaine qui pourrait amplement bénéficier du développement d'un système de ciblage, comme celui présenté dans le premier chapitre, puisque la libération des miARN de reprogrammation doit être ciblée vers les fibroblastes cardiaques. Pour cela, dans ce travail, l'élaboration de nanoparticules hybrides molles de type exosome-liposome a été proposée. Les propriétés physicochimiques de ces particules, leur biocompatibilité, leur possible absorption cellulaire ainsi que l'efficacité d'encapsulation des miARN et leur capacité de ciblage ont été étudiés. Comme les environnements de type hydrogel permettent généralement une efficacité de reprogrammation élevée, les nanoparticules hybrides de type exosome-liposome ont été incorporées dans des hydrogels à base de gélatine méthacrylée (GelMA). Une caractérisation physicochimique (porosité, propriétés mécaniques) et biologique (biocompatibilité, livraison efficace de miARN) de la matrice hybride a été réalisée. Pour compléter cette étude, la capacité de reprogrammation du GelMA hybride a été étudiée pendant 14 jours en utilisant le marqueur cardiaque Troponine I. Enfin, la capacité de biofabrication et de microfabrication du biomatériau hybride a été évaluée. Comme l'hydrogel hybride GelMA a été utilisé avec succès pour reprogrammer des cellules cardiaques et pour biofabriquer des architectures complexes, il peut être considéré comme une bioencres très prometteuse pour des applications de reprogrammation directe.



---

Article

## Reprogramming exosome-liposome hybrid bioink

Kamil Elkhoury<sup>1,2</sup>, Mo Chen<sup>1</sup>, Polen Koçak<sup>1,3</sup>, Eduardo Martinez<sup>1</sup>, Mariely Urbina<sup>1</sup>, Laura Sanchez-Gonzalez<sup>2</sup>, Elmira Arab-Tehrany<sup>2</sup>, Su Ryon Shin<sup>1</sup>

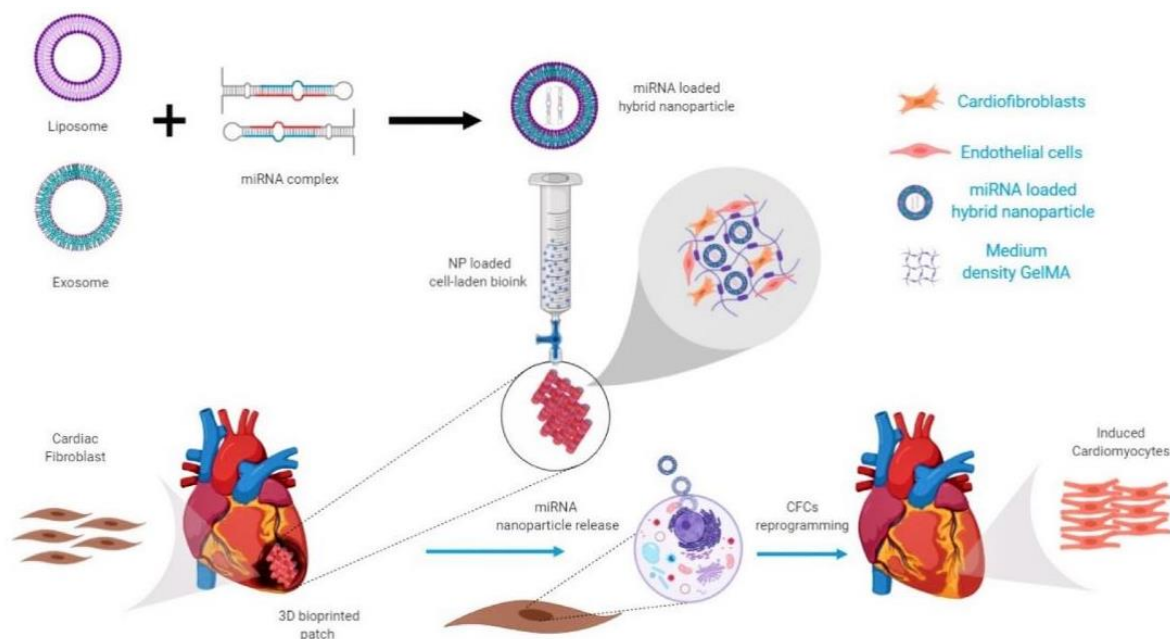
<sup>1</sup> Division of Engineering in Medicine, Department of Medicine, Brigham and Women's Hospital, Harvard Medical School, Cambridge, MA 02139, USA.

<sup>2</sup> LIBio, University of Lorraine, F-54000 Nancy, France.

<sup>3</sup> Department of Genetics and Bioengineering, Faculty of Engineering and Architecture, Yeditepe University, TR-34755 Istanbul, Turkey.

### Abstract

Coronary artery disease is the most common form of cardiovascular disease, which results in the loss of cardiomyocytes (CMs) at the site of myocardial infarction. Cardiac fibroblasts (CFs) quickly respond to this loss by forming chronic scar tissue. To restore the healthy heart muscle, the delivery of a specific combination of miRNAs can initiate a direct reprogramming of CFs into induced cardiac myocytes (iCMs). To increase the loading and targeting efficiency of miRNAs, hybrid exosome-liposome nanoparticles (hELs) were produced through membrane fusion of CFs-derived exosomes with salmon-derived liposomes *via* sonication. Following their characterization, hELs were found to be nanosized, negatively charged, and highly biocompatible. In addition, they successfully encapsulated and targeted the delivery of model miRNAs to CFs. Due to the increase in matrix metalloproteinases (MMPs) expression, three-dimensional (3D) hydrogel environments generally present a higher reprogramming efficiency. For this, gelatin methacryloyl (GelMA) was nanofunctionalized with hELs that improved its mechanical properties and decreased its pore size while maintaining its high biocompatibility. More importantly, CFs were successfully reprogrammed in 14 days when they were encapsulated in the GelMA-hELs hydrogel loaded with a miRNA reprogramming combo. Finally, the developed hybrid hydrogel was successfully biofabricated and microfabricated in complex shapes and forms, such as patches, hearts, triangles, and spirals, while maintaining a high biocompatibility.



**Keywords:** Liposomes; Exosomes; Hybrid Nanoparticles; Targeting Nanoparticles; Bioprinting; Direct Cardiac Reprogramming.

## 1. Introduction

According to the 2017 European Cardiovascular Disease Report, cardiovascular disease is causing 3.9 million deaths and accounts for 45% of all deaths in Europe [608]. Cardiac injury causes loss of nonregenerative cardiomyocytes, and consequently a fibrotic scar tissue is formed due to the expansion of cardiac fibroblasts (CFs). To that end, cardiac fibroblasts can be directly reprogrammed into cardiomyocyte-like cells using transcription factors and/or miRNAs [609]. However, the *in vitro* efficiency of direct reprogramming is relatively low [610]. When compared to two-dimensional (2D) cell culture, three-dimensional (3D) constructs have been shown to better mimic the native cardiac tissue environment [611].

Due to their tunable degradation properties porous structure, and high water-binding capacity, hydrogels have been widely used as 3D constructs for various tissue engineering applications [2]. Moreover, their shape can be tuned to form complex architectures using novel biofabrication techniques such as 3D bioprinting [14]. Gelatin methacryloyl (GelMA) are one of the most promising polymeric candidates for manufacturing hydrogel scaffolds for cardiac tissue repair owing to its advantageous chemical tunability, biocompatibility, and promising *in vitro* and *in vivo* bone regeneration [453,612]. Although GelMA is highly biocompatible, it has big pores which renders its use for controlled release inefficient [6]. To solve this issue, nanoparticles, such as liposomes, can be loaded with the bioactive molecule and then embedded in the GelMA matrix.

However, formulating biomaterials and nanoparticles that selectively deliver encapsulated therapeutics to specific cells remains one of the key challenges in bioengineering

and nanomedicine. Although, liposomes are well-established delivery nanoparticles, they require surface modifications to acquire the smart targeting capabilities. Nevertheless, some natural nanovesicles, such as exosomes, are granted this smart behavior by the donor cells in the form of lipid and cellular adhesion molecules expressed on their surfaces [8].

Exosomes and liposomes have many similarities and differences. Both nanoparticles range in size from 30 nm to 120 nm and are composed of lipid bilayers. However, the exosomal lipid composition and membrane proteins differentiate them from liposomes, as these unique lipid composition and membrane proteins play an important role in specific interactions with serum proteins, facilitate their cellular uptake, and increase their targeting efficiency. Exosomes are more biocompatible than liposomes and can evade phagocytosis [211–213]. However, efficient and reproducible drug loading in exosomes is still a big challenge. For this, many researchers have created hybrid liposome-exosome nanoparticles to preserve the advantages of both of these complimentary systems while eliminating their limitations [9–12].

Gathering on this, herein we first formulated hybrid exosome-liposome nanoparticles (hELs) by fusing the membrane of CFs-derived exosomes and salmon-derived liposomes and characterized its fusion, size, polydispersity, charge, biocompatibility, and cellular uptake, as well as its encapsulation efficiency and successful delivery of miRNAs. Then, the successfully produced hELs were incorporated in the GelMA matrix that was in turn characterized for its pore size, mechanical properties, and biocompatibility. Here, the successful delivery of miRNAs was again verified in 3D, in addition to the reprogramming ability of this hybrid hydrogel when encapsulating a reprogramming miRNA-combo composed of miRNAs 1, 133, 208, and 499. Finally, the possible biofabrication and microfabrication in complex shapes and forms of this novel reprogramming GelMA-hELs hydrogel was investigated.

## 2. Materials and Methods

Gelatin from porcine skin, photo-initiator (PI) 2-hydroxy-4'-(2-hydroxyethoxy)-2-methyl propiophenone (Irgacure D-2959), and paraformaldehyde ampules were purchased from Sigma-Aldrich (USA). Fetal bovine serum (FBS), Dulbecco's phosphate-buffered saline (DPBS), Dulbecco's modified Eagle medium (DMEM), and penicillin-streptomycin (P/S), were purchased from Thermo Fisher Scientific (USA).

### 2.1 Cell Isolation and Culture

Neonatal rat cardiac fibroblasts (CFs) and cardiomyocytes (CMs) were isolated from newborn rats following the previously published protocol approved by the Institution of Animal Care and Use Committee at Brigham's and Women's Hospital through a collagenase based enzymatic digestion [613]. Briefly, the hearts of neonatal pups were surgically removed from the thoracic cavity after euthanasia. Upon removing the atria, the ventricular tissues were cut

into multiple small pieces and incubated overnight (at 4 °C) on a shaker in a 0.05% (w/v) trypsin solution prepared in Hank's balanced salt solution (HBSS, Gibco, USA). The heart tissues were subjected to four collagenase type II (LS004176, Worthington, Lakewood, NJ) digestions (10 min, 37 °C, 80 rpm) to further digest the heart tissues. The cell suspension was then collected, centrifuged (1000 rpm) for 5 min, and pre-plated for 1 h to enrich CMs for immediate experimental use. The attached CFs were cultured for a maximum of three passages for future experimental use. CFs were cultured in Dulbecco's modified eagle medium (DMEM, Gibco USA) with 10% fetal bovine serum (FBS; Gibco, USA) and 1% penicillin/streptomycin (P/S; Gibco, USA).

### *2.2 Preparation and Characterization of Nanoparticles*

CFs were incubated with Serum free media for 6 hours for serum starvation. Media is then centrifuged at 300 x g for 10 minutes to get rid of detached cells. Supernatant was transferred to clean falcon tubes and DEX-PEG solution (1:1 volume ratio) was added to it. The solution was then centrifuged at 1000 x g for 10 minutes at -4 °C and at a low acceleration and deceleration rates. After centrifugation, the upper phase is discarded, and the bottom phase was washed with wash solution (1:1 ratio of distilled water to DEX-PEG solution) to increase the purity of exosomes. The solution was again centrifuged at 1000 x g for 10 minutes and the upper phase is again discarded. To completely purify exosomes, this washing step was repeated a second time. Then, the bottom phase composed of pure exosomes was filtered using a 0.22 µm filter inside laminar flow cabinet and stored at -80°C. To measure the concentration of exosomes, Bradford assay was used. Standard samples were prepared from protein standards in buffer 0.25, 0.5, 0.75, and 1 mg/mL using a BSA standard. 5 µL of each standard and 5 µL of the pure exosome solution were mixed with 250 µL of Bradford reagent and added into a 96-well-plate that was then incubated at room temperature for 30 minutes. the absorbance was measured at 595 nm.

Lecithin was enzymatically extracted from *Salmo salar* without the use of organic solvents as described previously [591]. A lecithin stock solution of 2% (w/v) was prepared under a nitrogen flow to prevent oxidation and stored in the dark at 4 °C. Fresh nanoliposomes were prepared via probe-sonication (Q500 Sonicator, QSonica) of the lecithin solution using a 3.2 mm microtip at 30% amplitude and a pulse mode for 4 mins (5 s on and 5 s off).

hELs were produced by incubating the same concentration of exosomes and liposomes at 37°C for 12 h followed by probe-sonication using the same liposome sonication parameters. The fusion between liposomes and exosomes was evaluated using fluorescence resonance energy transfer (FRET) assay. Liposomes were labelled with 2% (w/w) of NBD PE and Liss Rhod PE (Avanti Polar Lipids, USA) and mixed with different concentrations of exosomes (1:2,

1:1, and 2:1) to produce hELs. A fluorescence spectra of the mixture from 500 nm to 650 nm was measured using a microplate reader (SpectraMax Paradigm; Molecular Devices, USA) with an excitation at 460 nm.

The average hydrodynamic particle diameter, size distribution (PDI), and zeta potential of the nanoparticles were characterized by DLS with a Zetasizer Nano ZS equipment (Malvern Instruments Ltd). The samples' concentration was of 200 µg/ml. Measurements were performed in standard capillary electrophoresis cells equipped with gold electrodes at 25 °C with a fixed scattering angle of 173°, a refractive index of 1.471, and an absorbance of 0.01.

Loaded nanoparticles were prepared by the incubation of the bioactive molecule with exosomes and/or lecithin solution at 37 °C for 12 h followed by probe-sonication using the same liposome sonication parameters. Nanoparticles were then collected using Amicon Ultra-0.5 mL centrifugal filters with 10 kDa molecular weight cutoff (Millipore). The encapsulation of miRNA was quantified in RNase-free water. To quantify the encapsulated miRNA DY547, first a standard curve was prepared based on the dye fluorescence intensity (525/570), then the free miRNA amount was quantified by the ultracentrifugation of nanoparticles at 100,000 g for 70 mins at 4 °C, and the encapsulation efficiency was calculated as  $(1 - \text{Free drug}/\text{loaded drug}) \times 100$ .

### 2.3 Cell Viability and Proliferation

Cell viability and proliferation of cells and cell-laden constructs were assessed using live/dead assay (Thermo Fisher scientific, USA) and PrestoBlue kit (Thermo Fisher scientific, USA). The colorimetric assays were measured using a plate reader by measuring the absorbance at 570 nm with reference to 600 nm. The results were normalized to day 1 of culture.

### 2.4 PKH-labeled Nanoparticles Cellular Uptake

NPs were labeled with the green lipid membrane dye PKH67 (Sigma-Aldrich), according to the manufacturer's protocol. Briefly, NPs and PKH67 were separately diluted in 100 µL diluent C. NPs were mixed with the staining solution and incubated for 5 minutes at room temperature. Labeling was stopped by adding an equal volume of 1% BSA and the mixture was subsequently passed through 100 kDa Amicon filter to remove unincorporated dye. CFs were incubated with PKH67-labeled NPs for 8 hrs, then DAPI (4',6-diamidino-2-phenylindole, 1:1000, Sigma-Aldrich, USA) was added for 10 mins at room temperature, and the samples were washed three times with DPBS and assessed using fluorescent microscopy.

### 2.5 RNA Isolation and Reverse Transcriptase Polymerase Chain Reaction (RT-PCR)

RNA was extracted directly from dishes or from 3D constructs, after crushing in nitrogen, using TRIzol (Thermo Fisher Scientific); 2 µg of RNA for each sample were retro-transcribed

using the High-Capacity cDNA Reverse Transcription Kit (Thermo Fisher Scientific), according to the manufacturers' instructions. Glyceraldehyde 3-phosphate dehydrogenase (GAPDH) was selected as endogenous control after verifying its stable expression. Quantitative RT-PCR analysis was performed with a real-time PCR thermocycler (LightCycler, Roche). Each cDNA sample was amplified in triplicate using KAPA SYBR FAST qPCR kit Master Mix (Kapa Biosystems). Relative mRNA levels were calculated by the delta delta CT method. Primer specificity was confirmed by melting curve analysis.

### 2.6 Synthesis of GelMA

GelMA was prepared by following a previously reported protocol [4,310]. Briefly, a 10% w/v gelatin solution was prepared in DPBS and heated to 50 °C for 1 h. Methacrylic anhydride (400  $\mu\text{L g}^{-1}$  of gelatin) was added dropwise to this gelatin solution and was allowed to react for 2 h under constant stirring at 50 °C. The reaction was stopped by further adding two times the volume of DPBS to the gelatin-methacrylate mixture. This solution was then extensively dialyzed using a 12 kDa (MWCO) Spectraphor dialysis membrane against deionized water for 5 days at 40 °C, followed by freeze-drying. The freeze dried GelMA was dissolved in DPBS in the desired concentrations. 0.5% of photoinitiator was added to the GelMA solution prior to crosslinking using UV light for 20 s.

### 2.7 Scanning electron microscopy (SEM) analysis

SEM analysis was performed to evaluate the porosity of the crosslinked hydrogels. Samples were frozen at  $-80$  °C overnight and then dried under vacuum overnight. Samples were then lyophilized, and SEM images were obtained using a FEI/Phillips XL30 FEG SEM (15 kV), and lyophilized gels were coated with gold prior to analysis. The pore sizes of GelMA gels were averaged from at least 3 images from 3 samples for each condition ( $n = 50$ ).

### 2.8 Mechanical Characterization

Compression stress tests were performed using a parallel plate platform (ADMET, MTESTQuattro, USA). Samples with around 7 mm circular diameter and 1 mm thickness were loaded and tested until rupture. All measurements were performed at room temperature. Prior to all measurements, the zero gap was determined. Four samples of each condition were tested. To calculate Young's modulus, the elastic part (10–20% strain) of the stress–strain curve was used.

### 2.9 Immunostaining

Fixation of cell-laden constructs was done in the Nunc™ Lab-Tek™ II Chamber Slide™ System (Thermo Fisher Scientific, USA). Briefly, samples were treated with 4% paraformaldehyde solution (Thermo Fisher scientific, USA) for 15 mins and then permeabilized

using 0.2% Triton X (Sigma-Aldrich, USA). F-actin (1:40, Invitrogen, USA), anti-cardiac troponin I antibody (ab19615, Abcam, USA) were added to the samples for staining. The samples were incubated with the primary antibody overnight at 4 °C. Secondary antibodies (Alexa Fluor-594 goat anti-mouse for troponin I, Invitrogen, USA) were added to the samples, followed by incubation at room temperature for 60 mins. DAPI was then added for 10 mins at room temperature. Fresh DPBS was added to the sample and confocal images were taken using a ZEISS LSM 880 with Airyscan Microscope. Images were processed and analyzed in Fiji software.

### 2.10 Bioprinting and Microfabrication

To prepare the bioink, 7.5% GelMA (medium degree of MA), 5% gelatin, and 0.5% PI were used. GelMA, gelatin, and PI were added to DPBS covered by aluminum foil and incubated at 80 °C for 30 min. The bioink was then moved to the 37 °C incubator for 60 min, after which CFs and NPs were added to the bioink when needed. The bioink was then allowed to partially solidify in a fridge at 4 °C for 10 mins before bioprinting.

3D bioprinting was performed using a SUNP ALPHA-CPD1 bioprinter. A G-code readable by the bioprinter was uploaded. A 3 mL syringe (BD, USA) and 27-gauge needle (Fisnar, USA) were used for printing the bioink. The nozzle was covered by foil during the process to avoid random crosslinking of the gel. The 3D bioprinted construct was placed at a distance of 8 cm from an 800 mW UV light source (Omnicure S2000, Excelitas Technologies, USA) and allowed to crosslink for 20 s.

Microfabricated GelMA hydrogels were produced by first placing a 7.5% GelMA solution with 0.5% photoinitiator in special custom-made PDMS molds prior to crosslinking under UV light for 20 s.

### 2.11 Statistical Analysis

All data are expressed as mean  $\pm$  standard deviation. Results were statistically analyzed by one-way analysis of variance (ANOVA) with Tukey's test to evaluate the level of significance. A p-value of 0.05 was considered significant.

## 3. Results and Discussion

### 3.1 Preparation and Characterization of Nanoparticles (NPs)

Exosomes that were isolated from CFs culture media and liposomes that were enzymatically extracted from salmon fish were used to produce loaded hELs *via* probe-sonication as shown in **Figure 1A**. The successful membrane fusion between liposomes and exosomes was investigated by a FRET assay using a set of NBD and Rhod-labelled phospholipids. As can be seen in **Figure 1B**, when NBD phospholipids are excited at a

wavelength of 460 nm, NBD PE emit fluorescence at 530 nm and part of that energy is transferred to close Rhod PE that emit fluorescence at 580 nm. However, when new exosomal phospholipids and membrane components are introduced in the liposomal bilayer, the distance between fluorescent NBD and Rhod PEs increase, and as a result the fluorescence intensity at 530 nm increase and the intensity at 588 nm decrease. The production of hELs was verified to be successful as the fluorescence intensity at 530 nm increased and the intensity at 588 nm decreased when higher concentrations of exosomes are introduced to the liposomal solution (**Figure 1C**), which suggest that new exosomal phospholipids are being introduced in the liposomal bilayer.

Furthermore, the size, PDI, and zeta-potential of NPs were quantified by DLS (**Figure 1C, D**). The applied sonication parameters during the production process (**Figure 1A**) can affect the minimum size that can be achieved [614]. The size of the liposomes (~52 nm) was found to be larger than that of exosomes (~37 nm) and hELs (~37 nm) (**Figure 1E**). The formulated NPs were relatively monodisperse, presenting a low PDI (~0.25) associated with a narrow size distribution [595]. For nanoformulations used for drug delivery applications, a PDI value lower than 0.3 indicates a homogenous population and is considered to be acceptable [596]. Zeta-potential for nanoliposomes was negative (~ -36 mV), which is probably caused by the negatively charged phospholipids of salmon lecithin, such as phosphatidylserine, phosphatidic acid, phosphatidylglycerol, and phosphatidylinositol that can be exposed at the nanoliposomes surface [186]. The zeta-potential of exosomes was still negative (~ -6 mV) but closer to neutral than that of liposomes. The zeta-potential value of hELs (~ -12 mV) was closer to that of exosomes than that of liposomes. The zeta-potential of hELs might explain why their size is similar to exosomes and different than liposomes, as the less negative zeta-potential might lead to a lower repulsion between phospholipids, and thus lead to a decrease in the particle's size.

Moreover, the EE of miRNA by NPs was assessed using the fluorescent model miRNA DY547 (**Figure 1E**). Directly after encapsulation, the loaded NP suspensions were ultracentrifuged at 100,000 g for 70 mins at 4 °C, which separates the loaded NPs found in the pellet from the free miRNA found in the supernatant. The free miRNA DY547 concentration was quantified from a standard curve based on the dye fluorescence intensity (525/570). Based on this concentration the EE was calculated and was found to be around 63% for liposomes, 65% for hEL, and 76% for exosomes. These E values are probably governed by the NPs charge. Since miRNA are negatively charged, the higher the negative charge of the NPs the lower their EE will be due to the repulsive forces between similar charges [615].

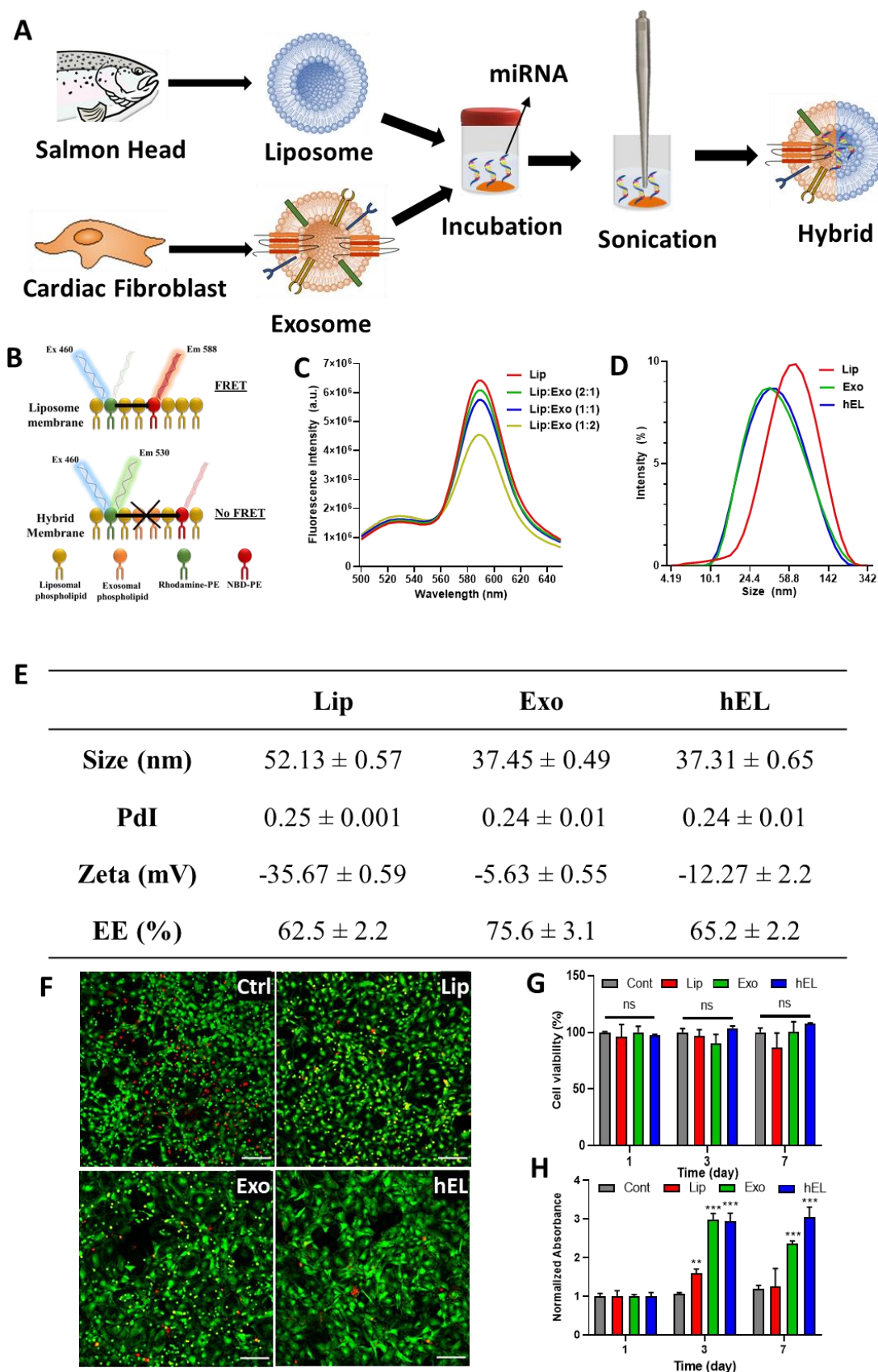


**Figure 1. Preparation and characterization of liposomes, exosomes, and hybrid (hEL) nanoparticles (NPs).** (A) Schematic of the method used to engineer hELs. (B) Fluorescence resonance energy transfer (FRET) assay with excitation at 460 nm. (C) Schematic of the FRET analysis assay used to monitor the fusion between exosomes and liposomes. (D) Size distribution measurements of NPs by dynamic light scattering. (E) Table showing the size, PdI, zeta-potential, and encapsulation efficiency of NPs. (F) Live/dead images of CFs cultured with NPs on Day 1. Scale bar: 200  $\mu$ m. (G) Live/dead assay showing the viability of CFs cultured with NPs for 7 days. (H) PrestoBlue results showing the cell proliferation of CFs cultured with NPs for 7 days.

Although salmon nanoliposomes have been found to be cytocompatible toward cortical neurons and Wharton's jelly human stem cells [117,186,583], investigating a possible cytotoxic response with a new cell type is an important requirement. The same requirement applies for hELs as it has not been previously fabricated from CFs-derived exosomes and salmon-derived liposomes. For this CFs were incubated with a  $100 \mu\text{g mL}^{-1}$  concentration of liposomes, exosomes, and hELs, and their viability and proliferation were measured at day 1, 3, and 7. CFs cultured with NPs showed a high viability as no significant difference in viability existed compared to the control (**Figure 1F,G**). Interestingly, CFs cultured with NPs had a significantly larger proliferation than the control (**Figure 1H**), with cells cultured with hELs showing the highest proliferation, followed by exosomes, then liposomes.

### 3.2 NPs Cellular uptake and Targeted Delivery

To determine whether CF-derived exosomes, salmon-derived liposomes, and their resulting hELs could be taken up by fibroblasts, NPs were labeled with PKH67, a fluorescent dye, and cultured with CFs for 8 hrs. Following incubation, fluorescence microscope imaging, presented in **Figure 2A**, showed the presence of PKH67-labeled NPs in recipient fibroblasts, suggesting that labeled exosomes, liposomes, and hELs can be successfully delivered to the cytoplasm of CFs. Moreover, the fluorescence intensity of PKH67-labeled NPs to the intensity of DAPI was quantified (**Figure 2B**). The intensity of PKH67-labeled exosomes (~75%) was significantly higher than that of labeled hELs (~60%) that is in turn significantly higher than that of labeled liposomes (~10%).

Furthermore, the successful cellular uptake and delivery of miRNA loaded in NPs to both CFs and CMs was investigated using miRNA GAPDH. RT-PCR was used to quantify the resulting downregulation of the mRNA GAPDH. As shown in **Figure 2C**, miRNA GAPDH-loaded exosomes induced the highest downregulation of the GAPDH gene (~0.3) in CFs, followed by loaded hELs (~0.4), then loaded liposomes (~0.5). **Figure 2D** shows the downregulation of the mRNA GAPDH in CMs by the miRNA GAPDH-loaded NPs. Interestingly, loaded exosomes and hELs did not induce any significant downregulation of the GAPDH gene, unlike loaded liposomes (~0.7). This specificity of exosomes and hELs to CFs might be due to the presence of fibroblastic specific receptors on the CFs-derived exosomes and hELs surfaces, which improved their cellular uptake by CFs and prevented their uptake by CMs. For liposomes, this specificity does not exist due to the absence of cell specific receptors and membrane proteins on their surfaces, which led to its uptake by both CFs and CMs, and to the downregulation of the GAPDH gene in both cell types. This might suggest that exosomes and hELs can be used for targeting drug delivery to CFs even when other cell types, such as CMs, are present.

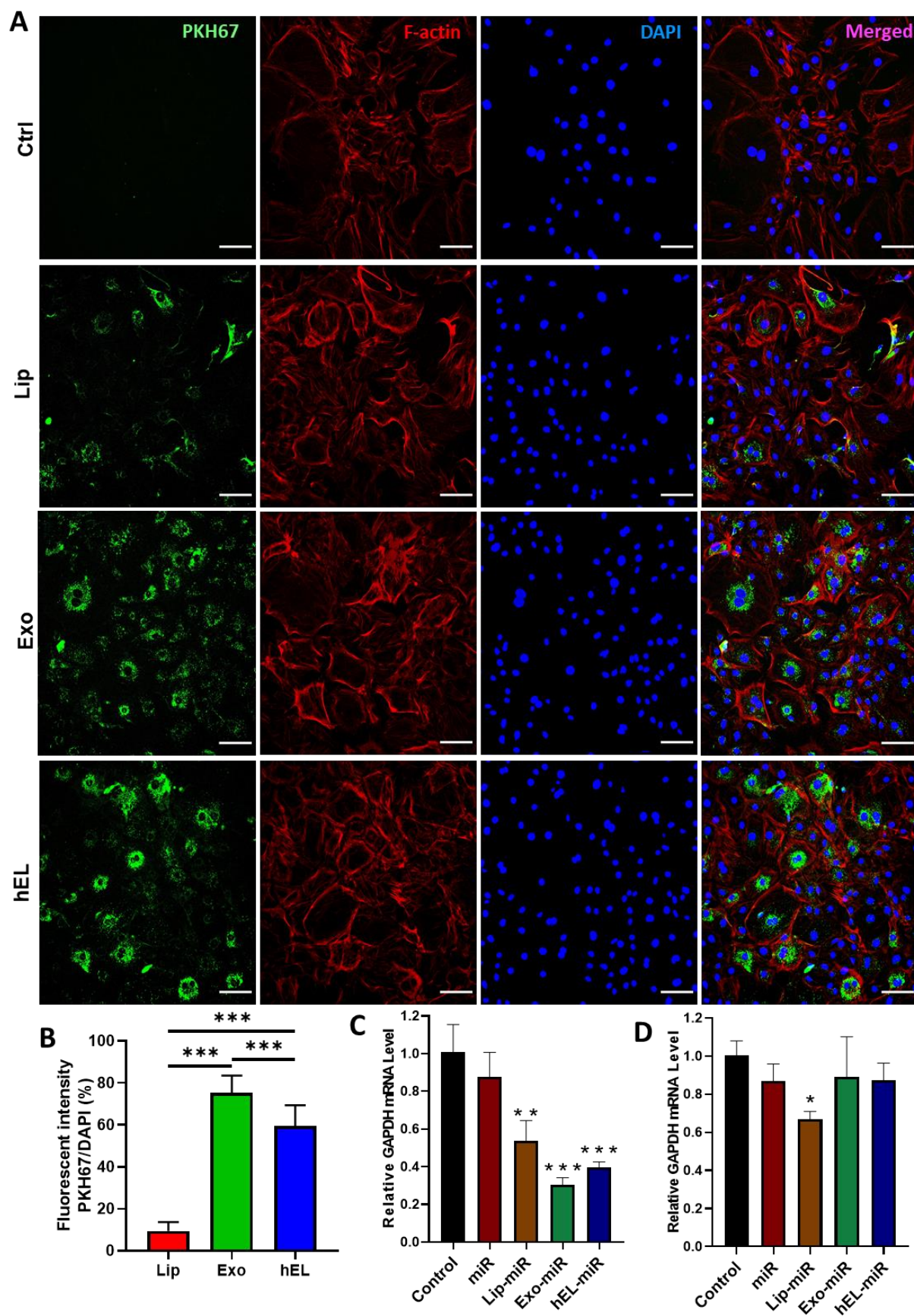


**Figure 2. Characterization of NPs uptake.** (A) Fluorescence images of PKH67-labeled NPs uptake by CFs. Scale bar: 100  $\mu$ m. (B) Fluorescent percentage of PKH67/DAPI. RT-PCR results of (C) CFs and (D) CMs.

### 3.3 Characterization of NPs-GelMA Hydrogels

To visualize the internal structures of GelMA hydrogels, the corresponding cross-sectional microstructures were examined by SEM (**Figure 3A**). The GelMA hydrogels' cross-sectional microstructures displayed a honeycomb-like structure, which was also visualized by Wang *et al.* [616]. The nanofunctionalization with soft NPs resulted in the observation of GelMA hydrogels with different pore sizes and morphologies (**Figure 3B**). GelMA hydrogels had a significantly higher pore size than all other GelMA-NPs hydrogels, with an average pore size diameters of about 60  $\mu\text{m}$ . GelMA-liposomes (Gel-Lip) hydrogels exhibited the smallest pores with an average pore diameters of around 35  $\mu\text{m}$ , followed by GelMA-hEL (Gel-hEL) hydrogels with an average pore size of around 45  $\mu\text{m}$ , and then GelMA-exosomes (Gel-Exo) hydrogels with an average pore size of about 50  $\mu\text{m}$ . This might be due to the presence stronger interactions between liposomes and the GelMA matrix than that of exosomes and the hydrogel's matrix. Those strong interactions will further increase the micro-crosslinking level of GelMA, which will lead to a higher decrease in pores' size.

To prove this hypothesis, the mechanical properties of GelMA-NPs hydrogels were characterized by performing compression tests using a universal testing machine. The Young's modulus was quantified based on the slope of the initial linear region (10%–20% strain) (**Figure 3C**). Indeed, Gel-Lip hydrogels had a higher Young's modulus ( $\sim 11$  kPa) than Gel-hEL ( $\sim 9.5$  kPa), Gel-Exo ( $\sim 8.5$  kPa), and GelMA hydrogels ( $\sim 5$  kPa). This further suggest that indeed strong hydrogen bonds exist between phosphorous heads of liposomes membrane and nitrogen present in the GelMA network, whereas weak peptide bonds exist between exosomes and GelMA due to the presence of membrane proteins on its surface, and a mix of both types of bonds exists between hELs and GelMA (**Figure 3D**).

The viability of encapsulated cells in the different GelMA hydrogels was assessed on day 1 using a Live/Dead assay to evaluate the impact of UV exposure on the CFs survival during the fabrication process (**Figure 3E**). **Figure 3F** illustrates the quantitative analysis of the percentage of the live cells, where it can be seen that the NPs incorporation in the GelMA matrix did not affect the CFs viability, as all hydrogels presented a non-significantly different viability that is higher than 84%. This high viability was found to be consistent with previously reported viabilities of cardiac cells encapsulated in GelMA hydrogels [617]. As for the proliferation of CFs in GelMA-NPs hydrogels, the PrestoBlue assay revealed a good proliferation of CFs with all cells having a non-significant proliferation than the control with the exception of cells encapsulated in Gel-hELs that showed a significantly higher proliferation on day 7 (**Figure 3G**).

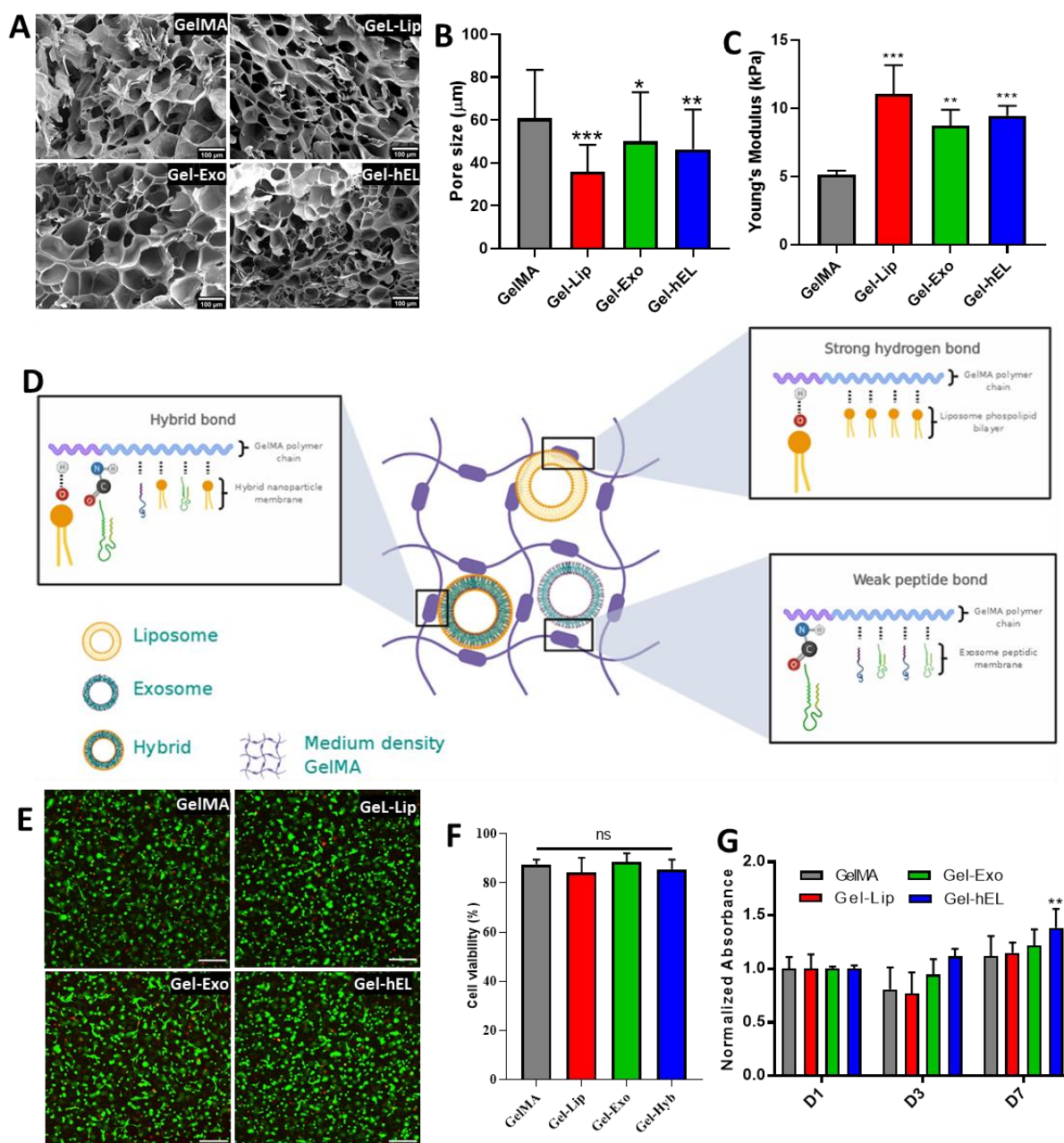


**Figure 3. Characterization of 3D CFs-laden Gel-NPs hydrogel.** (A) SEM images of Gel-NPs hydrogels. (B) Pore size measurements of Gel-NPs hydrogels. (C) Young's modulus of Gel-NPs hydrogels. (D) Schematic representation of electrostatic interactions between GelMA matrix and NPs. (E) Live/dead images of CFs-laden Gel-NPs hydrogels on Day 1. Scale bar: 200 µm. (F) Live/dead assay showing the viability of CFs-laden Gel-NPs hydrogels on Day 1. (G) PrestoBlue results showing the cell proliferation of CFs-laden Gel-NPs hydrogels for 7 days.

### 3.4 Delivery of miRNA in GelMA-NPs hydrogels

To check whether the GelMA matrix would hinder the delivery of miRNA loaded in NPs, miRNA DY547 (red) was loaded in GelMA-NPs hydrogels that in turn were immunostained with F-actin (green) and DAPI (blue). The staining on miRNA-loaded GelMA-NPs samples revealed that all NPs successfully delivery the miRNA DY547 to CFs, whereas this delivery was not achieved when using free miRNAs (**Figure 4A**).

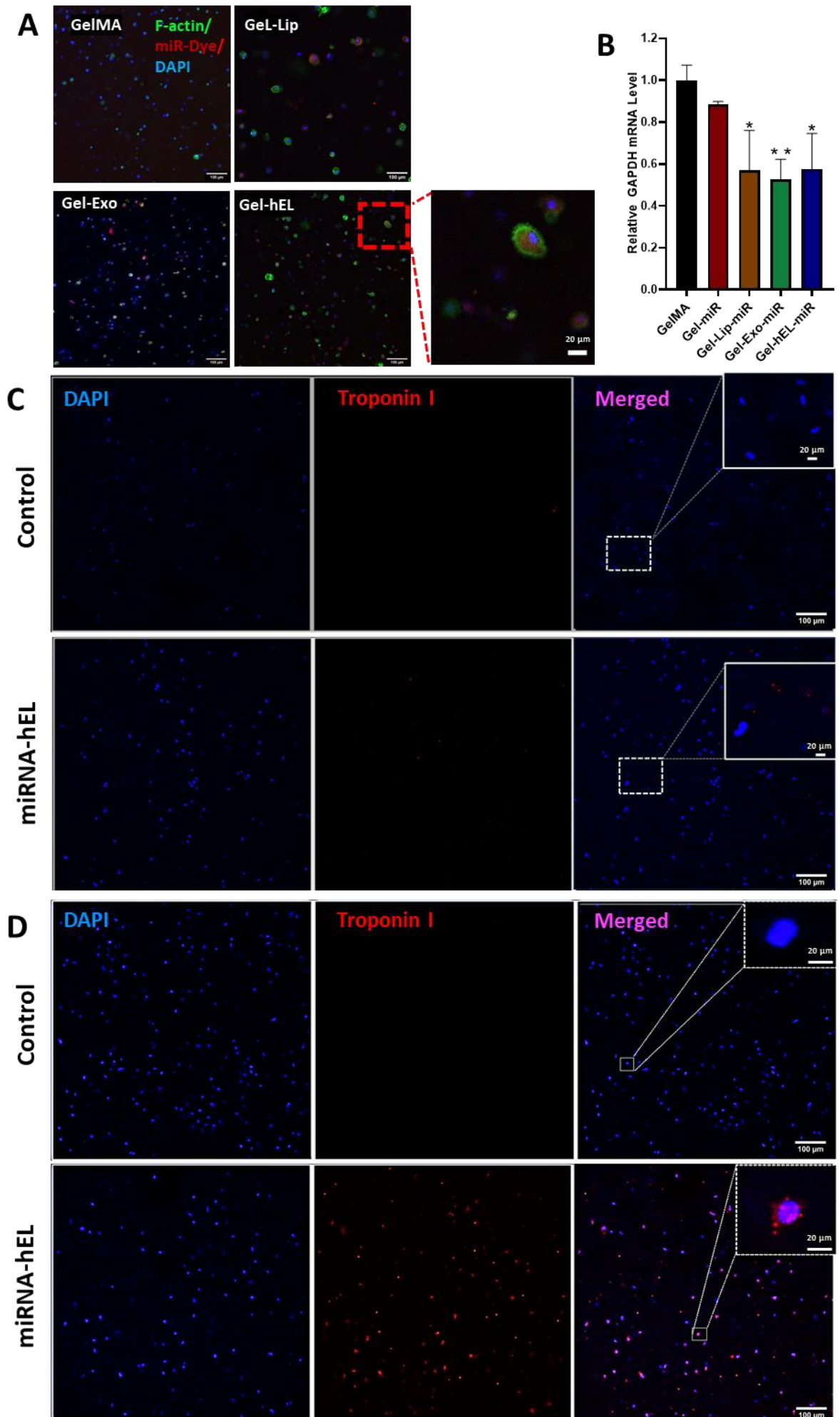


**Figure 4. Immunostained GelMA-NPs hydrogels.** (A) Images of CFs-laden Gel-NPs hydrogels loaded with miRNA DY547 (red) immunostained with F-actin (green) and DAPI (blue). (B) RT-PCR results of CFs-laden Gel-NPs hydrogels loaded with miRNA GAPDH. Images of CFs-laden Gel-hEL hydrogels loaded with miRNA reprogramming combo immunostained for Troponin I (red) and DAPI (blue) after (C) 7 and (D) 14 days of culture.

This delivery was further verified by RT-PCR of miRNA GAPDH loaded in GelMA-NPs hydrogels. Indeed, free miRNAs did not induce a significant downregulation of the GAPDH gene, whereas as miRNA-loaded NPs did (**Figure 4B**). This suggest that the GelMA matrix did not hinder the NPs ability to successfully deliver miRNAs to CFs.

For this, a miRNA-combo composed of miRNAs 1, 133, 208, and 499, known for its capability to induce the direct cardiac reprogramming of CFs to CM-like cells *in vitro* [609], was encapsulated in hELs which in turn was embedded in the CF-laden GelMA matrix to study its ability to induce the direct cardiac reprogramming. The reprogramming ability of miRNA-combo loaded in Gel-hEL hydrogels was assessed using immunofluorescence staining for the specific cardiac marker troponin I. Troponin I is a marker involved in cellular contraction, cytoskeletal organization, and muscle calcium binding [618]. The reprogramming using Gel-hEL resulted in only a small number of Troponin I stained cells at day 7 (**Figure 4C**), but a substantially larger number of Troponin I stained cells at day 14 (**Figure 4D**). The same larger number of stained cells at day 14 was also reported by Li *et al.* using CF-laden fibrin-based hydrogels [610]. To fully understand and characterize the reprogramming ability of the newly developed Gel-hEL hydrogel, more *in vitro* and *in vivo* experiments are required. However, for the scope of this work and as a proof of concept, it is safe to say that the 7.5% GelMA hydrogels nanofunctionalized with 100  $\mu\text{g/mL}$  of hybrid exosome-liposome nanoparticles encapsulating the reprogramming miRNA-combo (miRNAs 1, 133, 208, and 499) are very promising direct cardiac reprogramming platforms.

### 3.5 Biofabrication of GelMA-NPs hydrogels

After characterizing the Gel-hEL hydrogels biofunctionality, its printability was characterized. Biofabrication techniques, such as bioprinting, made the creation of complex structures, that can mimic the native ECM's complex architecture, possible. In **Figure 5A**, it can be seen that 7.5% GelMA can be 3D printed in different shapes, such as small and large patches with multiple layers and triangles. **Figure 5B** revealed no leakages of encapsulated fluorescein from 3D printed Gel-hEL complex shapes (patches, spirals, hearts), which suggest that the Gel-hEL can retain encapsulated materials which can maximize their bioactivity. Moreover, to check whether the harsh bioprinting process would hinder the viability of CFs, Live/Dead assay was performed on bioprinted CF-laden Gel-hEL patches after 3 days of culture. As can be seen from the green bioprinted construct with very few dead cells (red) in **Figure 5C**, the bioprinted construct had a high cell viability. Furthermore, Gel-hEL hydrogels were not

only successfully biofabricated but also microfabricated using specific molds. **Figure 5D** shows the successful microfabrication of well-structured PKH-labeled Gel-hEL hydrogels, which proves the high shape-tunability of this biomaterial.

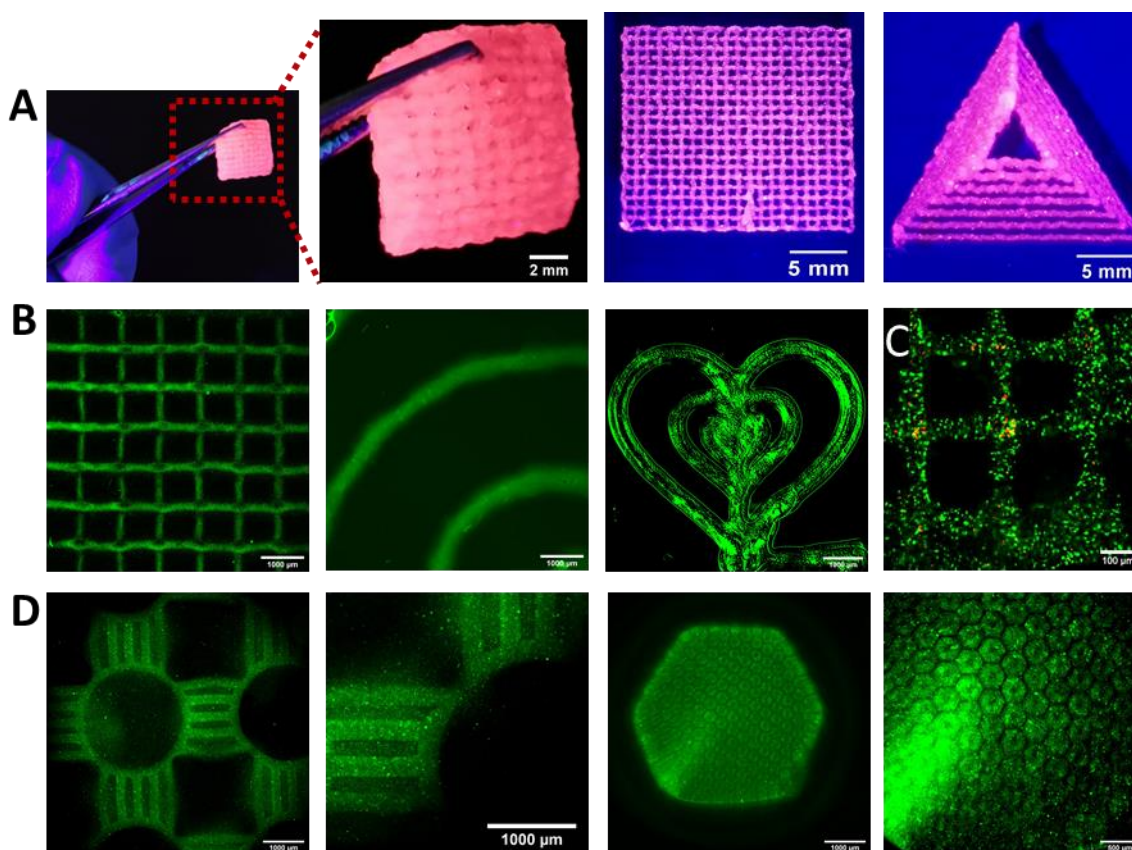


**Figure 5. Bio- and micro-fabricated Gel-hEL hydrogels.** (A) 3D printed tough patches and complex shapes using GelMA ink colored with pink food dye. (B) 3D printed complex shapes using fluorescein-loaded Gel-hEL ink. (C) Live/dead at Day 3 of CFs-laden bioprinted Gel-hEL bioink. (D) Microfabricated PKH67-labeled Gel-hEL hydrogels.

#### 4. Conclusions

Throughout this study, the development and characterization of a reprogramming hybrid hydrogel were achieved. First, hELs were produced from CF-derived exosomes and salmon-derived liposomes and were physicochemically and biologically characterized. Salmon-derived liposomes present a double functionality since they are rich in bioactive  $\omega$ -3 PUFAs and they can encapsulate bioactive molecules. On the other hand, exosomes present a smart behavior due to the presence of cell specific receptors and membrane proteins on their surfaces, which allows them to target specific cells. The hELs formation was verified using FRET analysis, and their nanometric size, narrow PDI, and negative zeta-potential were quantified using DLS. CFs cultured with hELs showed a high viability and a significantly improved proliferation. In addition, the successful cellular uptake of PKH67-labeled hELs by CFs was visualized using a fluorescent microscope and the successful delivery of miRNA loaded in hELs to CFs was verified using RT-PCR and confocal microscopy. Interestingly, although hELs successfully

delivered its cargo to CFs, it failed to do so with CMs, which suggest that the smart behavior was successfully passed to hELs from exosomes.

Moreover, the embedment of hELs in GelMA improved its mechanical properties and reduced its average pore size due to the presence of both strong hydrogen bonds inherited from liposomes and weak peptide bonds inherited from exosomes between hELs and the GelMA matrix. However, this embedment did not negatively affect the excellent biocompatibility of hELs toward CFs or their ability to deliver miRNA to CFs. In fact, it has significantly improved CFs proliferation in 3D environments. The cardiac reprogramming potential of hELs was verified with the increased numbers of immunostained cells with Troponin I 14 days after transfection. To add to all these beneficial characteristics, the Gel-hEL hydrogel was successfully microfabricated and bioprinted with excellent cell viability and in different sizes and shapes, which suggest that the natural hybrid bioink is very promising for the bioprinting of 3D direct reprogramming cardiac patches. Future *in vitro* and *in vivo* studies will focus further on the characterization of the reprogrammed CM-like cells using this novel exosome-liposome hybrid bioink.



# **Conclusion & Perspectives**



## Conclusion & Perspectives

---

Conventional and novel applications of tissue engineering require the design of scaffolds that are biocompatible and biodegradable, facilitate cell growth and nutrient transport, and mimic the architecture and physical properties of native tissues. The biomaterial used in scaffolding plays a key role in achieving this goal. Natural hydrogels have been widely used as scaffolds for tissue engineering due to their excellent biocompatibility, adjustable biodegradability, and low cytotoxicity.

For this reason, in this work, the physicochemical and biological properties of GelMA from pig and fish skin produced with low and high methacrylation degrees were studied and compared. The degree of substitution was found to be independent of the source of GelMA because it was similar between polymers with the same degree of methacrylation and significantly different between GelMA with low and high methacrylation. On the one hand, the level of methacrylation and the source of GelMA did not affect the thermal and water absorption properties. However, GelMA hydrogels derived from fish had a significantly higher swelling rate and lower elastic and compressive Young's modulus than GelMA derived from pork. On the other hand, as the degree of methacrylation increased, the swelling rate decreased, and the elastic and compressive Young's modulus increased. Although cell proliferation was only induced in GelMA with low methacrylation and better spreading was only observed in GelMA derived from fish, all GelMA hydrogels showed high biocompatibility towards encapsulated C2C12 myoblasts. Notably, GelMA derived from fish with low methacrylation showed the best proliferation and spread of C2C12-laden myoblasts, which encourages future investigations as a potential scaffold for skeletal muscle tissue engineering. Overall, for clinical, environmental, religious, and economical reasons, GelMA derived from marine sources could be a promising substitute for mammalian-derived GelMA for biomedical applications. Future studies will focus first on the *in vitro* differentiation of C2C12 myoblasts loaded in myotubes, followed by the bio-manufacturing, using a portable bio-printer, and nanofunctionalization, with nanoliposomes of plant and marine origin, of GelMA derived from fish for the *in vivo* treatment of skeletal muscle injury.

To improve their biological activity, these hydrogels can be functionalized by soft nanoparticles. These soft nanoparticles are highly biocompatible and do not adversely affect cell functions. Thus, the development of soft nanoparticles incorporated in natural hydrogels that can control the release of bioactive molecules would be an important step towards scaffold engineering for neural, muscle and heart tissue culture.

For this, in a second work, the development and characterization of a potential bone regeneration nanocomposite hydrogel was achieved. The nanofunctionalized platform was composed of a naturally available drug (naringin) encapsulated in nanoliposomes derived from salmon and integrated in GelMA hydrogels. The inclusion of naringin in the nanoliposomes

resulted in a high encapsulation efficiency and a controlled drug release profile. The loaded nanoliposomes showed no cytotoxicity to human adipose stem cells. The results of this study showed that naringin-loaded nanoliposomes are highly biocompatible and can be safely used for bone tissue engineering applications. Since nanoliposomes are derived from salmon fish, they are rich in polyunsaturated fatty acids  $\omega$ -3 which offer the dual functionality of being bioactive by themselves and being able to encapsulate bioactive molecules, further increasing their efficacy. In addition, the incorporation of nanoliposomes in GelMA has not only improved its mechanical and rheological properties but has also decreased its swelling rate and hydrophilicity and prolonged the release of naringin. Thus, nanoliposomes have strengthened the GelMA scaffold, made it more resistant to shape changes, and improved its barrier properties and drug release behavior. To add to all these advantages, the nanoliposomes formed no aggregates and had a homogeneous distribution in the GelMA scaffold after the bioprinting process, suggesting that the natural nanocomposite hydrogel composed of naringin-loaded nanoliposomes incorporated in GelMA may be a promising bioink candidate for bioprinting pro-osteogenic bioactive cell-laden constructs. Since GelMA printed structures suffer from poor resolution, the developed nanocomposite bioink will be further evaluated and optimized to balance printability and functionality. Future studies will also focus on the ability of naringin-loaded nanoliposomes to induce osteodifferentiation of stem cells in 2D cell culture, as well as in 3D cell culture when encapsulated within the GelMA hydrogel matrix.

An emerging field in drug delivery is the development of intelligent systems for the targeted delivery of bioactive compounds. This concept is also important in tissue engineering applications where different spatial and temporal concentrations of biological factors are required at different stages of tissue formation. Exosomes are naturally occurring nanovesicles that can target specific cells and tissues without special modifications. While liposomes are well-established drug delivery systems that can deliver heavy loads. These nanovesicles have many advantages, but each has its own drawbacks. To overcome their drawbacks, membrane fusion between exosomes and liposomes can generate superior hybrid nanovesicles. This new hybrid delivery system can be armed with both the intelligent targeting behavior of exosomes and the high loading capacity of liposomes.

In addition, to improve, control and prolong drug delivery, these nanovesicles can be loaded into naturally occurring hydrogels, which can then be administered by better routes, such as oral, nasal, parenteral, ocular, topical and cerebral, or biofabricated to create complex 3D tissue engineering scaffolds. Advances in biofabrication techniques, particularly 3D bioprinting techniques, are very promising in the fields of tissue engineering and regenerative medicine, as 3D it offers superior control over the architecture and resolution of the structure.

## Conclusion & Perspectives

---

For this, in a third work, the development of a bioink from GelMA hydrogels incorporating soft hybrid nanoparticles created by the fusion between exosomes and liposomes was carried out. Coronary heart disease is the most common form of cardiovascular disease, which leads to the loss of cardiomyocytes at the site of myocardial infarction. Cardiac fibroblasts respond rapidly to this loss by forming chronic scar tissue. To restore healthy heart muscle, the administration of a specific combination of miRNA can initiate direct reprogramming of cardiac fibroblasts into induced cardiomyocytes. To increase the loading and targeting efficiency of miRNAs, hybrid nanoparticles have been produced by membrane fusion of exosomes derived from cardiac fibroblasts with liposomes derived from salmon lecithin by sonication. Due to the increased expression of matrix metalloproteinases, 3D hydrogel environments generally exhibit higher reprogramming efficiency. Thus, GelMA hydrogel has been nanofunctionalized with these hybrid nanoparticles to form a reprogramming bioink that has been successfully used to bioprint 3D constructs and cardiac patches of different shapes and sizes.

In the future, there are many challenges and obstacles to the successful translation of biofabricated hydrogel products. This has not prevented the FDA from approving a number of marketed hydrogel products that are generally classified as Class I, II or III medical devices, depending on whether they are encapsulated drugs or bioactive compounds. Although a bright future lies ahead for marketed hydrogel products, due to recent developments in biofabrication techniques, the great challenge of large-scale functional tissue and organ engineering has not yet been resolved.

In conclusion, the work during this thesis has led to the successful biofabrication of a nanofunctionalized GelMA bioink with liposomal and exosomal soft nanoparticles. This new platform has been partially and fully tested for muscle, bone, and cardiac tissue engineering applications. Interestingly, it has the potential to be used for other tissue engineering applications and may one day be translated into clinical trials and if successful to the market.

Les applications nouvelles et conventionnelles en ingénierie tissulaire nécessitent la conception d'échafaudages biocompatibles et biodégradables, facilitant la croissance cellulaire et le transport des nutriments, et imitant l'architecture et les propriétés physiques des tissus natifs. La nature du biomatériau utilisé dans la fabrication de ces échafaudages joue un rôle clé dans l'atteinte de cet objectif. Les hydrogels naturels ont été largement utilisés comme échafaudages pour l'ingénierie tissulaire en raison de leur excellente biocompatibilité, de leur biodégradabilité ajustable et de leur faible cytotoxicité.

Pour cette raison, dans ce travail, les propriétés physicochimiques et biologiques de la gélatine méthacrylée (GelMA) issue de sources différentes (peau de porc ou de poisson) et présentant des degrés de méthacrylation faible ou élevé ont été étudiées et comparées. Le degré de substitution ne dépend pas de la source de GelMA utilisée car ce paramètre était similaire pour les deux polymères avec le même degré de méthacrylation, en revanche il est modifié par le degré de méthacrylation. D'une part, concernant les propriétés thermiques et la capacité d'absorption d'eau de la matrice, le niveau de méthacrylation et la source de GelMA n'ont pas modifié ces paramètres de façon significative. Cependant, les hydrogels GelMA de source marine présentent un taux de gonflement significativement plus élevé et un module d'élasticité et un module de compression plus faible que le GelMA dérivé du porc. D'autre part, avec l'augmentation du degré de méthacrylation, le taux de gonflement diminue et les modules de Young et de compression augmentent. Même si la prolifération cellulaire n'est induite que dans la matrice GelMA faiblement méthacrylée et qu'un meilleur étalement est observé pour la matrice de source marine, tous les hydrogels GelMA montrent une grande biocompatibilité envers les myoblastes C2C12 encapsulés. La matrice GelMA de source marine avec un faible degrés de méthacrylation présente les meilleurs résultats en termes de prolifération cellulaire et de propagation des myoblastes chargés en C2C12, il serait donc intéressant d'évaluer le potentiel de cette matrice pour des applications en tant qu'échafaudage en ingénierie des tissus musculaires squelettiques. Dans l'ensemble, pour des raisons cliniques, environnementales, religieuses et économiques, le GelMA de source marine s'avère être un substitut prometteur du GelMA de source porcine. En termes de perspectives, il serait intéressant d'aborder la différenciation *in vitro* des myoblastes C2C12 chargés en myotubes, puis de s'intéresser à la biofabrication de ce polymère, à l'aide d'une bioimprimante portable, et d'étudier la nanofonctionnalisation de cette matrice. Cette matrice ainsi produite et fonctionnalisée permettrait d'apporter des solutions pour le traitement *in vivo* des lésions musculaires squelettiques.

Dans le but d'améliorer leur activité biologique, ces hydrogels de type GelMA peuvent être fonctionnalisés par l'incorporation de nanoparticules molles dans la matrice. Ces nanoparticules molles sont hautement biocompatibles et n'affectent pas les fonctions cellulaires.

Ainsi, le développement de ces matrices hydrogel nanofonctionnalisées et naturelles permettraient un relargage contrôlé des molécules bioactives. Ces systèmes sont donc une étape importante vers l'ingénierie des échafaudages pour la culture de tissus neuraux, musculaires et cardiaques.

Pour cette raison, dans un deuxième travail de cette thèse, le développement et la caractérisation physico-chimique, biologique d'un hydrogel nanocomposite avec de possibles applications en régénération osseuse ont été réalisés. La matrice nanofonctionnalisée était composée d'un principe actif d'origine naturelle (naringine) encapsulé dans des nanoliposomes produits à partir de lécithine de saumon et intégrés dans des hydrogels à base de GelMA. Une efficacité d'encapsulation élevée est observée suite à l'incorporation de la naringine dans les nanoliposomes et ce système permet un relargage contrôlé du principe actif. Les nanoliposomes chargés ne montrent aucune cytotoxicité envers les cellules souches humaines d'origine adipeuse. Les résultats de cette étude montrent que les nanoliposomes chargés de naringine sont biocompatibles et peuvent être utilisés en toute sécurité pour des applications en ingénierie du tissu osseux. Étant donné que les nanoliposomes utilisés proviennent d'une source marine (saumon), ils sont riches en acides gras polyinsaturés  $\omega$ -3 et présentent donc une double fonctionnalité car ils sont eux-mêmes bioactifs et peuvent être utilisés comme vecteurs pour l'encapsulation de molécules actives, ce qui augmente encore leur intérêt. De plus, l'incorporation de nanoliposomes dans la matrice de type GelMA permet non seulement d'améliorer ses propriétés mécaniques et rhéologiques, mais également de diminuer son taux de gonflement et son caractère hydrophile tout en prolongeant la libération de la naringine. Ainsi, les nanoliposomes ont renforcé le support GelMA, en le rendant plus résistant aux modifications de forme/structure et ont amélioré ses propriétés barrière ainsi que le relargage contrôlé de principes actifs. En plus de ces avantages, les nanoliposomes n'ont formé aucun agrégat et avaient une distribution homogène dans la matrice GelMA après le procédé de bioimpression, ce qui suggère que l'hydrogel nanocomposite naturel composé de nanoliposomes chargés de naringine incorporés dans la matrice GelMA peut être un candidat bioencore prometteur pour la bioimpression de constructions cellulaires chargées pro-ostéogéniques bioactives. Puisque les structures GelMA imprimées souffrent d'une mauvaise résolution, la bioencore nanocomposite développée sera en outre évaluée et optimisée pour équilibrer son imprimabilité et sa fonctionnalité. En termes de perspectives pour cette partie, il serait intéressant d'évaluer la capacité des nanoliposomes chargés avec de la naringine à induire l'ostéo-différentiation des cellules souches en culture cellulaire 2D, ainsi que dans la culture cellulaire 3D lorsque celle-ci se trouve encapsulée à l'intérieur de la matrice d'hydrogel de type GelMA.

Un domaine émergent dans le domaine de l'administration de médicaments est le développement de systèmes intelligents pour la libération contrôlée de composés bioactifs. Ce concept est également important dans les applications d'ingénierie tissulaire où différentes concentrations spatiales et temporelles de facteurs biologiques sont nécessaires à différents stades de la formation des tissus. Les exosomes sont des nanovésicules d'origine naturelle qui peuvent cibler des cellules et des tissus spécifiques sans modifications particulières. Alors que les liposomes sont des vecteurs de molécules actives avec des applications bien établies dans le milieu médical notamment qui peuvent libérer des quantités importantes de principes actifs. Ces nanovésicules présentent de nombreux avantages, mais également des inconvénients. Pour surmonter les limites de ces systèmes, une fusion membranaire entre exosomes et liposomes peut générer des nanovésicules hybrides d'intérêt. Ce nouveau système hybride de libération contrôlée peut être armé à la fois du comportement de ciblage intelligent des exosomes et de la capacité de charge élevée des liposomes.

De plus, pour améliorer, contrôler et prolonger l'administration des principes actifs, ces nanovésicules peuvent être incorporées dans des hydrogels naturels, qui peuvent ensuite être administrés par de meilleures voies, telles que la voie orale, nasale, parentérale, oculaire, topique et cérébrale, ou être biofabriqués pour créer des supports d'ingénierie tissulaire complexes en 3D. Les progrès des techniques de biofabrication, en particulier des techniques de bioimpression en 3D, sont très prometteurs dans les domaines de l'ingénierie tissulaire et de la médecine régénérative, car elle offre un meilleur contrôle de l'architecture et de la résolution de la structure.

Pour ces raisons, dans un troisième travail, le développement d'une bioencore formulée à partir d'hydrogels de type GelMA incorporant des nanoparticules hybrides molles créées par la fusion entre exosomes et liposomes a été réalisée. La maladie coronarienne est la forme la plus courante de maladie cardiovasculaire, qui entraîne la perte de cardiomyocytes au site de l'infarctus du myocarde. Les fibroblastes cardiaques répondent rapidement à cette perte en formant du tissu cicatriciel chronique. Pour restaurer le muscle cardiaque sain, l'administration d'une combinaison spécifique de miARN peut initier une reprogrammation directe des fibroblastes cardiaques en cardiomyocytes induits. Pour augmenter l'efficacité de chargement et de ciblage des miARN, des nanoparticules hybrides (NP) ont été produites par la fusion membranaire d'exosomes dérivés de fibroblastes cardiaques avec des liposomes élaborés à partir de lécithine de saumon par sonication. En raison de l'augmentation de l'expression des métalloprotéinases matricielles, les environnements hydrogels 3D présentent généralement une efficacité de reprogrammation plus élevée. Ainsi, l'hydrogel de type GelMA a été fonctionnalisé avec ces nanoparticules hybrides pour former une bioencore fonctionnelle qui a été utilisée avec

succès pour bioimprimer des constructions 3D et des patchs cardiaques de différentes formes et tailles.

À l'avenir, pour aboutir à la commercialisation de produits à base d'hydrogel biofabriqués, de nombreux défis restent à relever. Notons cependant, que ceci n'a pas empêché la FDA d'autoriser depuis plusieurs années la mise sur le marché d'un certain nombre de produits à base d'hydrogel qui sont généralement classés comme des dispositifs médicaux de classe I, II ou III, selon les médicaments encapsulés ou les composés bioactifs. Même si des perspectives intéressantes peuvent être soulignées en termes de commercialisation pour les produits formulés à partir d'hydrogels, en raison des récents développements dans les techniques de biofabrication, le grand défi de l'ingénierie de tissus et d'organes fonctionnels à grande échelle n'est pas encore résolu.

En conclusion, les travaux de cette thèse ont mené à la biofabrication d'une bioencore de type GelMA nanofonctionnalisée avec des nanoparticules molles hybrides de type liposome-exosome. Cette nouvelle matrice a été testée pour des applications en ingénierie tissulaire musculaire, osseuse et cardiaque. Il est intéressant de noter qu'elle pourrait être utilisée pour d'autres applications en ingénierie tissulaire et pourrait peut-être un jour aboutir à une autorisation de mise sur le marché en cas d'essais cliniques concluants.



# **References**



1. Langer, R.; Vacanti, J. Tissue Engineering. *Science* **1993**, *260*, 920–926, doi:10.1126/science.8493529.
2. Elkhoury, K.; Russell, C.S.; Sanchez-Gonzalez, L.; Mostafavi, A.; Williams, T.J.; Kahn, C.; Peppas, N.A.; Arab-Tehrany, E.; Tamayol, A. Soft-Nanoparticle Functionalization of Natural Hydrogels for Tissue Engineering Applications. *Adv. Healthcare Mater.* **2019**, *8*, 1900506, doi:10.1002/adhm.201900506.
3. Yue, K.; Trujillo-de Santiago, G.; Alvarez, M.M.; Tamayol, A.; Annabi, N.; Khademhosseini, A. Synthesis, Properties, and Biomedical Applications of Gelatin Methacryloyl (GelMA) Hydrogels. *Biomaterials* **2015**, *73*, 254–271, doi:10.1016/j.biomaterials.2015.08.045.
4. Nichol, J.W.; Koshy, S.T.; Bae, H.; Hwang, C.M.; Yamanlar, S.; Khademhosseini, A. Cell-Laden Microengineered Gelatin Methacrylate Hydrogels. *Biomaterials* **2010**, *31*, 5536–5544, doi:10.1016/j.biomaterials.2010.03.064.
5. Zhao, F.; Yao, D.; Guo, R.; Deng, L.; Dong, A.; Zhang, J. Composites of Polymer Hydrogels and Nanoparticulate Systems for Biomedical and Pharmaceutical Applications. *Nanomaterials* **2015**, *5*, 2054–2130, doi:10.3390/nano5042054.
6. Elkhoury, K.; Koçak, P.; Kang, A.; Arab-Tehrany, E.; Ellis Ward, J.; Shin, S.R. Engineering Smart Targeting Nanovesicles and Their Combination with Hydrogels for Controlled Drug Delivery. *Pharmaceutics* **2020**, *12*, 849, doi:10.3390/pharmaceutics12090849.
7. Bulbake, U.; Doppalapudi, S.; Kommineni, N.; Khan, W. Liposomal Formulations in Clinical Use: An Updated Review. *Pharmaceutics* **2017**, *9*, 12, doi:10.3390/pharmaceutics9020012.
8. Liu, C.; Su, C. Design Strategies and Application Progress of Therapeutic Exosomes. *Theranostics* **2019**, *9*, 1015–1028, doi:10.7150/thno.30853.
9. Sato, Y.T.; Umezaki, K.; Sawada, S.; Mukai, S.; Sasaki, Y.; Harada, N.; Shiku, H.; Akiyoshi, K. Engineering Hybrid Exosomes by Membrane Fusion with Liposomes. *Sci Rep* **2016**, *6*, 21933, doi:10.1038/srep21933.
10. Piffoux, M.; Silva, A.K.A.; Wilhelm, C.; Gazeau, F.; Taresté, D. Modification of Extracellular Vesicles by Fusion with Liposomes for the Design of Personalized Biogenic Drug Delivery Systems. *ACS Nano* **2018**, *12*, 6830–6842, doi:10.1021/acsnano.8b02053.
11. Lin, Y.; Wu, J.; Gu, W.; Huang, Y.; Tong, Z.; Huang, L.; Tan, J. Exosome-Liposome Hybrid Nanoparticles Deliver CRISPR/Cas9 System in MSCs. *Adv. Sci.* **2018**, *5*, 1700611, doi:10.1002/advs.201700611.
12. Rayamajhi, S.; Nguyen, T.D.T.; Marasini, R.; Aryal, S. Macrophage-Derived Exosome-Mimetic Hybrid Vesicles for Tumor Targeted Drug Delivery. *Acta Biomaterialia* **2019**, *94*, 482–494, doi:10.1016/j.actbio.2019.05.054.
13. Liu, H.; Wang, Y.; Cui, K.; Guo, Y.; Zhang, X.; Qin, J. Advances in Hydrogels in Organoids and Organs-on-a-Chip. *Adv. Mater.* **2019**, *31*, 1902042, doi:10.1002/adma.201902042.
14. Pedde, R.D.; Mirani, B.; Navaei, A.; Styran, T.; Wong, S.; Mehrali, M.; Thakur, A.; Mohtaram, N.K.; Bayati, A.; Dolatshahi-Pirouz, A.; et al. Emerging Biofabrication Strategies for Engineering Complex Tissue Constructs. *Advanced Materials* **2017**, *29*, 1606061, doi:10.1002/adma.201606061.
15. Ashtari, K.; Nazari, H.; Ko, H.; Tebon, P.; Akhshik, M.; Akbari, M.; Alhosseini, S.N.; Mozafari, M.; Mehravi, B.; Soleimani, M.; et al. Electrically Conductive Nanomaterials for Cardiac Tissue Engineering. *Advanced Drug Delivery Reviews* **2019**, *144*, 162–179, doi:10.1016/j.addr.2019.06.001.
16. Sadeghi, A.; Moztarzadeh, F.; Aghazadeh Mohandesi, J. Investigating the Effect of Chitosan on Hydrophilicity and Bioactivity of Conductive Electrospun Composite Scaffold for Neural Tissue Engineering. *International Journal of Biological Macromolecules* **2019**, *121*, 625–632, doi:10.1016/j.ijbiomac.2018.10.022.

17. Moreno Madrid, A.P.; Vrech, S.M.; Sanchez, M.A.; Rodriguez, A.P. Advances in Additive Manufacturing for Bone Tissue Engineering Scaffolds. *Materials Science and Engineering: C* **2019**, *100*, 631–644, doi:10.1016/j.msec.2019.03.037.
18. Khademhosseini, A.; Langer, R.; Borenstein, J.; Vacanti, J.P. Microscale Technologies for Tissue Engineering and Biology. *Proceedings of the National Academy of Sciences* **2006**, *103*, 2480–2487, doi:10.1073/pnas.0507681102.
19. Gaharwar, A.K.; Peppas, N.A.; Khademhosseini, A. Nanocomposite Hydrogels for Biomedical Applications. *Biotechnol. Bioeng.* **2014**, *111*, 441–453, doi:10.1002/bit.25160.
20. Uto, K.; Tsui, J.H.; DeForest, C.A.; Kim, D.-H. Dynamically Tunable Cell Culture Platforms for Tissue Engineering and Mechanobiology. *Progress in Polymer Science* **2017**, *65*, 53–82, doi:10.1016/j.progpolymsci.2016.09.004.
21. Bhatia, S.N.; Underhill, G.H.; Zaret, K.S.; Fox, I.J. Cell and Tissue Engineering for Liver Disease. *Science Translational Medicine* **2014**, *6*, 245sr2–245sr2, doi:10.1126/scitranslmed.3005975.
22. Ma, X.; Qu, X.; Zhu, W.; Li, Y.-S.; Yuan, S.; Zhang, H.; Liu, J.; Wang, P.; Lai, C.S.E.; Zanella, F.; et al. Deterministically Patterned Biomimetic Human iPSC-Derived Hepatic Model via Rapid 3D Bioprinting. *Proceedings of the National Academy of Sciences* **2016**, *113*, 2206–2211, doi:10.1073/pnas.1524510113.
23. Faramarzi, N.; Yazdi, I.K.; Nabavinia, M.; Gemma, A.; Fanelli, A.; Caizzone, A.; Ptaszek, L.M.; Sinha, I.; Khademhosseini, A.; Ruskin, J.N.; et al. Patient-Specific Bioinks for 3D Bioprinting of Tissue Engineering Scaffolds. *Adv. Healthcare Mater.* **2018**, *7*, 1701347, doi:10.1002/adhm.201701347.
24. L'Heureux, N.; Dusserre, N.; Marini, A.; Garrido, S.; de la Fuente, L.; McAllister, T. Technology Insight: The Evolution of Tissue-Engineered Vascular Grafts—from Research to Clinical Practice. *Nature Clinical Practice Cardiovascular Medicine* **2007**, *4*, 389–395, doi:10.1038/ncpcardio0930.
25. Neves, L.S.; Rodrigues, M.T.; Reis, R.L.; Gomes, M.E. Current Approaches and Future Perspectives on Strategies for the Development of Personalized Tissue Engineering Therapies. *Expert Review of Precision Medicine and Drug Development* **2016**, *1*, 93–108, doi:10.1080/23808993.2016.1140004.
26. Bhatia, S.N.; Ingber, D.E. Microfluidic Organs-on-Chips. *Nature Biotechnology* **2014**, *32*, 760–772, doi:10.1038/nbt.2989.
27. Byambaa, B.; Annabi, N.; Yue, K.; Trujillo-de Santiago, G.; Alvarez, M.M.; Jia, W.; Kazemzadeh-Narbat, M.; Shin, S.R.; Tamayol, A.; Khademhosseini, A. Bioprinted Osteogenic and Vasculogenic Patterns for Engineering 3D Bone Tissue. *Advanced Healthcare Materials* **2017**, *6*, 1700015, doi:10.1002/adhm.201700015.
28. Caldorera-Moore, M.; Peppas, N.A. Micro- and Nanotechnologies for Intelligent and Responsive Biomaterial-Based Medical Systems. *Advanced Drug Delivery Reviews* **2009**, *61*, 1391–1401, doi:10.1016/j.addr.2009.09.002.
29. Culver, H.R.; Daily, A.M.; Khademhosseini, A.; Peppas, N.A. Intelligent Recognitive Systems in Nanomedicine. *Current Opinion in Chemical Engineering* **2014**, *4*, 105–113, doi:10.1016/j.coche.2014.02.001.
30. Huh, D.; Hamilton, G.A.; Ingber, D.E. From 3D Cell Culture to Organs-on-Chips. *Trends in Cell Biology* **2011**, *21*, 745–754, doi:10.1016/j.tcb.2011.09.005.
31. Khademhosseini, A.; Peppas, N.A. Micro- and Nanoengineering of Biomaterials for Healthcare Applications. *Advanced Healthcare Materials* **2013**, *2*, 10–12, doi:10.1002/adhm.201200444.
32. Liechty, W.B.; Caldorera-Moore, M.; Phillips, M.A.; Schoener, C.; Peppas, N.A. Advanced Molecular Design of Biopolymers for Transmucosal and Intracellular Delivery of Chemotherapeutic Agents and Biological Therapeutics. *Journal of Controlled Release* **2011**, *155*, 119–127, doi:10.1016/j.jconrel.2011.06.009.

33. Amini, A.R.; Laurencin, C.T.; Nukavarapu, S.P. Bone Tissue Engineering: Recent Advances and Challenges. *Crit Rev Biomed Eng* **2012**, *40*, 363–408, doi:10.1615/critrevbiomedeng.v40.i5.10.
34. Onoe, H.; Takeuchi, S. Cell-Laden Microfibers for Bottom-up Tissue Engineering. *Drug Discovery Today* **2015**, *20*, 236–246, doi:10.1016/j.drudis.2014.10.018.
35. Peppas, N.A.; Hoffman, A.S. Chapter I.2.5 - Hydrogels. In *Biomaterials Science (Third Edition)*; Academic Press, 2013; pp. 166–179 ISBN 978-0-12-374626-9.
36. Peppas, N.A.; Slaughter, B.V.; Kanzelberger, M.A. Hydrogels. In *Polymer Science: A Comprehensive Reference*; Elsevier, 2012; pp. 385–395 ISBN 978-0-08-087862-1.
37. Vacanti, J.P.; Vacanti, C.A. The History and Scope of Tissue Engineering. In *Principles of Tissue Engineering*; Elsevier, 2014; pp. 3–8 ISBN 978-0-12-398358-9.
38. Hay, E.D. *Cell Biology of Extracellular Matrix*; Springer Science & Business Media, 2013;
39. Hynes, R.O. The Extracellular Matrix: Not Just Pretty Fibrils. *Science* **2009**, *326*, 1216–1219, doi:10.1126/science.1176009.
40. Yannas, I.V. Hesitant Steps from the Artificial Skin to Organ Regeneration. *Regenerative Biomaterials* **2018**, doi:10.1093/rb/rby012.
41. Bae, H.; Puranik, A.S.; Gauvin, R.; Edalat, F.; Carrillo-Conde, B.; Peppas, N.A.; Khademhosseini, A. Building Vascular Networks. *Science Translational Medicine* **2012**, *4*, 160ps23-160ps23, doi:10.1126/scitranslmed.3003688.
42. De Witte, T.-M.; Fratila-Apachitei, L.E.; Zadpoor, A.A.; Peppas, N.A. Bone Tissue Engineering via Growth Factor Delivery: From Scaffolds to Complex Matrices. *Regenerative Biomaterials* **2018**, *5*, 197–211, doi:10.1093/rb/rby013.
43. Clegg, J.R.; Wechsler, M.E.; Peppas, N.A. Vision for Functionally Decorated and Molecularly Imprinted Polymers in Regenerative Engineering. *Regenerative Engineering and Translational Medicine* **2017**, *3*, 166–175, doi:10.1007/s40883-017-0028-9.
44. Culver, H.R.; Clegg, J.R.; Peppas, N.A. Analyte-Responsive Hydrogels: Intelligent Materials for Biosensing and Drug Delivery. *Accounts of Chemical Research* **2017**, *50*, 170–178, doi:10.1021/acs.accounts.6b00533.
45. Culver, H.R.; Peppas, N.A. Protein-Imprinted Polymers: The Shape of Things to Come? *Chemistry of Materials* **2017**, *29*, 5753–5761, doi:10.1021/acs.chemmater.7b01936.
46. Wagner, A.M.; Gran, M.P.; Peppas, N.A. Designing the New Generation of Intelligent Biocompatible Carriers for Protein and Peptide Delivery. *Acta Pharmaceutica Sinica B* **2018**, *8*, 147–164, doi:10.1016/j.apsb.2018.01.013.
47. Wagner, A.M.; Spencer, D.S.; Peppas, N.A. Advanced Architectures in the Design of Responsive Polymers for Cancer Nanomedicine: REVIEW. *Journal of Applied Polymer Science* **2018**, *135*, 46154, doi:10.1002/app.46154.
48. Peppas, N.A.; Vela Ramirez, J. Molecularly and Cellularly Imprinted, Intelligent Scaffolds for Tissue Engineering and Regenerative Medicine.; Beijing, 2018.
49. Peppas, N.A.; Hilt, J.Z.; Khademhosseini, A.; Langer, R. Hydrogels in Biology and Medicine: From Molecular Principles to Bionanotechnology. *Advanced Materials* **2006**, *18*, 1345–1360, doi:10.1002/adma.200501612.
50. Annabi, N.; Tamayol, A.; Uquillas, J.A.; Akbari, M.; Bertassoni, L.E.; Cha, C.; Camci-Unal, G.; Dokmeci, M.R.; Peppas, N.A.; Khademhosseini, A. 25th Anniversary Article: Rational Design and Applications of Hydrogels in Regenerative Medicine. *Adv. Mater.* **2014**, *26*, 85–124, doi:10.1002/adma.201303233.
51. Peppas, N.A.; Van Blarcom, D.S. Hydrogel-Based Biosensors and Sensing Devices for Drug Delivery. *Journal of Controlled Release* **2016**, *240*, 142–150, doi:10.1016/j.jconrel.2015.11.022.
52. Hoffman, A.S. Hydrogels for Biomedical Applications. *Advanced Drug Delivery Reviews* **2012**, *64*, 18–23, doi:10.1016/j.addr.2012.09.010.
53. Klouda, L.; Mikos, A.G. Thermoresponsive Hydrogels in Biomedical Applications. *European Journal of Pharmaceutics and Biopharmaceutics* **2008**, *68*, 34–45, doi:10.1016/j.ejpb.2007.02.025.

54. Koetting, M.C.; Peters, J.T.; Steichen, S.D.; Peppas, N.A. Stimulus-Responsive Hydrogels: Theory, Modern Advances, and Applications. *Materials Science and Engineering: R: Reports* **2015**, *93*, 1–49, doi:10.1016/j.mser.2015.04.001.
55. Caldorera-Moore, M.E.; Liechty, W.B.; Peppas, N.A. Responsive Theranostic Systems: Integration of Diagnostic Imaging Agents and Responsive Controlled Release Drug Delivery Carriers. *Accounts of Chemical Research* **2011**, *44*, 1061–1070, doi:10.1021/ar2001777.
56. Hoare, T.R.; Kohane, D.S. Hydrogels in Drug Delivery: Progress and Challenges. *Polymer* **2008**, *49*, 1993–2007, doi:10.1016/j.polymer.2008.01.027.
57. Peppas, N.A. Hydrogels and Drug Delivery. *Current Opinion in Colloid & Interface Science* **1997**, *2*, 531–537, doi:10.1016/S1359-0294(97)80103-3.
58. Qiu, Y.; Park, K. Environment-Sensitive Hydrogels for Drug Delivery. *Advanced Drug Delivery Reviews* **2001**, *53*, 321–339, doi:10.1016/S0169-409X(01)00203-4.
59. Drury, J.L.; Mooney, D.J. Hydrogels for Tissue Engineering: Scaffold Design Variables and Applications. *Biomaterials* **2003**, *24*, 4337–4351, doi:10.1016/S0142-9612(03)00340-5.
60. Lee, K.Y.; Mooney, D.J. Hydrogels for Tissue Engineering. *Chemical Reviews* **2001**, *101*, 1869–1880, doi:10.1021/cr000108x.
61. Slaughter, B.V.; Khurshid, S.S.; Fisher, O.Z.; Khademhosseini, A.; Peppas, N.A. Hydrogels in Regenerative Medicine. *Advanced Materials* **2009**, *21*, 3307–3329, doi:10.1002/adma.200802106.
62. Saghadzadeh, S.; Rinoldi, C.; Schot, M.; Kashaf, S.S.; Sharifi, F.; Jalilian, E.; Nuutila, K.; Giatsidis, G.; Mostafalu, P.; Derakhshandeh, H.; et al. Drug Delivery Systems and Materials for Wound Healing Applications. *Advanced Drug Delivery Reviews* **2018**, *127*, 138–166, doi:10.1016/j.addr.2018.04.008.
63. Thoniyot, P.; Tan, M.J.; Karim, A.A.; Young, D.J.; Loh, X.J. Nanoparticle-Hydrogel Composites: Concept, Design, and Applications of These Promising, Multi-Functional Materials. *Advanced Science* **2015**, *2*, 1400010, doi:10.1002/advs.201400010.
64. O'Brien, F.J. Biomaterials & Scaffolds for Tissue Engineering. *Materials Today* **2011**, *14*, 88–95, doi:10.1016/S1369-7021(11)70058-X.
65. Lee, K.Y.; Mooney, D.J. Alginate: Properties and Biomedical Applications. *Prog Polym Sci* **2012**, *37*, 106–126, doi:10.1016/j.progpolymsci.2011.06.003.
66. Croisier, F.; Jérôme, C. Chitosan-Based Biomaterials for Tissue Engineering. *European Polymer Journal* **2013**, *49*, 780–792, doi:10.1016/j.eurpolymj.2012.12.009.
67. Chang, C.; Zhang, L. Cellulose-Based Hydrogels: Present Status and Application Prospects. *Carbohydrate Polymers* **2011**, *84*, 40–53, doi:10.1016/j.carbpol.2010.12.023.
68. Burdick, J.A.; Prestwich, G.D. Hyaluronic Acid Hydrogels for Biomedical Applications. *Advanced Materials* **2011**, *23*, H41–H56, doi:10.1002/adma.201003963.
69. Antoine, E.E.; Vlachos, P.P.; Rylander, M.N. Review of Collagen I Hydrogels for Bioengineered Tissue Microenvironments: Characterization of Mechanics, Structure, and Transport. *Tissue Engineering Part B: Reviews* **2014**, *20*, 683–696, doi:10.1089/ten.teb.2014.0086.
70. Ahmed, E.M. Hydrogel: Preparation, Characterization, and Applications: A Review. *Journal of Advanced Research* **2015**, *6*, 105–121, doi:10.1016/j.jare.2013.07.006.
71. Zhao, W.; Jin, X.; Cong, Y.; Liu, Y.; Fu, J. Degradable Natural Polymer Hydrogels for Articular Cartilage Tissue Engineering: Degradable Natural Polymer Hydrogels for Articular Cartilage Tissue Engineering. *Journal of Chemical Technology & Biotechnology* **2013**, *88*, 327–339, doi:10.1002/jctb.3970.
72. Venkatesan, J.; Bhatnagar, I.; Manivasagan, P.; Kang, K.-H.; Kim, S.-K. Alginate Composites for Bone Tissue Engineering: A Review. *International Journal of Biological Macromolecules* **2015**, *72*, 269–281, doi:10.1016/j.ijbiomac.2014.07.008.
73. Madhally, S.V.; Matthew, H.W.T. Porous Chitosan Scaffolds for Tissue Engineering. *Biomaterials* **1999**, *20*, 1133–1142, doi:10.1016/S0142-9612(99)00011-3.

74. Collins, M.N.; Birkinshaw, C. Hyaluronic Acid Based Scaffolds for Tissue Engineering—A Review. *Carbohydrate Polymers* **2013**, *92*, 1262–1279, doi:10.1016/j.carbpol.2012.10.028.
75. Dugan, J.M.; Gough, J.E.; Eichhorn, S.J. Bacterial Cellulose Scaffolds and Cellulose Nanowhiskers for Tissue Engineering. *Nanomedicine* **2013**, *8*, 287–298, doi:10.2217/nnm.12.211.
76. Freier, T.; Montenegro, R.; Shan Koh, H.; Shoichet, M.S. Chitin-Based Tubes for Tissue Engineering in the Nervous System. *Biomaterials* **2005**, *26*, 4624–4632, doi:10.1016/j.biomaterials.2004.11.040.
77. Oliveira, J.T.; Martins, L.; Picciochi, R.; Malafaya, P.B.; Sousa, R.A.; Neves, N.M.; Mano, J.F.; Reis, R.L. Gellan Gum: A New Biomaterial for Cartilage Tissue Engineering Applications. *J. Biomed. Mater. Res.* **2009**, 9999A, NA-NA, doi:10.1002/jbm.a.32574.
78. Tamayol, A.; Najafabadi, A.H.; Aliakbarian, B.; Arab-Tehrany, E.; Akbari, M.; Annabi, N.; Juncker, D.; Khademhosseini, A. Hydrogel Templates for Rapid Manufacturing of Bioactive Fibers and 3D Constructs. *Adv. Healthcare Mater.* **2015**, *4*, 2146–2153, doi:10.1002/adhm.201500492.
79. Cen, L.; Liu, W.; Cui, L.; Zhang, W.; Cao, Y. Collagen Tissue Engineering: Development of Novel Biomaterials and Applications. *Pediatr Res* **2008**, *63*, 492–496, doi:10.1203/PDR.0b013e31816c5bc3.
80. Rezaei Nejad, H.; Goli Malekabadi, Z.; Kazemzadeh Narbat, M.; Annabi, N.; Mostafalu, P.; Tarlan, F.; Zhang, Y.S.; Hoorfar, M.; Tamayol, A.; Khademhosseini, A. Laterally Confined Microfluidic Patterning of Cells for Engineering Spatially Defined Vascularization. *Small* **2016**, *12*, 5132–5139, doi:10.1002/sml.201601391.
81. Tsigkou, O.; Pomerantseva, I.; Spencer, J.A.; Redondo, P.A.; Hart, A.R.; O'Doherty, E.; Lin, Y.; Friedrich, C.C.; Daheron, L.; Lin, C.P.; et al. Engineered Vascularized Bone Grafts. *Proc Natl Acad Sci USA* **2010**, *107*, 3311–3316, doi:10.1073/pnas.0905445107.
82. Annabi, N.; Shin, S.R.; Tamayol, A.; Miscuglio, M.; Bakooshli, M.A.; Assmann, A.; Mostafalu, P.; Sun, J.-Y.; Mithieux, S.; Cheung, L.; et al. Highly Elastic and Conductive Human-Based Protein Hybrid Hydrogels. *Advanced Materials* **2016**, *28*, 40–49, doi:10.1002/adma.201503255.
83. Xiao, W.; He, J.; Nichol, J.W.; Wang, L.; Hutson, C.B.; Wang, B.; Du, Y.; Fan, H.; Khademhosseini, A. Synthesis and Characterization of Photocrosslinkable Gelatin and Silk Fibroin Interpenetrating Polymer Network Hydrogels. *Acta Biomaterialia* **2011**, *7*, 2384–2393, doi:10.1016/j.actbio.2011.01.016.
84. Nitta, S.; Numata, K. Biopolymer-Based Nanoparticles for Drug/Gene Delivery and Tissue Engineering. *International Journal of Molecular Sciences* **2013**, *14*, 1629–1654, doi:10.3390/ijms14011629.
85. Smith, I.O.; Liu, X.H.; Smith, L.A.; Ma, P.X. Nanostructured Polymer Scaffolds for Tissue Engineering and Regenerative Medicine: Nanostructured Polymer Scaffolds. *Wiley Interdisciplinary Reviews: Nanomedicine and Nanobiotechnology* **2009**, *1*, 226–236, doi:10.1002/wnan.26.
86. Luo, X.; Morrin, A.; Killard, A.J.; Smyth, M.R. Application of Nanoparticles in Electrochemical Sensors and Biosensors. *Electroanalysis* **2006**, *18*, 319–326, doi:10.1002/elan.200503415.
87. VanBlarcom, D.S.; Peppas, N.A. Microcantilever Sensing Arrays from Biodegradable, PH-Responsive Hydrogels. *Biomedical Microdevices* **2011**, *13*, 829–836, doi:10.1007/s10544-011-9553-3.
88. Sharma, P.; Brown, S.; Walter, G.; Santra, S.; Moudgil, B. Nanoparticles for Bioimaging. *Advances in Colloid and Interface Science* **2006**, *123–126*, 471–485, doi:10.1016/j.cis.2006.05.026.
89. Yang, H.-H.; Zhang, S.-Q.; Chen, X.-L.; Zhuang, Z.-X.; Xu, J.-G.; Wang, X.-R. Magnetite-Containing Spherical Silica Nanoparticles for Biocatalysis and Bioseparations. *Analytical Chemistry* **2004**, *76*, 1316–1321, doi:10.1021/ac034920m.

90. Tomalia, D.A. In Quest of a Systematic Framework for Unifying and Defining Nanoscience. *Journal of Nanoparticle Research* **2009**, *11*, 1251–1310, doi:10.1007/s11051-009-9632-z.
91. Peters, J.T.; Hutchinson, S.S.; Lizana, N.; Verma, I.; Peppas, N.A. Synthesis and Characterization of Poly(N-Isopropyl Methacrylamide) Core/Shell Nanogels for Controlled Release of Chemotherapeutics. *Chemical Engineering Journal* **2018**, *340*, 58–65, doi:10.1016/j.cej.2018.01.009.
92. Peters, J.T.; Verghese, S.; Subramanian, D.; Peppas, N.A. Surface Hydrolysis-Mediated PEGylation of Poly(N-Isopropyl Acrylamide) Based Nanogels. *Regenerative Biomaterials* **2017**, *4*, 281–287, doi:10.1093/rb/rbx022.
93. Roohani-Esfahani, S.-I.; Zreiqat, H. Nanoparticles: A Promising New Therapeutic Platform for Bone Regeneration? *Nanomedicine* **2017**, *12*, 419–422, doi:10.2217/nnm-2016-0423.
94. Kim, T.; Hyeon, T. Applications of Inorganic Nanoparticles as Therapeutic Agents. *Nanotechnology* **2014**, *25*, 012001, doi:10.1088/0957-4484/25/1/012001.
95. Dykman, L.; Khlebtsov, N. Gold Nanoparticles in Biomedical Applications: Recent Advances and Perspectives. *Chem. Soc. Rev.* **2012**, *41*, 2256–2282, doi:10.1039/C1CS15166E.
96. Memic, A.; Alhadrami, H.A.; Hussain, M.A.; Aldahri, M.; Al Nowaiser, F.; Al-Hazmi, F.; Oklu, R.; Khademhosseini, A. Hydrogels 2.0: Improved Properties with Nanomaterial Composites for Biomedical Applications. *Biomedical Materials* **2015**, *11*, 014104, doi:10.1088/1748-6041/11/1/014104.
97. Bitounis, D.; Fanciullino, R.; Iliadis, A.; Ciccolini, J. Optimizing Druggability through Liposomal Formulations: New Approaches to an Old Concept. *ISRN Pharmaceutics* **2012**, *2012*, 1–11, doi:10.5402/2012/738432.
98. Gowda, R. Use of Nanotechnology to Develop Multi-Drug Inhibitors for Cancer Therapy. *Journal of Nanomedicine & Nanotechnology* **2013**, *04*, doi:10.4172/2157-7439.1000184.
99. Vahabi, S.; Eatemadi, A. Nanoliposome Encapsulated Anesthetics for Local Anesthesia Application. *Biomedicine & Pharmacotherapy* **2017**, *86*, 1–7, doi:10.1016/j.biopha.2016.11.137.
100. Fakhravar, Z.; Ebrahimnejad, P.; Daraee, H.; Akbarzadeh, A. Nanoliposomes: Synthesis Methods and Applications in Cosmetics. *Journal of Cosmetic and Laser Therapy* **2016**, *18*, 174–181, doi:10.3109/14764172.2015.1039040.
101. Mozafari, M.R. Nanoliposomes: Preparation and Analysis. In *Liposomes*; Weissig, V., Ed.; Humana Press: Totowa, NJ, 2010; Vol. 605, pp. 29–50 ISBN 978-1-60327-359-6.
102. Perisé-Barrios, A.J.; Sepúlveda-Crespo, D.; Shcharbin, D.; Rasines, B.; Gómez, R.; Klajnert-Maculewicz, B.; Bryszewska, M.; de la Mata, F.J.; Muñoz-Fernández, M.A. CHAPTER 7. Dendrimers. In *Nanoscience & Nanotechnology Series*; Callejas-Fernández, J., Estelrich, J., Quesada-Pérez, M., Forcada, J., Eds.; Royal Society of Chemistry: Cambridge, 2014; pp. 246–279 ISBN 978-1-84973-811-8.
103. Pearson, R.M.; Sunoqrot, S.; Hsu, H.; Bae, J.W.; Hong, S. Dendritic Nanoparticles: The next Generation of Nanocarriers? *Therapeutic delivery* **2012**, *3*, 941–959.
104. Taboada, P.; Barbosa, S.; Concheiro, A.; Alvarez-Lorenzo, C. CHAPTER 5. Polymeric Micelles. In *Nanoscience & Nanotechnology Series*; Callejas-Fernández, J., Estelrich, J., Quesada-Pérez, M., Forcada, J., Eds.; Royal Society of Chemistry: Cambridge, 2014; pp. 157–215 ISBN 978-1-84973-811-8.
105. Chen, H.; Khemtong, C.; Yang, X.; Chang, X.; Gao, J. Nanonization Strategies for Poorly Water-Soluble Drugs. *Drug Discovery Today* **2011**, *16*, 354–360, doi:10.1016/j.drudis.2010.02.009.
106. Yokoyama, M. Polymeric Micelles as a New Drug Carrier System and Their Required Considerations for Clinical Trials. *Expert Opinion on Drug Delivery* **2010**, *7*, 145–158, doi:10.1517/17425240903436479.
107. Ramos, J.; Pelaez-Fernandez, M.; Forcada, J.; Moncho-Jorda, A. CHAPTER 4. Nanogels for Drug Delivery: the Key Role of Nanogel&#8211;Drug Interactions. In *Nanoscience &*

- Nanotechnology Series*; Callejas-Fernández, J., Estelrich, J., Quesada-Pérez, M., Forcada, J., Eds.; Royal Society of Chemistry: Cambridge, 2014; pp. 133–156 ISBN 978-1-84973-811-8.
108. Neamtu, I.; Rusu, A.G.; Diaconu, A.; Nita, L.E.; Chiriac, A.P. Basic Concepts and Recent Advances in Nanogels as Carriers for Medical Applications. *Drug Delivery* **2017**, *24*, 539–557, doi:10.1080/10717544.2016.1276232.
  109. Bangham, A.D.; Horne, R.W. Negative Staining of Phospholipids and Their Structural Modification by Surface-Active Agents as Observed in the Electron Microscope. *Journal of Molecular Biology* **1964**, *8*, 660–IN10, doi:10.1016/S0022-2836(64)80115-7.
  110. Allen, T.M. Drug Delivery Systems: Entering the Mainstream. *Science* **2004**, *303*, 1818–1822, doi:10.1126/science.1095833.
  111. Allen, T.M.; Cullis, P.R. Liposomal Drug Delivery Systems: From Concept to Clinical Applications. *Advanced Drug Delivery Reviews* **2013**, *65*, 36–48, doi:10.1016/j.addr.2012.09.037.
  112. Korsmeyer, R. Critical Questions in Development of Targeted Nanoparticle Therapeutics. *Regenerative Biomaterials* **2016**, *3*, 143–147, doi:10.1093/rb/rbw011.
  113. Li, L.; He, Z.-Y.; Wei, X.-W.; Wei, Y.-Q. Recent Advances of Biomaterials in Biotherapy. *Regenerative Biomaterials* **2016**, *3*, 99–105, doi:10.1093/rb/rbw007.
  114. Kulkarni, M.; Greiser, U.; O'Brien, T.; Pandit, A. Liposomal Gene Delivery Mediated by Tissue-Engineered Scaffolds. *Trends in Biotechnology* **2010**, *28*, 28–36, doi:10.1016/j.tibtech.2009.10.003.
  115. Monteiro, N.; Martins, A.; Reis, R.L.; Neves, N.M. Liposomes in Tissue Engineering and Regenerative Medicine. *J R Soc Interface* **2014**, *11*, doi:10.1098/rsif.2014.0459.
  116. Hasan, M.; Elkhoury, K.; Kahn, C.J.F.; Arab-Tehrany, E.; Linder, M. Preparation, Characterization, and Release Kinetics of Chitosan-Coated Nanoliposomes Encapsulating Curcumin in Simulated Environments. *Molecules* **2019**, *24*, 2023, doi:10.3390/molecules24102023.
  117. Hasan, M.; Latifi, S.; Kahn, C.; Tamayol, A.; Habibey, R.; Passeri, E.; Linder, M.; Arab-Tehrany, E. The Positive Role of Curcumin-Loaded Salmon Nanoliposomes on the Culture of Primary Cortical Neurons. *Mar. Drugs* **2018**, *16*, 218, doi:10.3390/md16070218.
  118. Reza Mozafari, M.; Johnson, C.; Hatziantoniou, S.; Demetzos, C. Nanoliposomes and Their Applications in Food Nanotechnology. *Journal of Liposome Research* **2008**, *18*, 309–327, doi:10.1080/08982100802465941.
  119. Doll, T.A.P.F.; Raman, S.; Dey, R.; Burkhard, P. Nanoscale Assemblies and Their Biomedical Applications. *Journal of The Royal Society Interface* **2013**, *10*, 20120740–20120740, doi:10.1098/rsif.2012.0740.
  120. Díaz, M.; Vivas-Mejia, P. Nanoparticles as Drug Delivery Systems in Cancer Medicine: Emphasis on RNAi-Containing Nanoliposomes. *Pharmaceuticals* **2013**, *6*, 1361–1380, doi:10.3390/ph6111361.
  121. Cleymand, F.; Zhang, H.; Dostert, G.; Menu, P.; Arab-Tehrany, E.; Velot, E.; Mano, J.F. Membranes Combining Chitosan and Natural-Origin Nanoliposomes for Tissue Engineering. *RSC Advances* **2016**, *6*, 83626–83637, doi:10.1039/C6RA13568D.
  122. Hasan, M.; Ben Messaoud, G.; Michaux, F.; Tamayol, A.; Kahn, C.J.F.; Belhaj, N.; Linder, M.; Arab-Tehrany, E. Chitosan-Coated Liposomes Encapsulating Curcumin: Study of Lipid–Polysaccharide Interactions and Nanovesicle Behavior. *RSC Advances* **2016**, *6*, 45290–45304, doi:10.1039/C6RA05574E.
  123. Hasan, M.; Belhaj, N.; Benachour, H.; Barberi-Heyob, M.; Kahn, C.J.F.; Jabbari, E.; Linder, M.; Arab-Tehrany, E. Liposome Encapsulation of Curcumin: Physico-Chemical Characterizations and Effects on MCF7 Cancer Cell Proliferation. *Int. J. Pharm.* **2014**, *461*, 519–528.
  124. Lee, C.C.; MacKay, J.A.; Fréchet, J.M.J.; Szoka, F.C. Designing Dendrimers for Biological Applications. *Nature Biotechnology* **2005**, *23*, 1517–1526, doi:10.1038/nbt1171.

125. Kolhatkar, R.; Sweet, D.; Ghandehari, H. Functionalized Dendrimers as Nanoscale Drug Carriers. In *Multifunctional Pharmaceutical Nanocarriers*; Torchilin, V., Ed.; Springer New York: New York, NY, 2008; Vol. 4, pp. 201–232 ISBN 978-0-387-76551-8.
126. Nguyen, C.K.; Tran, N.Q.; Nguyen, T.P.; Nguyen, D.H. Biocompatible Nanomaterials Based on Dendrimers, Hydrogels and Hydrogel Nanocomposites for Use in Biomedicine. *Advances in Natural Sciences: Nanoscience and Nanotechnology* **2017**, *8*, 015001, doi:10.1088/2043-6254/8/1/015001.
127. Wiener, E.; Brechbiel, M.W.; Brothers, H.; Magin, R.L.; Gansow, O.A.; Tomalia, D.A.; Lauterbur, P.C. Dendrimer-Based Metal Chelates: A New Class of Magnetic Resonance Imaging Contrast Agents. *Magn. Reson. Med.* **1994**, *31*, 1–8, doi:10.1002/mrm.1910310102.
128. Supattapone, S.; Nguyen, H.-O.B.; Cohen, F.E.; Prusiner, S.B.; Scott, M.R. Elimination of Prions by Branched Polyamines and Implications for Therapeutics. *Proceedings of the National Academy of Sciences* **1999**, *96*, 14529–14534.
129. Kojima, C.; Kono, K.; Maruyama, K.; Takagishi, T. Synthesis of Polyamidoamine Dendrimers Having Poly(Ethylene Glycol) Grafts and Their Ability To Encapsulate Anticancer Drugs. *Bioconjugate Chemistry* **2000**, *11*, 910–917, doi:10.1021/bc0000583.
130. Tang, M.X.; Redemann, C.T.; Szoka, F.C. In Vitro Gene Delivery by Degraded Polyamidoamine Dendrimers. *Bioconjugate chemistry* **1996**, *7*, 703–714.
131. Wathier, M.; Jung, P.J.; Carnahan, M.A.; Kim, T.; Grinstaff, M.W. Dendritic Macromers as in Situ Polymerizing Biomaterials for Securing Cataract Incisions. *Journal of the American Chemical Society* **2004**, *126*, 12744–12745, doi:10.1021/ja045870l.
132. Velazquez, A.J.; Carnahan, M.A.; Kristinsson, J.; Stinnett, S.; Grinstaff, M.W.; Kim, T. New Dendritic Adhesives for Sutureless Ophthalmic Surgical Procedures: In Vitro Studies of Corneal Laceration Repair. *Archives of Ophthalmology* **2004**, *122*, 867–870.
133. King, H.D.; Dubowchik, G.M.; Mastalerz, H.; Willner, D.; Hofstead, S.J.; Firestone, R.A.; Lasch, S.J.; Trail, P.A. Monoclonal Antibody Conjugates of Doxorubicin Prepared with Branched Peptide Linkers: Inhibition of Aggregation by Methoxytriethyleneglycol Chains. *Journal of Medicinal Chemistry* **2002**, *45*, 4336–4343, doi:10.1021/jm020149g.
134. Morgan, M.T.; Carnahan, M.A.; Immoos, C.E.; Ribeiro, A.A.; Finkelstein, S.; Lee, S.J.; Grinstaff, M.W. Dendritic Molecular Capsules for Hydrophobic Compounds. *Journal of the American Chemical Society* **2003**, *125*, 15485–15489, doi:10.1021/ja0347383.
135. Estelrich, J.; Quesada-Pérez, M.; Forcada, J.; Callejas-Fernández, J. CHAPTER 1. Introductory Aspects of Soft Nanoparticles. In *Nanoscience & Nanotechnology Series*; Callejas-Fernández, J., Estelrich, J., Quesada-Pérez, M., Forcada, J., Eds.; Royal Society of Chemistry: Cambridge, 2014; pp. 1–18 ISBN 978-1-84973-811-8.
136. Letchford, K.; Burt, H. A Review of the Formation and Classification of Amphiphilic Block Copolymer Nanoparticulate Structures: Micelles, Nanospheres, Nanocapsules and Polymersomes. *European Journal of Pharmaceutics and Biopharmaceutics* **2007**, *65*, 259–269, doi:10.1016/j.ejpb.2006.11.009.
137. Jones, M.-C.; Leroux, J.-C. Polymeric Micelles—a New Generation of Colloidal Drug Carriers. *European journal of pharmaceutics and biopharmaceutics* **1999**, *48*, 101–111.
138. Sasaki, Y.; Akiyoshi, K. Nanogel Engineering for New Nanobiomaterials: From Chaperoning Engineering to Biomedical Applications. *The Chemical Record* **2010**, n/a-n/a, doi:10.1002/tcr.201000008.
139. Akiyoshi, K.; Deguchi, S.; Moriguchi, N.; Yamaguchi, S.; Sunamoto, J. Self-Aggregates of Hydrophobized Polysaccharides in Water. Formation and Characteristics of Nanoparticles. *Macromolecules* **1993**, *26*, 3062–3068, doi:10.1021/ma00064a011.
140. Vinogradov, S.; Batrakova, E.; Kabanov, A. Poly(Ethylene Glycol)–Polyethyleneimine NanoGel<sup>TM</sup> Particles: Novel Drug Delivery Systems for Antisense Oligonucleotides. *Colloids and Surfaces B: Biointerfaces* **1999**, *16*, 291–304, doi:10.1016/S0927-7765(99)00080-6.

141. Kabanov, A.V.; Vinogradov, S.V. Nanogels as Pharmaceutical Carriers: Finite Networks of Infinite Capabilities. *Angewandte Chemie International Edition* **2009**, *48*, 5418–5429, doi:10.1002/anie.200900441.
142. Chacko, R.T.; Ventura, J.; Zhuang, J.; Thayumanavan, S. Polymer Nanogels: A Versatile Nanoscopic Drug Delivery Platform. *Advanced Drug Delivery Reviews* **2012**, *64*, 836–851, doi:10.1016/j.addr.2012.02.002.
143. Culver, H.R.; Steichen, S.D.; Peppas, N.A. A Closer Look at the Impact of Molecular Imprinting on Adsorption Capacity and Selectivity for Protein Templates. *Biomacromolecules* **2016**, *17*, 4045–4053, doi:10.1021/acs.biomac.6b01482.
144. Neves, M.I.; Wechsler, M.E.; Gomes, M.E.; Reis, R.L.; Granja, P.L.; Peppas, N.A. Molecularly Imprinted Intelligent Scaffolds for Tissue Engineering Applications. *Tissue Engineering Part B: Reviews* **2017**, *23*, 27–43, doi:10.1089/ten.teb.2016.0202.
145. Zhang, Q.; Chen, X.; Geng, S.; Wei, L.; Miron, R.J.; Zhao, Y.; Zhang, Y. Nanogel-Based Scaffolds Fabricated for Bone Regeneration with Mesoporous Bioactive Glass and Strontium: In Vitro and in Vivo Characterization. *J. Biomed. Mater. Res.* **2017**, *105*, 1175–1183, doi:10.1002/jbm.a.35980.
146. Zhu, D.; Zhang, L.; Dong, X.; Sun, H.; Song, C.; Wang, C.; Kong, D. Folate-Modified Lipid–Polymer Hybrid Nanoparticles for Targeted Paclitaxel Delivery. *International Journal of Nanomedicine* **2015**, 2101, doi:10.2147/IJN.S77667.
147. Karanth, H.; Murthy, R.S.R. PH-Sensitive Liposomes-Principle and Application in Cancer Therapy. *Journal of Pharmacy and Pharmacology* **2007**, *59*, 469–483, doi:10.1211/jpp.59.4.0001.
148. Pridgen, E.M.; Alexis, F.; Farokhzad, O.C. Polymeric Nanoparticle Technologies for Oral Drug Delivery. *Clinical Gastroenterology and Hepatology* **2014**, *12*, 1605–1610, doi:10.1016/j.cgh.2014.06.018.
149. Liu, M.; Ishida, Y.; Ebina, Y.; Sasaki, T.; Aida, T. Photolatently Modulable Hydrogels Using Unilamellar Titania Nanosheets as Photocatalytic Crosslinkers. *Nature Communications* **2013**, *4*, doi:10.1038/ncomms3029.
150. Wu, H.; Yu, G.; Pan, L.; Liu, N.; McDowell, M.T.; Bao, Z.; Cui, Y. Stable Li-Ion Battery Anodes by in-Situ Polymerization of Conducting Hydrogel to Conformally Coat Silicon Nanoparticles. *Nature Communications* **2013**, *4*, doi:10.1038/ncomms2941.
151. Zhang, D.; Yang, J.; Bao, S.; Wu, Q.; Wang, Q. Semiconductor Nanoparticle-Based Hydrogels Prepared via Self-Initiated Polymerization under Sunlight, Even Visible Light. *Scientific Reports* **2013**, *3*, doi:10.1038/srep01399.
152. Pardo-Yissar, V.; Gabai, R.; Shipway, A.N.; Bourenko, T.; Willner, I. Gold Nanoparticle/Hydrogel Composites with Solvent-Switchable Electronic Properties. *Advanced Materials* **2001**, *13*, 1320, doi:10.1002/1521-4095(200109)13:17<1320::AID-ADMA1320>3.0.CO;2-8.
153. Saravanan, P.; Padmanabha Raju, M.; Alam, S. A Study on Synthesis and Properties of Ag Nanoparticles Immobilized Polyacrylamide Hydrogel Composites. *Materials Chemistry and Physics* **2007**, *103*, 278–282, doi:10.1016/j.matchemphys.2007.02.025.
154. Marcelo, G.; López-González, M.; Mendicuti, F.; Tarazona, M.P.; Valiente, M. Poly(*N*-Isopropylacrylamide)/Gold Hybrid Hydrogels Prepared by Catechol Redox Chemistry. Characterization and Smart Tunable Catalytic Activity. *Macromolecules* **2014**, *47*, 6028–6036, doi:10.1021/ma501214k.
155. Holtz, J.H.; Asher, S.A. Polymerized Colloidal Crystal Hydrogel Films as Intelligent Chemical Sensing Materials. *Nature* **1997**, *389*, 829–832, doi:10.1038/39834.
156. Lauten, E.H.; Peppas, N.A. Intelligent Drug Release Using Molecular Imprinting Methods Recognitive Systems for Angiotensin II. *Journal of Drug Delivery Science and Technology* **2009**, *19*, 391–399, doi:10.1016/S1773-2247(09)50082-2.
157. Souza, G.R.; Christianson, D.R.; Staquicini, F.I.; Ozawa, M.G.; Snyder, E.Y.; Sidman, R.L.; Miller, J.H.; Arap, W.; Pasqualini, R. Networks of Gold Nanoparticles and Bacteriophage as Biological Sensors and Cell-Targeting Agents. *Proceedings of the National Academy of Sciences* **2006**, *103*, 1215–1220, doi:10.1073/pnas.0509739103.

158. Jones, C.D.; Lyon, L.A. Photothermal Patterning of Microgel/Gold Nanoparticle Composite Colloidal Crystals. *Journal of the American Chemical Society* **2003**, *125*, 460–465, doi:10.1021/ja027431x.
159. Wang, C.; Flynn, N.T.; Langer, R. Controlled Structure and Properties of Thermoresponsive Nanoparticle–Hydrogel Composites. *Advanced Materials* **2004**, *16*, 1074–1079, doi:10.1002/adma.200306516.
160. Anderson, J.M. Future Challenges in the *in Vitro* and *in Vivo* Evaluation of Biomaterial Biocompatibility. *Regenerative Biomaterials* **2016**, *3*, 73–77, doi:10.1093/rb/rbw001.
161. Leijten, J.; Seo, J.; Yue, K.; Trujillo-de Santiago, G.; Tamayol, A.; Ruiz-Esparza, G.U.; Shin, S.R.; Sharifi, R.; Noshadi, I.; Álvarez, M.M.; et al. Spatially and Temporally Controlled Hydrogels for Tissue Engineering. *Materials Science and Engineering: R: Reports* **2017**, *119*, 1–35, doi:10.1016/j.mser.2017.07.001.
162. Choi, K.; Kuhn, J.L.; Ciarelli, M.J.; Goldstein, S.A. The Elastic Moduli of Human Subchondral, Trabecular, and Cortical Bone Tissue and the Size-Dependency of Cortical Bone Modulus. *Journal of Biomechanics* **1990**, *23*, 1103–1113, doi:10.1016/0021-9290(90)90003-L.
163. Kot, B.C.W.; Zhang, Z.J.; Lee, A.W.C.; Leung, V.Y.F.; Fu, S.N. Elastic Modulus of Muscle and Tendon with Shear Wave Ultrasound Elastography: Variations with Different Technical Settings. *PLoS ONE* **2012**, *7*, e44348, doi:10.1371/journal.pone.0044348.
164. Chen, Q.-Z.; Bismarck, A.; Hansen, U.; Junaid, S.; Tran, M.Q.; Harding, S.E.; Ali, N.N.; Boccaccini, A.R. Characterisation of a Soft Elastomer Poly(Glycerol Sebacate) Designed to Match the Mechanical Properties of Myocardial Tissue. *Biomaterials* **2008**, *29*, 47–57, doi:10.1016/j.biomaterials.2007.09.010.
165. Saraf, H.; Ramesh, K.T.; Lennon, A.M.; Merkle, A.C.; Roberts, J.C. Mechanical Properties of Soft Human Tissues under Dynamic Loading. *Journal of Biomechanics* **2007**, *40*, 1960–1967, doi:10.1016/j.jbiomech.2006.09.021.
166. Shin, S.R.; Li, Y.-C.; Jang, H.L.; Khoshakhlagh, P.; Akbari, M.; Nasajpour, A.; Zhang, Y.S.; Tamayol, A.; Khademhosseini, A. Graphene-Based Materials for Tissue Engineering. *Advanced Drug Delivery Reviews* **2016**, *105*, 255–274, doi:10.1016/j.addr.2016.03.007.
167. Xiao, L.; Liu, C.; Zhu, J.; Pochan, D.J.; Jia, X. Hybrid, Elastomeric Hydrogels Crosslinked by Multifunctional Block Copolymer Micelles. *Soft Matter* **2010**, *6*, 5293, doi:10.1039/c0sm00511h.
168. Duan, X.; Sheardown, H. Dendrimer Crosslinked Collagen as a Corneal Tissue Engineering Scaffold: Mechanical Properties and Corneal Epithelial Cell Interactions. *Biomaterials* **2006**, *27*, 4608–4617, doi:10.1016/j.biomaterials.2006.04.022.
169. Rahali, K.; Ben Messaoud, G.; Kahn, C.; Sanchez-Gonzalez, L.; Kaci, M.; Cleymand, F.; Fleutot, S.; Linder, M.; Desobry, S.; Arab-Tehrany, E. Synthesis and Characterization of Nanofunctionalized Gelatin Methacrylate Hydrogels. *International Journal of Molecular Sciences* **2017**, *18*, 2675, doi:10.3390/ijms18122675.
170. Kadri, R.; Ben Messaoud, G.; Tamayol, A.; Aliakbarian, B.; Zhang, H.Y.; Hasan, M.; Sánchez-González, L.; Arab-Tehrany, E. Preparation and Characterization of Nanofunctionalized Alginate/Methacrylated Gelatin Hybrid Hydrogels. *RSC Advances* **2016**, *6*, 27879–27884, doi:10.1039/C6RA03699F.
171. Biondi, M.; Ungaro, F.; Quaglia, F.; Netti, P.A. Controlled Drug Delivery in Tissue Engineering. *Advanced Drug Delivery Reviews* **2008**, *60*, 229–242, doi:10.1016/j.addr.2007.08.038.
172. Parker, J.; Mitrousis, N.; Shoichet, M.S. Hydrogel for Simultaneous Tunable Growth Factor Delivery and Enhanced Viability of Encapsulated Cells *in Vitro*. *Biomacromolecules* **2016**, *17*, 476–484, doi:10.1021/acs.biomac.5b01366.
173. Peng, L.-H.; Xu, S.-Y.; Shan, Y.-H.; Wei, W.; Liu, S.; Zhang, C.-Z.; Wu, J.-H.; Liang, W.-Q.; Gao, J.-Q. Sequential Release of Salidroside and Paeonol from a Nanosphere-Hydrogel System Inhibits Ultraviolet B-Induced Melanogenesis in Guinea Pig Skin. *International Journal of Nanomedicine* **2014**, 1897, doi:10.2147/IJN.S59290.

174. Pulat, M.; Kahraman, A.S.; Tan, N.; Gümüşderelioğlu, M. Sequential Antibiotic and Growth Factor Releasing Chitosan-PAAm Semi-IPN Hydrogel as a Novel Wound Dressing. *Journal of Biomaterials Science, Polymer Edition* **2013**, *24*, 807–819, doi:10.1080/09205063.2012.718613.
175. Hao, X.; Silva, E.; Manssonbroberg, A.; Grinnemo, K.; Siddiqui, A.; Dellgren, G.; Wardell, E.; Brodin, L.; Mooney, D.; Sylven, C. Angiogenic Effects of Sequential Release of VEGF-A165 and PDGF-BB with Alginate Hydrogels after Myocardial Infarction. *Cardiovascular Research* **2007**, *75*, 178–185, doi:10.1016/j.cardiores.2007.03.028.
176. Nelson, D.M.; Ma, Z.; Leeson, C.E.; Wagner, W.R. Extended and Sequential Delivery of Protein from Injectable Thermoresponsive Hydrogels. *Journal of Biomedical Materials Research Part A* **2012**, *100A*, 776–785, doi:10.1002/jbm.a.34015.
177. Quinlan, E.; López-Noriega, A.; Thompson, E.; Kelly, H.M.; Cryan, S.A.; O'Brien, F.J. Development of Collagen–Hydroxyapatite Scaffolds Incorporating PLGA and Alginate Microparticles for the Controlled Delivery of RhBMP-2 for Bone Tissue Engineering. *Journal of Controlled Release* **2015**, *198*, 71–79, doi:10.1016/j.jconrel.2014.11.021.
178. Taetz, S.; Bochot, A.; Surace, C.; Arpicco, S.; Renoir, J.-M.; Schaefer, U.F.; Marsaud, V.; Kerdine-Roemer, S.; Lehr, C.-M.; Fattal, E. Hyaluronic Acid-Modified DOTAP/DOPE Liposomes for the Targeted Delivery of Anti-Telomerase siRNA to CD44-Expressing Lung Cancer Cells. *Oligonucleotides* **2009**, *19*, 103–116, doi:10.1089/oli.2008.0168.
179. Pederson, A. Thermal Assembly of a Biomimetic Mineral/Collagen Composite. *Biomaterials* **2003**, *24*, 4881–4890, doi:10.1016/S0142-9612(03)00369-7.
180. Samadikuchaksaraei, A.; Gholipourmalekabadi, M.; Erfani Ezadyar, E.; Azami, M.; Mozafari, M.; Johari, B.; Kargozar, S.; Jameie, S.B.; Korourian, A.; Seifalian, A.M. Fabrication and in Vivo Evaluation of an Osteoblast-Conditioned Nano-Hydroxyapatite/Gelatin Composite Scaffold for Bone Tissue Regeneration. *Journal of Biomedical Materials Research Part A* **2016**, *104*, 2001–2010, doi:10.1002/jbm.a.35731.
181. Ochi, M.; Adachi, N.; Nobuto, H.; Yanada, S.; Ito, Y.; Agung, M. Articular Cartilage Repair Using Tissue Engineering Technique—Novel Approach with Minimally Invasive Procedure. *Artificial Organs* **2004**, *28*, 28–32, doi:10.1111/j.1525-1594.2004.07317.x.
182. Reya, T.; Morrison, S.J.; Clarke, M.F.; Weissman, I.L. Stem Cells, Cancer, and Cancer Stem Cells. *nature* **2001**, *414*, 105.
183. Narita, Y.; Yamawaki, A.; Kagami, H.; Ueda, M.; Ueda, Y. Effects of Transforming Growth Factor-Beta 1 and Ascorbic Acid on Differentiation of Human Bone-Marrow-Derived Mesenchymal Stem Cells into Smooth Muscle Cell Lineage. *Cell and Tissue Research* **2008**, *333*, 449–459, doi:10.1007/s00441-008-0654-0.
184. Miller, M.W.; Luo, J. Effects of Ethanol and Transforming Growth Factor Beta (TGFbeta) on Neuronal Proliferation and NCAM Expression. *Alcoholism: Clinical and Experimental Research* **2002**, *26*, 1281–1285, doi:10.1111/j.1530-0277.2002.tb02668.x.
185. Hosseinzadeh, Z.; Schmid, E.; Shumilina, E.; Laufer, S.; Borst, O.; Gawaz, M.; Lang, F. Effect of TGFβ on Na<sup>+</sup>/K<sup>+</sup> ATPase Activity in Megakaryocytes. *Biochemical and Biophysical Research Communications* **2014**, *452*, 537–541, doi:10.1016/j.bbrc.2014.08.093.
186. Dostert, G.; Kahn, C.J.F.; Menu, P.; Mesure, B.; Cleymand, F.; Linder, M.; Velot, é.; Arab-Tehrany, E. Nanoliposomes of Marine Lecithin, a New Way to Deliver TGF-β 1. *J. Biomater. Tissue Eng* **2017**, *7*, 1163–1170, doi:10.1166/jbt.2017.1670.
187. Fujioka-Kobayashi, M.; Ota, M.S.; Shimoda, A.; Nakahama, K.; Akiyoshi, K.; Miyamoto, Y.; Iseki, S. Cholesteryl Group- and Acryloyl Group-Bearing Pullulan Nanogel to Deliver BMP2 and FGF18 for Bone Tissue Engineering. *Biomaterials* **2012**, *33*, 7613–7620, doi:10.1016/j.biomaterials.2012.06.075.
188. Joo, V.; Ramasamy, T.; Haidar, Z.S. A Novel Self-Assembled Liposome-Based Polymeric Hydrogel for Cranio-Maxillofacial Applications: Preliminary Findings. *Polymers* **2011**, *3*, 967–974, doi:10.3390/polym3020967.

189. Record, M.; Subra, C.; Silvente-Poirot, S.; Poirot, M. Exosomes as Intercellular Signalosomes and Pharmacological Effectors. *Biochemical Pharmacology* **2011**, *81*, 1171–1182, doi:10.1016/j.bcp.2011.02.011.
190. Liu, X.; Yang, Y.; Li, Y.; Niu, X.; Zhao, B.; Wang, Y.; Bao, C.; Xie, Z.; Lin, Q.; Zhu, L. Integration of Stem Cell-Derived Exosomes with in Situ Hydrogel Glue as a Promising Tissue Patch for Articular Cartilage Regeneration. *Nanoscale* **2017**, *9*, 4430–4438, doi:10.1039/C7NR00352H.
191. Siddappa, R.; Licht, R.; van Blitterswijk, C.; de Boer, J. Donor Variation and Loss of Multipotency during in Vitro Expansion of Human Mesenchymal Stem Cells for Bone Tissue Engineering. *Journal of Orthopaedic Research* **2007**, *25*, 1029–1041, doi:10.1002/jor.20402.
192. Shi, Q.; Qian, Z.; Liu, D.; Sun, J.; Wang, X.; Liu, H.; Xu, J.; Guo, X. GMSC-Derived Exosomes Combined with a Chitosan/Silk Hydrogel Sponge Accelerates Wound Healing in a Diabetic Rat Skin Defect Model. *Frontiers in Physiology* **2017**, *8*, doi:10.3389/fphys.2017.00904.
193. Fisher, O.Z.; Khademhosseini, A.; Langer, R.; Peppas, N.A. Bioinspired Materials for Controlling Stem Cell Fate. *Accounts of Chemical Research* **2010**, *43*, 419–428, doi:10.1021/ar900226q.
194. Peng, L.; Cheng, X.; Zhuo, R.; Lan, J.; Wang, Y.; Shi, B.; Li, S. Novel Gene-Activated Matrix with Embedded Chitosan/Plasmid DNA Nanoparticles Encoding PDGF for Periodontal Tissue Engineering. *J. Biomed. Mater. Res.* **2009**, *90A*, 564–576, doi:10.1002/jbm.a.32117.
195. Raftery, R.M.; Tierney, E.G.; Curtin, C.M.; Cryan, S.-A.; O'Brien, F.J. Development of a Gene-Activated Scaffold Platform for Tissue Engineering Applications Using Chitosan-PDNA Nanoparticles on Collagen-Based Scaffolds. *Journal of Controlled Release* **2015**, *210*, 84–94, doi:10.1016/j.jconrel.2015.05.005.
196. Smith, A.M.; Harris, J.J.; Shelton, R.M.; Perrie, Y. 3D Culture of Bone-Derived Cells Immobilised in Alginate Following Light-Triggered Gelation. *Journal of Controlled Release* **2007**, *119*, 94–101, doi:10.1016/j.jconrel.2007.01.011.
197. Wu, S.Y.; Chang, H.-I.; Burgess, M.; McMillan, N.A.J. Vaginal Delivery of siRNA Using a Novel PEGylated Lipoplex-Entrapped Alginate Scaffold System. *Journal of Controlled Release* **2011**, *155*, 418–426, doi:10.1016/j.jconrel.2011.02.002.
198. Dai, C.; Wang, B.; Zhao, H.; Li, B.; Wang, J. Preparation and Characterization of Liposomes-in-Alginate (LIA) for Protein Delivery System. *Colloids and Surfaces B: Biointerfaces* **2006**, *47*, 205–210, doi:10.1016/j.colsurfb.2005.07.013.
199. Weiner, A.L.; Carpenter-Green, S.S.; Soehngen, E.C.; Lenk, R.P.; Popescu, M.C. Liposome–Collagen Gel Matrix: A Novel Sustained Drug Delivery System. *Journal of pharmaceutical sciences* **1985**, *74*, 922–925.
200. Lee, J.-H.; Oh, H.; Baxa, U.; Raghavan, S.R.; Blumenthal, R. Biopolymer-Connected Liposome Networks as Injectable Biomaterials Capable of Sustained Local Drug Delivery. *Biomacromolecules* **2012**, *13*, 3388–3394, doi:10.1021/bm301143d.
201. Lajavardi, L.; Camelo, S.; Agnely, F.; Luo, W.; Goldenberg, B.; Naud, M.-C.; Behar-Cohen, F.; de Kozak, Y.; Bochot, A. New Formulation of Vasoactive Intestinal Peptide Using Liposomes in Hyaluronic Acid Gel for Uveitis. *Journal of Controlled Release* **2009**, *139*, 22–30, doi:10.1016/j.jconrel.2009.05.033.
202. Walsh, D.P.; Heise, A.; O'Brien, F.J.; Cryan, S.-A. An Efficient, Non-Viral Dendritic Vector for Gene Delivery in Tissue Engineering. *Gene Therapy* **2017**, *24*, 681–691, doi:10.1038/gt.2017.58.
203. Xiao, L.; Tong, Z.; Chen, Y.; Pochan, D.J.; Sabanayagam, C.R.; Jia, X. Hyaluronic Acid-Based Hydrogels Containing Covalently Integrated Drug Depots: Implication for Controlling Inflammation in Mechanically Stressed Tissues. *Biomacromolecules* **2013**, *14*, 3808–3819, doi:10.1021/bm4011276.

204. Derakhshandeh, H.; Kashaf, S.S.; Aghabaglou, F.; Ghanavati, I.O.; Tamayol, A. Smart Bandages: The Future of Wound Care. *Trends in Biotechnology* **2018**, doi:10.1016/j.tibtech.2018.07.007.
205. Patel, G.; Dalwadi, C. Recent Patents on Stimuli Responsive Hydrogel Drug Delivery System. *Recent Patents on Drug Delivery & Formulation* **2013**, *7*, 206–215, doi:10.2174/1872211307666131118141600.
206. *FDA Executive Summary: Classification of Wound Dressings Combined with Drugs*; 2016;
207. He, H.; Lu, Y.; Qi, J.; Zhu, Q.; Chen, Z.; Wu, W. Adapting Liposomes for Oral Drug Delivery. *Acta Pharmaceutica Sinica B* **2019**, *9*, 36–48, doi:10.1016/j.apsb.2018.06.005.
208. Bianchi, A.; Velot, É.; Kempf, H.; Elkhoury, K.; Sanchez-Gonzalez, L.; Linder, M.; Kahn, C.; Arab-Tehrany, E. Nanoliposomes from Agro-Resources as Promising Delivery Systems for Chondrocytes. *IJMS* **2020**, *21*, 3436, doi:10.3390/ijms21103436.
209. Antimisiaris, S.; Mourtas, S.; Marazioti, A. Exosomes and Exosome-Inspired Vesicles for Targeted Drug Delivery. *Pharmaceutics* **2018**, *10*, 218, doi:10.3390/pharmaceutics10040218.
210. Johnsen, K.B.; Gudbergsson, J.M.; Skov, M.N.; Pilgaard, L.; Moos, T.; Duroux, M. A Comprehensive Overview of Exosomes as Drug Delivery Vehicles — Endogenous Nanocarriers for Targeted Cancer Therapy. *Biochimica et Biophysica Acta (BBA) - Reviews on Cancer* **2014**, *1846*, 75–87, doi:10.1016/j.bbcan.2014.04.005.
211. Wang, P.; Wang, H.; Huang, Q.; Peng, C.; Yao, L.; Chen, H.; Qiu, Z.; Wu, Y.; Wang, L.; Chen, W. Exosomes from M1-Polarized Macrophages Enhance Paclitaxel Antitumor Activity by Activating Macrophages-Mediated Inflammation. *Theranostics* **2019**, *9*, 1714–1727, doi:10.7150/thno.30716.
212. Ohno, S.; Takanashi, M.; Sudo, K.; Ueda, S.; Ishikawa, A.; Matsuyama, N.; Fujita, K.; Mizutani, T.; Ohgi, T.; Ochiya, T.; et al. Systemically Injected Exosomes Targeted to EGFR Deliver Antitumor MicroRNA to Breast Cancer Cells. *Molecular Therapy* **2013**, *21*, 185–191, doi:10.1038/mt.2012.180.
213. Turturici, G.; Tinnirello, R.; Sconzo, G.; Geraci, F. Extracellular Membrane Vesicles as a Mechanism of Cell-to-Cell Communication: Advantages and Disadvantages. *American Journal of Physiology-Cell Physiology* **2014**, *306*, C621–C633, doi:10.1152/ajpcell.00228.2013.
214. Johnsen, K.B.; Gudbergsson, J.M.; Duroux, M.; Moos, T.; Andresen, T.L.; Simonsen, J.B. On the Use of Liposome Controls in Studies Investigating the Clinical Potential of Extracellular Vesicle-Based Drug Delivery Systems – A Commentary. *Journal of Controlled Release* **2018**, *269*, 10–14, doi:10.1016/j.jconrel.2017.11.002.
215. Cheng, R.; Yan, Y.; Liu, H.; Chen, H.; Pan, G.; Deng, L.; Cui, W. Mechanically Enhanced Lipo-Hydrogel with Controlled Release of Multi-Type Drugs for Bone Regeneration. *Applied Materials Today* **2018**, *12*, 294–308, doi:10.1016/j.apmt.2018.06.008.
216. Wang, C.; Wang, M.; Xu, T.; Zhang, X.; Lin, C.; Gao, W.; Xu, H.; Lei, B.; Mao, C. Engineering Bioactive Self-Healing Antibacterial Exosomes Hydrogel for Promoting Chronic Diabetic Wound Healing and Complete Skin Regeneration. *Theranostics* **2019**, *9*, 65–76, doi:10.7150/thno.29766.
217. Rasoulzadehzali, M.; Namazi, H. Facile Preparation of Antibacterial Chitosan/Graphene Oxide-Ag Bio-Nanocomposite Hydrogel Beads for Controlled Release of Doxorubicin. *International Journal of Biological Macromolecules* **2018**, *116*, 54–63, doi:10.1016/j.ijbiomac.2018.04.140.
218. Zhang, K.; Zhao, X.; Chen, X.; Wei, Y.; Du, W.; Wang, Y.; Liu, L.; Zhao, W.; Han, Z.; Kong, D.; et al. Enhanced Therapeutic Effects of Mesenchymal Stem Cell-Derived Exosomes with an Injectable Hydrogel for Hindlimb Ischemia Treatment. *ACS Appl. Mater. Interfaces* **2018**, *10*, 30081–30091, doi:10.1021/acsami.8b08449.
219. Shafei, S.; Khanmohammadi, M.; Heidari, R.; Ghanbari, H.; Taghdiri Nooshabadi, V.; Farzamfar, S.; Akbariqomi, M.; Sanikhani, N.S.; Absalan, M.; Tavoosidana, G. Exosome

- Loaded Alginate Hydrogel Promotes Tissue Regeneration in Full-thickness Skin Wounds: An in Vivo Study. *J Biomed Mater Res* **2020**, *108*, 545–556, doi:10.1002/jbm.a.36835.
220. Lyu, D.; Chen, S.; Guo, W. Liposome Crosslinked Polyacrylamide/DNA Hydrogel: A Smart Controlled-Release System for Small Molecular Payloads. *Small* **2018**, *14*, 1704039, doi:10.1002/sml.201704039.
221. Biondi, M.; Borzacchiello, A.; Mayol, L.; Ambrosio, L. Nanoparticle-Integrated Hydrogels as Multifunctional Composite Materials for Biomedical Applications. *Gels* **2015**, *1*, 162–178, doi:10.3390/gels1020162.
222. Bangham, A.D.; Standish, M.M.; Watkins, J.C. Diffusion of Univalent Ions across the Lamellae of Swollen Phospholipids. *Journal of Molecular Biology* **1965**, *13*, 238-IN27.
223. Pattni, B.S.; Chupin, V.V.; Torchilin, V.P. New Developments in Liposomal Drug Delivery. *Chem. Rev.* **2015**, *115*, 10938–10966, doi:10.1021/acs.chemrev.5b00046.
224. Li, J.; Elkhoury, K.; Barbieux, C.; Linder, M.; Grandemange, S.; Tamayol, A.; Francius, G.; Arab-Tehrany, E. Effects of Bioactive Marine-Derived Liposomes on Two Human Breast Cancer Cell Lines. *Mar. Drugs* **2020**, *18*, 211, doi:10.3390/md18040211.
225. Lasic, D.D. Novel Applications of Liposomes. *Trends Biotechnol.* **1998**, *16*, 307–321.
226. Israelachvili, J.N.; Marčelja, S.; Horn, R.G. Physical Principles of Membrane Organization. *Quart. Rev. Biophys.* **1980**, *13*, 121–200, doi:10.1017/S0033583500001645.
227. Hasan, M.; Elkhoury, K.; Belhaj, N.; Kahn, C.; Tamayol, A.; Barberi-Heyob, M.; Arab-Tehrany, E.; Linder, M. Growth-Inhibitory Effect of Chitosan-Coated Liposomes Encapsulating Curcumin on MCF-7 Breast Cancer Cells. *Mar. Drugs* **2020**, *18*, 217, doi:10.3390/md18040217.
228. Duplessis, J.; Ramachandran, C.; Weiner, N.; Muller, D. The Influence of Lipid Composition and Lamellarity of Liposomes on the Physical Stability of Liposomes upon Storage. *Int. J. Pharm.* **1996**, *127*, 273–278, doi:10.1016/0378-5173(95)04281-4.
229. Fröhlich, M.; Brecht, V.; Peschka-Süss, R. Parameters Influencing the Determination of Liposome Lamellarity by <sup>31</sup>P-NMR. *Chemistry and Physics of Lipids* **2001**, *109*, 103–112, doi:10.1016/S0009-3084(00)00220-6.
230. Torchilin, V.P. Recent Advances with Liposomes as Pharmaceutical Carriers. *Nat Rev Drug Discov* **2005**, *4*, 145–160, doi:10.1038/nrd1632.
231. Nag, O.; Awasthi, V. Surface Engineering of Liposomes for Stealth Behavior. *Pharmaceutics* **2013**, *5*, 542–569, doi:10.3390/pharmaceutics5040542.
232. Riaz, M.; Riaz, M.; Zhang, X.; Lin, C.; Wong, K.; Chen, X.; Zhang, G.; Lu, A.; Yang, Z. Surface Functionalization and Targeting Strategies of Liposomes in Solid Tumor Therapy: A Review. *IJMS* **2018**, *19*, 195, doi:10.3390/ijms19010195.
233. Hatakeyama, H.; Akita, H.; Harashima, H. The Polyethyleneglycol Dilemma: Advantage and Disadvantage of PEGylation of Liposomes for Systemic Genes and Nucleic Acids Delivery to Tumors. *Biological Pharmaceutical Bulletin* **2013**, *36*, 892–899, doi:10.1248/bpb.b13-00059.
234. Salmaso, S.; Caliceti, P. Stealth Properties to Improve Therapeutic Efficacy of Drug Nanocarriers. *Journal of Drug Delivery* **2013**, *2013*, 1–19, doi:10.1155/2013/374252.
235. Lasic, D.D.; Needham, David. The “Stealth” Liposome: A Prototypical Biomaterial. *Chem. Rev.* **1995**, *95*, 2601–2628, doi:10.1021/cr00040a001.
236. Woodle, M.C.; Lasic, D.D. Sterically Stabilized Liposomes. *Biochim Biophys Acta Biomembr* **1992**, *1113*, 171–199, doi:10.1016/0304-4157(92)90038-C.
237. Milla, P.; Dosio, F.; Cattel, L. PEGylation of Proteins and Liposomes: A Powerful and Flexible Strategy to Improve the Drug Delivery. *CDM* **2012**, *13*, 105–119, doi:10.2174/138920012798356934.
238. Harris, J.M.; Martin, N.E.; Modi, M. Pegylation: A Novel Process for Modifying Pharmacokinetics. *Clinical Pharmacokinetics* **2001**, *40*, 539–551, doi:10.2165/00003088-200140070-00005.
239. Roberts, M.J.; Bentley, M.D.; Harris, J.M. Chemistry for Peptide and Protein PEGylation. *Advanced Drug Delivery Reviews* **2002**, *54*, 459–476, doi:10.1016/S0169-409X(02)00022-4.

240. Barenholz, Y. (Chezy) Doxil® — The First FDA-Approved Nano-Drug: Lessons Learned. *Journal of Controlled Release* **2012**, *160*, 117–134, doi:10.1016/j.jconrel.2012.03.020.
241. Gabizon, A.; Catane, R.; Uziely, B.; Kaufman, B.; Safra, T.; Cohen, R.; Martin, F.; Huang, A.; Barenholz, Y. Prolonged Circulation Time and Enhanced Accumulation in Malignant Exudates of Doxorubicin Encapsulated in Polyethylene-Glycol Coated Liposomes. *Cancer Res.* **1994**, *54*, 987–992.
242. Gabizon, A.; Shmeeda, H.; Barenholz, Y. Pharmacokinetics of Pegylated Liposomal Doxorubicin: Review of Animal and Human Studies. *Clinical Pharmacokinetics* **2003**, *42*, 419–436, doi:10.2165/00003088-200342050-00002.
243. Hong, R.L.; Huang, C.J.; Tseng, Y.L.; Pang, V.F.; Chen, S.T.; Liu, J.J.; Chang, F.H. Direct Comparison of Liposomal Doxorubicin with or without Polyethylene Glycol Coating in C-26 Tumor-Bearing Mice: Is Surface Coating with Polyethylene Glycol Beneficial? *Clin. Cancer Res.* **1999**, *5*, 3645–3652.
244. Zhang, Y.; Huang, L. Liposomal delivery system. In *Nanoparticles for Biomedical Applications*; Elsevier, 2020; pp. 145–152 ISBN 978-0-12-816662-8.
245. Lohade, A.A.; Jain, R.R.; Iyer, K.; Roy, S.K.; Shimpi, H.H.; Pawar, Y.; Rajan, M.G.R.; Menon, M.D. A Novel Folate-Targeted Nanoliposomal System of Doxorubicin for Cancer Targeting. *AAPS PharmSciTech* **2016**, *17*, 1298–1311, doi:10.1208/s12249-015-0462-2.
246. Moghimipour, E.; Rezaei, M.; Ramezani, Z.; Kouchak, M.; Amini, M.; Angali, K.A.; Dorkoosh, F.A.; Handali, S. Folic Acid-Modified Liposomal Drug Delivery Strategy for Tumor Targeting of 5-Fluorouracil. *European Journal of Pharmaceutical Sciences* **2018**, *114*, 166–174, doi:10.1016/j.ejps.2017.12.011.
247. Sriraman, S.K.; Salzano, G.; Sarisozen, C.; Torchilin, V. Anti-Cancer Activity of Doxorubicin-Loaded Liposomes Co-Modified with Transferrin and Folic Acid. *European Journal of Pharmaceutics and Biopharmaceutics* **2016**, *105*, 40–49, doi:10.1016/j.ejpb.2016.05.023.
248. Dasargyri, A.; Kümin, C.D.; Leroux, J.-C. Targeting Nanocarriers with Anisamide: Fact or Artifact? *Adv. Mater.* **2017**, *29*, 1603451, doi:10.1002/adma.201603451.
249. Chen, Y.; Bathula, S.R.; Yang, Q.; Huang, L. Targeted Nanoparticles Deliver SiRNA to Melanoma. *Journal of Investigative Dermatology* **2010**, *130*, 2790–2798, doi:10.1038/jid.2010.222.
250. Li, S.-D.; Chen, Y.-C.; Hackett, M.J.; Huang, L. Tumor-Targeted Delivery of SiRNA by Self-Assembled Nanoparticles. *Molecular Therapy* **2008**, *16*, 163–169, doi:10.1038/sj.mt.6300323.
251. Banerjee, R.; Tyagi, P.; Li, S.; Huang, L. Anisamide-Targeted Stealth Liposomes: A Potent Carrier for Targeting Doxorubicin to Human Prostate Cancer Cells. *Int. J. Cancer* **2004**, *112*, 693–700, doi:10.1002/ijc.20452.
252. Plourde, K.; Derbali, R.M.; Desrosiers, A.; Dubath, C.; Vallée-Bélisle, A.; Leblond, J. Aptamer-Based Liposomes Improve Specific Drug Loading and Release. *Journal of Controlled Release* **2017**, *251*, 82–91, doi:10.1016/j.jconrel.2017.02.026.
253. Baek, S.E.; Lee, K.H.; Park, Y.S.; Oh, D.-K.; Oh, S.; Kim, K.-S.; Kim, D.-E. RNA Aptamer-Conjugated Liposome as an Efficient Anticancer Drug Delivery Vehicle Targeting Cancer Cells in Vivo. *Journal of Controlled Release* **2014**, *196*, 234–242, doi:10.1016/j.jconrel.2014.10.018.
254. Dissanayake, S.; Denny, W.A.; Gamage, S.; Sarojini, V. Recent Developments in Anticancer Drug Delivery Using Cell Penetrating and Tumor Targeting Peptides. *Journal of Controlled Release* **2017**, *250*, 62–76, doi:10.1016/j.jconrel.2017.02.006.
255. Zhang, X.; Lin, C.; Lu, A.; Lin, G.; Chen, H.; Liu, Q.; Yang, Z.; Zhang, H. Liposomes Equipped with Cell Penetrating Peptide BR2 Enhances Chemotherapeutic Effects of Cantharidin against Hepatocellular Carcinoma. *Drug Delivery* **2017**, *24*, 986–998, doi:10.1080/10717544.2017.1340361.
256. Chen, Z.; Deng; Zhao; Tao Cyclic RGD Peptide-Modified Liposomal Drug Delivery System: Enhanced Cellular Uptake in Vitro and Improved Pharmacokinetics in Rats. *IJN* **2012**, 3803, doi:10.2147/IJN.S33541.

257. Koren, E.; Torchilin, V.P. Cell-Penetrating Peptides: Breaking through to the Other Side. *Trends in Molecular Medicine* **2012**, *18*, 385–393, doi:10.1016/j.molmed.2012.04.012.
258. Xie, Y.; Ding, Y.; Sun, D.; Wang, G.; Yang, H.; Xu, H.; Wang, Z.; Chen, J. An Efficient PEGylated Liposomal Nanocarrier Containing Cell-Penetrating Peptide and PH-Sensitive Hydrazone Bond for Enhancing Tumor-Targeted Drug Delivery. *IJN* **2015**, 6199, doi:10.2147/IJN.S92519.
259. Eloy, J.O.; Petrilli, R.; Trevizan, L.N.F.; Chorilli, M. Immunoliposomes: A Review on Functionalization Strategies and Targets for Drug Delivery. *Colloids and Surfaces B: Biointerfaces* **2017**, *159*, 454–467, doi:10.1016/j.colsurfb.2017.07.085.
260. Manjappa, A.S.; Chaudhari, K.R.; Venkataraju, M.P.; Dantuluri, P.; Nanda, B.; Sidda, C.; Sawant, K.K.; Ramachandra Murthy, R.S. Antibody Derivatization and Conjugation Strategies: Application in Preparation of Stealth Immunoliposome to Target Chemotherapeutics to Tumor. *Journal of Controlled Release* **2011**, *150*, 2–22, doi:10.1016/j.jconrel.2010.11.002.
261. Ordóñez-Gutiérrez, L.; Posado-Fernández, A.; Ahmadvand, D.; Lettiero, B.; Wu, L.; Antón, M.; Flores, O.; Moghimi, S.M.; Wandosell, F. ImmunoPEGliposome-Mediated Reduction of Blood and Brain Amyloid Levels in a Mouse Model of Alzheimer's Disease Is Restricted to Aged Animals. *Biomaterials* **2017**, *112*, 141–152, doi:10.1016/j.biomaterials.2016.07.027.
262. Corrado, C.; Raimondo, S.; Chiesi, A.; Ciccia, F.; De Leo, G.; Alessandro, R. Exosomes as Intercellular Signaling Organelles Involved in Health and Disease: Basic Science and Clinical Applications. *IJMS* **2013**, *14*, 5338–5366, doi:10.3390/ijms14035338.
263. Simons, M.; Raposo, G. Exosomes – Vesicular Carriers for Intercellular Communication. *Current Opinion in Cell Biology* **2009**, *21*, 575–581, doi:10.1016/j.ceb.2009.03.007.
264. Kapsogeorgou, E.K.; Abu-Helu, R.F.; Moutsopoulos, H.M.; Manoussakis, M.N. Salivary Gland Epithelial Cell Exosomes: A Source of Autoantigenic Ribonucleoproteins. *Arthritis Rheum* **2005**, *52*, 1517–1521, doi:10.1002/art.21005.
265. Lai, R.C.; Arslan, F.; Lee, M.M.; Sze, N.S.K.; Choo, A.; Chen, T.S.; Salto-Tellez, M.; Timmers, L.; Lee, C.N.; El Oakley, R.M.; et al. Exosome Secreted by MSC Reduces Myocardial Ischemia/Reperfusion Injury. *Stem Cell Research* **2010**, *4*, 214–222, doi:10.1016/j.scr.2009.12.003.
266. Mallegol, J.; Van Niel, G.; Lebreton, C.; Lepelletier, Y.; Candalh, C.; Dugave, C.; Heath, J.K.; Raposo, G.; Cerf-Bensussan, N.; Heyman, M. T84-Intestinal Epithelial Exosomes Bear MHC Class II/Peptide Complexes Potentiating Antigen Presentation by Dendritic Cells. *Gastroenterology* **2007**, *132*, 1866–1876, doi:10.1053/j.gastro.2007.02.043.
267. Ristorcelli, E.; Beraud, E.; Verrando, P.; Villard, C.; Lafitte, D.; Sbarra, V.; Lombardo, D.; Verine, A. Human Tumor Nanoparticles Induce Apoptosis of Pancreatic Cancer Cells. *The FASEB Journal* **2008**, *22*, 3358–3369, doi:10.1096/fj.07-102855.
268. Théry, C.; Regnault, A.; Garin, J.; Wolfers, J.; Zitvogel, L.; Ricciardi-Castagnoli, P.; Raposo, G.; Amigorena, S. Molecular Characterization of Dendritic Cell-Derived Exosomes. *The Journal of Cell Biology* **1999**, *147*, 599–610, doi:10.1083/jcb.147.3.599.
269. Zech, D.; Rana, S.; Büchler, M.W.; Zöller, M. Tumor-Exosomes and Leukocyte Activation: An Ambivalent Crosstalk. *Cell Commun Signal* **2012**, *10*, 37, doi:10.1186/1478-811X-10-37.
270. Gutiérrez-Vázquez, C.; Villarroya-Beltri, C.; Mittelbrunn, M.; Sánchez-Madrid, F. Transfer of Extracellular Vesicles during Immune Cell-Cell Interactions. *Immunol Rev* **2013**, *251*, 125–142, doi:10.1111/imr.12013.
271. Bang, C.; Thum, T. Exosomes: New Players in Cell-Cell Communication. *The International Journal of Biochemistry & Cell Biology* **2012**, *44*, 2060–2064, doi:10.1016/j.biocel.2012.08.007.
272. Fais, S.; O'Driscoll, L.; Borrás, F.E.; Buzas, E.; Camussi, G.; Cappello, F.; Carvalho, J.; Cordeiro da Silva, A.; Del Portillo, H.; El Andaloussi, S.; et al. Evidence-Based Clinical Use of Nanoscale Extracellular Vesicles in Nanomedicine. *ACS Nano* **2016**, *10*, 3886–3899, doi:10.1021/acsnano.5b08015.

273. Yakimchuk, K. Exosomes: Isolation Methods and Specific Markers. *MATER METHODS* **2015**, *5*, doi:10.13070/mm.en.5.1450.
274. Contreras-Naranjo, J.C.; Wu, H.-J.; Ugaz, V.M. Microfluidics for Exosome Isolation and Analysis: Enabling Liquid Biopsy for Personalized Medicine. *Lab Chip* **2017**, *17*, 3558–3577, doi:10.1039/C7LC00592J.
275. Allmann, C. Functions of the Exosome in RRNA, SnoRNA and SnRNA Synthesis. *The EMBO Journal* **1999**, *18*, 5399–5410, doi:10.1093/emboj/18.19.5399.
276. Gruenberg, J.; Stenmark, H. The Biogenesis of Multivesicular Endosomes. *Nat Rev Mol Cell Biol* **2004**, *5*, 317–323, doi:10.1038/nrm1360.
277. Théry, C.; Zitvogel, L.; Amigorena, S. Exosomes: Composition, Biogenesis and Function. *Nat Rev Immunol* **2002**, *2*, 569–579, doi:10.1038/nri855.
278. Urbanelli, L.; Magini, A.; Buratta, S.; Brozzi, A.; Sagini, K.; Polchi, A.; Tancini, B.; Emiliani, C. Signaling Pathways in Exosomes Biogenesis, Secretion and Fate. *Genes* **2013**, *4*, 152–170, doi:10.3390/genes4020152.
279. Subra, C.; Laulagnier, K.; Perret, B.; Record, M. Exosome Lipidomics Unravels Lipid Sorting at the Level of Multivesicular Bodies. *Biochimie* **2007**, *89*, 205–212, doi:10.1016/j.biochi.2006.10.014.
280. Subra, C.; Grand, D.; Laulagnier, K.; Stella, A.; Lambeau, G.; Paillasse, M.; De Medina, P.; Monsarrat, B.; Perret, B.; Silvente-Poirot, S.; et al. Exosomes Account for Vesicle-Mediated Transcellular Transport of Activatable Phospholipases and Prostaglandins. *J. Lipid Res.* **2010**, *51*, 2105–2120, doi:10.1194/jlr.M003657.
281. Valadi, H.; Ekström, K.; Bossios, A.; Sjöstrand, M.; Lee, J.J.; Lötvall, J.O. Exosome-Mediated Transfer of MRNAs and MicroRNAs Is a Novel Mechanism of Genetic Exchange between Cells. *Nat Cell Biol* **2007**, *9*, 654–659, doi:10.1038/ncb1596.
282. van Niel, G.; Porto-Carreiro, I.; Simoes, S.; Raposo, G. Exosomes: A Common Pathway for a Specialized Function. *The Journal of Biochemistry* **2006**, *140*, 13–21, doi:10.1093/jb/mvj128.
283. Mathivanan, S.; Ji, H.; Simpson, R.J. Exosomes: Extracellular Organelles Important in Intercellular Communication. *Journal of Proteomics* **2010**, *73*, 1907–1920, doi:10.1016/j.jprot.2010.06.006.
284. D’Asti, E.; Garnier, D.; Lee, T.H.; Montermini, L.; Meehan, B.; Rak, J. Oncogenic Extracellular Vesicles in Brain Tumor Progression. *Front. Physiol.* **2012**, *3*, doi:10.3389/fphys.2012.00294.
285. Cordonnier, M.; Chanteloup, G.; Isambert, N.; Seigneuric, R.; Fumoleau, P.; Garrido, C.; Gobbo, J. Exosomes in Cancer Theranostic: Diamonds in the Rough. *Cell Adhesion & Migration* **2017**, *11*, 151–163, doi:10.1080/19336918.2016.1250999.
286. Soung, Y.H.; Nguyen, T.; Cao, H.; Lee, J.; Chung, J. Emerging Roles of Exosomes in Cancer Invasion and Metastasis. *BMB Reports* **2016**, *49*, 18–25, doi:10.5483/BMBRep.2016.49.1.239.
287. Blaser, M.C.; Aikawa, E. Differential MiRNA Loading Underpins Dual Harmful and Protective Roles for Extracellular Vesicles in Atherogenesis. *Circ Res* **2019**, *124*, 467–469, doi:10.1161/CIRCRESAHA.119.314596.
288. Bang, C.; Batkai, S.; Dangwal, S.; Gupta, S.K.; Foinquinos, A.; Holzmann, A.; Just, A.; Remke, J.; Zimmer, K.; Zeug, A.; et al. Cardiac Fibroblast-Derived MicroRNA Passenger Strand-Enriched Exosomes Mediate Cardiomyocyte Hypertrophy. *J. Clin. Invest.* **2014**, *124*, 2136–2146, doi:10.1172/JCI70577.
289. Dangwal, S.; Thum, T. MicroRNA Therapeutics in Cardiovascular Disease Models. *Annu. Rev. Pharmacol. Toxicol.* **2014**, *54*, 185–203, doi:10.1146/annurev-pharmtox-011613-135957.
290. Koles, K.; Budnik, V. Exosomes Go with the Wnt. *Cellular Logistics* **2012**, *2*, 169–173, doi:10.4161/cl.21981.
291. Maggio, S.; Ceccaroli, P.; Polidori, E.; Cioccoloni, A.; Stocchi, V.; Guescini, M. Signal Exchange through Extracellular Vesicles in Neuromuscular Junction Establishment and

- Maintenance: From Physiology to Pathology. *IJMS* **2019**, *20*, 2804, doi:10.3390/ijms20112804.
292. Chairoungdua, A.; Smith, D.L.; Pochard, P.; Hull, M.; Caplan, M.J. Exosome Release of  $\beta$ -Catenin: A Novel Mechanism That Antagonizes Wnt Signaling. *The Journal of Cell Biology* **2010**, *190*, 1079–1091, doi:10.1083/jcb.201002049.
293. Bunggulawa, E.J.; Wang, W.; Yin, T.; Wang, N.; Durkan, C.; Wang, Y.; Wang, G. Recent Advancements in the Use of Exosomes as Drug Delivery Systems. *J Nanobiotechnol* **2018**, *16*, 81, doi:10.1186/s12951-018-0403-9.
294. Van Hove, A.H.; Benoit, D.S.W. Depot-Based Delivery Systems for Pro-Angiogenic Peptides: A Review. *Front. Bioeng. Biotechnol.* **2015**, *3*, doi:10.3389/fbioe.2015.00102.
295. Peers, S.; Alcouffe, P.; Montembault, A.; Ladavière, C. Embedment of Liposomes into Chitosan Physical Hydrogel for the Delayed Release of Antibiotics or Anaesthetics, and Its First ESEM Characterization. *Carbohydrate Polymers* **2020**, *229*, 115532, doi:10.1016/j.carbpol.2019.115532.
296. Wu, W.; Dai, Y.; Liu, H.; Cheng, R.; Ni, Q.; Ye, T.; Cui, W. Local Release of Gemcitabine via *in Situ* UV-Crosslinked Lipid-Strengthened Hydrogel for Inhibiting Osteosarcoma. *Drug Delivery* **2018**, *25*, 1642–1651, doi:10.1080/10717544.2018.1497105.
297. Xiao, L.; Lin, J.; Chen, R.; Huang, Y.; Liu, Y.; Bai, J.; Ge, G.; Shi, X.; Chen, Y.; Shi, J.; et al. Sustained Release of Melatonin from GelMA Liposomes Reduced Osteoblast Apoptosis and Improved Implant Osseointegration in Osteoporosis. *Oxidative Medicine and Cellular Longevity* **2020**, *2020*, 1–20, doi:10.1155/2020/6797154.
298. Yu, J.R.; Janssen, M.; Liang, B.J.; Huang, H.-C.; Fisher, J.P. A Liposome/Gelatin Methacrylate Nanocomposite Hydrogel System for Delivery of Stromal Cell-Derived Factor-1 $\alpha$  and Stimulation of Cell Migration. *Acta Biomaterialia* **2020**, *108*, 67–76, doi:10.1016/j.actbio.2020.03.015.
299. Kadri, R.; Bacharouch, J.; Elkhoury, K.; Ben Messaoud, G.; Kahn, C.; Desobry, S.; Linder, M.; Tamayol, A.; Francius, G.; Mano, J.F.; et al. Role of Active Nanoliposomes in the Surface and Bulk Mechanical Properties of Hybrid Hydrogels. *Mater. Today Bio* **2020**, *6*, 100046, doi:10.1016/j.mtbio.2020.100046.
300. Chang, M.-C.; Kuo, Y.-J.; Hung, K.-H.; Peng, C.-L.; Chen, K.-Y.; Yeh, L.-K. Liposomal Dexamethasone–Moxifloxacin Nanoparticles Combinations with Collagen/Gelatin/Alginate Hydrogel for Corneal Infection Treatment and Wound Healing. *Biomed. Mater.* **2020**, doi:10.1088/1748-605X/ab9510.
301. Yan, J.; Chen, R.; Zhang, H.; Bryers, J.D. Injectable Biodegradable Chitosan-Alginate 3D Porous Gel Scaffold for mRNA Vaccine Delivery. *Macromol. Biosci.* **2019**, *19*, 1800242, doi:10.1002/mabi.201800242.
302. Li, R.; Liu, Q.; Wu, H.; Wang, K.; Li, L.; Zhou, C.; Ao, N. Preparation and Characterization of In-Situ Formable Liposome/Chitosan Composite Hydrogels. *Materials Letters* **2018**, *220*, 289–292, doi:10.1016/j.matlet.2018.03.052.
303. Qu, Y.; Tang, J.; Liu, L.; Song, L.; Chen, S.; Gao, Y.  $\alpha$ -Tocopherol Liposome Loaded Chitosan Hydrogel to Suppress Oxidative Stress Injury in Cardiomyocytes. *International Journal of Biological Macromolecules* **2019**, *125*, 1192–1202, doi:10.1016/j.ijbiomac.2018.09.092.
304. Yang, S.; Zhu, B.; Yin, P.; Zhao, L.; Wang, Y.; Fu, Z.; Dang, R.; Xu, J.; Zhang, J.; Wen, N. Integration of Human Umbilical Cord Mesenchymal Stem Cells-Derived Exosomes with Hydroxyapatite-Embedded Hyaluronic Acid-Alginate Hydrogel for Bone Regeneration. *ACS Biomater. Sci. Eng.* **2020**, *6*, 1590–1602, doi:10.1021/acsbiomaterials.9b01363.
305. Chen, C.W.; Wang, L.L.; Zaman, S.; Gordon, J.; Arisi, M.F.; Venkataraman, C.M.; Chung, J.J.; Hung, G.; Gaffey, A.C.; Spruce, L.A.; et al. Sustained Release of Endothelial Progenitor Cell-Derived Extracellular Vesicles from Shear-Thinning Hydrogels Improves Angiogenesis and Promotes Function after Myocardial Infarction. *Cardiovascular Research* **2018**, *114*, 1029–1040, doi:10.1093/cvr/cvy067.

306. Han, C.; Zhou, J.; Liu, B.; Liang, C.; Pan, X.; Zhang, Y.; Zhang, Y.; Wang, Y.; Shao, L.; Zhu, B.; et al. Delivery of MiR-675 by Stem Cell-Derived Exosomes Encapsulated in Silk Fibrin Hydrogel Prevents Aging-Induced Vascular Dysfunction in Mouse Hindlimb. *Materials Science and Engineering: C* **2019**, *99*, 322–332, doi:10.1016/j.msec.2019.01.122.
307. Lv, K.; Li, Q.; Zhang, L.; Wang, Y.; Zhong, Z.; Zhao, J.; Lin, X.; Wang, J.; Zhu, K.; Xiao, C.; et al. Incorporation of Small Extracellular Vesicles in Sodium Alginate Hydrogel as a Novel Therapeutic Strategy for Myocardial Infarction. *Theranostics* **2019**, *9*, 7403–7416, doi:10.7150/thno.32637.
308. Tao, S.-C.; Guo, S.-C.; Li, M.; Ke, Q.-F.; Guo, Y.-P.; Zhang, C.-Q. Chitosan Wound Dressings Incorporating Exosomes Derived from MicroRNA-126-Overexpressing Synovium Mesenchymal Stem Cells Provide Sustained Release of Exosomes and Heal Full-Thickness Skin Defects in a Diabetic Rat Model. *Stem Cells Transl Med* **2017**, *6*, 736–747, doi:10.5966/sctm.2016-0275.
309. Shi, Q.; Qian, Z.; Liu, D.; Sun, J.; Wang, X.; Liu, H.; Xu, J.; Guo, X. GMSC-Derived Exosomes Combined with a Chitosan/Silk Hydrogel Sponge Accelerates Wound Healing in a Diabetic Rat Skin Defect Model. *Front Physiol* **2017**, *8*, 904, doi:10.3389/fphys.2017.00904.
310. Van Den Bulcke, A.I.; Bogdanov, B.; De Rooze, N.; Schacht, E.H.; Cornelissen, M.; Berghmans, H. Structural and Rheological Properties of Methacrylamide Modified Gelatin Hydrogels. *Biomacromolecules* **2000**, *1*, 31–38, doi:10.1021/bm990017d.
311. Kean, T.; Thanou, M. Biodegradation, Biodistribution and Toxicity of Chitosan. *Advanced Drug Delivery Reviews* **2010**, *62*, 3–11, doi:10.1016/j.addr.2009.09.004.
312. Li, R.; Lin, Z.; Zhang, Q.; Zhang, Y.; Liu, Y.; Lyu, Y.; Li, X.; Zhou, C.; Wu, G.; Ao, N.; et al. Injectable and *In Situ* -Formable Thiolated Chitosan-Coated Liposomal Hydrogels as Curcumin Carriers for Prevention of *In Vivo* Breast Cancer Recurrence. *ACS Appl. Mater. Interfaces* **2020**, *12*, 17936–17948, doi:10.1021/acsami.9b21528.
313. Wang, S.-S.; Yang, M.-C.; Chung, T.-W. Liposomes/Chitosan Scaffold/Human Fibrin Gel Composite Systems for Delivering Hydrophilic Drugs—Release Behaviors of Tirofiban *In Vitro*. *Drug Delivery* **2008**, *15*, 149–157, doi:10.1080/10717540801952456.
314. Spicer, P.P.; Mikos, A.G. Fibrin Glue as a Drug Delivery System. *Journal of Controlled Release* **2010**, *148*, 49–55, doi:10.1016/j.jconrel.2010.06.025.
315. Mufamadi, M.S.; Pillay, V.; Choonara, Y.E.; Du Toit, L.C.; Modi, G.; Naidoo, D.; Ndesendo, V.M.K. A Review on Composite Liposomal Technologies for Specialized Drug Delivery. *Journal of Drug Delivery* **2011**, *2011*, 1–19, doi:10.1155/2011/939851.
316. Monshipouri, M.; Rudolph, A.S. Liposome-Encapsulated Alginate: Controlled Hydrogel Particle Formation and Release. *Journal of Microencapsulation* **1995**, *12*, 117–127, doi:10.3109/02652049509015282.
317. Dhoot, N.O.; Wheatley, M.A. Microencapsulated Liposomes in Controlled Drug Delivery: Strategies to Modulate Drug Release and Eliminate the Burst Effect. *Journal of Pharmaceutical Sciences* **2003**, *92*, 679–689, doi:10.1002/jps.19104.
318. Erol, O.; Pantula, A.; Liu, W.; Gracias, D.H. Transformer Hydrogels: A Review. *Adv. Mater. Technol.* **2019**, *4*, 1900043, doi:10.1002/admt.201900043.
319. White, E.M.; Yatvin, J.; Grubbs, J.B.; Bilbrey, J.A.; Locklin, J. Advances in Smart Materials: Stimuli-Responsive Hydrogel Thin Films. *J. Polym. Sci. Part B: Polym. Phys.* **2013**, *51*, 1084–1099, doi:10.1002/polb.23312.
320. Morishita, M.; Goto, T.; Nakamura, K.; Lowman, A.M.; Takayama, K.; Peppas, N.A. Novel Oral Insulin Delivery Systems Based on Complexation Polymer Hydrogels: Single and Multiple Administration Studies in Type 1 and 2 Diabetic Rats. *Journal of Controlled Release* **2006**, *110*, 587–594, doi:10.1016/j.jconrel.2005.10.029.
321. Gutowska, A.; Seok Bark, J.; Chan Kwon, I.; Han Bae, Y.; Cha, Y.; Wan Kim, S. Squeezing Hydrogels for Controlled Oral Drug Delivery. *Journal of Controlled Release* **1997**, *48*, 141–148, doi:10.1016/S0168-3659(97)00041-2.

322. Sharpe, L.A.; Daily, A.M.; Horava, S.D.; Peppas, N.A. Therapeutic Applications of Hydrogels in Oral Drug Delivery. *Expert Opinion on Drug Delivery* **2014**, *11*, 901–915, doi:10.1517/17425247.2014.902047.
323. Ghasemiyeh, P.; Mohammadi-Samani, S. Hydrogels as Drug Delivery Systems; Pros and Cons. *Trends in Pharmaceutical Sciences* **2019**, *5*, doi:10.30476/tips.2019.81604.1002.
324. Illum, L. Nasal Drug Delivery—Possibilities, Problems and Solutions. *Journal of Controlled Release* **2003**, *87*, 187–198, doi:10.1016/S0168-3659(02)00363-2.
325. Wu, J.; Wei, W.; Wang, L.-Y.; Su, Z.-G.; Ma, G.-H. A Thermosensitive Hydrogel Based on Quaternized Chitosan and Poly(Ethylene Glycol) for Nasal Drug Delivery System. *Biomaterials* **2007**, *28*, 2220–2232, doi:10.1016/j.biomaterials.2006.12.024.
326. Gaudana, R.; Ananthula, H.K.; Parenky, A.; Mitra, A.K. Ocular Drug Delivery. *AAPS J* **2010**, *12*, 348–360, doi:10.1208/s12248-010-9183-3.
327. Gulsen, D.; Chauhan, A. Dispersion of Microemulsion Drops in HEMA Hydrogel: A Potential Ophthalmic Drug Delivery Vehicle. *International Journal of Pharmaceutics* **2005**, *292*, 95–117, doi:10.1016/j.ijpharm.2004.11.033.
328. Kang Derwent, J.J.; Mieler, W.F. Thermoresponsive Hydrogels as a New Ocular Drug Delivery Platform to the Posterior Segment of the Eye. *Trans Am Ophthalmol Soc* **2008**, *106*, 206–213; discussion 213-214.
329. Liu, W.; Griffith, M.; Li, F. Alginate Microsphere-Collagen Composite Hydrogel for Ocular Drug Delivery and Implantation. *J Mater Sci: Mater Med* **2008**, *19*, 3365–3371, doi:10.1007/s10856-008-3486-2.
330. Prausnitz, M.R.; Langer, R. Transdermal Drug Delivery. *Nat Biotechnol* **2008**, *26*, 1261–1268, doi:10.1038/nbt.1504.
331. Calixto, G.; Yoshii, A.C.; Rocha e Silva, H.; Stringhetti Ferreira Cury, B.; Chorilli, M. Polyacrylic Acid Polymers Hydrogels Intended to Topical Drug Delivery: Preparation and Characterization. *Pharmaceutical Development and Technology* **2015**, *20*, 490–496, doi:10.3109/10837450.2014.882941.
332. Reimer, K.; Vogt, P.M.; Broegmann, B.; Hauser, J.; Rossbach, O.; Kramer, A.; Rudolph, P.; Bosse, B.; Schreier, H.; Fleischer, W. An Innovative Topical Drug Formulation for Wound Healing and Infection Treatment: In Vitro and in Vivo Investigations of a Povidone-Iodine Liposome Hydrogel. *Dermatology* **2000**, *201*, 235–241, doi:10.1159/000018494.
333. Kreuter, J. Nanoparticulate Systems for Brain Delivery of Drugs. *Advanced Drug Delivery Reviews* **2001**, *47*, 65–81, doi:10.1016/S0169-409X(00)00122-8.
334. Wang, Y.; Cooke, M.J.; Morshead, C.M.; Shoichet, M.S. Hydrogel Delivery of Erythropoietin to the Brain for Endogenous Stem Cell Stimulation after Stroke Injury. *Biomaterials* **2012**, *33*, 2681–2692, doi:10.1016/j.biomaterials.2011.12.031.
335. Anselmo, A.C.; Mitragotri, S. Nanoparticles in the Clinic: Nanoparticles in the Clinic. *Bioengineering & Translational Medicine* **2016**, *1*, 10–29, doi:10.1002/btm2.10003.
336. Anselmo, A.C.; Mitragotri, S. Nanoparticles in the Clinic: An Update. *Bioeng Transl Med* **2019**, *4*, doi:10.1002/btm2.10143.
337. Mandal, A.; Clegg, J.R.; Anselmo, A.C.; Mitragotri, S. Hydrogels in the Clinic. *Bioeng Transl Med* **2020**, *5*.
338. Ingber, D.E. Is It Time for Reviewer 3 to Request Human Organ Chip Experiments Instead of Animal Validation Studies? *Adv. Sci.* **2020**, 2002030, doi:10.1002/advs.202002030.
339. Walus, K.; Beyer, S.; Willerth, S.M. Three-Dimensional Bioprinting Healthy and Diseased Models of the Brain Tissue Using Stem Cells. *Current Opinion in Biomedical Engineering* **2020**, *14*, 25–33, doi:10.1016/j.cobme.2020.03.002.
340. Barros, A.S.; Costa, A.; Sarmiento, B. Building Three-Dimensional Lung Models for Studying Pharmacokinetics of Inhaled Drugs. *Advanced Drug Delivery Reviews* **2020**, S0169409X20301320, doi:10.1016/j.addr.2020.09.008.
341. Harris, J.P.; Burrell, J.C.; Struzyna, L.A.; Chen, H.I.; Serruya, M.D.; Wolf, J.A.; Duda, J.E.; Cullen, D.K. Emerging Regenerative Medicine and Tissue Engineering Strategies for Parkinson's Disease. *npj Parkinsons Dis.* **2020**, *6*, 4, doi:10.1038/s41531-019-0105-5.

342. Khademhosseini, A.; Langer, R. A Decade of Progress in Tissue Engineering. *Nat Protoc* **2016**, *11*, 1775–1781, doi:10.1038/nprot.2016.123.
343. Armstrong, J.P.K.; Stevens, M.M. Emerging Technologies for Tissue Engineering: From Gene Editing to Personalized Medicine. *Tissue Engineering Part A* **2019**, *25*, 688–692, doi:10.1089/ten.tea.2019.0026.
344. Ghosh, S.; Burks, A.C.; Akulian, J.A. Customizable Airway Stents-Personalized Medicine Reaches the Airways. *J Thorac Dis* **2019**, *11*, S1129–S1131, doi:10.21037/jtd.2019.03.100.
345. Hoffman, T.; Khademhosseini, A.; Langer, R. Chasing the Paradigm: Clinical Translation of 25 Years of Tissue Engineering. *Tissue Engineering Part A* **2019**, *25*, 679–687, doi:10.1089/ten.tea.2019.0032.
346. Da Silva, K.; Kumar, P.; Choonara, Y.E.; du Toit, L.C.; Pillay, V. Three-dimensional Printing of Extracellular Matrix (ECM)-mimicking Scaffolds: A Critical Review of the Current ECM Materials. *J Biomed Mater Res* **2020**, *108*, 2324–2350, doi:10.1002/jbm.a.36981.
347. Castilho, M.; de Ruijter, M.; Beirne, S.; Villette, C.C.; Ito, K.; Wallace, G.G.; Malda, J. Multitechnology Biofabrication: A New Approach for the Manufacturing of Functional Tissue Structures? *Trends in Biotechnology* **2020**, S0167779920301190, doi:10.1016/j.tibtech.2020.04.014.
348. Bonani, W.; Cagol, N.; Maniglio, D. Alginate Hydrogels: A Tool for 3D Cell Encapsulation, Tissue Engineering, and Biofabrication. In *Biomimicked Biomaterials*; Chun, H.J., Reis, R.L., Motta, A., Khang, G., Eds.; Advances in Experimental Medicine and Biology; Springer Singapore: Singapore, 2020; Vol. 1250, pp. 49–61 ISBN 9789811532610.
349. Kumar, H.; Sakthivel, K.; Mohamed, M.G.A.; Boras, E.; Shin, S.R.; Kim, K. Designing Gelatin Methacryloyl (GelMA)-Based Biinks for Visible Light Stereolithographic 3D Biofabrication. *Macromol. Biosci.* **2020**, 2000317, doi:10.1002/mabi.202000317.
350. Fallahi, A.; Yazdi, I.K.; Serex, L.; Lasha, E.; Faramarzi, N.; Tarlan, F.; Avci, H.; Costa-Almeida, R.; Sharifi, F.; Rinoldi, C.; et al. Customizable Composite Fibers for Engineering Skeletal Muscle Models. *ACS Biomater. Sci. Eng.* **2020**, *6*, 1112–1123, doi:10.1021/acsbiomaterials.9b00992.
351. Fallahi, A.; Khademhosseini, A.; Tamayol, A. Textile Processes for Engineering Tissues with Biomimetic Architectures and Properties. *Trends in Biotechnology* **2016**, *34*, 683–685, doi:10.1016/j.tibtech.2016.07.001.
352. Ahadian, S.; Khademhosseini, A. Smart Scaffolds in Tissue Regeneration. *Regenerative Biomaterials* **2018**, *5*, 125–128, doi:10.1093/rb/rby007.
353. Annabi, N.; Nichol, J.W.; Zhong, X.; Ji, C.; Koshy, S.; Khademhosseini, A.; Dehghani, F. Controlling the Porosity and Microarchitecture of Hydrogels for Tissue Engineering. *Tissue Eng Part B Rev* **2010**, *16*, 371–383, doi:10.1089/ten.teb.2009.0639.
354. Gerecht, S.; Townsend, S.A.; Pressler, H.; Zhu, H.; Nijst, C.L.E.; Bruggeman, J.P.; Nichol, J.W.; Langer, R. A Porous Photocurable Elastomer for Cell Encapsulation and Culture. *Biomaterials* **2007**, *28*, 4826–4835, doi:10.1016/j.biomaterials.2007.07.039.
355. Lien, S.-M.; Ko, L.-Y.; Huang, T.-J. Effect of Pore Size on ECM Secretion and Cell Growth in Gelatin Scaffold for Articular Cartilage Tissue Engineering. *Acta Biomaterialia* **2009**, *5*, 670–679, doi:10.1016/j.actbio.2008.09.020.
356. Mandal, B.B.; Kundu, S.C. Cell Proliferation and Migration in Silk Fibroin 3D Scaffolds. *Biomaterials* **2009**, *30*, 2956–2965, doi:10.1016/j.biomaterials.2009.02.006.
357. Akbari, M.; Tamayol, A.; Bagherifard, S.; Serex, L.; Mostafalu, P.; Faramarzi, N.; Mohammadi, M.H.; Khademhosseini, A. Textile Technologies and Tissue Engineering: A Path Toward Organ Weaving. *Advanced Healthcare Materials* **2016**, *5*, 751–766, doi:10.1002/adhm.201500517.
358. Walsh, T.; Karperien, L.; Dabiri, S.M.H.; Akbari, M. Fiber-Based Microphysiological Systems: A Powerful Tool for High Throughput Drug Screening. *Microphysiol Syst* **2019**, *3*, 3–3, doi:10.21037/mps.2019.08.01.

359. Chatterjee, K.; Ghosh, T.K. 3D Printing of Textiles: Potential Roadmap to Printing with Fibers. *Adv. Mater.* **2020**, *32*, 1902086, doi:10.1002/adma.201902086.
360. Kolesky, D.B.; Homan, K.A.; Skylar-Scott, M.A.; Lewis, J.A. Three-Dimensional Bioprinting of Thick Vascularized Tissues. *Proc Natl Acad Sci U S A* **2016**, *113*, 3179–3184, doi:10.1073/pnas.1521342113.
361. Spearman, B.S.; Agrawal, N.K.; Rubiano, A.; Simmons, C.S.; Mobini, S.; Schmidt, C.E. Tunable Methacrylated Hyaluronic Acid-based Hydrogels as Scaffolds for Soft Tissue Engineering Applications. *J Biomed Mater Res* **2020**, *108*, 279–291, doi:10.1002/jbm.a.36814.
362. Aubin, H.; Nichol, J.W.; Hutson, C.B.; Bae, H.; Sieminski, A.L.; Cropek, D.M.; Akhyari, P.; Khademhosseini, A. Directed 3D Cell Alignment and Elongation in Microengineered Hydrogels. *Biomaterials* **2010**, *31*, 6941–6951, doi:10.1016/j.biomaterials.2010.05.056.
363. Noshadi, I.; Hong, S.; Sullivan, K.E.; Shirzaei Sani, E.; Portillo-Lara, R.; Tamayol, A.; Shin, S.R.; Gao, A.E.; Stoppel, W.L.; Black III, L.D.; et al. In Vitro and in Vivo Analysis of Visible Light Crosslinkable Gelatin Methacryloyl (GelMA) Hydrogels. *Biomaterials Science* **2017**, *5*, 2093–2105, doi:10.1039/C7BM00110J.
364. Yue, K.; Liu, Y.; Byambaa, B.; Singh, V.; Liu, W.; Li, X.; Sun, Y.; Zhang, Y.S.; Tamayol, A.; Zhang, P.; et al. Visible Light Crosslinkable Human Hair Keratin Hydrogels: YUE et al. *Bioengineering & Translational Medicine* **2018**, *3*, 37–48, doi:10.1002/btm2.10077.
365. Xie, R.; Zheng, W.; Guan, L.; Ai, Y.; Liang, Q. Engineering of Hydrogel Materials with Perfusable Microchannels for Building Vascularized Tissues. *Small* **2020**, *16*, 1902838, doi:10.1002/sml.201902838.
366. He, J.; Mao, M.; Liu, Y.; Shao, J.; Jin, Z.; Li, D. Fabrication of Nature-Inspired Microfluidic Network for Perfusable Tissue Constructs. *Advanced Healthcare Materials* **2013**, *2*, 1108–1113, doi:10.1002/adhm.201200404.
367. Rinoldi, C.; Fallahi, A.; Yazdi, I.K.; Campos Paras, J.; Kijeńska-Gawrońska, E.; Trujillo-de Santiago, G.; Tuoheti, A.; Demarchi, D.; Annabi, N.; Khademhosseini, A.; et al. Mechanical and Biochemical Stimulation of 3D Multilayered Scaffolds for Tendon Tissue Engineering. *ACS Biomater. Sci. Eng.* **2019**, *5*, 2953–2964, doi:10.1021/acsbomaterials.8b01647.
368. Alimohammadi, M.; Aghli, Y.; Fakhraei, O.; Moradi, A.; Passandideh-Fard, M.; Ebrahimzadeh, M.H.; Khademhosseini, A.; Tamayol, A.; Mousavi Shaegh, S.A. Electrospun Nanofibrous Membranes for Preventing Tendon Adhesion. *ACS Biomater. Sci. Eng.* **2020**, *6*, 4356–4376, doi:10.1021/acsbomaterials.0c00201.
369. Tamayol, A.; Akbari, M.; Annabi, N.; Paul, A.; Khademhosseini, A.; Juncker, D. Fiber-Based Tissue Engineering: Progress, Challenges, and Opportunities. *Biotechnology Advances* **2013**, *31*, 669–687, doi:10.1016/j.biotechadv.2012.11.007.
370. Zhang, K.; Liimatainen, H. Hierarchical Assembly of Nanocellulose-Based Filaments by Interfacial Complexation. *Small* **2018**, *14*, 1801937, doi:10.1002/sml.201801937.
371. Wan, A.C.A.; Liao, I.-C.; Yim, E.K.F.; Leong, K.W. Mechanism of Fiber Formation by Interfacial Polyelectrolyte Complexation. *Macromolecules* **2004**, *37*, 7019–7025, doi:10.1021/ma0498868.
372. Wan, A.C.A.; Yim, E.K.F.; Liao, I.-C.; Le Visage, C.; Leong, K.W. Encapsulation of Biologics in Self-Assembled Fibers as Biostructural Units for Tissue Engineering. *Journal of Biomedical Materials Research* **2004**, *71A*, 586–595, doi:10.1002/jbm.a.30158.
373. Leong, M.F.; Toh, J.K.C.; Du, C.; Narayanan, K.; Lu, H.F.; Lim, T.C.; Wan, A.C.A.; Ying, J.Y. Patterned Prevascularised Tissue Constructs by Assembly of Polyelectrolyte Hydrogel Fibres. *Nat Commun* **2013**, *4*, 2353, doi:10.1038/ncomms3353.
374. Levenberg, S.; Rouwkema, J.; Macdonald, M.; Garfein, E.S.; Kohane, D.S.; Darland, D.C.; Marini, R.; van Blitterswijk, C.A.; Mulligan, R.C.; D'Amore, P.A.; et al. Engineering Vascularized Skeletal Muscle Tissue. *Nature Biotechnology* **2005**, *23*, 879–884, doi:10.1038/nbt1109.
375. Asakawa, N.; Shimizu, T.; Tsuda, Y.; Sekiya, S.; Sasagawa, T.; Yamato, M.; Fukai, F.; Okano, T. Pre-Vascularization of in Vitro Three-Dimensional Tissues Created by Cell

- Sheet Engineering. *Biomaterials* **2010**, *31*, 3903–3909, doi:10.1016/j.biomaterials.2010.01.105.
376. Alajati, A.; Laib, A.M.; Weber, H.; Boos, A.M.; Bartol, A.; Ikenberg, K.; Korff, T.; Zentgraf, H.; Obodozie, C.; Graeser, R.; et al. Spheroid-Based Engineering of a Human Vasculature in Mice. *Nature Methods* **2008**, *5*, 439–445, doi:10.1038/nmeth.1198.
377. Katoh, K.; Shibayama, M.; Tanabe, T.; Yamauchi, K. Preparation and Properties of Keratin-Poly(Vinyl Alcohol) Blend Fiber. *Journal of Applied Polymer Science* **2004**, *91*, 756–762, doi:10.1002/app.13236.
378. Mirani, B.; Pagan, E.; Shojaei, S.; Dabiri, S.M.H.; Savoji, H.; Mehrali, M.; Sam, M.; Alsaif, J.; Bhiladvala, R.B.; Dolatshahi-Pirouz, A.; et al. Facile Method for Fabrication of Meter-Long Multifunctional Hydrogel Fibers with Controllable Biophysical and Biochemical Features. *ACS Appl. Mater. Interfaces* **2020**, *12*, 9080–9089, doi:10.1021/acsami.9b23063.
379. Yang, Y.; Sun, J.; Liu, X.; Guo, Z.; He, Y.; Wei, D.; Zhong, M.; Guo, L.; Fan, H.; Zhang, X. Wet-Spinning Fabrication of Shear-Patterned Alginate Hydrogel Microfibers and the Guidance of Cell Alignment. *Regenerative Biomaterials* **2017**, *4*, 299–307, doi:10.1093/rb/rbx017.
380. Yao, K.; Li, W.; Li, K.; Wu, Q.; Gu, Y.; Zhao, L.; Zhang, Y.; Gao, X. Simple Fabrication of Multicomponent Heterogeneous Fibers for Cell Co-Culture via Microfluidic Spinning. *Macromol. Biosci.* **2020**, *20*, 1900395, doi:10.1002/mabi.201900395.
381. Wang, X.; Liu, J.; Wang, P.; deMello, A.; Feng, L.; Zhu, X.; Wen, W.; Kodzius, R.; Gong, X. Synthesis of Biomaterials Utilizing Microfluidic Technology. *Genes* **2018**, *9*, 283, doi:10.3390/genes9060283.
382. Cheng, J.; Jun, Y.; Qin, J.; Lee, S.-H. Electrospinning versus Microfluidic Spinning of Functional Fibers for Biomedical Applications. *Biomaterials* **2017**, *114*, 121–143, doi:10.1016/j.biomaterials.2016.10.040.
383. Zuo, Y.; He, X.; Yang, Y.; Wei, D.; Sun, J.; Zhong, M.; Xie, R.; Fan, H.; Zhang, X. Microfluidic-Based Generation of Functional Microfibers for Biomimetic Complex Tissue Construction. *Acta Biomaterialia* **2016**, *38*, 153–162, doi:10.1016/j.actbio.2016.04.036.
384. Akbari, M.; Tamayol, A.; Laforte, V.; Annabi, N.; Najafabadi, A.H.; Khademhosseini, A.; Juncker, D. Composite Living Fibers for Creating Tissue Constructs Using Textile Techniques. *Adv. Funct. Mater.* **2014**, *24*, 4060–4067, doi:10.1002/adfm.201303655.
385. Onoe, H.; Okitsu, T.; Itou, A.; Kato-Negishi, M.; Gojo, R.; Kiriya, D.; Sato, K.; Miura, S.; Iwanaga, S.; Kuribayashi-Shigetomi, K.; et al. Metre-Long Cell-Laden Microfibres Exhibit Tissue Morphologies and Functions. *Nature Materials* **2013**, *12*, 584–590, doi:10.1038/nmat3606.
386. Peppas, N.A.; Khademhosseini, A. Make Better, Safer Biomaterials. *Nature* **2016**, *540*, 335–337, doi:10.1038/540335a.
387. Farzin, A.; Miri, A.K.; Sharifi, F.; Faramarzi, N.; Jaber, A.; Mostafavi, A.; Solorzano, R.; Zhang, Y.S.; Annabi, N.; Khademhosseini, A.; et al. 3D-Printed Sugar-Based Stents Facilitating Vascular Anastomosis. *Adv. Healthcare Mater.* **2018**, *7*, 1800702, doi:10.1002/adhm.201800702.
388. Derakhshandeh, H.; Aghabaglou, F.; McCarthy, A.; Mostafavi, A.; Wiseman, C.; Bonick, Z.; Ghanavati, I.; Harris, S.; Kreikemeier-Bower, C.; Moosavi Basri, S.M.; et al. A Wirelessly Controlled Smart Bandage with 3D-Printed Miniaturized Needle Arrays. *Adv. Funct. Mater.* **2020**, *30*, 1905544, doi:10.1002/adfm.201905544.
389. Murphy, S.V.; Atala, A. 3D Bioprinting of Tissues and Organs. *Nature Biotechnology* **2014**, *32*, 773–785, doi:10.1038/nbt.2958.
390. Zheng, Z.; Eglin, D.; Alini, M.; Richards, G.R.; Qin, L.; Lai, Y. Visible Light-Induced 3D Bioprinting Technologies and Corresponding Bioink Materials for Tissue Engineering: A Review. *Engineering* **2020**, S2095809920302496, doi:10.1016/j.eng.2020.05.021.
391. Bedell, M.L.; Navara, A.M.; Du, Y.; Zhang, S.; Mikos, A.G. Polymeric Systems for Bioprinting. *Chem. Rev.* **2020**, *120*, 10744–10792, doi:10.1021/acs.chemrev.9b00834.

392. Unagolla, J.M.; Jayasuriya, A.C. Hydrogel-Based 3D Bioprinting: A Comprehensive Review on Cell-Laden Hydrogels, Bioink Formulations, and Future Perspectives. *Applied Materials Today* **2020**, *18*, 100479, doi:10.1016/j.apmt.2019.100479.
393. Ashammakhi, N.; Hasan, A.; Kaarela, O.; Byambaa, B.; Sheikhi, A.; Gaharwar, A.K.; Khademhosseini, A. Advancing Frontiers in Bone Bioprinting. *Adv. Healthcare Mater.* **2019**, *8*, 1801048, doi:10.1002/adhm.201801048.
394. Duarte Campos, D.F.; Blaeser, A.; Buellbach, K.; Sen, K.S.; Xun, W.; Tillmann, W.; Fischer, H. Bioprinting Organotypic Hydrogels with Improved Mesenchymal Stem Cell Remodeling and Mineralization Properties for Bone Tissue Engineering. *Adv. Healthcare Mater.* **2016**, *5*, 1336–1345, doi:10.1002/adhm.201501033.
395. Gao, G.; Yonezawa, T.; Hubbell, K.; Dai, G.; Cui, X. Inkjet-Bioprinted Acrylated Peptides and PEG Hydrogel with Human Mesenchymal Stem Cells Promote Robust Bone and Cartilage Formation with Minimal Printhead Clogging. *Biotechnology Journal* **2015**, *10*, 1568–1577, doi:10.1002/biot.201400635.
396. Cui, X.; Gao, G.; Yonezawa, T.; Dai, G. Human Cartilage Tissue Fabrication Using Three-Dimensional Inkjet Printing Technology. *JoVE* **2014**, 51294, doi:10.3791/51294.
397. Tse, C.; Whiteley, R.; Yu, T.; Stringer, J.; MacNeil, S.; Haycock, J.W.; Smith, P.J. Inkjet Printing Schwann Cells and Neuronal Analogue NG108-15 Cells. *Biofabrication* **2016**, *8*, 015017, doi:10.1088/1758-5090/8/1/015017.
398. Xu, T.; Baicu, C.; Aho, M.; Zile, M.; Boland, T. Fabrication and Characterization of Bio-Engineered Cardiac Pseudo Tissues. *Biofabrication* **2009**, *1*, 035001, doi:10.1088/1758-5082/1/3/035001.
399. Binder, K.W.; Zhao, W.; Aboushwareb, T.; Dice, D.; Atala, A.; Yoo, J.J. In Situ Bioprinting of the Skin for Burns. *Journal of the American College of Surgeons* **2010**, *211*, S76, doi:10.1016/j.jamcollsurg.2010.06.198.
400. Gao, G.; Schilling, A.F.; Hubbell, K.; Yonezawa, T.; Truong, D.; Hong, Y.; Dai, G.; Cui, X. Improved Properties of Bone and Cartilage Tissue from 3D Inkjet-Bioprinted Human Mesenchymal Stem Cells by Simultaneous Deposition and Photocrosslinking in PEG-GelMA. *Biotechnology Letters* **2015**, *37*, 2349–2355, doi:10.1007/s10529-015-1921-2.
401. Teo, M.Y.; Kee, S.; RaviChandran, N.; Stuart, L.; Aw, K.C.; Stringer, J. Enabling Free-Standing 3D Hydrogel Microstructures with Microreactive Inkjet Printing. *ACS Appl. Mater. Interfaces* **2020**, *12*, 1832–1839, doi:10.1021/acsami.9b17192.
402. Lee, A.; Hudson, A.R.; Shiwerski, D.J.; Tashman, J.W.; Hinton, T.J.; Yerneni, S.; Bliley, J.M.; Campbell, P.G.; Feinberg, A.W. 3D Bioprinting of Collagen to Rebuild Components of the Human Heart. *Science* **2019**, *365*, 482–487, doi:10.1126/science.aav9051.
403. Colina, M.; Serra, P.; Fernández-Pradas, J.M.; Sevilla, L.; Morenza, J.L. DNA Deposition through Laser Induced Forward Transfer. *Biosensors and Bioelectronics* **2005**, *20*, 1638–1642, doi:10.1016/j.bios.2004.08.047.
404. Dinca, V.; Kasotakis, E.; Catherine, J.; Mourka, A.; Ranella, A.; Ovsianikov, A.; Chichkov, B.N.; Farsari, M.; Mitraki, A.; Fotakis, C. Directed Three-Dimensional Patterning of Self-Assembled Peptide Fibrils. *Nano Letters* **2008**, *8*, 538–543, doi:10.1021/nl072798r.
405. Ringeisen, B.R.; Kim, H.; Barron, J.A.; Krizman, D.B.; Chrisey, D.B.; Jackman, S.; Auyeung, R.Y.C.; Spargo, B.J. Laser Printing of Pluripotent Embryonal Carcinoma Cells. *Tissue Engineering* **2004**, *10*, 483–491, doi:10.1089/107632704323061843.
406. Chrisey, D.B. MATERIALS PROCESSING: The Power of Direct Writing. *Science* **2000**, *289*, 879–881, doi:10.1126/science.289.5481.879.
407. Hakobyan, D.; Kerouredan, O.; Remy, M.; Dusserre, N.; Medina, C.; Devillard, R.; Fricain, J.-C.; Oliveira, H. Laser-Assisted Bioprinting for Bone Repair. In *3D Bioprinting*; Crook, J.M., Ed.; Methods in Molecular Biology; Springer US: New York, NY, 2020; Vol. 2140, pp. 135–144 ISBN 978-1-07-160519-6.
408. Koch, L.; Kuhn, S.; Sorg, H.; Gruene, M.; Schlie, S.; Gaebel, R.; Polchow, B.; Reimers, K.; Stoelting, S.; Ma, N.; et al. Laser Printing of Skin Cells and Human Stem Cells. *Tissue Engineering Part C: Methods* **2010**, *16*, 847–854, doi:10.1089/ten.tec.2009.0397.

409. Koch, L.; Deiwick, A.; Schlie, S.; Michael, S.; Gruene, M.; Coger, V.; Zychlinski, D.; Schambach, A.; Reimers, K.; Vogt, P.M.; et al. Skin Tissue Generation by Laser Cell Printing. *Biotechnology and Bioengineering* **2012**, *109*, 1855–1863, doi:10.1002/bit.24455.
410. Michael, S.; Sorg, H.; Peck, C.-T.; Koch, L.; Deiwick, A.; Chichkov, B.; Vogt, P.M.; Reimers, K. Tissue Engineered Skin Substitutes Created by Laser-Assisted Bioprinting Form Skin-Like Structures in the Dorsal Skin Fold Chamber in Mice. *PLoS ONE* **2013**, *8*, e57741, doi:10.1371/journal.pone.0057741.
411. Gruene, M.; Unger, C.; Koch, L.; Deiwick, A.; Chichkov, B. Dispensing Pico to Nanolitre of a Natural Hydrogel by Laser-Assisted Bioprinting. *BioMedical Engineering OnLine* **2011**, *10*, 19, doi:10.1186/1475-925X-10-19.
412. Dolatshahi-Pirouz, A.; Nikkhah, M.; Gaharwar, A.K.; Hashmi, B.; Guermani, E.; Aliabadi, H.; Camci-Unal, G.; Ferrante, T.; Foss, M.; Ingber, D.E.; et al. A Combinatorial Cell-Laden Gel Microarray for Inducing Osteogenic Differentiation of Human Mesenchymal Stem Cells. *Sci Rep* **2015**, *4*, 3896, doi:10.1038/srep03896.
413. Xu, N.; Ye, X.; Wei, D.; Zhong, J.; Chen, Y.; Xu, G.; He, D. 3D Artificial Bones for Bone Repair Prepared by Computed Tomography-Guided Fused Deposition Modeling for Bone Repair. *ACS Applied Materials & Interfaces* **2014**, *6*, 14952–14963, doi:10.1021/am502716t.
414. Kang, H.-W.; Lee, S.J.; Ko, I.K.; Kengla, C.; Yoo, J.J.; Atala, A. A 3D Bioprinting System to Produce Human-Scale Tissue Constructs with Structural Integrity. *Nature Biotechnology* **2016**, *34*, 312–319, doi:10.1038/nbt.3413.
415. Pati, F.; Jang, J.; Ha, D.-H.; Won Kim, S.; Rhie, J.-W.; Shim, J.-H.; Kim, D.-H.; Cho, D.-W. Printing Three-Dimensional Tissue Analogues with Decellularized Extracellular Matrix Bioink. *Nat Commun* **2014**, *5*, 3935, doi:10.1038/ncomms4935.
416. Hsieh, F.-Y.; Hsu, S. 3D Bioprinting: A New Insight into the Therapeutic Strategy of Neural Tissue Regeneration. *Organogenesis* **2015**, *11*, 153–158, doi:10.1080/15476278.2015.1123360.
417. Hsieh, F.-Y.; Lin, H.-H.; Hsu, S. 3D Bioprinting of Neural Stem Cell-Laden Thermoresponsive Biodegradable Polyurethane Hydrogel and Potential in Central Nervous System Repair. *Biomaterials* **2015**, *71*, 48–57, doi:10.1016/j.biomaterials.2015.08.028.
418. Zhang, Y.S.; Arneri, A.; Bersini, S.; Shin, S.-R.; Zhu, K.; Goli-Malekabadi, Z.; Aleman, J.; Colosi, C.; Busignani, F.; Dell’Erba, V.; et al. Bioprinting 3D Microfibrous Scaffolds for Engineering Endothelialized Myocardium and Heart-on-a-Chip. *Biomaterials* **2016**, *110*, 45–59, doi:10.1016/j.biomaterials.2016.09.003.
419. Gaetani, R.; Doevendans, P.A.; Metz, C.H.G.; Alblas, J.; Messina, E.; Giacomello, A.; Sluijter, J.P.G. Cardiac Tissue Engineering Using Tissue Printing Technology and Human Cardiac Progenitor Cells. *Biomaterials* **2012**, *33*, 1782–1790, doi:10.1016/j.biomaterials.2011.11.003.
420. Pourchet, L.J.; Thepot, A.; Albouy, M.; Courtial, E.J.; Boher, A.; Blum, L.J.; Marquette, C.A. Human Skin 3D Bioprinting Using Scaffold-Free Approach. *Advanced Healthcare Materials* **2017**, *6*, 1601101, doi:10.1002/adhm.201601101.
421. Huang, S.; Yao, B.; Xie, J.; Fu, X. 3D Bioprinted Extracellular Matrix Mimics Facilitate Directed Differentiation of Epithelial Progenitors for Sweat Gland Regeneration. *Acta Biomaterialia* **2016**, *32*, 170–177, doi:10.1016/j.actbio.2015.12.039.
422. Chang, R.; Emami, K.; Wu, H.; Sun, W. Biofabrication of a Three-Dimensional Liver Micro-Organ as an *in Vitro* Drug Metabolism Model. *Biofabrication* **2010**, *2*, 045004, doi:10.1088/1758-5082/2/4/045004.
423. Snyder, J.E.; Hamid, Q.; Wang, C.; Chang, R.; Emami, K.; Wu, H.; Sun, W. Bioprinting Cell-Laden Matrigel for Radioprotection Study of Liver by pro-Drug Conversion in a Dual-Tissue Microfluidic Chip. *Biofabrication* **2011**, *3*, 034112, doi:10.1088/1758-5082/3/3/034112.

424. Merceron, T.K.; Burt, M.; Seol, Y.-J.; Kang, H.-W.; Lee, S.J.; Yoo, J.J.; Atala, A. A 3D Bioprinted Complex Structure for Engineering the Muscle–Tendon Unit. *Biofabrication* **2015**, *7*, 035003, doi:10.1088/1758-5090/7/3/035003.
425. Billiet, T.; Gevaert, E.; De Schryver, T.; Cornelissen, M.; Dubruel, P. The 3D Printing of Gelatin Methacrylamide Cell-Laden Tissue-Engineered Constructs with High Cell Viability. *Biomaterials* **2014**, *35*, 49–62, doi:10.1016/j.biomaterials.2013.09.078.
426. Markstedt, K.; Mantas, A.; Tournier, I.; Martínez Ávila, H.; Hägg, D.; Gatenholm, P. 3D Bioprinting Human Chondrocytes with Nanocellulose–Alginate Bioink for Cartilage Tissue Engineering Applications. *Biomacromolecules* **2015**, *16*, 1489–1496, doi:10.1021/acs.biomac.5b00188.
427. Martínez Ávila, H.; Schwarz, S.; Rotter, N.; Gatenholm, P. 3D Bioprinting of Human Chondrocyte-Laden Nanocellulose Hydrogels for Patient-Specific Auricular Cartilage Regeneration. *Bioprinting* **2016**, *1–2*, 22–35, doi:10.1016/j.bprint.2016.08.003.
428. Yang, Q.; Gao, B.; Xu, F. Recent Advances in 4D Bioprinting. *Biotechnol. J.* **2020**, *15*, 1900086, doi:10.1002/biot.201900086.
429. Gao, B.; Yang, Q.; Zhao, X.; Jin, G.; Ma, Y.; Xu, F. 4D Bioprinting for Biomedical Applications. *Trends in Biotechnology* **2016**, *34*, 746–756, doi:10.1016/j.tibtech.2016.03.004.
430. Ong, C.S.; Nam, L.; Ong, K.; Krishnan, A.; Huang, C.Y.; Fukunishi, T.; Hibino, N. 3D and 4D Bioprinting of the Myocardium: Current Approaches, Challenges, and Future Prospects. *BioMed Research International* **2018**, *2018*, 1–11, doi:10.1155/2018/6497242.
431. *3D Bioprinting in Regenerative Engineering: Principles and Applications*; Khademhosseini, A., Camci-Unal, G., Eds.; Taylor & Francis: Boca Raton, 2018; ISBN 978-1-138-19717-6.
432. Kirillova, A.; Maxson, R.; Stoychev, G.; Gomillion, C.T.; Ionov, L. 4D Biofabrication Using Shape-Morphing Hydrogels. *Advanced Materials* **2017**, *29*, 1703443, doi:10.1002/adma.201703443.
433. Mironov, V.; Visconti, R.P.; Kasyanov, V.; Forgacs, G.; Drake, C.J.; Markwald, R.R. Organ Printing: Tissue Spheroids as Building Blocks. *Biomaterials* **2009**, *30*, 2164–2174, doi:10.1016/j.biomaterials.2008.12.084.
434. Miller, J.S.; Stevens, K.R.; Yang, M.T.; Baker, B.M.; Nguyen, D.-H.T.; Cohen, D.M.; Toro, E.; Chen, A.A.; Galie, P.A.; Yu, X.; et al. Rapid Casting of Patterned Vascular Networks for Perfusible Engineered Three-Dimensional Tissues. *Nature Materials* **2012**, *11*, 768–774, doi:10.1038/nmat3357.
435. Blakely, A.M.; Manning, K.L.; Tripathi, A.; Morgan, J.R. Bio-Pick, Place, and Perfuse: A New Instrument for Three-Dimensional Tissue Engineering. *Tissue Engineering Part C: Methods* **2015**, *21*, 737–746, doi:10.1089/ten.tec.2014.0439.
436. Rutz, A.L.; Hyland, K.E.; Jakus, A.E.; Burghardt, W.R.; Shah, R.N. A Multimaterial Bioink Method for 3D Printing Tunable, Cell-Compatible Hydrogels. *Advanced Materials* **2015**, *27*, 1607–1614, doi:10.1002/adma.201405076.
437. Zhu, K.; Shin, S.R.; van Kempen, T.; Li, Y.-C.; Ponraj, V.; Nasajpour, A.; Mandla, S.; Hu, N.; Liu, X.; Leijten, J.; et al. Gold Nanocomposite Bioink for Printing 3D Cardiac Constructs. *Advanced Functional Materials* **2017**, *27*, 1605352, doi:10.1002/adfm.201605352.
438. Yang, J.; Sun, X.; Zhang, Y.; Chen, Y. Chapter 10 - The application of natural polymer-based hydrogels in tissue engineering. In *Hydrogels Based on Natural Polymers*; Chen, Y., Ed.; Elsevier, 2020; pp. 273–307 ISBN 978-0-12-816421-1.
439. Naahidi, S.; Jafari, M.; Logan, M.; Wang, Y.; Yuan, Y.; Bae, H.; Dixon, B.; Chen, P. Biocompatibility of Hydrogel-Based Scaffolds for Tissue Engineering Applications. *Biotechnology Advances* **2017**, *35*, 530–544, doi:10.1016/j.biotechadv.2017.05.006.
440. Mantha, S.; Pillai, S.; Khayambashi, P.; Upadhyay, A.; Zhang, Y.; Tao, O.; Pham, H.M.; Tran, S.D. Smart Hydrogels in Tissue Engineering and Regenerative Medicine. *Materials* **2019**, *12*, 3323, doi:10.3390/ma12203323.

441. Catoira, M.C.; Fusaro, L.; Di Francesco, D.; Ramella, M.; Boccafoschi, F. Overview of Natural Hydrogels for Regenerative Medicine Applications. *J Mater Sci: Mater Med* **2019**, *30*, 115, doi:10.1007/s10856-019-6318-7.
442. Bajaj, P.; Schweller, R.M.; Khademhosseini, A.; West, J.L.; Bashir, R. 3D Biofabrication Strategies for Tissue Engineering and Regenerative Medicine. *Annu Rev Biomed Eng* **2014**, *16*, 247–276, doi:10.1146/annurev-bioeng-071813-105155.
443. Bao, W.; Li, M.; Yang, Y.; Wan, Y.; Wang, X.; Bi, N.; Li, C. Advancements and Frontiers in the High Performance of Natural Hydrogels for Cartilage Tissue Engineering. *Front. Chem.* **2020**, *8*, 53, doi:10.3389/fchem.2020.00053.
444. Sahana, T.G.; Rekha, P.D. Biopolymers: Applications in Wound Healing and Skin Tissue Engineering. *Mol Biol Rep* **2018**, *45*, 2857–2867, doi:10.1007/s11033-018-4296-3.
445. Hunt, J.A.; Chen, R.; Veen, T. van; Bryan, N. Hydrogels for Tissue Engineering and Regenerative Medicine. *J. Mater. Chem. B* **2014**, *2*, 5319–5338, doi:10.1039/C4TB00775A.
446. Nguyen, A.H.; Marsh, P.; Schmiess-Heine, L.; Burke, P.J.; Lee, A.; Lee, J.; Cao, H. Cardiac Tissue Engineering: State-of-the-Art Methods and Outlook. *Journal of Biological Engineering* **2019**, *13*, 57, doi:10.1186/s13036-019-0185-0.
447. Rodrigues, I.C.P.; Kaasi, A.; Maciel Filho, R.; Jardini, A.L.; Gabriel, L.P. Cardiac Tissue Engineering: Current State-of-the-Art Materials, Cells and Tissue Formation. *Einstein (São Paulo)* **2018**, *16*, doi:10.1590/s1679-45082018rb4538.
448. Radisic, M.; Christman, K.L. Materials Science and Tissue Engineering: Repairing the Heart. *Mayo Clin Proc* **2013**, *88*, 884–898, doi:10.1016/j.mayocp.2013.05.003.
449. Feyen, D.A.M.; Gaetani, R.; Doevendans, P.A.; Sluijter, J.P.G. Stem Cell-Based Therapy: Improving Myocardial Cell Delivery. *Advanced Drug Delivery Reviews* **2016**, *106*, 104–115, doi:10.1016/j.addr.2016.04.023.
450. Lee, J.; Manoharan, V.; Cheung, L.; Lee, S.; Cha, B.-H.; Newman, P.; Farzad, R.; Mehrotra, S.; Zhang, K.; Khan, F.; et al. Nanoparticle-Based Hybrid Scaffolds for Deciphering the Role of Multimodal Cues in Cardiac Tissue Engineering. *ACS Nano* **2019**, *13*, 12525–12539, doi:10.1021/acsnano.9b03050.
451. Shin, S.R.; Jung, S.M.; Zalabany, M.; Kim, K.; Zorlutuna, P.; Kim, S. bok; Nikkhah, M.; Khabiry, M.; Azize, M.; Kong, J.; et al. Carbon-Nanotube-Embedded Hydrogel Sheets for Engineering Cardiac Constructs and Bioactuators. *ACS Nano* **2013**, *7*, 2369–2380, doi:10.1021/nn305559j.
452. Zielińska, A.; Costa, B.; Ferreira, M.V.; Miguéis, D.; Louros, J.M.S.; Durazzo, A.; Lucarini, M.; Eder, P.; V. Chaud, M.; Morsink, M.; et al. Nanotoxicology and Nanosafety: Safety-by-Design and Testing at a Glance. *International Journal of Environmental Research and Public Health* **2020**, *17*, 4657, doi:10.3390/ijerph17134657.
453. Koti, P.; Muselimyan, N.; Mirdamadi, E.; Asfour, H.; Sarvazyan, N.A. Use of GelMA for 3D Printing of Cardiac Myocytes and Fibroblasts. *Journal of 3D Printing in Medicine* **2019**, *3*, 11–22, doi:10.2217/3dp-2018-0017.
454. Li, X.-P.; Qu, K.-Y.; Zhang, F.; Jiang, H.-N.; Zhang, N.; Nihad, C.; Liu, C.-M.; Wu, K.-H.; Wang, X.-W.; Huang, N.-P. High-Aspect-Ratio Water-Dispersed Gold Nanowires Incorporated within Gelatin Methacrylate Hydrogels for Constructing Cardiac Tissues in Vitro. *J. Mater. Chem. B* **2020**, *8*, 7213–7224, doi:10.1039/D0TB00768D.
455. Yadid, M.; Feiner, R.; Dvir, T. Gold Nanoparticle-Integrated Scaffolds for Tissue Engineering and Regenerative Medicine. *Nano Lett.* **2019**, *19*, 2198–2206, doi:10.1021/acs.nanolett.9b00472.
456. Baei, P.; Jalili-Firoozinezhad, S.; Rajabi-Zeleti, S.; Tafazzoli-Shadpour, M.; Baharvand, H.; Aghdami, N. Electrically Conductive Gold Nanoparticle-Chitosan Thermosensitive Hydrogels for Cardiac Tissue Engineering. *Materials Science and Engineering: C* **2016**, *63*, 131–141, doi:10.1016/j.msec.2016.02.056.
457. Saravanan, S.; Sareen, N.; Abu-El-Rub, E.; Ashour, H.; Sequiera, G.L.; Ammar, H.I.; Gopinath, V.; Shamaa, A.A.; Sayed, S.S.E.; Moudgil, M.; et al. Graphene Oxide-Gold Nanosheets Containing Chitosan Scaffold Improves Ventricular Contractility and

- Function After Implantation into Infarcted Heart. *Scientific Reports* **2018**, *8*, 15069, doi:10.1038/s41598-018-33144-0.
458. Li, Y.; Shi, X.; Tian, L.; Sun, H.; Wu, Y.; Li, X.; Li, J.; Wei, Y.; Han, X.; Zhang, J.; et al. AuNP–Collagen Matrix with Localized Stiffness for Cardiac-Tissue Engineering: Enhancing the Assembly of Intercalated Discs by B1-Integrin-Mediated Signaling. *Advanced Materials* **2016**, *28*, 10230–10235, doi:10.1002/adma.201603027.
459. Hosoyama, K.; Ahumada, M.; McTiernan, C.D.; Davis, D.R.; Variola, F.; Ruel, M.; Liang, W.; Suuronen, E.J.; Alarcon, E.I. Nanoengineered Electroconductive Collagen-Based Cardiac Patch for Infarcted Myocardium Repair. *ACS Appl. Mater. Interfaces* **2018**, *10*, 44668–44677, doi:10.1021/acsmi.8b18844.
460. Yu, H.; Zhao, H.; Huang, C.; Du, Y. Mechanically and Electrically Enhanced CNT–Collagen Hydrogels As Potential Scaffolds for Engineered Cardiac Constructs. *ACS Biomater. Sci. Eng.* **2017**, *3*, 3017–3021, doi:10.1021/acsbiomaterials.6b00620.
461. Liberski, A.; Latif, N.; Raynaud, C.; Bollensdorff, C.; Yacoub, M. Alginate for Cardiac Regeneration: From Seaweed to Clinical Trials. *gcsp* **2016**, *2016*, doi:10.21542/gcsp.2016.4.
462. Cattelan, G.; Guerrero Gerbolés, A.; Foresti, R.; Pramstaller, P.P.; Rossini, A.; Miragoli, M.; Caffarra Malvezzi, C. Alginate Formulations: Current Developments in the Race for Hydrogel-Based Cardiac Regeneration. *Front. Bioeng. Biotechnol.* **2020**, *8*, 414, doi:10.3389/fbioe.2020.00414.
463. Anker, S.D.; Coats, A.J.S.; Cristian, G.; Dragomir, D.; Pusineri, E.; Piredda, M.; Bettari, L.; Dowling, R.; Volterrani, M.; Kirwan, B.-A.; et al. A Prospective Comparison of Alginate-Hydrogel with Standard Medical Therapy to Determine Impact on Functional Capacity and Clinical Outcomes in Patients with Advanced Heart Failure (AUGMENT-HF Trial). *Eur. Heart J.* **2015**, *36*, 2297–2309, doi:10.1093/eurheartj/ehv259.
464. Hayoun-Neeman, D.; Korover, N.; Etzion, S.; Ofir, R.; Lichtenstein, R.G.; Cohen, S. Exploring Peptide-Functionalized Alginate Scaffolds for Engineering Cardiac Tissue from Human Embryonic Stem Cell-Derived Cardiomyocytes in Serum-Free Medium. *Polymers for Advanced Technologies* **2019**, *30*, 2493–2505, doi:10.1002/pat.4602.
465. R.M. Lombardi, V. New Challenges in CNS Repair: The Immune and Nervous Connection. *CIR* **2012**, *8*, 87–93, doi:10.2174/157339512798991272.
466. Steward, M.M.; Sridhar, A.; Meyer, J.S. Neural Regeneration. *Curr. Top. Microbiol. Immunol.* **2013**, *367*, 163–191, doi:10.1007/82\_2012\_302.
467. Boni, R.; Ali, A.; Shavandi, A.; Clarkson, A.N. Current and Novel Polymeric Biomaterials for Neural Tissue Engineering. *Journal of Biomedical Science* **2018**, *25*, 90, doi:10.1186/s12929-018-0491-8.
468. Madhusudan, P.; Raju, G.; Shankarappa, S. Hydrogel Systems and Their Role in Neural Tissue Engineering. *Journal of The Royal Society Interface* **2020**, *17*, 20190505, doi:10.1098/rsif.2019.0505.
469. George, J.; Hsu, C.-C.; Nguyen, L.T.B.; Ye, H.; Cui, Z. Neural Tissue Engineering with Structured Hydrogels in CNS Models and Therapies. *Biotechnology Advances* **2020**, *42*, 107370, doi:10.1016/j.biotechadv.2019.03.009.
470. Uz, M.; Mallapragada, S.K. Conductive Polymers and Hydrogels for Neural Tissue Engineering. *J Indian Inst Sci* **2019**, *99*, 489–510, doi:10.1007/s41745-019-00126-8.
471. Ucar, B.; Humpel, C. Collagen for Brain Repair: Therapeutic Perspectives. *Neural Regen Res* **2018**, *13*, 595, doi:10.4103/1673-5374.230273.
472. Bozkurt, A.; Claeys, K.G.; Schrading, S.; Rödler, J.V.; Altinova, H.; Schulz, J.B.; Weis, J.; Pallua, N.; van Neerven, S.G.A. Clinical and Biometrical 12-Month Follow-up in Patients after Reconstruction of the Sural Nerve Biopsy Defect by the Collagen-Based Nerve Guide Neuromaix. *European Journal of Medical Research* **2017**, *22*, 34, doi:10.1186/s40001-017-0279-4.
473. Wangensteen, K.J.; Kalliainen, L.K. Collagen Tube Conduits in Peripheral Nerve Repair: A Retrospective Analysis. *Hand (New York, N.Y.)* **2010**, *5*, 273–277, doi:10.1007/s11552-009-9245-0.

474. O'Rourke, C.; Day, A.G.E.; Murray-Dunning, C.; Thanabalasundaram, L.; Cowan, J.; Stevanato, L.; Grace, N.; Cameron, G.; Drake, R. a. L.; Sinden, J.; et al. An Allogeneic 'off the Shelf' Therapeutic Strategy for Peripheral Nerve Tissue Engineering Using Clinical Grade Human Neural Stem Cells. *Scientific Reports* **2018**, *8*, 2951, doi:10.1038/s41598-018-20927-8.
475. Schuh, C.M.A.P.; Day, A.G.E.; Redl, H.; Phillips, J. An Optimized Collagen-Fibrin Blend Engineered Neural Tissue Promotes Peripheral Nerve Repair. *Tissue Engineering Part A* **2018**, *24*, 1332–1340, doi:10.1089/ten.tea.2017.0457.
476. Yu, Z.; Li, H.; Xia, P.; Kong, W.; Chang, Y.; Fu, C.; Wang, K.; Yang, X.; Qi, Z. Application of Fibrin-Based Hydrogels for Nerve Protection and Regeneration after Spinal Cord Injury. *Journal of Biological Engineering* **2020**, *14*, 22, doi:10.1186/s13036-020-00244-3.
477. Hasanzadeh, E.; Ebrahimi-Barough, S.; Mirzaei, E.; Azami, M.; Tavangar, S.M.; Mahmoodi, N.; Basiri, A.; Ai, J. Preparation of Fibrin Gel Scaffolds Containing MWCNT/PU Nanofibers for Neural Tissue Engineering. *Journal of Biomedical Materials Research Part A* **2019**, *107*, 802–814, doi:10.1002/jbm.a.36596.
478. Sill, T.J.; von Recum, H.A. Electrospinning: Applications in Drug Delivery and Tissue Engineering. *Biomaterials* **2008**, *29*, 1989–2006, doi:10.1016/j.biomaterials.2008.01.011.
479. Faghihi, F.; Mirzaei, E.; Ai, J.; Lotfi, A.; Sayahpour, F.A.; Barough, S.E.; Joghataei, M.T. Differentiation Potential of Human Chorion-Derived Mesenchymal Stem Cells into Motor Neuron-Like Cells in Two- and Three-Dimensional Culture Systems. *Mol. Neurobiol.* **2016**, *53*, 1862–1872, doi:10.1007/s12035-015-9129-y.
480. Gnavi, S.; Fornasari, B.E.; Tonda-Turo, C.; Laurano, R.; Zanetti, M.; Ciardelli, G.; Geuna, S. The Effect of Electrospun Gelatin Fibers Alignment on Schwann Cell and Axon Behavior and Organization in the Perspective of Artificial Nerve Design. *Int J Mol Sci* **2015**, *16*, 12925–12942, doi:10.3390/ijms160612925.
481. Baiguera, S.; Del Gaudio, C.; Lucatelli, E.; Kuevda, E.; Boieri, M.; Mazzanti, B.; Bianco, A.; Macchiarini, P. Electrospun Gelatin Scaffolds Incorporating Rat Decellularized Brain Extracellular Matrix for Neural Tissue Engineering. *Biomaterials* **2014**, *35*, 1205–1214, doi:10.1016/j.biomaterials.2013.10.060.
482. Gunasekaran, H.; Acutis, A.D.; Montemurro, F.; Maria, C.D.; Vozzi, G. Fabrication and Characterization of Gelatin/Carbon Black–Based Scaffolds for Neural Tissue Engineering Applications. *MPC* **2019**, *8*, 301–315, doi:10.1520/MPC20180165.
483. Wang, S.; Sun, C.; Guan, S.; Li, W.; Xu, J.; Ge, D.; Zhuang, M.; Liu, T.; Ma, X. Chitosan/Gelatin Porous Scaffolds Assembled with Conductive Poly(3,4-Ethylenedioxythiophene) Nanoparticles for Neural Tissue Engineering. *J. Mater. Chem. B* **2017**, *5*, 4774–4788, doi:10.1039/C7TB00608J.
484. Rifai, N.A.; Hasan, A.; Kobeissy, F.; Hasan, A.; Rifai, N.A.; Gazalah, H.; Charara, J. Culture of PC12 Neuronal Cells in GelMA Hydrogel for Brain Tissue Engineering. In Proceedings of the 2015 International Conference on Advances in Biomedical Engineering (ICABME); September 2015; pp. 254–257.
485. Ye, W.; Li, H.; Yu, K.; Xie, C.; Wang, P.; Zheng, Y.; Zhang, P.; Xiu, J.; Yang, Y.; Zhang, F.; et al. 3D Printing of Gelatin Methacrylate-Based Nerve Guidance Conduits with Multiple Channels. *Materials & Design* **2020**, *192*, 108757, doi:10.1016/j.matdes.2020.108757.
486. Sitoci-Ficici, K.H.; Matyash, M.; Uckermann, O.; Galli, R.; Leipnitz, E.; Later, R.; Ikonomidou, C.; Gelinsky, M.; Schackert, G.; Kirsch, M. Non-Functionalized Soft Alginate Hydrogel Promotes Locomotor Recovery after Spinal Cord Injury in a Rat Hemimyelonection Model. *Acta Neurochir* **2018**, *160*, 449–457, doi:10.1007/s00701-017-3389-4.
487. Golafshan, N.; Kharaziha, M.; Fathi, M. Tough and Conductive Hybrid Graphene-PVA: Alginate Fibrous Scaffolds for Engineering Neural Construct. *Carbon* **2017**, *111*, 752–763, doi:10.1016/j.carbon.2016.10.042.

488. Homaeigohar, S.; Tsai, T.-Y.; Young, T.-H.; Yang, H.J.; Ji, Y.-R. An Electroactive Alginate Hydrogel Nanocomposite Reinforced by Functionalized Graphite Nanofilaments for Neural Tissue Engineering. *Carbohydrate Polymers* **2019**, *224*, 115112, doi:10.1016/j.carbpol.2019.115112.
489. Wang, G.; Wang, X.; Huang, L. Feasibility of Chitosan-Alginate (Chi-Alg) Hydrogel Used as Scaffold for Neural Tissue Engineering: A Pilot Study in Vitro. *Biotechnology & Biotechnological Equipment* **2017**, *31*, 766–773, doi:10.1080/13102818.2017.1332493.
490. Li, R.; Liu, H.; Huang, H.; Bi, W.; Yan, R.; Tan, X.; Wen, W.; Wang, C.; Song, W.; Zhang, Y.; et al. Chitosan Conduit Combined with Hyaluronic Acid Prevent Sciatic Nerve Scar in a Rat Model of Peripheral Nerve Crush Injury. *Molecular Medicine Reports* **2018**, *17*, 4360–4368, doi:10.3892/mmr.2018.8388.
491. Li, G.; Chen, K.; You, D.; Xia, M.; Li, W.; Fan, S.; Chai, R.; Zhang, Y.; Li, H.; Sun, S. Laminin-Coated Electrospun Regenerated Silk Fibroin Mats Promote Neural Progenitor Cell Proliferation, Differentiation, and Survival in Vitro. *Front. Bioeng. Biotechnol.* **2019**, *7*, 190, doi:10.3389/fbioe.2019.00190.
492. Nune, M.; Manchineella, S.; T., G.; K.s., N. Melanin Incorporated Electroactive and Antioxidant Silk Fibroin Nanofibrous Scaffolds for Nerve Tissue Engineering. *Materials Science and Engineering: C* **2019**, *94*, 17–25, doi:10.1016/j.msec.2018.09.014.
493. Schemitsch, E.H. Size Matters: Defining Critical in Bone Defect Size! *Journal of Orthopaedic Trauma* **2017**, *31*, S20, doi:10.1097/BOT.0000000000000978.
494. Henkel, J.; Woodruff, M.A.; Epari, D.R.; Steck, R.; Glatt, V.; Dickinson, I.C.; Choong, P.F.M.; Schuetz, M.A.; Huttmacher, D.W. Bone Regeneration Based on Tissue Engineering Conceptions — A 21st Century Perspective. *Bone Res* **2013**, *1*, 216–248, doi:10.4248/BR201303002.
495. Mittwede, P.N.; Gottardi, R.; Alexander, P.G.; Tarkin, I.S.; Tuan, R.S. Clinical Applications of Bone Tissue Engineering in Orthopedic Trauma. *Curr Pathobiol Rep* **2018**, *6*, 99–108, doi:10.1007/s40139-018-0166-x.
496. Perez, J.R.; Kouroupis, D.; Li, D.J.; Best, T.M.; Kaplan, L.; Correa, D. Tissue Engineering and Cell-Based Therapies for Fractures and Bone Defects. *Front. Bioeng. Biotechnol.* **2018**, *6*, 105, doi:10.3389/fbioe.2018.00105.
497. Bai, X.; Gao, M.; Syed, S.; Zhuang, J.; Xu, X.; Zhang, X.-Q. Bioactive Hydrogels for Bone Regeneration. *Bioact Mater* **2018**, *3*, 401–417, doi:10.1016/j.bioactmat.2018.05.006.
498. Koons, G.L.; Diba, M.; Mikos, A.G. Materials Design for Bone-Tissue Engineering. *Nature Reviews Materials* **2020**, *5*, 584–603, doi:10.1038/s41578-020-0204-2.
499. Ferreira, A.M.; Gentile, P.; Chiono, V.; Ciardelli, G. Collagen for Bone Tissue Regeneration. *Acta Biomaterialia* **2012**, *8*, 3191–3200, doi:10.1016/j.actbio.2012.06.014.
500. Lindsey, W.H.; Ogle, R.C.; Morgan, R.F.; Cantrell, R.W.; Sweeney, T.M. Nasal Reconstruction Using an Osteoconductive Collagen Gel Matrix. *Arch. Otolaryngol. Head Neck Surg.* **1996**, *122*, 37–40, doi:10.1001/archotol.1996.01890130031004.
501. Stuckensen, K.; Schwab, A.; Knauer, M.; Muiños-López, E.; Ehlicke, F.; Reboredo, J.; Granero-Moltó, F.; Gbureck, U.; Prósper, F.; Walles, H.; et al. Tissue Mimicry in Morphology and Composition Promotes Hierarchical Matrix Remodeling of Invading Stem Cells in Osteochondral and Meniscus Scaffolds. *Advanced Materials* **2018**, *30*, 1706754, doi:10.1002/adma.201706754.
502. Clarke, B. Normal Bone Anatomy and Physiology. *Clin J Am Soc Nephrol* **2008**, *3 Suppl 3*, S131-139, doi:10.2215/CJN.04151206.
503. Nijssure, M.P.; Kishore, V. Collagen-Based Scaffolds for Bone Tissue Engineering Applications. In *Orthopedic Biomaterials: Advances and Applications*; Li, B., Webster, T., Eds.; Springer International Publishing: Cham, 2017; pp. 187–224 ISBN 978-3-319-73664-8.
504. Meyer, M. Processing of Collagen Based Biomaterials and the Resulting Materials Properties. *BioMedical Engineering OnLine* **2019**, *18*, 24, doi:10.1186/s12938-019-0647-0.

505. Villa, M.M.; Wang, L.; Huang, J.; Rowe, D.W.; Wei, M. Bone Tissue Engineering with a Collagen–Hydroxyapatite Scaffold and Culture Expanded Bone Marrow Stromal Cells. *J Biomed Mater Res B Appl Biomater* **2015**, *103*, 243–253, doi:10.1002/jbm.b.33225.
506. Chen, L.; Wu, Z.; Zhou, Y.; Li, L.; Wang, Y.; Wang, Z.; Chen, Y.; Zhang, P. Biomimetic Porous Collagen/Hydroxyapatite Scaffold for Bone Tissue Engineering. *Journal of Applied Polymer Science* **2017**, *134*, 45271, doi:10.1002/app.45271.
507. Kang, H.-W.; Tabata, Y.; Ikada, Y. Fabrication of Porous Gelatin Scaffolds for Tissue Engineering. *Biomaterials* **1999**, *20*, 1339–1344, doi:10.1016/S0142-9612(99)00036-8.
508. Raucci, M.G.; D'Amora, U.; Ronca, A.; Demitri, C.; Ambrosio, L. Bioactivation Routes of Gelatin-Based Scaffolds to Enhance at Nanoscale Level Bone Tissue Regeneration. *Front. Bioeng. Biotechnol.* **2019**, *7*, 27, doi:10.3389/fbioe.2019.00027.
509. Celikkin, N.; Mastrogiacomo, S.; Jaroszewicz, J.; Walboomers, X.F.; Swieszkowski, W. Gelatin Methacrylate Scaffold for Bone Tissue Engineering: The Influence of Polymer Concentration: GELATIN METHACRYLATE SCAFFOLD FOR BONE TISSUE ENGINEERING. *J. Biomed. Mater. Res.* **2018**, *106*, 201–209, doi:10.1002/jbm.a.36226.
510. Irmak, G.; Demirtaş, T.T.; Gümüşderelioğlu, M. Highly Methacrylated Gelatin Bioink for Bone Tissue Engineering. *ACS Biomater. Sci. Eng.* **2019**, *5*, 831–845, doi:10.1021/acsbomaterials.8b00778.
511. Byambaa, B.; Annabi, N.; Yue, K.; Santiago, G.T.; Alvarez, M.M.; Jia, W.; Kazemzadeh-Narbat, M.; Shin, S.R.; Tamayol, A.; Khademhosseini, A. Bioprinted Osteogenic and Vasculogenic Patterns for Engineering 3D Bone Tissue. *Advanced Healthcare Materials* **2017**, *6*, 1700015, doi:10.1002/adhm.201700015.
512. Luo, Z.; Zhang, S.; Pan, J.; Shi, R.; Liu, H.; Lyu, Y.; Han, X.; Li, Y.; Yang, Y.; Xu, Z.; et al. Time-Responsive Osteogenic Niche of Stem Cells: A Sequentially Triggered, Dual-Peptide Loaded, Alginate Hybrid System for Promoting Cell Activity and Osteo-Differentiation. *Biomaterials* **2018**, *163*, 25–42, doi:10.1016/j.biomaterials.2018.02.025.
513. Shi, L.; Wang, F.; Zhu, W.; Xu, Z.; Fuchs, S.; Hilborn, J.; Zhu, L.; Ma, Q.; Wang, Y.; Weng, X.; et al. Self-Healing Silk Fibroin-Based Hydrogel for Bone Regeneration: Dynamic Metal-Ligand Self-Assembly Approach. *Advanced Functional Materials* **2017**, *27*, 1700591, doi:10.1002/adfm.201700591.
514. Gerdes, S.; Mostafavi, A.; Ramesh, S.; Memic, A.; Rivero, I.V.; Rao, P.; Tamayol, A. Process–Structure–Quality Relationships of Three-Dimensional Printed Poly(Caprolactone)-Hydroxyapatite Scaffolds. *Tissue Engineering Part A* **2020**, *26*, 279–291, doi:10.1089/ten.tea.2019.0237.
515. Russell, C.S.; Mostafavi, A.; Quint, J.P.; Panayi, A.C.; Baldino, K.; Williams, T.J.; Daubendiek, J.G.; Hugo Sánchez, V.; Bonick, Z.; Trujillo-Miranda, M.; et al. *In Situ* Printing of Adhesive Hydrogel Scaffolds for the Treatment of Skeletal Muscle Injuries. *ACS Appl. Bio Mater.* **2020**, *3*, 1568–1579, doi:10.1021/acsbm.9b01176.
516. Cheng, R.Y.; Eylert, G.; Garipey, J.-M.; He, S.; Ahmad, H.; Gao, Y.; Priore, S.; Hakimi, N.; Jeschke, M.G.; Günther, A. Handheld Instrument for Wound-Conformal Delivery of Skin Precursor Sheets Improves Healing in Full-Thickness Burns. *Biofabrication* **2020**, *12*, 025002, doi:10.1088/1758-5090/ab6413.
517. Chen, Y.; Zhang, J.; Liu, X.; Wang, S.; Tao, J.; Huang, Y.; Wu, W.; Li, Y.; Zhou, K.; Wei, X.; et al. Noninvasive in Vivo 3D Bioprinting. *Sci. Adv.* **2020**, *6*, eaba7406, doi:10.1126/sciadv.aba7406.
518. Zhang, B.; Radisic, M. Organ-Level Vascularization: The Mars Mission of Bioengineering. *The Journal of Thoracic and Cardiovascular Surgery* **2020**, *159*, 2003–2007, doi:10.1016/j.jtcvs.2019.08.128.
519. Karim, A.A.; Bhat, R. Fish Gelatin: Properties, Challenges, and Prospects as an Alternative to Mammalian Gelatins. *Food Hydrocolloids* **2009**, *23*, 563–576, doi:10.1016/j.foodhyd.2008.07.002.
520. Elzoghby, A.O. Gelatin-Based Nanoparticles as Drug and Gene Delivery Systems: Reviewing Three Decades of Research. *Journal of Controlled Release* **2013**, *172*, 1075–1091, doi:10.1016/j.jconrel.2013.09.019.

521. Foox, M.; Zilberman, M. Drug Delivery from Gelatin-Based Systems. *Expert Opinion on Drug Delivery* **2015**, *12*, 1547–1563, doi:10.1517/17425247.2015.1037272.
522. Etxabide, A.; Uranga, J.; Guerrero, P.; de la Caba, K. Development of Active Gelatin Films by Means of Valorisation of Food Processing Waste: A Review. *Food Hydrocolloids* **2017**, *68*, 192–198, doi:10.1016/j.foodhyd.2016.08.021.
523. Farris, S.; Schaich, K.M.; Liu, L.; Piergiovanni, L.; Yam, K.L. Development of Polyion-Complex Hydrogels as an Alternative Approach for the Production of Bio-Based Polymers for Food Packaging Applications: A Review. *Trends in Food Science & Technology* **2009**, *20*, 316–332, doi:10.1016/j.tifs.2009.04.003.
524. Liu, Y.; Chan-Park, M.B. A Biomimetic Hydrogel Based on Methacrylated Dextran-Graft-Lysine and Gelatin for 3D Smooth Muscle Cell Culture. *Biomaterials* **2010**, *31*, 1158–1170, doi:10.1016/j.biomaterials.2009.10.040.
525. Vandooren, J.; Van den Steen, P.E.; Opdenakker, G. Biochemistry and Molecular Biology of Gelatinase B or Matrix Metalloproteinase-9 (MMP-9): The next Decade. *Critical Reviews in Biochemistry and Molecular Biology* **2013**, *48*, 222–272, doi:10.3109/10409238.2013.770819.
526. Rose, J.; Pacelli, S.; Haj, A.; Dua, H.; Hopkinson, A.; White, L.; Rose, F. Gelatin-Based Materials in Ocular Tissue Engineering. *Materials* **2014**, *7*, 3106–3135, doi:10.3390/ma7043106.
527. Hosseini, V.; Ahadian, S.; Ostrovidov, S.; Camci-Unal, G.; Chen, S.; Kaji, H.; Ramalingam, M.; Khademhosseini, A. Engineered Contractile Skeletal Muscle Tissue on a Microgrooved Methacrylated Gelatin Substrate. *Tissue Engineering Part A* **2012**, *18*, 2453–2465, doi:10.1089/ten.tea.2012.0181.
528. Xu, F.; Wu, C.M.; Rengarajan, V.; Finley, T.D.; Keles, H.O.; Sung, Y.; Li, B.; Gurkan, U.A.; Demirci, U. Three-Dimensional Magnetic Assembly of Microscale Hydrogels. *Advanced Materials* **2011**, *23*, 4254–4260, doi:10.1002/adma.201101962.
529. Piraino, F.; Camci-Unal, G.; Hancock, M.J.; Rasponi, M.; Khademhosseini, A. Multi-Gradient Hydrogels Produced Layer by Layer with Capillary Flow and Crosslinking in Open Microchannels. *Lab Chip* **2012**, *12*, 659–661, doi:10.1039/C2LC20515G.
530. Shi, X.; Ostrovidov, S.; Zhao, Y.; Liang, X.; Kasuya, M.; Kurihara, K.; Nakajima, K.; Bae, H.; Wu, H.; Khademhosseini, A. Microfluidic Spinning of Cell-Responsive Grooved Microfibers. *Advanced Functional Materials* **2015**, *25*, 2250–2259, doi:10.1002/adfm.201404531.
531. Bertassoni, L.E.; Cardoso, J.C.; Manoharan, V.; Cristino, A.L.; Bhise, N.S.; Araujo, W.A.; Zorlutuna, P.; Vrana, N.E.; Ghaemmaghami, A.M.; Dokmeci, M.R.; et al. Direct-Write Bioprinting of Cell-Laden Methacrylated Gelatin Hydrogels. *Biofabrication* **2014**, *6*, 024105, doi:10.1088/1758-5082/6/2/024105.
532. Suresh, P.V.; Kudre, T.G.; Johny, L.C. Sustainable Valorization of Seafood Processing By-Product/Discard. In *Waste to Wealth*; Singhania, R.R., Agarwal, R.A., Kumar, R.P., Sukumaran, R.K., Eds.; Springer Singapore: Singapore, 2018; pp. 111–139 ISBN 978-981-10-7430-1.
533. Badii, F.; Howell, N. Fish Gelatin: Structure, Gelling Properties and Interaction with Egg Albumen Proteins. *Food Hydrocolloids* **2006**, *20*, 630–640, doi:10.1016/j.foodhyd.2005.06.006.
534. Karim, A.A.; Bhat, R. Gelatin Alternatives for the Food Industry: Recent Developments, Challenges and Prospects. *Trends in Food Science & Technology* **2008**, *19*, 644–656, doi:10.1016/j.tifs.2008.08.001.
535. Yoon, H.J.; Shin, S.R.; Cha, J.M.; Lee, S.-H.; Kim, J.-H.; Do, J.T.; Song, H.; Bae, H. Cold Water Fish Gelatin Methacryloyl Hydrogel for Tissue Engineering Application. *PLOS ONE* **2016**, *11*, e0163902, doi:10.1371/journal.pone.0163902.
536. Wang, Z.; Tian, Z.; Menard, F.; Kim, K. Comparative Study of Gelatin Methacrylate Hydrogels from Different Sources for Biofabrication Applications. *Biofabrication* **2017**, *9*, 044101, doi:10.1088/1758-5090/aa83cf.

537. Costantini, M.; Testa, S.; Fornetti, E.; Barbetta, A.; Trombetta, M.; Cannata, S.M.; Gargioli, C.; Rainer, A. Engineering Muscle Networks in 3D Gelatin Methacryloyl Hydrogels: Influence of Mechanical Stiffness and Geometrical Confinement. *Front. Bioeng. Biotechnol.* **2017**, *5*, doi:10.3389/fbioe.2017.00022.
538. Seyedmahmoud; Çelebi-Saltik; Barros; Nasiri; Banton; Shamloo; Ashammakhi; Dokmeci; Ahadian Three-Dimensional Bioprinting of Functional Skeletal Muscle Tissue Using GelatinMethacryloyl-Alginate Bioinks. *Micromachines* **2019**, *10*, 679, doi:10.3390/mi10100679.
539. Ebrahimi, M.; Ostrovidov, S.; Salehi, S.; Kim, S.B.; Bae, H.; Khademhosseini, A. Enhanced Skeletal Muscle Formation on Microfluidic Spun Gelatin Methacryloyl (GelMA) Fibres Using Surface Patterning and Agrin Treatment. *J Tissue Eng Regen Med* **2018**, *12*, 2151–2163, doi:10.1002/term.2738.
540. Habeeb, A.F. Determination of Free Amino Groups in Proteins by Trinitrobenzenesulfonic Acid. *Anal. Biochem.* **1966**, *14*, 328–336, doi:10.1016/0003-2697(66)90275-2.
541. Anirudhan, T.S.; Mohan, A.M. Novel PH Switchable Gelatin Based Hydrogel for the Controlled Delivery of the Anti Cancer Drug 5-Fluorouracil. *RSC Adv.* **2014**, *4*, 12109, doi:10.1039/c3ra47991a.
542. Anirudhan, T.S.; Mohan, A.M. Novel PH Sensitive Dual Drug Loaded-Gelatin Methacrylate/Methacrylic Acid Hydrogel for the Controlled Release of Antibiotics. *International Journal of Biological Macromolecules* **2018**, *110*, 167–178, doi:10.1016/j.ijbiomac.2018.01.220.
543. Aldana, A.; Malatto, L.; Rehman, M.; Boccaccini, A.; Abraham, G. Fabrication of Gelatin Methacrylate (GelMA) Scaffolds with Nano- and Micro-Topographical and Morphological Features. *Nanomaterials* **2019**, *9*, 120, doi:10.3390/nano9010120.
544. Erkoç, P.; Seker, F.; Bağcı-Onder, T.; Kizilel, S. Gelatin Methacryloyl Hydrogels in the Absence of a Crosslinker as 3D Glioblastoma Multiforme (GBM)-Mimetic Microenvironment. *Macromolecular Bioscience* **2018**, *18*, 1700369, doi:10.1002/mabi.201700369.
545. Neelam, A.; Hany, O.; Ishteyaq, S.; Nawaz, K.; Mahmood, S.J.; Siddique, M. Analysis of Physical, Mechanical and Thermal Degradation of Gelatin-Based Film—Exploring the Biopolymer for Plastic Advancement. *Journal of Applied and Emerging Sciences* **2018**, *8*, pp39–47.
546. Mahmood, K.; Kamilah, H.; Sudesh, K.; Karim, A.A.; Ariffin, F. Study of Electrospun Fish Gelatin Nanofilms from Benign Organic Acids as Solvents. *Food Packaging and Shelf Life* **2019**, *19*, 66–75, doi:10.1016/j.fpsl.2018.11.018.
547. Kołbuk, D.; Sajkiewicz, P.; Maniura-Weber, K.; Fortunato, G. Structure and Morphology of Electrospun Polycaprolactone/Gelatine Nanofibres. *European Polymer Journal* **2013**, *49*, 2052–2061, doi:10.1016/j.eurpolymj.2013.04.036.
548. Gupta, S.S.; Meena, A.; Parikh, T.; Serajuddin, A.T. Investigation of Thermal and Viscoelastic Properties of Polymers Relevant to Hot Melt Extrusion-I: Polyvinylpyrrolidone and Related Polymers. *Journal of Excipients and Food Chemicals* **2016**, *5*, 1001.
549. Van Vlierberghe, S.; Dubruel, P.; Lippens, E.; Cornelissen, M.; Schacht, E. Correlation Between Cryogenic Parameters and Physico-Chemical Properties of Porous Gelatin Cryogels. *Journal of Biomaterials Science, Polymer Edition* **2009**, *20*, 1417–1438, doi:10.1163/092050609X12457418905508.
550. Bravo-Osuna, I.; Ferrero, C.; Jiménez-Castellanos, M.R. Water Sorption–Desorption Behaviour of Methyl Methacrylate–Starch Copolymers: Effect of Hydrophobic Graft and Drying Method. *European Journal of Pharmaceutics and Biopharmaceutics* **2005**, *59*, 537–548, doi:10.1016/j.ejpb.2004.10.003.
551. Ayranci, E. Moisture sorption of cellulose based edible films. *Nahrung* **1996**, *40*, 274–276, doi:10.1002/food.19960400510.
552. Kim, S.W.; Bae, Y.H.; Okano, T. Hydrogels: Swelling, Drug Loading, and Release. *Pharmaceutical Research* **1992**, *09*, 283–290, doi:10.1023/A:1015887213431.

553. Araghi, M.; Moslehi, Z.; Mohammadi Nafchi, A.; Mostahsan, A.; Salamat, N.; Daraei Garmakhany, A. Cold Water Fish Gelatin Modification by a Natural Phenolic Cross-Linker (Ferulic Acid and Caffeic Acid). *Food Sci Nutr* **2015**, *3*, 370–375, doi:10.1002/fsn3.230.
554. Muyonga, J.H.; Cole, C.G.B.; Duodu, K.G. Extraction and Physico-Chemical Characterisation of Nile Perch (*Lates niloticus*) Skin and Bone Gelatin. *Food Hydrocolloids* **2004**, *18*, 581–592, doi:10.1016/j.foodhyd.2003.08.009.
555. Haug, I.J.; Draget, K.I.; Smidsrød, O. Physical Behaviour of Fish Gelatin- $\kappa$ -Carrageenan Mixtures. *Carbohydrate Polymers* **2004**, *56*, 11–19, doi:10.1016/j.carbpol.2003.10.014.
556. Wells, R.G. The Role of Matrix Stiffness in Regulating Cell Behavior. *Hepatology* **2008**, *47*, 1394–1400, doi:10.1002/hep.22193.
557. Chatterjee, K.; Lin-Gibson, S.; Wallace, W.E.; Parekh, S.H.; Lee, Y.J.; Cicerone, M.T.; Young, M.F.; Simon, C.G. The Effect of 3D Hydrogel Scaffold Modulus on Osteoblast Differentiation and Mineralization Revealed by Combinatorial Screening. *Biomaterials* **2010**, *31*, 5051–5062, doi:10.1016/j.biomaterials.2010.03.024.
558. Young, J.L.; Engler, A.J. Hydrogels with Time-Dependent Material Properties Enhance Cardiomyocyte Differentiation in Vitro. *Biomaterials* **2011**, *32*, 1002–1009, doi:10.1016/j.biomaterials.2010.10.020.
559. Banerjee, A.; Arha, M.; Choudhary, S.; Ashton, R.S.; Bhatia, S.R.; Schaffer, D.V.; Kane, R.S. The Influence of Hydrogel Modulus on the Proliferation and Differentiation of Encapsulated Neural Stem Cells. *Biomaterials* **2009**, *30*, 4695–4699, doi:10.1016/j.biomaterials.2009.05.050.
560. Eastoe, J.E. The Amino Acid Composition of Fish Collagen and Gelatin. *Biochemical Journal* **1957**, *65*, 363–368, doi:10.1042/bj0650363.
561. Kang, M.G.; Lee, M.Y.; Cha, J.M.; Lee, J.K.; Lee, S.C.; Kim, J.; Hwang, Y.-S.; Bae, H. Nanogels Derived from Fish Gelatin: Application to Drug Delivery System. *Mar. Drugs* **2019**, *17*, 246, doi:10.3390/md17040246.
562. Pepelanova, I.; Kruppa, K.; Scheper, T.; Lavrentieva, A. Gelatin-Methacryloyl (GelMA) Hydrogels with Defined Degree of Functionalization as a Versatile Toolkit for 3D Cell Culture and Extrusion Bioprinting. *Bioengineering* **2018**, *5*, 55, doi:10.3390/bioengineering5030055.
563. Zhu, M.; Wang, Y.; Ferracci, G.; Zheng, J.; Cho, N.-J.; Lee, B.H. Gelatin Methacryloyl and Its Hydrogels with an Exceptional Degree of Controllability and Batch-to-Batch Consistency. *Sci Rep* **2019**, *9*, 6863, doi:10.1038/s41598-019-42186-x.
564. Zaupa, A.; Byres, N.; Dal Zovo, C.; Acevedo, C.A.; Angelopoulos, I.; Terraza, C.; Nestle, N.; Abarzúa-Illanes, P.N.; Quero, F.; Díaz-Calderón, P.; et al. Cold-Adaptation of a Methacrylamide Gelatin towards the Expansion of the Biomaterial Toolbox for Specialized Functionalities in Tissue Engineering. *Materials Science and Engineering: C* **2019**, *102*, 373–390, doi:10.1016/j.msec.2019.04.020.
565. Klotz, B.J.; Gawlitta, D.; Rosenberg, A.J.W.P.; Malda, J.; Melchels, F.P.W. Gelatin-Methacryloyl Hydrogels: Towards Biofabrication-Based Tissue Repair. *Trends in Biotechnology* **2016**, *34*, 394–407, doi:10.1016/j.tibtech.2016.01.002.
566. Arab-Tehrany, E.; Elkhoury, K.; Francius, G.; Jierry, L.; Mano, J.F.; Kahn, C.; Linder, M. Curcumin Loaded Nanoliposomes Localization by Nanoscale Characterization. *IJMS* **2020**, *21*, 7276, doi:10.3390/ijms21197276.
567. Koons, G.L.; Diba, M.; Mikos, A.G. Materials Design for Bone-Tissue Engineering. *Nat Rev Mater* **2020**, doi:10.1038/s41578-020-0204-2.
568. Frese, L.; Dijkman, P.E.; Hoerstrup, S.P. Adipose Tissue-Derived Stem Cells in Regenerative Medicine. *Transfusion Medicine and Hemotherapy* **2016**, *43*, 268–274, doi:10.1159/000448180.
569. Lavrador, P.; Gaspar, V.M.; Mano, J.F. Bioinspired Bone Therapies Using Naringin: Applications and Advances. *Drug Discovery Today* **2018**, *23*, 1293–1304, doi:10.1016/j.drudis.2018.05.012.

570. Rao, K.; Imran, M.; Jabri, T.; Ali, I.; Perveen, S.; Shafiullah; Ahmed, S.; Shah, M.R. Gum Tragacanth Stabilized Green Gold Nanoparticles as Cargos for Naringin Loading: A Morphological Investigation through AFM. *Carbohydrate Polymers* **2017**, *174*, 243–252, doi:10.1016/j.carbpol.2017.06.071.
571. Fan, J.; Li, J.; Fan, Q. Naringin Promotes Differentiation of Bone Marrow Stem Cells into Osteoblasts by Upregulating the Expression Levels of MicroRNA-20a and Downregulating the Expression Levels of PPAR $\gamma$ . *Molecular Medicine Reports* **2015**, *12*, 4759–4765, doi:10.3892/mmr.2015.3996.
572. Yu, G.; Zheng, G.; Chang, B.; Hu, Q.; Lin, F.; Liu, D.; Wu, C.; Du, S.; Li, X. Naringin Stimulates Osteogenic Differentiation of Rat Bone Marrow Stromal Cells via Activation of the Notch Signaling Pathway. *Stem Cells International* **2016**, *2016*, 1–8, doi:10.1155/2016/7130653.
573. Osathanon, T.; Subbalekha, K.; Sastravaha, P.; Pavasant, P. Notch Signalling Inhibits the Adipogenic Differentiation of Single-Cell-Derived Mesenchymal Stem Cell Clones Isolated from Human Adipose Tissue. *Cell Biology International* **2012**, *36*, 1161–1170, doi:10.1042/CBI20120288.
574. Wu, J.-B.; Fong, Y.-C.; Tsai, H.-Y.; Chen, Y.-F.; Tsuzuki, M.; Tang, C.-H. Naringin-Induced Bone Morphogenetic Protein-2 Expression via PI3K, Akt, c-Fos/c-Jun and AP-1 Pathway in Osteoblasts. *European Journal of Pharmacology* **2008**, *588*, 333–341, doi:10.1016/j.ejphar.2008.04.030.
575. Gaoli, X.; Yi, L.; Lili, W.; Qiutao, S.; Guang, H.; Zhiyuan, G. [Effect of naringin combined with bone morphogenetic protein-2 on the proliferation and differentiation of MC3T3-E1 cells]. *Hua Xi Kou Qiang Yi Xue Za Zhi* **2017**, *35*, 275–280, doi:10.7518/hxkq.2017.03.009.
576. Lavrador, P.; Gaspar, V.M.; Mano, J.F. Bioinstructive Naringin-Loaded Micelles for Guiding Stem Cell Osteodifferentiation. *Advanced Healthcare Materials* **2018**, *7*, 1800890, doi:10.1002/adhm.201800890.
577. Wang, H.; Li, C.; Li, J.; Zhu, Y.; Jia, Y.; Zhang, Y.; Zhang, X.; Li, W.; Cui, L.; Li, W.; et al. Naringin Enhances Osteogenic Differentiation through the Activation of ERK Signaling in Human Bone Marrow Mesenchymal Stem Cells. *Iranian Journal of Basic Medical Sciences* **2017**, *20*, doi:10.22038/ijbms.2017.8582.
578. Liu, M.; Li, Y.; Yang, S.-T. Effects of Naringin on the Proliferation and Osteogenic Differentiation of Human Amniotic Fluid-Derived Stem Cells: Effects of Naringin on Osteogenic Differentiation of HAFSCs. *J Tissue Eng Regen Med* **2017**, *11*, 276–284, doi:10.1002/term.1911.
579. Yin, L.; Cheng, W.; Qin, Z.; Yu, H.; Yu, Z.; Zhong, M.; Sun, K.; Zhang, W. Effects of Naringin on Proliferation and Osteogenic Differentiation of Human Periodontal Ligament Stem Cells In Vitro and In Vivo. *Stem Cells International* **2015**, *2015*, 1–9, doi:10.1155/2015/758706.
580. Walle, T. Absorption and Metabolism of Flavonoids. *Free Radical Biology and Medicine* **2004**, *36*, 829–837, doi:10.1016/j.freeradbiomed.2004.01.002.
581. Cassidy, A.; Minihane, A.-M. The Role of Metabolism (and the Microbiome) in Defining the Clinical Efficacy of Dietary Flavonoids. *The American Journal of Clinical Nutrition* **2017**, *105*, 10–22, doi:10.3945/ajcn.116.136051.
582. Maherani, B.; Arab-Tehrany, E.; Kheiriloomoom, A.; Geny, D.; Linder, M. Calcein Release Behavior from Liposomal Bilayer; Influence of Physicochemical/Mechanical/Structural Properties of Lipids. *Biochimie* **2013**, *95*, 2018–2033, doi:10.1016/j.biochi.2013.07.006.
583. Latifi, S.; Tamayol, A.; Habibey, R.; Sabzevari, R.; Kahn, C.; Geny, D.; Eftekharpour, E.; Annabi, N.; Blau, A.; Linder, M.; et al. Natural Lecithin Promotes Neural Network Complexity and Activity. *Sci Rep* **2016**, *6*, 25777, doi:10.1038/srep25777.
584. Elbahnasawy, A.S.; Valeeva, E.R.; El-Sayed, E.M.; Stepanova, N.V. Protective Effect of Dietary Oils Containing Omega-3 Fatty Acids against Glucocorticoid-Induced Osteoporosis. *J Nutr Health* **2019**, *52*, 323, doi:10.4163/jnh.2019.52.4.323.

585. Banu, J.; Bhattacharya, A.; Rahman, M.; Fernandes, G. Beneficial Effects of Conjugated Linoleic Acid and Exercise on Bone of Middle-Aged Female Mice. *J Bone Miner Metab* **2008**, *26*, 436–445, doi:10.1007/s00774-008-0863-3.
586. Fang, X.; Xie, J.; Zhong, L.; Li, J.; Rong, D.; Li, X.; Ouyang, J. Biomimetic Gelatin Methacrylamide Hydrogel Scaffolds for Bone Tissue Engineering. *J. Mater. Chem. B* **2016**, *4*, 1070–1080, doi:10.1039/C5TB02251G.
587. Visser, J.; Gawlitta, D.; Benders, K.E.M.; Toma, S.M.H.; Pouran, B.; van Weeren, P.R.; Dhert, W.J.A.; Malda, J. Endochondral Bone Formation in Gelatin Methacrylamide Hydrogel with Embedded Cartilage-Derived Matrix Particles. *Biomaterials* **2015**, *37*, 174–182, doi:10.1016/j.biomaterials.2014.10.020.
588. Zhou, L.; Tan, G.; Tan, Y.; Wang, H.; Liao, J.; Ning, C. Biomimetic Mineralization of Anionic Gelatin Hydrogels: Effect of Degree of Methacrylation. *RSC Adv.* **2014**, *4*, 21997–22008, doi:10.1039/C4RA02271H.
589. Celikkin, N.; Mastrogiacomo, S.; Walboomers, X.; Swieszkowski, W. Enhancing X-Ray Attenuation of 3D Printed Gelatin Methacrylate (GelMA) Hydrogels Utilizing Gold Nanoparticles for Bone Tissue Engineering Applications. *Polymers* **2019**, *11*, 367, doi:10.3390/polym11020367.
590. Kang, H.; Shih, Y.-R.V.; Hwang, Y.; Wen, C.; Rao, V.; Seo, T.; Varghese, S. Mineralized Gelatin Methacrylate-Based Matrices Induce Osteogenic Differentiation of Human Induced Pluripotent Stem Cells. *Acta Biomaterialia* **2014**, *10*, 4961–4970, doi:10.1016/j.actbio.2014.08.010.
591. Linder, M.; Matouba, E.; Fanni, J.; Parmentier, M. Enrichment of Salmon Oil with N-3 PUFA by Lipolysis, Filtration and Enzymatic Re-Esterification. *European journal of lipid science and technology (Print)* **2002**, *104*, 455–462.
592. Colas, J.C.; Shi, W.L.; Rao, V.; Omri, A.; Mozafari, M.R.; Singh, H. Microscopical Investigations of Nisin-Loaded Nanoliposomes Prepared by Mozafari Method and Their Bacterial Targeting. *Micron* **2007**, *38*, 841–847, doi:10.1016/j.micron.2007.06.013.
593. Owens, D.K.; Wendt, R.C. Estimation of the Surface Free Energy of Polymers. *J. Appl. Polym. Sci.* **1969**, *13*, 1741–1747, doi:10.1002/app.1969.070130815.
594. Pleguezuelos-Villa, M.; Mir-Palomo, S.; Díez-Sales, O.; Buso, M.A.O.V.; Sauri, A.R.; Náchter, A. A Novel Ultradeformable Liposomes of Naringin for Anti-Inflammatory Therapy. *Colloids and Surfaces B: Biointerfaces* **2018**, *162*, 265–270, doi:10.1016/j.colsurfb.2017.11.068.
595. Yen, F.-L.; Wu, T.-H.; Lin, L.-T.; Cham, T.-M.; Lin, C.-C. Nanoparticles Formulation of *Cuscuta Chinensis* Prevents Acetaminophen-Induced Hepatotoxicity in Rats. *Food and Chemical Toxicology* **2008**, *46*, 1771–1777, doi:10.1016/j.fct.2008.01.021.
596. Danaei, M.; Dehghankhold, M.; Ataie, S.; Hasanzadeh Davarani, F.; Javanmard, R.; Dokhani, A.; Khorasani, S.; Mozafari, M. Impact of Particle Size and Polydispersity Index on the Clinical Applications of Lipidic Nanocarrier Systems. *Pharmaceutics* **2018**, *10*, 57, doi:10.3390/pharmaceutics10020057.
597. Tsai, M.-J.; Huang, Y.-B.; Fang, J.-W.; Fu, Y.-S.; Wu, P.-C. Preparation and Characterization of Naringenin-Loaded Elastic Liposomes for Topical Application. *PLOS ONE* **2015**, *10*, e0131026, doi:10.1371/journal.pone.0131026.
598. Ducy, P.; Zhang, R.; Geoffroy, V.; Ridall, A.L.; Karsenty, G. *Osf2/Cbfa1*: A Transcriptional Activator of Osteoblast Differentiation. *Cell* **1997**, *89*, 747–754, doi:10.1016/S0092-8674(00)80257-3.
599. Watkins, B.A.; Li, Y.; Lippman, H.E.; Feng, S. Modulatory Effect of Omega-3 Polyunsaturated Fatty Acids on Osteoblast Function and Bone Metabolism. *Prostaglandins, Leukotrienes and Essential Fatty Acids* **2003**, *68*, 387–398, doi:10.1016/S0952-3278(03)00063-2.
600. Abou-Saleh, H.; Ouhtit, A.; Halade, G.V.; Rahman, M.M. Bone Benefits of Fish Oil Supplementation Depend on Its EPA and DHA Content. *Nutrients* **2019**, *11*, 2701, doi:10.3390/nu11112701.

601. Casado-Díaz, A.; Santiago-Mora, R.; Dorado, G.; Quesada-Gómez, J.M. The Omega-6 Arachidonic Fatty Acid, but Not the Omega-3 Fatty Acids, Inhibits Osteoblastogenesis and Induces Adipogenesis of Human Mesenchymal Stem Cells: Potential Implication in Osteoporosis. *Osteoporos Int* **2013**, *24*, 1647–1661, doi:10.1007/s00198-012-2138-z.
602. Li, L.; Zeng, Z.; Cai, G. Comparison of Neoferocitrin and Naringin on Proliferation and Osteogenic Differentiation in MC3T3-E1. *Phytomedicine* **2011**, *18*, 985–989, doi:10.1016/j.phymed.2011.03.002.
603. Li, F.; Meng, F.; Xiong, Z.; Li, Y.; Liu, R.; Liu, H. Stimulative Activity of *Drynaria Fortunei* (Kunze) J. Sm. Extracts and Two of Its Flavonoids on the Proliferation of Osteoblastic like Cells. *Pharmazie* **2006**, *61*, 962–965.
604. Pacelli, S.; Maloney, R.; Chakravarti, A.R.; Whitlow, J.; Basu, S.; Modaresi, S.; Gehrke, S.; Paul, A. Controlling Adult Stem Cell Behavior Using Nanodiamond-Reinforced Hydrogel: Implication in Bone Regeneration Therapy. *Sci Rep* **2017**, *7*, 6577, doi:10.1038/s41598-017-06028-y.
605. Shao, Y.; You, D.; Lou, Y.; Li, J.; Ying, B.; Cheng, K.; Weng, W.; Wang, H.; Yu, M.; Dong, L. Controlled Release of Naringin in GelMA-Incorporated Rutile Nanorod Films to Regulate Osteogenic Differentiation of Mesenchymal Stem Cells. *ACS Omega* **2019**, *4*, 19350–19357, doi:10.1021/acsomega.9b02751.
606. Maisani, M.; Pezzoli, D.; Chassande, O.; Mantovani, D. Cellularizing Hydrogel-Based Scaffolds to Repair Bone Tissue: How to Create a Physiologically Relevant Micro-Environment? *Journal of Tissue Engineering* **2017**, *8*, 204173141771207, doi:10.1177/2041731417712073.
607. Ciobanu, B.C.; Cadinoiu, A.N.; Popa, M.; Desbrières, J.; Peptu, C.A. Modulated Release from Liposomes Entrapped in Chitosan/Gelatin Hydrogels. *Materials Science and Engineering: C* **2014**, *43*, 383–391, doi:10.1016/j.msec.2014.07.036.
608. Wilkins, E.; Wilson, L.; Wickramasinghe, K.; Bhatnagar, P.; Leal, J.; Luengo-Fernandez, R.; Burns, R.; Rayner, M.; Townsend, N. European Cardiovascular Disease Statistics 2017. **2017**.
609. Jayawardena, T.M.; Egemnazarov, B.; Finch, E.A.; Zhang, L.; Payne, J.A.; Pandya, K.; Zhang, Z.; Rosenberg, P.; Mirotso, M.; Dzau, V.J. MicroRNA-Mediated In Vitro and In Vivo Direct Reprogramming of Cardiac Fibroblasts to Cardiomyocytes. *Circ Res* **2012**, *110*, 1465–1473, doi:10.1161/CIRCRESAHA.112.269035.
610. Li, Y.; Dal-Pra, S.; Mirotso, M.; Jayawardena, T.M.; Hodgkinson, C.P.; Bursac, N.; Dzau, V.J. Tissue-Engineered 3-Dimensional (3D) Microenvironment Enhances the Direct Reprogramming of Fibroblasts into Cardiomyocytes by MicroRNAs. *Sci Rep* **2016**, *6*, 38815, doi:10.1038/srep38815.
611. Zhang, D.; Shadrin, I.Y.; Lam, J.; Xian, H.-Q.; Snodgrass, H.R.; Bursac, N. Tissue-Engineered Cardiac Patch for Advanced Functional Maturation of Human ESC-Derived Cardiomyocytes. *Biomaterials* **2013**, *34*, 5813–5820, doi:10.1016/j.biomaterials.2013.04.026.
612. Shin, S.R.; Zihlmann, C.; Akbari, M.; Assawes, P.; Cheung, L.; Zhang, K.; Manoharan, V.; Zhang, Y.S.; Yükksekaya, M.; Wan, K.; et al. Reduced Graphene Oxide-GelMA Hybrid Hydrogels as Scaffolds for Cardiac Tissue Engineering. *Small* **2016**, *12*, 3677–3689, doi:10.1002/sml.201600178.
613. Sadeghi, A.H.; Shin, S.R.; Deddens, J.C.; Fratta, G.; Mandla, S.; Yazdi, I.K.; Prakash, G.; Antona, S.; Demarchi, D.; Buijsrogge, M.P.; et al. Engineered 3D Cardiac Fibrotic Tissue to Study Fibrotic Remodeling. *Adv. Healthcare Mater.* **2017**, *6*, 1601434, doi:10.1002/adhm.201601434.
614. Elkhoury, K.; Sanchez-Gonzalez, L.; Lavrador, P.; Almeida, R.; Gaspar, V.; Kahn, C.; Cleymand, F.; Arab-Tehrany, E.; Mano, J.F. Gelatin Methacryloyl (GelMA) Nanocomposite Hydrogels Embedding Bioactive Naringin Liposomes. *Polymers* **2020**, *12*, 2944, doi:10.3390/polym12122944.

- 
615. Lee, S.W.L.; Paoletti, C.; Campisi, M.; Osaki, T.; Adriani, G.; Kamm, R.D.; Mattu, C.; Chiono, V. MicroRNA Delivery through Nanoparticles. *Journal of Controlled Release* **2019**, *313*, 80–95, doi:10.1016/j.jconrel.2019.10.007.
  616. Wang, H.; Zhou, L.; Liao, J.; Tan, Y.; Ouyang, K.; Ning, C.; Ni, G.; Tan, G. Cell-Laden Photocrosslinked GelMA–DexMA Copolymer Hydrogels with Tunable Mechanical Properties for Tissue Engineering. *J Mater Sci: Mater Med* **2014**, *25*, 2173–2183, doi:10.1007/s10856-014-5261-x.
  617. Sadeghi, A.H.; Shin, S.R.; Deddens, J.C.; Fratta, G.; Mandla, S.; Yazdi, I.K.; Prakash, G.; Antona, S.; Demarchi, D.; Buijsrogge, M.P.; et al. Engineered 3D Cardiac Fibrotic Tissue to Study Fibrotic Remodeling. *Adv. Healthcare Mater.* **2017**, *6*, 1601434, doi:10.1002/adhm.201601434.
  618. Valarmathi, M.T.; Goodwin, R.L.; Fuseler, J.W.; Davis, J.M.; Yost, M.J.; Potts, J.D. A 3-D Cardiac Muscle Construct for Exploring Adult Marrow Stem Cell Based Myocardial Regeneration. *Biomaterials* **2010**, *31*, 3185–3200, doi:10.1016/j.biomaterials.2010.01.041.



## Abstract

The main objective of this thesis is to develop a new natural material based on methacrylated gelatin (GelMA) nanofunctionalized by the incorporation of nanoliposomes or soft hybrid exosome-liposome nanoparticles. The physicochemical and biological properties of these hydrogel matrices were characterized in order to evaluate their potential use for tissue engineering applications. GelMA is prepared by the chemical modification of gelatin when methacrylate groups are attached to side groups containing amine functions. In a first part of this work, the influence of the gelatin source (pork or fish) and the degree of methacrylation on the physicochemical and biological properties of hydrogels was studied. In a second part of this work, the GelMA matrix was nanofunctionalized by the incorporation of nanoliposomes, which are soft and natural nanoparticles with remarkable self-assembly properties. These well-established drug delivery systems are formed of lipid bilayers and can transport and release hydrophobic, hydrophilic, and amphiphilic molecules. In this study, naringin, an active molecule that can guide the differentiation process of stem cells to the osteoblastic lineage, was encapsulated in nanoliposomes before their incorporation into the GelMA polymeric matrix in order to develop a system of interest for bone regeneration applications. This nanocomposite material was physicochemically and biologically characterized and the release profile of naringin was investigated. In a third and final part of this work, the GelMA matrix was nanofunctionalized by the incorporation of exosome-liposome soft hybrid nanoparticles. Exosomes, natural nanovesicles secreted by cells, are of increasing interest for targeted drug delivery applications due to the presence of cell specific receptors on their surface. The hybrid GelMA hydrogels were physicochemically and biologically characterized for applications in cardiac reprogramming and was successfully bioprinted and microfabricated. Biofabricated GelMA hydrogels nanofunctionalized with nanoliposomes or hybrid exosome-liposome nanoparticles are promising platforms for the controlled release of bioactive molecules and for tissue engineering applications.

---

---

## Résumé

L'objectif principal de cette thèse est de développer un nouveau matériau naturel à base de gélatine modifiée par méthacrylation (GelMA) nanofonctionnalisé par l'incorporation de nanoliposomes ou de nanoparticules hybrides molles de type exosome-liposome. Ces matrices hydrogel sont caractérisées d'un point de vue physicochimique et biologique afin d'évaluer leur potentiel en ingénierie tissulaire. Le GelMA est préparé par modification chimique de la gélatine, lorsque des groupements méthacrylate sont fixés sur des groupes latéraux contenant des fonctions amine. Dans une première partie de ce travail, l'influence de la source de la gélatine utilisée (porc ou poisson) et du degré de méthacrylation sur les propriétés physicochimiques et biologiques des hydrogels a été étudiée. Dans une deuxième partie de ce travail, la matrice GelMA a été nanofonctionnalisée par l'incorporation de nanoliposomes, nanoparticules molles et naturelles présentant des propriétés d'auto-assemblage remarquables. Ces vecteurs utilisés notamment dans le domaine médical sont formés de bicouches lipidiques et peuvent transporter et libérer des molécules hydrophobes, hydrophiles ou amphiphiles. Dans cette étude la naringine, une molécule active qui peut guider le processus de différenciation des cellules souches vers la lignée ostéoblastique, a été encapsulée dans les nanoliposomes avant leur incorporation dans la matrice polymérique afin de développer un hydrogel d'intérêt pour des applications en régénération osseuse. Ce matériau nanocomposite a été caractérisé d'un point de vue physicochimique, biologique et le profil de libération de la naringine est étudié. Dans une troisième et dernière partie de ce travail, la matrice GelMA a été nanofonctionnalisée par l'incorporation de nanoparticules hybrides molles de type exosome-liposome. Les exosomes, nanovésicules naturelles sécrétées par les cellules, présentent un intérêt croissant pour l'administration ciblée de médicaments en raison de la présence de récepteurs spécifiques aux cellules sur leur surface. L'hydrogel GelMA-nanoparticules hybrides a été caractérisée d'un point de vue physicochimique et biologique pour des applications en reprogrammation cardiaque et a été bioimprimé et microfabriqué avec succès. Les hydrogels GelMA biofabriqués et nanofonctionnalisés avec des nanoliposomes ou des nanoparticules hybrides molles de type exosome-liposome sont des systèmes prometteurs pour la libération contrôlée de molécules bioactives et pour des applications en ingénierie tissulaire.